



**Effects of ocean acidification and warming on shallow subtidal
temperate seaweed assemblages in eastern Tasmania, Australia:
implications for the blacklip abalone (*Haliotis rubra*)**

Damon Britton

BMarSc (First Class Honours)

Institute for Marine and Antarctic Studies (IMAS)
University of Tasmania
November 2020

Thesis submitted in fulfilment of the requirements for the degree of:
Doctor of Philosophy in Marine Science

Declaration of Originality

This thesis contains no material which has been accepted for a degree or diploma by the University or any other institution, except by way of background information and duly acknowledged in the thesis, and to the best of my knowledge and belief no material previously published or written by another person except where due acknowledgement is made in the text of the thesis, nor does the thesis contain any material that infringes copyright.

Signed:

(Damon Britton)

Date: 25/03/2020

Statement of Authority of Access

The publishers of the papers comprising Chapters 3 and 4 hold the copyright for that content and access to the material should be sought from the respective journals. The remaining unpublished content of the thesis may be made available for loan and limited copying and communication in accordance with the Copyright Act 1968.

A version of Chapter 3 has been published as:

Britton, D., Mundy, C. N., McGraw, C. M., Revill, A. T., & Hurd, C. L. (2019). Responses of seaweeds that use CO₂ as their sole inorganic carbon source to ocean acidification: differential effects of fluctuating pH but little benefit of CO₂ enrichment. *ICES Journal of Marine Science*. doi:10.1093/icesjms/fsz070

A version of Chapter 4 has been published as:

Britton, D., Schmid, M., Noisette, F., Havenhand, J.N., Paine, E.R., McGraw, C.M. et al. (2020). Adjustments in fatty acid composition is a mechanism that can explain resilience to marine heatwaves and future ocean conditions in the habitat-forming seaweed *Phyllospora comosa* (Labillardière) C.Agardh. *Global Change Biology*. <https://doi.org/10.1111/gcb.15052>

Signed:

(Damon Britton)

Date: 25/03/2020

Statement of co-authorship

Chapters 2 – 5 of this thesis has been prepared as submissions, have been submitted to or are published in peer-reviewed journals. The design and implementation of experiments and surveys, the development of methods, data analysis, interpretation of results and the preparation of manuscripts for submission was the responsibility of the candidate but was carried out in collaboration with supervisors and other co-authors.

The following people and institutions contributed to the publication of work undertaken as part of this thesis.

Candidate: Damon Britton (candidate), Institute for Marine and Antarctic Studies

Author 1: Prof. Catriona Hurd, Institute for Marine and Antarctic Studies

Author 2: Dr. Craig Mundy, Institute for Marine and Antarctic Studies

Author 3: Dr. Matthias Schmid, Institute for Marine and Antarctic Studies

Author 4: Dr. Fanny Noisette, Université du Québec à Rimouski

Author 5: Dr. Christina McGraw, University of Otago

Author 6: Dr. Andrew Revill, CSIRO Oceans and Atmosphere

Author 7: Dr. Patti Virtue, Institute for Marine and Antarctic Studies

Author 8: Dr. Peter Nichols, CSIRO Oceans and Atmosphere

Author 9: Prof. Jonathan Havenhand, University of Gothenburg

Author 10: Ms. Ellie Paine, Institute for Marine and Antarctic Studies

Chapter 2: Seasonal and site-specific variation in the nutritional quality of temperate seaweed assemblages: implications for grazing invertebrates and the commercial exploitation of seaweeds.

Craig Mundy and Catriona Hurd contributed to the design of the study. Matthias Schmid conducted the fatty acid extractions and analysis. Andrew Revill conducted the analysis of nitrogen content. Peter Nichols, Patti Virtue and Matthias Schmid assisted with the interpretation of the fatty acid data. Craig Mundy and Catriona Hurd contributed to the data analysis. All authors provided comments on the manuscript.

Chapter 3: Responses of seaweeds that use CO₂ as their sole inorganic carbon source to ocean acidification: differential effects of fluctuating pH but little benefit of CO₂ enrichment.

Craig Mundy and Catriona Hurd contributed to the design the study. Christina McGraw designed and built the automated culture system. Christina McGraw and Andrew Revill assisted in post-experiment data and sample processing. Craig Mundy and Catriona Hurd assisted with the data analysis. All authors provided comments on the manuscript.

Chapter 4: Adjustments in fatty acid composition is a mechanism that can explain resilience to marine heatwaves and future ocean conditions in the habitat-forming seaweed *Phyllospora comosa* (Labillardière) C.Agardh.

Craig Mundy, Catriona Hurd, Jonathan Havenhand and Fanny Noisette contributed to the design of the experiment. Matthias Schmid undertook the fatty acid extraction and analysis and assisted with interpretation of the data. Andrew Revill conducted the stable isotope analysis and assisted in interpretation. Christina McGraw designed the experimental system and assisted with post-experiment processing of experimental data. Fanny Noisette and Ellie

Paine assisted with the field and laboratory components of the study and interpretation of results. Peter Nichols, Patti Virtue and Matthias Schmid assisted with the interpretation of the fatty acid data. Craig Mundy, Catriona Hurd, Jonathan Havenhand and Fanny Noisette assisted with data analysis. All authors provided comments on the manuscript.

Chapter 5: Crustose coralline algae are sensitive to near-future global ocean change scenarios.

Craig Mundy, Catriona Hurd and Fanny Noisette contributed to the design of the study. Christina McGraw designed the experimental system and assisted with post-experimental processing of chemical data. Fanny Noisette undertook analysis of samples for total alkalinity and assisted with the calculation and interpretation of calcification rates. Catriona Hurd and Craig Mundy assisted with the data analysis. All authors provided comments on the manuscript.

We the undersigned agree with the above stated “proportion of work undertaken” for each of the above published (or submitted/in preparation) peer-reviewed manuscripts contributing to this thesis:

Damon Britton
Candidate
Institute for Marine and Antarctic Studies (IMAS)
Ecology and Biodiversity
University of Tasmania
November 2020

Professor Catriona Hurd
Primary Supervisor
Institute for Marine and Antarctic Studies (IMAS)
Ecology and Biodiversity
University of Tasmania
March 2020

Professor Catriona MacLeod
Institute for Marine and Antarctic Studies (IMAS)
Centre Head – Ecology and Biodiversity
University of Tasmania
March 2020

Acknowledgements

I would like to extend a thank you to my research organisation, the Institute for Marine and Antarctic Studies (IMAS) and the University of Tasmania, without which the preparation and submission of this thesis would not have been possible. I am grateful to the assistance and encouragement given to me by numerous people throughout the course of my PhD and would like to extend a thank you to the following people in particular:

To my supervisors Catriona Hurd and Craig Mundy, I am extremely grateful to both of you for the opportunity to undertake this project and providing me with the guidance, support, knowledge and funding to successfully complete the research. The skills I have learnt from you will prove invaluable over the course of my career and I would like to extend a special thank you for your patience and enthusiasm throughout my PhD.

Thank you to Jonathan Havenhand, Matthias Schmid, Fanny Noisette and Cayne Layton. All four of you have provided substantial support and advice to me over the course of this thesis and I feel very privileged to have been able to access your help when required. Thankyou also to all members of the Hurd lab group over the last few years, in particular Ellie Paine, Pamela Fernandez, Joanna Smart, Pablo Leal and our visiting collaborators Christina McGraw and Louise Kregting. I would also like to thank Victor Shelamoff for numerous discussions about results and marine science in general and providing me with an alternative viewpoint.

The fieldwork conducted in these experiments would not have been possible without the assistance of numerous people. I would like to thank Sarah Pyke, David Faloon, Ruari Colquhoun, Jaime McAllister, Jane Ruckert, Kylie Cahill and Graeme Ewing for helping me undertake the fieldwork and teaching me a range of practical skills along the way.

Additionally, I would like to thank Camille White, Sam Kruimink, Simon Talbot, Vallorie Hodges and all volunteers who helped complete the fieldwork, Kathryn Willis in particular.

To all the other students at IMAS and the University of Tasmania more broadly, thank you for your support and good humour. Thank you also to both of my parents, Helen and Glenn for your endless support.

Lastly, I would like to thank Ella for your unlimited support and patience throughout this thesis. You have truly made the entire journey far more manageable and enjoyable.

Contents

Chapter 1. Introduction	1
Global ocean change	2
Impacts of ocean acidification of seaweeds	3
Fluctuating pH in coastal systems: influences on responses to ocean acidification	5
Impacts of elevated temperature on seaweeds	6
Interactive effects of global ocean change stressors	7
Reliance of abalone on seaweeds	7
Thesis structure	10
Chapter 2: Seasonal and site-specific variation in the nutritional quality of temperate seaweed assemblages: implications for grazing invertebrates and the commercial exploitation of seaweeds.	10
Chapter 3: Responses of seaweeds that use CO ₂ as their sole inorganic carbon source to ocean acidification: differential effects of fluctuating pH but little benefit of CO ₂ enrichment.	11
Chapter 4: Adjustments in fatty acid composition is a mechanism that can explain resilience to marine heatwaves and future ocean conditions in the habitat-forming seaweed <i>Phyllospora comosa</i> (Labillardière) C.Agardh.	11
Chapter 5: Crustose coralline algae are sensitive to near-future global ocean change scenarios.	12
Chapter 6: General Discussion	12
References	12
 Chapter 2. Seasonal and site-specific variation in the nutritional quality of temperate seaweed assemblages: implications for grazing invertebrates and the commercial exploitation of seaweeds.	 20
Abstract	20
Introduction	22
Methods	25
Seasonal sampling for biomass and species composition	25
Sampling for biochemical composition	28
	x

Fatty acid analysis	29
Analysis of % N content	29
Analysis and statistics on biochemical composition data	30
Spatial and seasonal variation in fatty acid composition, nitrogen content and biomass of red and brown seaweeds	30
Seasonal variation in individual seaweed species	32
Results	32
Overstory canopy description and biomass of understory species	32
Spatial and seasonal variation in nutritional quality of red and brown seaweeds	34
Overview of nutritionally important compounds in the reds and browns	36
Seasonal variation in fatty acids at the species level	39
Site 1	39
Site 2	39
Site 3	40
Discussion	43
Differences in the nutritional quality between sites is driven by the red seaweeds	44
Implications of variability in the nutritional quality of red seaweeds for commercial fisheries	45
Seasonal variability in fatty acids at the species level	47
Implications of species and site-specific variability in fatty acids for commercial exploitation of seaweeds	48
Summary	49
Acknowledgements	50
References	50
Appendices	56
References	63
 Chapter 3. Responses of seaweeds that use CO₂ as their sole inorganic carbon source to ocean acidification: differential effects of fluctuating pH but little benefit of CO₂ enrichment.	 64
Abstract	64
Introduction	66
Methods	69
	xi

Seaweed collection	69
Pre-experimental treatment	70
Experimental culture conditions	70
Experimental treatments	71
Biotic responses	72
Relative growth rates (wet weight)	72
Photosynthetic and respiration rates	72
Pigment content, tissue C and N and stable C isotopes	73
Statistical analysis	74
Results	75
Experimental culture conditions	75
Biotic responses	75
Relative growth rates (wet weight)	75
Photosynthetic and respiration rates	76
Pigment content, tissue C and N, stable C isotopes,	77
Discussion	81
Responses to fluctuating pH	82
Comparing studies that use different methods to fluctuate pH	85
Responses to OA	87
Interactive effects of pH fluctuations and OA: important implications for interpretations of species and community responses to OA	88
Acknowledgements	89
Funding sources	89
References	90
Appendices	95

Chapter 4. Adjustments in fatty acid composition is a mechanism that can explain resilience to marine heatwaves and future ocean conditions in the habitat-forming seaweed *Phyllospora comosa* (Labillardière) C.Agardh. 98

Abstract	98
Introduction	100
Materials and methods	104

Field conditions	104
Seaweed collection and pre-experimental treatment	105
Experimental culture conditions	106
Experimental treatments	107
Biotic responses	110
Relative growth rates (wet weight)	110
Pigment content, stable C isotopes, % tissue nitrogen and fatty acid profiles	110
Statistical analysis	112
Results	113
Field pH and light measurements	113
Experimental culture conditions	114
Biotic responses	115
Relative growth rates (wet weight)	115
Photosynthetic and respiration rates	115
Pigment content, stable carbon isotopes and % tissue nitrogen	117
Fatty acid profiles	119
Discussion	123
Implications for management	126
Funding sources	127
References	127
Appendices	133
Supplementary methods – pH logger calibration	133
Supplementary methods – light logger calibration	134
 Chapter 5. Crustose coralline algae are sensitive to near future global ocean change scenarios.	 139
Abstract	139
Introduction	140
Materials and methods	144
Deployment and collection of settlement plates and in situ CCA cover estimates	144
Pre-experimental treatment	144
	xiii

Experimental culture conditions	145
Determination of carbonate chemistry	146
Experimental treatments	146
Biotic responses	147
Relative growth rates (RGR) and percentage bleaching	147
Net photosynthesis	147
Net calcification	148
Statistical analysis	148
Results	150
Percentage cover of CCA in situ	150
Experimental culture conditions	150
Biotic responses	151
Relative growth rates (RGR) and percentage bleaching	151
Net photosynthesis	153
Calcification	153
Discussion	155
Rates of change: implications for adaptation	157
Ecological considerations	159
Acknowledgments	161
References	161
Appendices	168
 Chapter 6. General Discussion	 172
Current communities: have they already changed?	173
Indirect effects of global ocean change are likely to have differential effects on the life-stages of <i>H. rubra</i>	174
Limitations/key questions remaining	178
Inorganic carbon uptake strategy as a tool to predict responses of seaweeds to global ocean change	180
Projecting forward/conclusions	181
References	183

List of Figures

Figure 2.1: Map of Tasmania, Australia showing the location of the three sites in eastern Tasmania. Inset shows the location of Tasmania (red outline) in relation to mainland Australia.

Figure 2.2: Biomass (g dry weight m⁻²) of understory seaweeds at each site each season. Brown bars refer to brown seaweeds (species pooled) and red bars refer to the red seaweeds (species pooled). Data is presented as means \pm standard error.

Figure 2.3: Principal Coordinates Analysis (PCoA) of fatty acids that were on average at least 1 % of total fatty acids (TFA). The PCoA is based on a resemblance matrix using the Bray-Curtis Similarity measure. Brown symbols refer to brown seaweeds (species pooled) and red symbols refer to the red seaweeds (species pooled). Stars refer to samples from site 1, filled triangles refer to samples from site 2, and open circles refer to samples from site 3.

Figure 2.4: Boxplots of the nutritionally important fatty acids arachidonic acid (ARA, % dry weight, a, b, c) and eicosapentanoic acid (EPA, % TFA, d, e, f) at each site in each season for the red (red boxes) and brown (brown boxes) seaweeds sampled. The black lines display the median, boxes cover interquartile range and error bars display the maximum and minimum values. Outliers are displayed as points. No red species were sampled for biochemical composition at site 1.

Figure 2.5: Boxplots of the nutritionally important fatty acid group C₁₈ n-3 PUFA (% TFA, a, b, c) and percentage nitrogen (d, e, f) at each site in each season for the red (red boxes) and brown (brown boxes) seaweeds sampled. The black lines display the median, boxes cover interquartile range and error bars display the maximum and minimum values. Outliers are displayed as points. No red species were sampled for biochemical composition at site 1.

Figure 2.6: Levels of saturated fatty acids (SFA, % TFA) and polyunsaturated fatty acids (PUFA % TFA) for understory species sampled in at least 3 seasons at site 1 (a, d), site 2 (b, e), and site 3 (c, f). Seasons sharing the same letter were not found to be significantly different in THSD post-hoc tests. Differences in SFA and PUFA were compared across seasons in site 1 on pooled data for all species as no significant interactions between site and species were detected in the two-way ANOVA. All other sites had SFA and PUFA content compared across seasons separately for each species with one-way ANOVAs as a significant interaction between site and species was detected in the 2-way ANOVAs. Brown seaweeds are coloured brown and red seaweeds are coloured red. N.D refers to no data for a species in that season and site combination (*P. comosa* in spring at site 1 and *P. novaehollandiae* at site 2 in spring). Seasons are abbreviated: Sp = spring, Su = summer, Au = autumn, Wi = winter. Data is presented as means \pm standard error.

Figure 3.1: Average pH_T of seawater for each treatment following a seawater refresh of the culture chambers (4-hour intervals), error bars are standard error (measurements of pH_T for each treatment: n = 144 – 153).

Figure 3.2: Responses of *C. lambertii* (left) and *P. dilatatum* (right) to current and future ocean pH after 14 days in culture. Shaded bars refer to treatments where pH was static and white bars refer to treatments where pH was fluctuating. Response variables and significant differences are as follows: a) Relative growth rates (RGR, day⁻¹), *C. lambertii*: Static > Fluctuating ($p = 0.007$), *P. dilatatum*: no significant differences; b) Net photosynthesis ($\mu\text{mol O}_2 \text{ g}^{-1} \text{ h}^{-1}$), *C. lambertii*: Static > Fluctuating ($p = 0.007$), Future > Current ($p = 0.041$), *P. dilatatum*: no significant differences, and; c) Respiration ($\mu\text{mol O}_2 \text{ g}^{-1} \text{ h}^{-1}$) *C. lambertii*: Future > Current ($p = 0.0008$), *P. dilatatum*: Future > Current ($p = 0.013$). Data are presented as means \pm standard error, $n = 4 - 6$. All rates are calculated on a wet weight basis.

Figure 3.3: Responses of *C. lambertii* (left) and *P. dilatatum* (right) to current and future ocean pH after 14 days in culture. Shaded bars refer to treatments where pH was static and white bars refer to treatments where pH was fluctuating. Response variables and significant differences are as follows: a) C:N ratios, *C. lambertii*: Static > Fluctuating ($p = 0.035$), *P. dilatatum*: Fluctuating > Static ($p = 0.022$); b) % C, *C. lambertii*: Interaction ($p = 0.009$), *P. dilatatum*: no significant differences, and; c) % N, *C. lambertii*: Interaction ($p = 0.008$), *P. dilatatum*: Static > Fluctuating ($p = 0.043$). Data are presented as means \pm standard error, $n = 4 - 6$.

Figure 4.1: Top panel: pH and temperature conditions in each of the four experimental treatments. Blue boxes indicate the current scenario and red boxes the future scenario. Within each scenario, solid lines refer to baseline treatments in which temperature was constant for the duration of the experiment, whereas dashed lines refer to treatments in which a 6 day 3 °C heatwave was superimposed on the baseline temperature. **Bottom panel:** timeline of the sampling regime and the temperature levels in each treatment over the duration of the experiment. The first sampling was undertaken on the final day of the “heatwave period” and the final sampling was undertaken on the final day of the “recovery period.” For ease of visualisation overlapping lines are slightly offset despite having the same temperature. See results for precise temperature levels in each treatment.

Figure 4.2: Responses of juvenile *Phyllospora comosa* at the end of the heatwave period (first sampling, left panels) and following the recovery period (final sampling, right panels). *P. comosa* juveniles were cultured in current (today’s temperature and pH) and future (2100 temperature and pH projections) scenarios. Shaded bars refer to baseline temperature treatments and white bars refer to treatments where a 6 day 3 °C heatwave was superimposed on the baseline temperature in a given scenario. Response variables and significant differences are described for each panel. **Top row:** relative growth rates (RGR, day⁻¹); no significant differences at either sampling. **Middle row:** net photosynthesis ($\mu\text{mol O}_2 \text{ L}^{-1} \text{ g}^{-1} \text{ h}^{-1}$); first sampling, future > current ($p = 0.006$), heatwave < baseline ($p = 0.0002$); final sampling, no significant differences. **Bottom row:** respiration ($\mu\text{mol O}_2 \text{ L}^{-1} \text{ g}^{-1} \text{ h}^{-1}$); first sampling, interaction near significant ($p = 0.059$), final sampling, future < current ($p = 0.02$). Data are presented as means \pm standard error, $n = 6$ for all treatments at both sampling points excluding net photosynthesis in the future heatwave treatment at the first sampling ($n = 5$). All rates are calculated on a wet weight basis.

Figure 4.3: Responses of juvenile *Phyllospora comosa* at the end of the heatwave period (first sampling, left panels) and following the recovery period (final sampling, right panels). *P. comosa* juveniles were cultured in current (today’s temperature and pH) and future (2100 temperature and pH projections) scenarios. Shaded bars refer to baseline temperature treatments, and white bars refer to treatments where a 6 day 3 °C heatwave was

superimposed on the baseline temperature in a given scenario. Response variables and significant differences are described for each panel. **Top row:** chlorophyll a content (mg g^{-1}); first sampling, no significant differences, final sampling, future < current ($p = 0.013$). **Middle row:** fucoxanthin content (mg g^{-1}); first sampling, no significant differences; final sampling: future < current ($p = 0.042$). **Bottom row:** $\delta^{13}\text{C}$; first sampling, no significant differences, final sampling: future < current ($p = 0.002$). Data are presented as means \pm standard error, $n = 6$ for all treatments at both sampling points excluding chlorophyll a and fucoxanthin content in the future baseline and future heatwave treatment at the first sampling ($n = 5$). Chlorophyll a and fucoxanthin content are calculated on a dry weight basis.

Figure 4.4: Responses of juvenile *Phyllospora comosa* at the end of the heatwave period (first sampling, left panels) and following the recovery period (final sampling, right panels). *P. comosa* juveniles were cultured in current (today's temperature and pH) and future (2100 temperature and pH projections) scenarios. Shaded bars refer to baseline temperature treatments, and white bars refer to treatments where a 6 day 3 °C heatwave was superimposed on the baseline temperature in a given scenario. Response variables and significant differences are described for each panel. **Top row:** total fatty acids (TFA, % dry weight); first sampling, no significant differences; final sampling, interaction significant ($p = 0.003$). **Middle row:** saturated fatty acids (SFA, % TFA); first sampling, future < current ($p = 0.022$); final sampling: interaction ($p = 0.002$). **Bottom row:** polyunsaturated fatty acids (PUFA, % TFA); first sampling, future > current ($p = 0.028$); final sampling, interaction significant ($p = 0.003$). Data are presented as means \pm standard error, $n = 6$. For significant interactions, treatments displaying the same letter were not significantly different in THSD post-hoc tests. TFA is calculated on a dry weight basis.

Figure 5.1: Relative growth rates (RGR, day^{-1} , top panel) and % tissue bleached (bottom panel) of crustose coralline algae (CCA) cultured for 29 days under current ocean pH and temperature and pH and temperature projected by 2100 under the RCP emission scenarios (low = RCP 2.6, medium = RCP 4.5, and high RCP 8.5, IPCC 2014). Treatments with an asterisk were significantly different from the Current scenario at $\alpha = 0.05$ in the a-priori planned comparisons. Data are presented as means \pm standard error, $n = 8$ for all treatments except for % tissue bleached in the RCP 2.6 treatment ($n = 7$).

Figure 5.2: Net photosynthetic rates ($\mu\text{mol O}_2 \text{ cm}^{-2} \text{ h}^{-1}$, top panel) and net calcification rates ($\mu\text{mol CaCO}_3 \text{ cm}^{-2} \text{ h}^{-1}$, bottom panel) of crustose coralline algae (CCA) cultured for 29 days under current ocean pH and temperature and pH and temperature projected by 2100 under the RCP emission scenarios (low = RCP 2.6, medium = RCP 4.5, and high RCP 8.5, IPCC 2014). Treatments with an asterisk were significantly different from the current scenario at $\alpha = 0.05$ in the a-priori planned comparisons. Data are presented as means \pm standard error, $n = 8$ in all treatments for net photosynthesis, $n = 8$ in RCP 2.6, $n = 7$ in Current, RCP 8.5 and $n = 5$ in RCP 4.5.

Figure 5.3: Conceptual diagram displaying the change in ocean conditions until 2100 according to the IPCC *Representative Concentration Pathways* (RCP) emission scenarios 2.6 (low emissions), 4.5 (medium emissions), and 8.5 (high emissions). The y-axis displays the ocean conditions projected in 2100 under each emission scenario. Arrows mark the year when the conditions projected to occur in 2100 under the RCP 2.6 and 4.5 scenarios will occur in the high emissions RCP 8.5 scenario. Under the RCP 8.5 scenario the impacts

detected in this study in the RCP 2.6 scenario will occur ~ 2030 and the impacts detected in the RCP 4.5 scenario will occur ~ 2050. The “Equivalent ocean condition at 2100” scale is approximate and is for conceptual purposes only.

Figure 6.1: Conceptual diagram showing the ways in which the blacklip abalone (*Haliotis rubra*) relies on seaweed (left), the impacts of global ocean change on these seaweed detected in laboratory experiments (middle left), the likely indirect effects on *H. rubra* arising from the impacts on the seaweeds (middle right) and the potential ecological consequences of the indirect impacts (right). Red arrows refer to negative impacts and the grey dash refers to no impact.

List of Tables

Table 2.1: Analysis of Variance (ANOVA) table showing degrees of freedom (df), F – values and *p* – values for seasonal differences in polyunsaturated fatty acids (PUFA) and saturated fatty acids (SFA). For site 1, there was no significant interaction between season and species detected in the 2-way ANOVAs for PUFA or SFA and as such when the main effect of season was significant at $\alpha = 0.05$, differences between season were assessed across all species using Tukey’s Honestly Significant Different (THSD) post-hoc tests. For sites 2 and 3 a significant interaction between site and season were detected and as such, all species were analysed separately within each site. When these ANOVAs detected significant differences at $\alpha = 0.05$, *p*-values are displayed in bold and THSD post-hoc tests were conducted. Significant differences ($\alpha = 0.05$) between seasons detected in THSD post-hoc tests are displayed, and abbreviations of seasons are given: Sp = spring, Su = summer, Au = autumn and Wi = winter.

Table 3.1: Analysis of Variance (ANOVA) table for all response variables. The table displays *p*-values, transformations and the nature of differences for both *C. lambertii* and *P. dilatatum*. Significant effects ($\alpha = 0.05$) have *p*-values displayed in bold. For differences in main effects ‘Type’ (Two levels: static and fluctuating pH) and ‘Era’ (Two levels: Current and Future), acronyms are displayed: F = future, C = current, S = static and FL = fluctuating. For significant interactions, differences between ‘Type’ are displayed in bold when differences were significant at $\alpha = 0.05$ using separate one-way ANOVAs at each level of ‘Era’. Treatment acronyms: CF = current fluctuating, CS = current static, FF = future fluctuating, FS = future static. Degrees of Freedom = 1 for main effects and the interaction and 17 - 18 for residuals.

Table 3.2: Carbonate system parameters at the mean pH_T of each treatment. pH_T, and salinity were measured while A_T, DIC at mean treatment pH_T, CO₂ and [H⁺] were calculated at the mean pH_T of each treatment using the program CO2Calc (Robbins et al., 2010) from the DIC samples measured at pH_T 8.01 and 7.64 and the known salinity, pH_T and temperature of the seawater.

Table 3.3: Published responses of photosynthetic organisms to diel fluctuations in pH under ambient and OA conditions. All responses are relative to static pH at the mean pH of the respective scenario (i.e. ~ pH 8.0 and ~ pH 7.7). G = growth, PS = photosynthesis, R = respiration and C = calcification. ‘–’ refers to no effect and blank spaces indicate the variable was not measured or not tested by the authors. The calcification response of *H. reinboldii* under ambient pH from Cornwall et al. (2018) was dependent on the location individuals were collected from. Individuals collected at a site with high pH variability responded positively to fluctuating pH, while those from a site with low pH variability were unaffected.

Table 4.1: Mean, minimum, maximum and range of pH_T values recorded by the pH loggers deployed at Coal Point over the two logger deployments. Deployment 1 consisted of two loggers between the 24th January to 9th February 2018 (Jan-Feb) and deployment 2 consisted of one logger between the 27th February and 14th April 2018 (Feb-April).

Table 4.2: Mean pH_T , DIC, A_T and temperature (outside of and during the heatwaves) for each treatment. All pH values were measured, while DIC and A_T were calculated from the mean pH_T of each treatment and the relationship between pH_T and DIC. This relationship was constructed from the DIC values measured over pH_T values that spanned the range used in the experiment and the known salinity of the seawater.

Table 4.3: Linear mixed model table for all response variables. The table displays p -values and the nature of differences at both sampling points. Significant effects ($\alpha = 0.05$) have p -values displayed in bold. Near significant differences ($\alpha < 0.1$) have p -values displayed in italics. For differences in the main effects of “Scenario” (Two levels: current and future) and “Temperature regime” (Two levels: baseline or heatwave), factor names are displayed showing the nature of differences. For significant interactions, significant differences ($\alpha < 0.05$) between treatments identified using THSD post-hoc tests are displayed. Near significant differences ($\alpha < 0.1$) between treatments detected in THSD post-hoc tests are displayed in italics with p -values displayed in parentheses. Response variables displayed as acronyms: RGR = relative growth rates, TFA = total fatty acids, SFA = saturated fatty acids, PUFA = polyunsaturated fatty acids. Treatment acronyms: CB = current baseline, CH = current heatwave, FB = future baseline, FH = future heatwave. Degrees of Freedom = 1 for main effects and the interaction and 17 - 20 for residuals.

Table 5.1: Carbonate system parameters at the mean pH_T and temperature of each treatment. A_T , pH_T , temperature and salinity were measured and DIC was calculated in the program in CO2calc (Robbins, Hansen et al. 2010).

Abstract

This study investigated how the combined stressors of ocean warming and acidification (reduced pH and elevated CO₂) impact seaweed species that the commercially exploited blacklip abalone (*Haliotis rubra*) relies on for all components of its life cycle. The impacts of warming and acidification on seaweeds that provide habitat, a food source or induce settlement of larvae, were assessed through a series of manipulative laboratory experiments.

To provide context for experimental work, a field survey was undertaken that examined seaweed biomass, species composition and nutritional quality (fatty acid composition and nitrogen content) in three sites that spanned a latitudinal gradient in eastern Tasmania (Chapter 2). Results showed that the nutritional quality of the understory seaweeds consumed by *H. rubra* increased from the northern to southern site. This increase was consistent with higher productivity of *H. rubra* in the southern region and was driven by a higher biomass of red species at the southern sites, which were rich in polyunsaturated fatty acids (PUFA) and nitrogen.

Most studies examining the response of seaweeds to ocean acidification in laboratory studies have used experimental treatments based on future projections for the open ocean. This is problematic as pH within seaweed beds is highly variable (compared to stable open ocean), and pH fluctuations can influence the response of seaweeds to acidification. Chapter 3 examined the effect of fluctuating pH on two sympatric red seaweeds (*Callophyllis lambertii* and *Plocamium dilatatum*) under both current and future ocean pH. Only *C. lambertii* was affected by fluctuating pH, with reduced growth and photosynthetic rates relative to the static conditions. The differential responses of two sympatric red seaweeds led to the incorporation of pH fluctuations in the treatments of all subsequent experiments, to provide environmental realism.

Chapter 4 investigated the influence of marine heatwaves along with future warming and acidification on the brown seaweed *Phyllospora comosa*, which forms primary habitat for *H. rubra* and is an important food source. *P. comosa* was physiologically tolerant to marine heatwaves under both current and future ocean conditions. This tolerance was likely due to an adjustment in fatty acid composition with a reduction in the proportion of PUFA to saturated fatty acids (SFA) maintaining optimum membrane fluidity at elevated temperatures. Furthermore, energetic savings arising from increased CO₂ supply (i.e. acidification) may have facilitated this adjustment when marine heatwaves were superimposed on future ocean warming and acidification.

Chapter 5 examined the effects of warming and acidification on crustose coralline algae (CCA) that are known to induce settlement of *H. rubra* larvae. A scenario-based approach was used in which the responses of CCA (genus *Sporolithon*) cultured under current ocean temperature and pH were compared to responses under temperature and pH levels expected by 2030, 2050 and 2100 (RCP 8.5 emissions scenario). Results suggest that CCA are likely to be significantly negatively affected by combined warming and acidification as soon as 2030.

The findings of this thesis suggest that the key habitat forming seaweed in abalone habitat, *P. comosa*, is likely to acclimate to future ocean conditions. However, this acclimation mechanism (reduction in PUFA), along with a reduction in nitrogen content observed under global ocean change in both *P. comosa* and *C. lambertii*, may lead to a significant reduction the nutritional quality of these seaweeds for *H. rubra*. Whether other seaweeds utilised as food sources such as the red seaweeds that were abundant in our southern field sites will respond in similar ways requires investigation. Recruitment of *H. rubra* larvae may be negatively impacted within the next two decades via adverse impacts of climate change on CCA assemblages. These findings highlight the need for managers of commercially exploited species to consider the effects of climate change on the seaweeds they rely on.

Chapter 1. Introduction

Seaweed beds are diverse and productive communities that dominate rocky reefs in the temperate to sub-polar regions (Steneck et al., 2002; Hurd et al., 2014). They typically consist as a multi-tiered canopy, with large canopy forming browns (Phylum Ochrophyta, Class Phaeophyceae) forming an overstory, smaller species of red (Phylum Rhodophyta), green (Phylum Chlorophyta) and browns forming the understory, and encrusting species of reds such as coralline algae covering the rock surface (Steneck et al., 2002; Hurd et al., 2014). Seaweed beds support diverse communities of invertebrates (Teagle et al., 2018), from cryptic fauna associated with kelp holdfasts, to epifaunal communities and larger macro-invertebrate grazers such as abalone and urchins, which rely on seaweeds for the entire benthic phase of their life cycle. The seaweeds provide habitat and a food source (Steneck et al., 2002; Hurd et al., 2014), promote settlement cues for larvae (Pearce and Scheibling, 1991; Daume et al., 1999; Heyward and Negri, 1999; Roberts, 2001) and provide shelter from predation (Steneck et al., 2002; Hurd et al., 2014). Seaweeds have important roles in coastal nutrient cycling (Hurd et al., 2014), modify the physical environment by reducing light and water flow (Eckman et al., 1989; Kennelly, 1989; Layton et al., 2019) and alter the chemistry of the surrounding seawater (Cornwall et al., 2013; Britton et al., 2016). Anthropogenically induced stressors including eutrophication, invasive species and climate change are impacting seaweeds globally (Ling et al., 2009; Mineur et al., 2015; Krumhansl et al., 2016; Wernberg et al., 2016; Filbee-Dexter and Wernberg, 2018). These impacts on seaweeds are likely to indirectly affect species from higher trophic levels that rely on them. As such, understanding how seaweeds will respond in a future ocean is critical to predicting how the species and communities they support may be indirectly affected.

Global ocean change

Since the industrial revolution, anthropogenic greenhouse gas emissions have caused a suite of changes in the chemical and physical characteristics of the global oceans (IPCC, 2014), collectively referred to as global ocean change (Boyd et al., 2018). Two of the main changes that are likely to affect seaweeds are ocean acidification and ocean warming (IPCC, 2014). Ocean acidification refers to the sustained absorption of increased atmospheric CO₂, which causes a range of chemical changes to the seawater carbonate system (Feely et al., 2004; Doney et al., 2009). Since ~ 1880, the pH of the surface ocean has declined on average by ~ 0.1 units globally and a further decline of ~ 0.3 units is predicted by 2100 under the Intergovernmental Panel for Climate Change (IPCC) Representative Concentration Pathway (RCP) 8.5 scenario (IPCC, 2014). This decline in pH will correspond to an approximate increase in the concentrations of H⁺, CO₂ and HCO₃⁻ of ~ 100 %, 200 % and 14 % respectively (Hurd et al., 2009; IPCC, 2014, Hurd et al., 2018). In seaweed beds, ocean acidification is further complicated by the fact that biological activity modifies the carbonate chemistry within the canopy; uptake of CO₂ by the primary producers and release of CO₂ through community respiration results in diel fluctuations in pH and CO₂ (Delille et al., 2009; Hofmann et al., 2011; Cornwall et al., 2013). This variability, which can be up to ~ 1 pH unit in dense seaweed assemblages (Delille et al., 2009; Hofmann et al., 2011; Cornwall et al., 2013), is likely to influence response of species to ocean acidification in coastal systems.

Concurrently with ocean acidification, the average global sea surface temperatures have increased by ~ 1 °C since 1880 and a further increase of ~ 3 °C is projected by the end of the century under the RCP 8.5 scenario (IPCC, 2014). Although ocean warming is a global phenomenon, there is pronounced regional variability with some ‘hotspots’ warming at 3 – 4 times the global average (Hobday and Pecl, 2014). Furthermore, in addition to the gradual increase in temperature, discrete extreme warming events referred to as marine heatwaves are projected to increase in duration and frequency under global ocean change (Oliver et al.,

2017; Oliver et al., 2018a). These events can have substantial impacts on marine communities either as acute increases in local temperatures over short time scales (Wernberg et al., 2016; Rogers-Bennett and Catton, 2019), or elevated temperatures can be sustained over several months, creating physiological stress and increased susceptibility to disease (Oliver et al., 2017). Both warming and acidification in conjunction with marine heatwaves are likely to influence seaweeds in the future with consequences for the species that rely on them. However, predicting how seaweeds will respond is difficult due to different ways in which each stressor may influence the physiology of seaweeds and interactions between them.

Impacts of ocean acidification of seaweeds

The effects of ocean acidification on seaweeds are likely to be varied and dependent on physiological differences between species and broader taxonomic groups. There is substantial evidence that calcified seaweeds will respond negatively to ocean acidification as their calcium carbonate structures are more difficult to maintain under reduced pH (Fabricius et al., 2015; McCoy and Kamenos, 2015; Cornwall et al., 2017a). However, some species are capable to adapting to acidification in a few generations (Cornwall et al., 2020) and elevated pH during daylight due to canopy photosynthesis may provide a refugia for calcified species (Hurd, 2015). As such, assessing how species will respond to near future ocean conditions and incorporating natural fluctuations in pH into experimental treatments will assist in accurately predicting how calcified species will respond in a future ocean.

The response of fleshy (non-calcified) seaweeds to ocean acidification is more complicated than for calcified species, and dependent on inorganic carbon uptake strategies and species-specific sensitivity to reduced pH (Cornwall et al., 2017b; van der Loos et al., 2019).

Seaweeds convert dissolved inorganic carbon (DIC) to organic carbon during photosynthesis via the enzyme RuBisCO (Hurd et al., 2014). However, in seawater, DIC available for

photosynthesis exists as either CO_2 or HCO_3^- , and seaweeds differ in their ability to utilise both forms as an inorganic carbon source. All seaweeds are able to utilise CO_2 , which is taken into the cell via passive diffusion. This uptake process is energetically inexpensive, but only ~ 1 % of DIC in seawater is present as CO_2 (Giordano et al., 2005; Raven et al., 2005). As such, the productivity of species that rely exclusively on CO_2 may be carbon limited under present day CO_2 levels (Hepburn et al., 2011; Raven, 2011; Kübler and Dudgeon, 2015). However, most seaweed species (~ 65 %) have developed mechanisms to utilise HCO_3^- (the most abundant form of DIC in seawater, ~ 90 %) via carbon dioxide concentrating mechanisms (CCMs, Giordano et al. 2005). There is a large range of CCMs, but all function as a mechanism to concentrate CO_2 at the site of RuBisCO, albeit at an energetic cost (Giordano et al., 2005; Raven and Beardall, 2014). The response of species that have a CCM (CCM species) to acidification are likely to be positive if they have CCMs with a low affinity for DIC or can down-regulate the CCM to rely more on diffusive CO_2 , or neutral if they are unable to down-regulate CCM activity (Cornwall et al., 2017b; van der Loos et al., 2019). In contrast, those that rely only on diffusive CO_2 (non-CCM species) will theoretically benefit from acidification due to elevated CO_2 alleviating carbon limitation at today's concentrations (Hepburn et al., 2011; Raven, 2011; Kübler and Dudgeon, 2015). However, experimental studies on the response of CCM species to ocean acidification do not always find benefits arising from CCM down-regulation (Britton et al., 2016; van der Loos et al., 2019) and only a few studies have assessed the response of non-CCM species to elevated CO_2 , with contrasting results (Kübler et al., 1999; Cornwall et al., 2012; van der Loos et al., 2019; Cornwall and Hurd, 2019). This disagreement between the theoretical and observed responses may be due to species-specific sensitivity to elevated $[\text{H}^+]$, which is yet to be investigated in detail but has the potential to impact intracellular pH regulation (Bach et al., 2013; Raven and Smith, 2013; van der Loos et al., 2019).

Fluctuating pH in coastal systems: influences on responses to ocean acidification

Most studies assessing the response of seaweeds to ocean acidification have been based on projections for the open ocean where pH is relatively stable (Hofmann et al., 2011). However, in seaweed beds pH is highly variable and driven by the metabolic activity of the community. During daylight, pH increases due to uptake of CO₂ by seaweeds (and other primary producers) and during the night pH declines due to CO₂ release from community respiration (Delille et al., 2009; Hofmann et al., 2011; Cornwall et al., 2013). This results in diel cycles of pH (and DIC) that can be as large as 1 unit in dense seaweed assemblages (Delille et al., 2009; Hofmann et al., 2011; Cornwall et al., 2013). Studies have shown that seaweed responses to ocean acidification are strongly influenced by fluctuations in pH (Cornwall et al., 2013; Johnson et al., 2014; Britton et al., 2016). However, the effect of fluctuating pH on seaweeds has only been investigated for corallines and two CCM species. Corallines generally respond negatively (Cornwall et al., 2013; Johnson et al., 2014; Roleda et al., 2015), however see (Cornwall et al., 2018; Cornwall et al., 2020) and the two CCM species have contrasting responses: the kelp *Ecklonia radiata* benefited from fluctuations around current pH, yet this was reversed under ocean acidification (Britton et al., 2016), while the opposite pattern was observed in the red seaweed *Gracillaria lemaneiformis*. The effect of fluctuating pH on non-CCM seaweeds is yet to be investigated but these species are likely to be particularly affected as high pH during the day could result in CO₂ limitation, which may be alleviated under ocean acidification. Given that some seaweed communities comprise of up 90 % non-CCM species (Cornwall et al., 2015), research on how these species respond to fluctuations in pH is required.

Impacts of elevated temperature on seaweeds

Temperature determines the rates of all chemical reactions and as such regulates the rates of key metabolic processes such as growth, photosynthesis and respiration (Raven and Geider, 1988; Davison, 1991). The relationship between temperature and metabolic rates in seaweeds can be described by thermal performance curves (Eggert, 2012). Thermal performance curves are bell-shaped where rates increase from cooler to warmer temperatures until a maximum rate is achieved at certain temperature (thermal optimum), after which they rapidly decrease (Eggert, 2012). The local temperature at which a population of seaweeds exists and what this temperature is relative to the thermal optimum of a species will theoretically determine their response to ocean warming and extreme events such as marine heatwaves; as temperature increases, populations that exist below the thermal optimum will benefit and those that exist at or above thermal optimum will be negatively affected. However, thermal performance curves are not well described for most seaweeds and responses to changing temperature will depend on the magnitude of the temperature increase (i.e, whether temperatures are pushed above optimum), interactions with other environmental variables, life-history stage and adaption of populations to local temperature regimes (Machalek et al., 1996; Eggert, 2012; Hurd et al., 2014; Bennett et al., 2015b).

Seaweeds also have the capacity to physiologically adapt to changes in temperature, which may mitigate negative impacts of warming. For example, membrane fluidity increases with increasing temperature (Los and Murata, 2004) and seaweeds may adjust the fatty acid composition of cellular membranes, by increasing chain lengths or saturation state, both of which act to increase the rigidity of membranes (Becker et al., 2010). Alternatively, seaweeds may produce heat shock proteins under high temperatures (Ireland et al., 2004; Eggert, 2012), produce antioxidants to protect against elevated concentrations of reactive oxygen species under thermal stress (Collén et al., 2007; Eggert, 2012) or alter the structure and abundance of enzymes to compensate for temperature induced changes in reaction rates (Eggert et al.,

2003; Hurd et al., 2014). However, all of these processes require energy and whether they mitigate against negative impacts of elevated temperatures will largely depend on whether the benefit of increased physiological performance is greater than the energetic cost.

Interactive effects of global ocean change stressors

Both ocean warming and acidification are occurring concurrently and seaweeds in a future ocean will be affected by both of these stressors, which may have synergistic (Anthony et al., 2008; Martin and Gattuso, 2009; Connell and Russell, 2010; Gaitán-Espitia et al., 2014), antagonistic (Campbell et al., 2016) or independent effects (Al-Janabi et al., 2016a; Rich et al., 2018). Furthermore, the combined stressors of warming and acidification may interact with local environmental conditions such as eutrophication (Al-Janabi et al., 2016b) and, although it is yet to be investigated, marine heatwaves. Experiments investigating how seaweeds will respond to global ocean change will ideally include all relevant environmental changes. However, undertaking multiple stressor laboratory experiments can be logistically challenging and resource intensive (Boyd et al. 2016; Boyd et al. 2018). To deal with this, novel experimental approaches have been developed which focus resources on examining the drivers of interest and making predictions rather than identifying mechanisms (Boyd et al. 2016; Boyd et al. 2018). These methods provide a promising new avenue through which we can improve our understanding of how seaweeds will respond to global ocean change.

Reliance of abalone on seaweeds

Abalone are dominant herbivores in temperate reef systems and form the basis of highly productive fisheries (Cook, 2016; Mundy and Jones, 2016; Rogers-Bennet and Catton, 2019). They rely on seaweeds for all facets of their life cycle to provide habitat, a food source and to provide chemical cues to induce settlement of larvae. Abalone prefer the three-dimensional structure provided by large brown seaweeds to provide the primary habitat and utilise understory seaweeds as both habitat and a food source (Shepherd and Steinberg, 1992;

Steneck et al., 2002; Hurd et al., 2014). Crustose coralline algae (CCA) provide critical chemical cues that induce settlement and metamorphosis of larvae (Daume et al., 1999; Roberts, 2001), while post-larvae feed on the microbial communities present on the surface of CCA crusts (Daume et al., 1997). The reliance of abalone on seaweeds across multiple life stages suggests they will be highly sensitive to any changes in the seaweeds arising from global ocean change. For example, large canopy-forming brown seaweeds are susceptible to warming, acidification and extreme events such as marine heatwaves (Johnson et al., 2011; Britton et al., 2016; Filbee-Dexter et al., 2016; Wernberg et al., 2016; Thomsen et al., 2019), which may result in reduced availability of suitable habitat in a future ocean. Likewise, CCA are highly susceptible to ocean acidification (Kroeker et al., 2013; Fabricius et al., 2015; McCoy and Kamenos, 2015; Cornwall et al., 2017a), which may reduce the availability of suitable settlement substratum or influence the microbial communities that post-larvae feed on.

The availability or quality of food sources may also be altered under global ocean change, through either declines in abundance key understory seaweeds or through changes in their biochemical composition (Duarte et al., 2016; Rogers-Bennet and Catton, 2019; Benthuisen et al., 2020). For example, long-chain ($\geq C_{20}$) PUFA (LC-PUFA) and nitrogen content are considered particularly important for abalone nutrition (McShane et al., 1994; Fleming, 1995; Mai et al., 1996; Nelson et al., 2002), and these may become reduced under global ocean change (Becker et al., 2010; Gosch et al., 2015), with potential implications on abalone productivity. However, there is little information on the nutritional quality of most seaweed species and spatial and seasonal variability in this quality is poorly understood for most regions. Given that abalone are likely to be indirectly affected by global ocean change due to impacts on seaweeds and that these effects are likely to impact multiple life-history stages, understanding how global ocean change will affect seaweeds is necessary if we are to have a chance of mitigating impacts.

Seaweed communities in Tasmania, Australia

The ‘Great Southern Reef’ is a diverse and productive reef system that extends 6000 kms along the temperate Australian coastline (Bennett et al., 2015a). Approximately 1500 species of seaweed are described from this system, which collectively covers an area of ~ 70 000 km² (Waters et al., 2010; Wernberg et al., 2013; Bennett et al., 2015a). The seaweeds and the communities they support have an estimated economic value of AU \$10 billion per year (Bennett et al., 2015a), yet knowledge of them is limited. The southernmost state of Australia, the island of Tasmania, has a particularly diverse seaweed flora that supports valuable fisheries, including the blacklip abalone fishery (*Haliotis rubra*). *H. rubra* is distributed south of Rottnest Island in Western Australia and Coffs Harbour in New South Wales, with the largest populations found in Tasmania, despite temperatures being sub optimal for growth (Shepherd, 1973; Gilroy and Edwards, 1998). The *H. rubra* fishery is the most productive wild caught abalone fishery in the world and accounts for nearly a third of the global wild harvest (28 % in 2015, Cook 2016; Mundy and Jones 2016). Despite the importance of the *H. rubra* fishery in Tasmania, little is known about the seaweeds it relies on and how these seaweeds may respond to global ocean change. Ocean conditions in eastern Tasmania are rapidly changing as a result of global ocean change: the area is an ocean warming hotspot and is warming at 3 – 4 times the global average (Hobday and Pecl, 2014) and significant declines in habitat forming kelps such as *Macrocystis pyrifera* have already occurred (95 % decline since 1980 Johnson et al., 2011). Furthermore, recent marine heatwave events have had substantial impacts on seaweeds and the associated communities (Oliver et al., 2017; Oliver et al., 2018b) and these are projected to increase in the future (Oliver et al., 2018a; Oliver et al., 2018b). These changes, in conjunction with the potential impacts of ocean acidification (which is understudied in Tasmania but see Britton et al., 2016; van der Loos et al., 2019), suggest that seaweed beds in Tasmania may be substantially impacted in a future ocean. As such, understanding which species will be affected and how the effects will manifest is key to understanding how species such as *H. rubra* will be indirectly affected by global ocean change.

Thesis structure

The primary aim of this thesis was to assess how global ocean change (warming, acidification and marine heatwaves) will impact seaweed species that are key to the life cycle of *H. rubra*. Seaweed species examined were those that provide habitat, a food source, or a settlement substratum for *H. rubra*. Species were chosen based on prior studies from the region and a field survey conducted examining the spatial and seasonal variation in the abundance and nutritional quality of seaweeds in eastern Tasmania (Chapter 2). Manipulative laboratory experiments were undertaken that examined the response of selected seaweeds to ocean acidification, warming or marine heatwaves (Chapters 3, 4 and 5). Responses of seaweeds to global ocean change are interpreted in the context of how they may indirectly affect *H. rubra* in the general discussion (Chapter 6).

Chapter 2: Seasonal and site-specific variation in the nutritional quality of temperate seaweed assemblages: implications for grazing invertebrates and the commercial exploitation of seaweeds.

There is little information on the nutritional quality of seaweeds in Tasmania and even less on how this quality varies spatially and seasonally. Given that changes in nutritional quality are likely to have substantial impacts on abalone populations, establishing a baseline of the nutritional quality of seaweed assemblages and how this varies between sites and seasons is essential for interpreting how changes in a future ocean may impact abalone productivity. This chapter investigated seasonal variability in biomass and species composition of fleshy understory seaweeds in three sites in eastern Tasmania (1 northern and 2 southern sites). Fatty acid profiles and nitrogen content of the abundant species at each site in each season were analysed to provide information on the nutritional quality of the seaweed assemblages at each site.

Chapter 3: Responses of seaweeds that use CO₂ as their sole inorganic carbon source to ocean acidification: differential effects of fluctuating pH but little benefit of CO₂ enrichment.

pH in seaweed beds fluctuates on diel cycles and is driven by the metabolic activity of the community. Studies have shown that fluctuations in pH can influence the response of coralline algae and CCM seaweeds to ocean acidification, however none have assessed the response of non-CCM species. To fill this knowledge gap, a manipulative laboratory experiment was conducted in which two ecologically dominant non-CCM red seaweeds (*Callophyllis lambertii* and *Plocamium dilatatum*) were exposed to both fluctuating and static pH at the mean pH of today (~ 8.0) and that projected under ocean acidification (~ 7.7). Results from this experiment were used to inform whether pH fluctuations were included as part of experimental treatments in subsequent experiments.

Chapter 4: Adjustments in fatty acid composition is a mechanism that can explain resilience to marine heatwaves and future ocean conditions in the habitat-forming seaweed *Phyllospora comosa* (Labillardière) C.Agardh.

The seaweed *Phyllospora comosa* the primary habitat-forming seaweed for *H. rubra*. To determine how *P. comosa* may respond to the combined stressors of warming, acidification and marine heatwaves a laboratory experiment was conducted in which *P. comosa* was exposed to marine heatwaves superimposed on current and future ocean conditions. Fatty acid profiles were determined to identify if adjustments of fatty acid composition could provide a mechanism of tolerance to global ocean change.

Chapter 5: Crustose coralline algae are sensitive to near-future global ocean change scenarios.

The final data chapter examined the response of CCA assemblages known to induce settlement of *H. rubra* larvae to combined warming and acidification in a laboratory experiment. CCA assemblages were developed on settlement plates deployed in the field for 1.5 years. These assemblages were then exposed to multiple levels of future ocean conditions in a novel scenario based approach that simulated the different emissions scenarios projected by the IPCC.

Chapter 6: General Discussion

This chapter briefly summarises the main findings of the thesis and then discusses these results in the context of the implications for *H. rubra* populations. The main mechanisms through which *H. rubra* may be impacted by the responses of the seaweeds are discussed for each life stage. Critical areas of future research that build on the work presented here are identified and discussed in the context of how *H. rubra* populations may be affected by global ocean change.

References

- Al-Janabi, B., Kruse, I., Graiff, A., Karsten, U., and Wahl, M. 2016a. Genotypic variation influences tolerance to warming and acidification of early life-stage *Fucus vesiculosus* L. (Phaeophyceae) in a seasonally fluctuating environment. *Marine Biology*, 163 (14).
- Al-Janabi, B., Kruse, I., Graiff, A., Winde, V., Lenz, M., and Wahl, M. 2016b. Buffering and amplifying interactions among OAW (Ocean Acidification & Warming) and nutrient enrichment on early life-stage *Fucus vesiculosus* L. (Phaeophyceae) and their carry over effects to hypoxia impact. *PLoS ONE*, 11: e0152948-e0152948.
- Anthony, K. R. N., Kline, D. I., Diaz-Pulido, G., Dove, S., and Hoegh-Guldberg, O. 2008. Ocean acidification causes bleaching and productivity loss in coral reef builders. *Proceedings of the National Academy of Sciences*, 105 (45): 17442-17446.

- Bach, L. T., Mackinder, L. C. M., Schulz, K. G., Wheeler, G., Schroeder, D. C., Brownlee, C., and Riebesell, U. 2013. Dissecting the impact of CO₂ and pH on the mechanisms of photosynthesis and calcification in the coccolithophore *Emiliania huxleyi*. *New Phytologist*, 199: 121-134.
- Becker, S., Graeve, M., and Bischof, K. 2010. Photosynthesis and lipid composition of the Antarctic endemic rhodophyte *Palmaria decipiens*: effects of changing light and temperature levels. *Polar Biology*, 33: 945-955.
- Bennett, S., Wernberg, T., Connell, S. D., Hobday, A. J., Johnson, C. R., and Poloczanska, E. S. 2015a. The 'Great Southern Reef': social, ecological and economic value of Australia's neglected kelp forests. *Marine and Freshwater Research*, 67: 47-56.
- Bennett, S., Wernberg, T., Joy, B. A., De Bettignies, T., and Campbell, A. H. 2015b. Central and rear-edge populations can be equally vulnerable to warming. *Nature Communications*, 6.
- Benthuisen, J. A., Oliver, E. C. J., Chen, K., and Wernberg, T. 2020. Editorial: advances in understanding marine heatwaves and their impacts. *Frontiers in Marine Science*, 7 (147).
- Boyd, P. W., Collins, S., Dupont, S., Fabricius, K., Gattuso, J.-P., Havenhand, J., . . . Pörtner, H.-O. (2018). Experimental strategies to assess the biological ramifications of multiple drivers of global ocean change—A review. *Global Change Biology*, 24(6), 2239-2261. doi:10.1111/gcb.14102
- Britton, D., Cornwall, C. E., Revill, A. T., Hurd, C. L., and Johnson, C. R. 2016. Ocean acidification reverses the positive effects of seawater pH fluctuations on growth and photosynthesis of the habitat-forming kelp, *Ecklonia radiata*. *Scientific Reports*, 6: 26036.
- Campbell, J. E., Fisch, J., Langdon, C., and Paul, V. J. 2016. Increased temperature mitigates the effects of ocean acidification in calcified green algae (*Halimeda spp.*). *Coral Reefs*, 35: 357-368.
- Collén, J., Guisle-Marsollier, I., Léger, J. J., and Boyen, C. 2007. Response of the transcriptome of the intertidal red seaweed *Chondrus crispus* to controlled and natural stresses. *New Phytologist*, 176: 45-55.
- Connell, S. D., and Russell, B. D. 2010. The direct effects of increasing CO₂ and temperature on non-calcifying organisms: increasing the potential for phase shifts in kelp forests. *Proceedings of the Royal Society B: Biological Sciences*, 277: 1409-1415.
- Cook, P. 2016. Recent trends in worldwide abalone production. *Journal of Shellfish Research*, 35: 581-583.
- Cornwall, C. E., Comeau, S., DeCarlo, T. M., Larcombe, E., Moore, B., Giltrow, K., Puerzer, F., et al. 2020. A coralline alga gains tolerance to ocean acidification over multiple generations of exposure. *Nature Climate Change*. 10:143–146. <https://doi.org/10.1038/s41558-019-0681-8>
- Cornwall, C. E., Comeau, S., DeCarlo, T. M., Moore, B., D'Alexis, Q., and McCulloch, M. T. 2018. Resistance of corals and coralline algae to ocean acidification: physiological control of calcification under natural pH variability. *Proceedings of the Royal Society B: Biological Sciences*, 285: 20181168.

Cornwall, C. E., Comeau, S., and McCulloch, M. T. 2017a. Coralline algae elevate pH at the site of calcification under ocean acidification. *Global Change Biology*, 23: 4245-4256.

Cornwall, C. E., Hepburn, C. D., Pritchard, D., Currie, K. I., McGraw, C. M., Hunter, K. A., and Hurd, C. L. 2012. Carbon-use strategies in macroalgae: differential responses to lowered pH and implications for ocean acidification. *Journal of Phycology*, 48: 137-144.

Cornwall, C. E., and Hurd, C. L. 2019. Variability in the benefits of ocean acidification to photosynthetic rates of macroalgae without CO₂-concentrating mechanisms. *Marine and Freshwater Research*, 71: 275-280.

Cornwall, C. E., Hepburn, C. D., McGraw, C. M., Currie, K. I., Pilditch, C. A., Hunter, K. A., Boyd, P. W., et al. 2013. Diurnal fluctuations in seawater pH influence the response of a calcifying macroalga to ocean acidification. *Proceedings of the Royal Society B: Biological Sciences*, 280: 20132201.

Cornwall, C. E., Revill, A. T., Hall-Spencer, J. M., Milazzo, M., Raven, J. A., and Hurd, C. L. 2017b. Inorganic carbon physiology underpins macroalgal responses to elevated CO₂. *Scientific Reports*, 7: 46297.

Cornwall, C. E., Revill, A. T., and Hurd, C. L. 2015. High prevalence of diffusive uptake of CO₂ by macroalgae in a temperate subtidal ecosystem. *Photosynthesis Research*, 124: 181-190.

Daume, S., Brand-Gardner, S., and Woelkerling, W. J. 1999. Preferential settlement of abalone larvae: diatom films vs. non-geniculate coralline red algae. *Aquaculture*, 174: 243-254.

Daume, S., Brand, S., and Woelkerling, J. 1997. Effects of post-larval abalone (*Haliotis rubra*) grazing on the epiphytic diatom assemblage of coralline red algae. *Molluscan Research*, 18: 119-130.

Davison, I. R. 1991. Environmental effects on algal photosynthesis: temperature. *Journal of Phycology*, 27: 2-8.

Delille, B., Borges, A. V., and Delille, D. 2009. Influence of giant kelp beds (*Macrocystis pyrifera*) on diel cycles of pCO₂ and DIC in the Sub-Antarctic coastal area. *Estuarine, Coastal and Shelf Science*, 81: 114-122.

Doney, S. C., Fabry, V. J., Feely, R. A., and Kleypas, J. A. 2009. Ocean acidification: the other CO₂ problem. *Annual Review of Marine Science*, 1: 169-192.

Duarte, C., López, J., Benítez, S., Manríquez, P. H., Navarro, J. M., Bonta, C. C., Torres, R., et al. 2016. Ocean acidification induces changes in algal palatability and herbivore feeding behavior and performance. *Oecologia*, 180: 453-462.

Eckman, J. E., Duggins, D. O., and Sewell, A. T. 1989. Ecology of under story kelp environments. I. Effects of kelps on flow and particle transport near the bottom. *Journal of Experimental Marine Biology and Ecology*, 129: 173-187.

- Eggert, A. 2012. Seaweed Responses to Temperature. *In* Seaweed Biology: Novel Insights into Ecophysiology, Ecology and Utilization, pp. 47-66. Ed. by C. Wiencke, and K. Bischof. Springer Berlin Heidelberg, Berlin, Heidelberg.
- Eggert, A., Burger, E. M., and Breeman, A. M. 2003. Ecotypic differentiation in thermal traits in the tropical to warm-temperate green macrophyte *Valonia utricularis*. *In* Botanica Marina, p. 69.
- Fabricius, K. E., Klumbenschiedl, A., Harrington, L., Noonan, S., and De'Ath, G. 2015. *In situ* changes of tropical crustose coralline algae along carbon dioxide gradients. Scientific Reports, 5.
- Feely, R. A., Sabine, C. L., Lee, K., Berelson, W., Kleypas, J., Fabry, V. J., and Millero, F. J. 2004. Impact of anthropogenic CO₂ on the CaCO₃ system in the oceans. Science, 305: 362-366.
- Filbee-Dexter, K., Feehan, C. J., and Scheibling, R. E. 2016. Large-scale degradation of a kelp ecosystem in an ocean warming hotspot. Marine Ecology Progress Series, 543: 141-152.
- Filbee-Dexter, K., and Wernberg, T. 2018. Rise of Turfs: a new battlefront for globally declining kelp forests. BioScience, 68: 64-76.
- Fleming, A. E. 1995. Digestive efficiency of the Australian abalone *Haliotis rubra* in relation to growth and feed preference. Aquaculture, 134: 279-293.
- Gaitán-Espitia, J. D., Hancock, J. R., Padilla-Gamiño, J. L., Rivest, E. B., Blanchette, C. A., Reed, D. C., and Hofmann, G. E. 2014. Interactive effects of elevated temperature and pCO₂ on early-life-history stages of the giant kelp *Macrocystis pyrifera*. Journal of Experimental Marine Biology and Ecology, 457: 51-58.
- Gilroy, A. and S.J. Edwards, Optimum temperature for growth of Australian abalone: Preferred temperature and critical thermal maximum for blacklip abalone, *Haliotis rubra* (Leach), and greenlip abalone, *Haliotis laevis* (Leach). Aquaculture Research, 1998. 29(7): p. 481-485.
- Giordano, M., Beardall, J., and Raven, J. A. 2005. CO₂ concentrating mechanisms in algae: Mechanisms, environmental modulation, and evolution. Annual Review of Plant Biology, 56: 99-131.
- Gosch, B. J., Paul, N. A., de Nys, R., and Magnusson, M. 2015. Spatial, seasonal, and within-plant variation in total fatty acid content and composition in the brown seaweeds *Dictyota bartayresii* and *Dictyopteris australis* (Dictyotales, Phaeophyceae). Journal of Applied Phycology, 27: 1607-1622.
- Hepburn, C. D., Pritchard, D. W., Cornwall, C. E., McLeod, R. J., Beardall, J., Raven, J. A., and Hurd, C. L. 2011. Diversity of carbon use strategies in a kelp forest community: Implications for a high CO₂ ocean. Global Change Biology, 17: 2488-2497.
- Heyward, A. J., and Negri, A. P. 1999. Natural inducers for coral larval metamorphosis. Coral Reefs, 18: 273-279.

Hobday, A. J., and Pecl, G. T. 2014. Identification of global marine hotspots: sentinels for change and vanguards for adaptation action. *Reviews in Fish Biology and Fisheries*, 24: 415-425.

Hofmann, G. E., Smith, J. E., Johnson, K. S., Send, U., Levin, L. A., Micheli, F., Paytan, A., et al. 2011. High-frequency dynamics of ocean pH: a multi-ecosystem comparison. *PLoS ONE*, 6: e28983.

Hurd, C. L. 2015. Slow-flow habitats as refugia for coastal calcifiers from ocean acidification. *Journal of Phycology*, 51: 599-605.

Hurd, C. L., Harrison, P. J., Bischof, K., and Lobban, C. S. 2014. *Seaweed ecology and physiology*, Cambridge University Press, Cambridge.

Hurd, C. L., Hepburn, C. D., Currie, K. I., Raven, J. A., and Hunter, K. A. 2009. Testing the effects of ocean acidification on algal metabolism: Considerations for experimental designs. *Journal of Phycology*, 45: 1236-1251.

Hurd, C. L., Lenton, A., Tilbrook, B., & Boyd, P. W. (2018). Current understanding and challenges for oceans in a higher-CO₂ world. *Nature Climate Change*, 8: 686-694. doi:10.1038/s41558-018-0211-0

IPCC. 2014. *Climate Change 2014: Synthesis Report. Contribution of Working Groups I, II and III to the Fifth Assessment Report of the Intergovernmental Panel on Climate Change* [Core Writing Team, R.K. Pachauri and L.A. Meyer (eds.)]. IPCC, Geneva, Switzerland. 151 pp.

Ireland, H. E., Harding, S. J., Bonwick, G. A., Jones, M., Smith, C. J., and Williams, J. H. H. 2004. Evaluation of heat shock protein 70 as a biomarker of environmental stress in *Fucus serratus* and *Lemna minor*. *Biomarkers*, 9: 139-155.

Johnson, C. R., Banks, S. C., Barrett, N. S., Cazassus, F., Dunstan, P. K., Edgar, G. J., Frusher, S. D., et al. 2011. Climate change cascades: shifts in oceanography, species' ranges and subtidal marine community dynamics in eastern Tasmania. *Journal of Experimental Marine Biology and Ecology*, 400: 17-32.

Johnson, M. D., Moriarty, V. W., and Carpenter, R. C. 2014. Acclimatization of the crustose coralline alga *Porolithon onkodes* to variable pCO₂. *PLoS ONE*, 9: e87678.

Kennelly, S. J. 1989. Effects of kelp canopies on understory species due to shade and scour. *Marine ecology progress series*. Oldendorf, 50: 215-224.

Kroeker, K. J., Kordas, R. L., Crim, R., Hendriks, I. E., Ramajo, L., Singh, G. S., Duarte, C. M., et al. 2013. Impacts of ocean acidification on marine organisms: quantifying sensitivities and interaction with warming. *Global Change Biology*, 19: 1884-1896.

Krumhansl, K. A., Okamoto, D. K., Rassweiler, A., Novak, M., Bolton, J. J., Cavanaugh, K. C., Connell, S. D., et al. 2016. Global patterns of kelp forest change over the past half-century. *Proceedings of the National Academy of Sciences*, 113: 13785.

Kübler, J. E., and Dudgeon, S. R. 2015. Predicting effects of ocean acidification and warming on algae lacking carbon concentrating mechanisms. *PLoS ONE*, 10: e0132806.

Kübler, J. E., Johnston, A. M., and Raven, J. A. 1999. The effects of reduced and elevated CO₂ and O₂ on the seaweed *Lomentaria articulata*. *Plant, Cell and Environment*, 22: 1303-1310.

Layton, C., Shelamoff, V., Cameron, M. J., Tatsumi, M., Wright, J. T., and Johnson, C. R. 2019. Resilience and stability of kelp forests: the importance of patch dynamics and environment-engineer feedbacks. *PLoS ONE*, 14: e0210220.

Ling, S. D., Johnson, C. R., Frusher, S. D., and Ridgway, K. R. 2009. Overfishing reduces resilience of kelp beds to climate-driven catastrophic phase shift. *Proceedings of the National Academy of Sciences of the United States of America*, 106: 22341-22345.

Los, D. A., and Murata, N. 2004. Membrane fluidity and its roles in the perception of environmental signals. *Biochimica et Biophysica Acta (BBA) - Biomembranes*, 1666: 142-157.

Machalek, K. M., Davison, I. R., and Falkowski, P. G. 1996. Thermal acclimation and photoacclimation of photosynthesis in the brown alga *Laminaria saccharina*. *Plant, Cell & Environment*, 19: 1005-1016.

Mai, K., Mercer, J. P., and Donlon, J. 1996. Comparative studies on the nutrition of two species of abalone, *Haliotis tuberculata* L. and *Haliotis discus hannai* Ino. V. The role of polyunsaturated fatty acids of macroalgae in abalone nutrition. *Aquaculture*, 139: 77-89.

Chapter 2. Martin, S., and Gattuso, J. P. 2009. Response of Mediterranean coralline algae to ocean acidification and elevated temperature. *Global Change Biology*, 15: 2089-2100.

McCoy, S. J., and Kamenos, N. A. 2015. Coralline algae (Rhodophyta) in a changing world: Integrating ecological, physiological, and geochemical responses to global change. *Journal of Phycology*, 51: 6-24.

McShane, P. E., Gorfine, H. K., and Knuckey, I. A. 1994. Factors influencing food selection in the abalone *Haliotis rubra* (Mollusca: Gastropoda). *Journal of Experimental Marine Biology and Ecology*, 176: 27-37.

Mineur, F., Arenas, F., Assis, J., Davies, A. J., Engelen, A. H., Fernandes, F., Malta, E. J., et al. 2015. European seaweeds under pressure: consequences for communities and ecosystem functioning. *Journal of Sea Research*, 98: 91-108.

Nelson, M. M., Leighton, D. L., Phleger, C. F., and Nichols, P. D. 2002. Comparison of growth and lipid composition in the green abalone, *Haliotis fulgens*, provided specific macroalgal diets. *Comp Biochem Physiol B Biochem Mol Biol*, 131: 695-712.

Oliver, E. C. J., Benthuyssen, J. A., Bindoff, N. L., Hobday, A. J., Holbrook, N. J., Mundy, C. N., and Perkins-Kirkpatrick, S. E. 2017. The unprecedented 2015/16 Tasman Sea marine heatwave. *Nature Communications*, 8: 16101.

Oliver, E. C. J., Donat, M. G., Burrows, M. T., Moore, P. J., Smale, D. A., Alexander, L. V., Benthuyssen, J. A., et al. 2018a. Longer and more frequent marine heatwaves over the past century. *Nature Communications*, 9: 1324.

- Oliver, E. C. J., Lago, V., Hobday, A. J., Holbrook, N. J., Ling, S. D., and Mundy, C. N. 2018b. Marine heatwaves off eastern Tasmania: trends, interannual variability, and predictability. *Progress in Oceanography*, 161: 116-130.
- Pearce, C. M., and Scheibling, R. E. 1991. Effect of macroalgae, microbial films, and conspecifics on the induction of metamorphosis of the green sea urchin *Strongylocentrotus droebachiensis* (Müller). *Journal of Experimental Marine Biology and Ecology*, 147: 147-162.
- Qu, L., Xu, J., Sun, J., Li, X., and Gao, K. 2017. Diurnal pH fluctuations of seawater influence the responses of an economic red macroalga *Gracilaria lemaneiformis* to future CO₂-induced seawater acidification. *Aquaculture*, 473: 383-388.
- Raven, J., and Smith, F. 2013. The regulation of intracellular pH as a fundamental biological process. *Ion Transport in Plants*, Academic Press Inc. London: 271-278.
- Raven, J. A. 2011. Effects on marine algae of changed seawater chemistry with increasing atmospheric CO₂. *Biology and Environment*, 111: 1-17.
- Raven, J. A., Ball, L. A., Beardall, J., Giordano, M., and Maberly, S. C. 2005. Algae lacking carbon-concentrating mechanisms. *Canadian Journal of Botany*, 83: 879-890.
- Raven, J. A., and Beardall, J. 2014. CO₂ concentrating mechanisms and environmental change. *Aquatic Botany*, 118: 24-37.
- Raven, J. A., and Geider, R. J. 1988. Temperature and algal growth. *New Phytologist*, 110: 441-461.
- Rich, W. A., Schubert, N., Schläpfer, N., Carvalho, V. F., Horta, A. C. L., and Horta, P. A. 2018. Physiological and biochemical responses of a coralline alga and a sea urchin to climate change: implications for herbivory.
- Roberts, R. 2001. A review of settlement cues for larval abalone (*Haliotis spp.*). *Journal of Shellfish Research*, 20: 571-586.
- Rogers-Bennett, L., & Catton, C. A. (2019). Marine heat wave and multiple stressors tip bull kelp forest to sea urchin barrens. *Scientific Reports*, 9(1), 15050. doi:10.1038/s41598-019-51114-y
- Roleda, M. Y., Cornwall, C. E., Feng, Y., McGraw, C. M., Smith, A. M., and Hurd, C. L. 2015. Effect of ocean acidification and pH fluctuations on the growth and development of coralline algal recruits, and an associated benthic algal assemblage. *PLoS ONE*, 10.
- Shepherd, S.A., Studies on southern Australian abalone (Genus *Haliotis*). i. Ecology of five sympatric species. *Marine and Freshwater Research*, 1973. 24(3): p. 217-258.
- Shepherd, S., and Steinberg, P. D. 1992. Abalone of the World: Biology, Fisheries and Culture. Food preferences of three Australian abalone species with a review of the algal food of abalone, Wiley Blackwell, New Jersey: 169-181.

Steneck, R. S., Graham, M. H., Bourque, B. J., Corbett, D., Erlandson, J. M., Estes, J. A., and Tegner, M. J. 2002. Kelp forest ecosystems: biodiversity, stability, resilience and future. *Environmental Conservation*, 29: 436-459.

Teagle, H., Moore, P. J., Jenkins, H., & Smale, D. A. (2018). Spatial variability in the diversity and structure of faunal assemblages associated with kelp holdfasts (*Laminaria hyperborea*) in the northeast Atlantic. *PLoS ONE*, 13(7), e0200411. doi:10.1371/journal.pone.0200411

Thomsen, M. S., Mondardini, L., Alestra, T., Gerrity, S., Tait, L., South, P. M., Lilley, S. A., et al. 2019. Local Extinction of bull kelp (*Durvillaea spp.*) due to a marine heatwave. *Frontiers in Marine Science*, 6: 84.

van der Loos, L. M., Schmid, M., Leal, P. P., McGraw, C. M., Britton, D., Revill, A. T., Virtue, P., et al. 2019. Responses of macroalgae to CO₂ enrichment cannot be inferred solely from their inorganic carbon uptake strategy. *Ecology and Evolution*, 9: 125-140.

Waters, J. M., Wernberg, T., Connell, S. D., Thomsen, M. S., Zuccarello, G. C., Kraft, G. T., Sanderson, J. C., et al. 2010. Australia's marine biogeography revisited: back to the future? *Austral Ecology*, 35: 988-992.

Wernberg, T., Bennett, S., Babcock, R. C., De Bettignies, T., Cure, K., Depczynski, M., Dufois, F., et al. 2016. Climate-driven regime shift of a temperate marine ecosystem. *Science*, 353: 169-172.

Wernberg, T., Thomsen, M. S., Connell, S. D., Russell, B. D., Waters, J. M., Zuccarello, G. C., Kraft, G. T., et al. 2013. The footprint of continental-scale ocean currents on the biogeography of seaweeds. *PLoS ONE*, 8: e80168.

Chapter 2. Seasonal and site-specific variation in the nutritional quality of temperate seaweed assemblages: implications for grazing invertebrates and the commercial exploitation of seaweeds.

Damon Britton, Matthias Schmid, Andrew T. Revill, Patti Virtue, Peter D. Nichols, Catriona L. Hurd, Craig N. Mundy

A version of this chapter has been published as Britton, D., Schmid, M., Revill, A.T., Virtue, P., Nichols, P.D., Hurd, C.L., & Mundy, C.N. (2020). Seasonal and site-specific variation in the nutritional quality of temperate seaweed assemblages: implications for grazing invertebrates and the commercial exploitation of seaweeds. *Journal of Applied Phycology*. <https://doi.org/10.1007/s10811-020-02302-1>

Abstract

In coastal ecosystems, seaweeds provide habitat and a food source for a variety of species including herbivores of commercial importance. In these systems seaweeds are the ultimate source of energy with any changes in the seaweeds invariably affecting species of higher trophic levels. Seaweeds are rich sources of nutritionally important compounds such as polyunsaturated fatty acids (PUFA) and are particularly rich in long-chain ($\geq C_{20}$) PUFA (LC-PUFA). In southern Australia, the ‘Great Southern Reef’ has one of the most diverse assemblages of seaweeds in the world, which support highly productive fisheries and have been recognised as a promising resource of omega-3 LC-PUFA. Despite this, there is little information on the biochemical composition of most species and how it varies between sites and seasons. To address this knowledge gap, we undertook a survey to assess seasonal variability in the nutritional quality (fatty acids and nitrogen content) of abundant understory seaweeds across three sites in eastern Tasmania. The nutritional quality of the seaweed assemblages differed between sites and was primarily driven by differences in the biomass

and the biochemical composition of the nutritious red seaweeds at each site. This variability may have implications for regional differences in the productivity of grazing invertebrates. At the species level, seasonal changes in fatty acid composition were highly variable between species and sites, indicating that multiple environmental drivers influence fatty acid composition of seaweeds in this system. This finding suggests that commercial harvest of seaweeds from eastern Tasmania will need to consider species and site-specific variability in fatty acid composition.

Introduction

Seaweed beds are diverse and productive communities that provide essential services (Hurd et al., 2014; Steneck et al., 2002): they form habitat for numerous species (Hurd et al., 2014), release chemical cues that induce invertebrate larval settlement (Roberts 2001; Roberts et al., 2010), play important roles in nutrient cycling (Hurd et al., 2014) and provide a food source for herbivores (Hurd et al., 2014; Steneck et al., 2002). Within rocky reef ecosystems, seaweeds underpin the entire food web, are the ultimate source of energy for higher trophic levels, and support highly productive fisheries (Hurd et al., 2014; Steneck et al., 2002). In addition to their ecological importance, seaweeds are becoming increasingly recognised for their commercial value (Schmid et al., 2018; Wells et al., 2017). They are highly nutritious and, as a result, demand for seaweeds as functional foods or nutraceuticals is increasing worldwide (Wells et al., 2017). Seaweeds are also being suggested as alternatives to the use of fish in feedstock applications, in part to combat the overreliance on depleted wild fish stocks (Gosch et al., 2012). Despite their ecological and commercial importance, there is little known about the biochemical composition of most species, particularly in terms of nutritionally important compounds such as fatty acids. Furthermore, knowledge on the seasonal variability in biochemical composition is lacking for most regions (Gosch et al., 2015b; Schmid et al., 2014, 2017a).

Two important indicators of nutritional quality in seaweeds are polyunsaturated fatty acids (PUFA), particularly long-chain ($\geq C_{20}$) PUFA (LC-PUFA) and overall tissue nitrogen content (Falkenberg et al., 2013; Gosch et al., 2015b; Poore et al., 2013; Schmid et al., 2018; Wells et al., 2017). LC-PUFA are particularly important for animal nutrition as they provide an important energy source and comprise the structural components of the lipid bi-layer in cellular membranes. Most animals, including humans, are unable to synthesise LC-PUFA *de novo* or can obtain them more efficiently through their diet (Galloway et al., 2012; Wells et al., 2017). Seaweeds have particularly high proportions of LC-PUFA in the omega-3 and

omega-6 classes (Galloway et al., 2012; Schmid et al., 2018). These LC-PUFA are considered particularly beneficial; they have health promoting properties such as disease prevention in humans (Cottin et al., 2011) and are positively correlated with elevated growth rates in marine grazers (Mai et al., 1996; Nelson et al., 2002a). Nitrogen is an essential component of amino acids, which form the building blocks of proteins. As such, % tissue nitrogen is often used as a proxy for protein content (Angell et al., 2016). Species containing high levels of nitrogen are considered to be particularly nutritious and high nitrogen content is known to promote growth in grazers (Fleming 1995a; McShane et al., 1994).

Abiotic conditions in the marine environment are highly variable. This affects the physiological performance (e.g. growth and reproduction) of seaweeds (Hurd et al., 2014), species composition within communities (Goldberg 2005; Wernberg and Goldberg 2008), and their biochemical composition (Nelson et al., 2002b; Schmid et al., 2014; Venkatesalu et al., 2012). For example, temperature is known to influence fatty acid composition in seaweeds due to its effects on membrane fluidity (Los and Murata 2004). Membrane fluidity increases with increasing temperature and seaweeds maintain optimum fluidity by reducing the proportion of PUFA relative to saturated fatty acids (SFA) or by elongation of fatty acid chain length (Los and Murata 2004). A pattern of a decrease in PUFA in the summer followed by an increase throughout winter has been observed in the field (Schmid et al., 2017a) and laboratory studies have shown decreases in PUFA and increases in SFA with elevated temperatures (Al-Hasan et al., 1991; Britton et al., 2020; Schmid et al., *in review*). However, this pattern is not ubiquitous as variation in other factors including light (Hotimchenko 2002; Khotimchenko and Yakovleva 2005), salinity (Floreto et al., 1993; Floreto and Teshima 1998; Kumar et al., 2010) and nutrient concentrations (Floreto et al., 1993; Gómez Pinchetti et al., 1998; Gordillo et al., 2001; Kumari et al., 2013) all affect fatty acid composition. Nitrogen content in seaweeds is also influenced by abiotic conditions. Nitrogen is the major limiting nutrient for seaweed growth and reproduction (Hurd et al.,

2014), and higher seawater inorganic nitrogen concentrations typically lead to higher internal nitrogen levels (Brown et al., 1997). However, factors such as light and temperature also influence nitrogen content in seaweeds, meaning that high concentrations of dissolved nitrogen in seawater is not always reflected in the nitrogen content of seaweed tissue (Hurd et al., 2014). The influence of abiotic factors on the biochemical composition of seaweeds has important ecological considerations: the nutritional quality of seaweeds will likely fluctuate seasonally or spatially, with flow on effects to secondary productivity by grazers. These fluctuations will also affect commercial ventures as optimal harvest times of seaweeds will vary with ongoing implications for food and aquaculture applications. As such, baseline knowledge of seasonal and spatial variation in biochemical composition of seaweeds is fundamental to understanding how they support secondary productivity in shallow reef systems, and how they may be commercially exploited in the future.

The Great Southern Reef, which spans 6000 kms of the temperate coastline of Australia is comprised of one of the most diverse seaweed assemblages in the world (Bennett et al., 2015; Waters et al., 2010; Wernberg et al., 2013). Approximately 1500 described species of seaweed occupy a reef area of approximately 70 000 km² (Bennett et al., 2015; Waters et al., 2010; Wernberg et al., 2013). The diverse seaweed assemblage and the coastal food webs they underpin have an estimated economic value of AU\$10 billion per year (Bennett et al., 2015). Despite this diversity and economic importance, knowledge of seaweeds in this system is limited (Bennett et al., 2015). The southernmost state of Australia, the island of Tasmania, has a particularly diverse seaweed assemblage that supports valuable fisheries including the blacklip abalone (*Haliotis rubra*) fishery which is the most productive wild caught abalone fishery in the world (28% of global wild harvest in 2015 – Cook 2016; Mundy and Jones 2016). The *H. rubra* fishery has substantial regional variability in productivity with the highest catch rates occurring in the southern region of the state (Mundy and McAllister 2019). This high productivity, at the southern distributional margin of *H.*

rubra, occurs despite temperatures being sub-optimal for growth in this species (Gilroy and Edwards 1998). Reasons for this are unclear but may be driven by differences in the nutritional quality and availability of the seaweeds in each region. However, this is yet to be investigated. Seaweeds in Tasmania have been identified as a promising source of PUFA and LC-PUFA (Schmid et al., 2018) and are likely to be valuable resources for functional foods, nutraceuticals and in feed and aquaculture operations. However, there is little information on how they vary seasonally, and whether any seasonality is consistent across species and locations. As such, the aim of this study was to describe the seasonal variability in the nutritional quality of abundant understory red and brown seaweeds on shallow subtidal reef systems at three sites spanning the east coast of Tasmania. Observed patterns are discussed in the context of the implications for commercial harvest of seaweeds and abalone ecology.

Methods

Seasonal sampling for biomass and species composition

Sampling was undertaken at three sites that spanned the east coast of Tasmania, Australia. Site 1 (Bicheno, -41.870240° S, 148.303234° E) was located on the mid-east coast, site 2 (Coal Point, 43.335287° S, 147.324707° E) was located off the east coast of Bruny Island in south-eastern Tasmania, and site 3 (Mouldy Hole, 43.595252° S, 146.922055° E) was located on the southern coast (Figure 2.1). All three sites were representative of the typical seaweed beds in these areas. Estimates of understory biomass and composition were undertaken at all three sites at the end of each season (specific dates of each sampling can be seen in Appendix 2.1). The understory was defined as seaweeds that were < 50 cm high. Biomass and species composition were estimated by divers on SCUBA who destructively sampled all seaweed species less than 50 cm high in eight 0.25 m² quadrats placed haphazardly along a 20 m transect at 7 m depth. Samples from each quadrat were placed in mesh bags and transported to the laboratory where they were frozen at – 20 °C until later sorting. Due to difficulties in

collecting all individuals < 2 cm high, and the fact that these individuals contributed only a small percentage of the overall biomass, they were excluded from the biomass estimates. Heavily calcified coralline species were excluded from the estimates as they were unlikely to form major components of abalone diets, however the lightly calcified *Peyssonnelia novaehollandiae* was included. To provide a description of the overstory canopy the density of each species > 50 cm high was estimated by counting the number of individuals in each of the eight quadrats. Daily sea surface temperatures (SST) spanning the duration of the study at each site were sourced from the NOAA Daily SST database (Banzon et al., 2016).

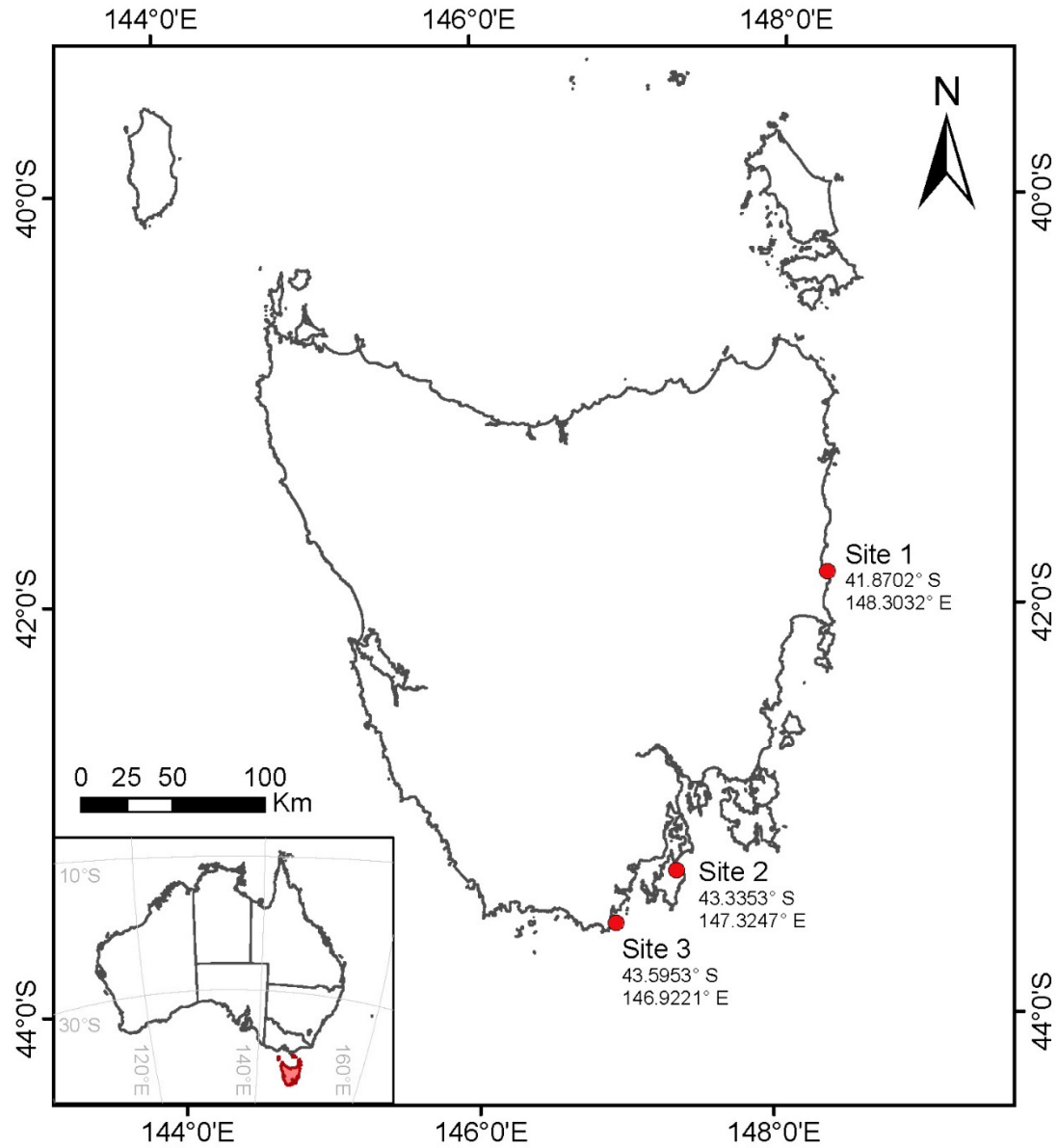


Figure 2.1: Map of Tasmania, Australia showing the location of the three sites in eastern Tasmania. Inset shows the location of Tasmania (red outline) in relation to mainland Australia.

For sorting, frozen samples from each quadrat were thawed, separated into species, dried at 60 °C and weighed. The species that comprised most of the overall biomass (typically 80 – 90 %) were identified to species level and if this was not possible then they were identified to genus. Species of low abundance were pooled into functional groups of: ‘filamentous reds’, ‘foliose reds’, ‘filamentous browns’, ‘foliose browns’, ‘other – green’ and ‘other – brown’. Biomass estimates were used to inform sampling for biochemical composition, with the three most abundant species by dry weight at each site, each season, being further sampled for fatty acid composition and nitrogen content. On three occasions (site 2 in spring, site 3 in summer and winter), a species that was in the three most abundant by biomass at that site was present in one or two quadrats in high biomass, but no other individuals were found in the other quadrats or observed along the transect. In these cases, as there were not enough replicate individuals of these species for analysis of fatty acid composition and nitrogen content, the 4th most abundant species were sampled. During summer at site 2 and site 3 and autumn at site 2 an extra species was sampled for fatty acid composition in addition to the three most abundant species: these were *Ecklonia radiata* in summer at site 2, *Sargassum spp.* in summer at site 3 and *Phyllospora comosa* in autumn at site 2. These additional species were sampled in these seasons to provide a full time-series of fatty acids across seasons. We were unable to undertake analysis of nitrogen content on these additional samples.

Sampling for biochemical composition

Concurrently with biomass sampling, 5 individual replicates of the most visually abundant species (typically 6 – 7 species) were collected into mesh bags and kept on ice in an insulated container until these samples were frozen at – 20 °C ~ 3 hours after collection. These samples were collected separately to biomass samples and frozen as soon as possible to ensure the material for biochemical analysis remained unchanged. Frozen samples for biochemical analysis were freeze-dried the day after freezing (Labconco® FreezeZone® 4.5) and stored at

– 20° C until analysis of biochemical composition. An issue during collection resulted in only two species being sampled at site 1 in spring for biochemical composition.

Fatty acid analysis

Fatty acids were extracted and analysed by the direct-transmethylation method described in Schmid et al. (2018). A known amount (~ 20 mg) of ground, freeze-dried biomass was transferred into borosilicate glass test tubes fitted with a PTFE-lined screw cap. The samples were directly transmethyated using methanol: dichloromethane (DCM): concentrated hydrochloric acid (3 ml, 10:1:1 v/v/v) and placed in a heating block at 80 – 85 °C for two hours, after which samples were cooled to room temperature. Following cooling, 1 ml of Milli-Q water was added and fatty acid methyl esters (FAME) were extracted three times by addition of 2 ml of hexane/DCM (4:1, v/v). FAME samples were evaporated under nitrogen gas flow and re-dissolved in 0.5 ml of DCM containing a known amount of 23:0 added as an internal injection standard. Samples were analysed by gas chromatography (7890 GC, Agilent Technologies, USA) coupled with a flame ionisation detector, with analytical conditions as described in Parrish et al. (2015). Individual fatty acids were confirmed by gas chromatography–mass spectrometry (1310 GC, ThermoFisher Scientific, USA) coupled with a triple quadrupole mass spectrometer (TSQ 8000, Thermo Fisher Scientific, USA). Samples were injected using an auto sampler (TriPlus RSH, ThermoFisher Scientific, USA) with a non-polar HP-5 Ultra 2 bonded-phase column (50 m × 0.32 mm internal diameter × 0.17 µm film thickness). The system conditions were as described in White et al. (2017). Mass spectra data were acquired and processed with Xcalibur™ software (ThermoFisher Scientific, USA).

Analysis of % N content

Percentage N was determined using the methods outlined in Britton et al. (2019). Dried samples (~ 5 mg) were weighed into tin cups (Sercon, U.K.) and analysed using an elemental

analyser (NA1500, Fisons Instruments, UK) coupled to an isotope ratio mass spectrometer (Delta V Plus, ThermoFisher Scientific, USA) via a Universal Continuous Flow Interface (Conflo IV, ThermoFisher Scientific, USA). Combustion and reduction were achieved at 1020 °C and 650 °C respectively. % N composition was calculated by comparison of mass spectrometer peak areas to those of standards with known concentrations.

Analysis and statistics on biochemical composition data

Spatial and seasonal variation in fatty acid composition, nitrogen content and biomass of red and brown seaweeds

Fatty acid composition and % N of the red and brown seaweeds at each site at each season were used as a proxy of nutritional quality of each group at different sites and seasons.

Principal Coordinates Analysis (PCoA) was used to visualise differences in fatty acid composition in multivariate space for all 3 sites and seasons. A Permutational Multivariate Analysis of Variance (PERMANOVA) was undertaken with the fixed factors: “Group” (2 levels: Red and Brown) and “Season” (4 levels: Spring, Summer, Autumn, Winter), “Site” (2 levels: site 2 and site 3) and all 2-way and 3-way interactions. Site 1 was excluded from this PERMANOVA as only browns were sampled for biochemical composition at this site, due to reds being in low abundance. A 3-way interaction was detected in the initial PERMANOVA (Appendix 2.2) and as such, each group was analysed separately with the fixed factors ‘Site’ (Browns: 3 levels: sites 1, 2 and 3, Reds: sites 2 and 3) and ‘Season’ (4 levels: Spring, Summer, Autumn, Winter) and the Site × Season interaction. If significant interactions were detected in these models, then differences between seasons were analysed within each site using pairwise tests. Type III sums of squares and unrestricted permutation of raw data were selected for all models. The Bray-Curtis dissimilarity measure was used as the measure of similarity for all resemblance matrices and no transformation of the data was undertaken. Resemblance matrices were calculated using fatty acids that contributed on average at least 1

% of total fatty acids (TFA). All multivariate analyses were undertaken in the software PRIMER v7 with the PERMANOVA+ add on (Anderson 2001).

To visualise differences in the nutritionally important compounds of C₁₈ chain n-3 PUFA, arachidonic acid (20:4 n-6, ARA), eicosapentaenoic acid (20:5 n-3, EPA) and % N, boxplots were produced for each site and season combination within each group. To test for differences between the total biomass of the red and brown seaweeds in each site, biomass was calculated as g dry weight m⁻² for each group and a 3-way Analysis of Variance (ANOVA) was conducted. This model included the fixed factors: 'Site' (3 levels: site 1, site 2 and site 3), 'Season' (4 levels: spring, summer, autumn and winter), 'Group' (2 levels: reds and browns) and all 2 and 3-way interactions. A significant 2-way interaction between Group and Site was detected in the 3-way ANOVA, while no effects of Season or any of its associated interactions were detected (Appendix 2.3). As such, separate 1-way ANOVAs were conducted separately for each group with the factors Group and Season and all associated interactions removed. When the ANOVAs indicated significant main effects at $\alpha = 0.05$, Tukey's Honestly Significant Different (THSD) post-hoc tests were conducted to identify differences between locations. The green seaweeds were excluded from this analysis as they contributed only ~ 1 % to the overall biomass across sites. All models were inspected to ensure they conformed to the assumptions of homogeneity of variances and normality of residuals using normal Q-Q plots and residual versus fitted plots and all three models required a transformation of $Y^{0.2}$. This transformation was determined using the Box-Cox method (Box and Cox 1964). The statistical software R v. 3.6.1 (R Core Team 2019) was used for fitting these models.

Seasonal variation in individual seaweed species

Seasonal variation in SFA and PUFA of individual species was analysed for 3 species at site 1 (*E. radiata*, *P. comosa* and *Zonaria turneriana*), 3 species at site 2 (*E. radiata*, *P. comosa* and *P. novaehollandiae*), and 2 species at site 3 (*Plocamium angustum* and *Sargassum spp.*). These species were sampled during all four seasons at each site, except for *P. comosa* at site 1 and *P. novaehollandiae* at site 2 which were not sampled in spring. An initial 2-way ANOVA was conducted separately for each site with the fixed effects: ‘Season’ (4 levels: Spring, Summer, Autumn and Winter) and ‘Species’ (site 1: 3 levels, site 2: 3 levels, site 3: 2 levels) and the ‘Season’ \times ‘Species’ interaction. If a significant interaction was determined for a site, a separate 1-way ANOVA for each species was conducted with the fixed effect of ‘Season’. When the ANOVAs indicated significant main effects at $\alpha = 0.05$, THSD post-hoc tests were conducted to identify differences between seasons. All models were inspected to ensure they conformed to the assumptions of homogeneity of variances and normality of residuals using normal Q-Q plots and residual versus fitted plots and no transformations were required. These analyses were conducted in R v. 3.6.1 (R Core Team 2019).

Results

Overstory canopy description and biomass of understory species

The overstory at sites 1 and 2 consisted of a mixed assemblage of *E. radiata* and *P. comosa*, while the overstory at site 3 was primarily of *P. comosa*, with low densities of other large browns (e.g. *E. radiata*, *Cystophora spp.*) interspersed among them (Appendix 2.4). The abundant understory species at site 1 were juvenile *E. radiata*, juvenile *P. comosa* and *Z. turneriana*, which comprised most of the biomass (ca. 90 – 95 %), with no clear seasonal variation in their abundance (Appendix 2.5). Foliose and filamentous reds comprised only a small proportion of the biomass and did not vary seasonally. The most abundant species at site 2 were juvenile *P. comosa*, juvenile *E. radiata* and *P. novaehollandiae*. *Callophyllis*

lambertii and *Z. turneriana* were also common (Appendix 2.5). There were some differences in the abundant species between seasons with *P. novaehollandiae* not detected in spring and other species such as *Carpoglossum confluens* and *Sargassum spp.* only detected in autumn and winter respectively (Appendix 2.5). Site 3 had the most diverse assemblage of abundant species with a mixture of reds and browns comprising the understory. *P. angustum* and *Sargassum spp.* were consistently abundant across all seasons, while *Phacelocarpus peperocarpus* and *Xiphophora gladiata* were abundant in some seasons but not others. Clear, consistent seasonal patterns were not apparent; however, the abundance of individual species was highly variable at this site between seasons. The biomass of both the red and brown understory seaweeds differed between sites (reds, ANOVA: $F_{(2,93)} = 30.45$, $p < 0.0001$ and browns, ANOVA: $F_{(2,93)} = 4.25$, $p < 0.017$, Figure 2.2). For the reds, site 2 had 4.3 times the biomass of site 1, while site 3 had 13.5 times the biomass of site 1 and 3.1 times the biomass of site 2. These differences were significant in THSD post-hoc tests. For the browns, site 3 had significantly more biomass than site 2 (2.6 times as much), while no other sites were significantly different from each other. SST over the duration of the study can be seen in Appendix 2.6 (site 1), Appendix 2.7 (site 2) and Appendix 2.8 (site 3).

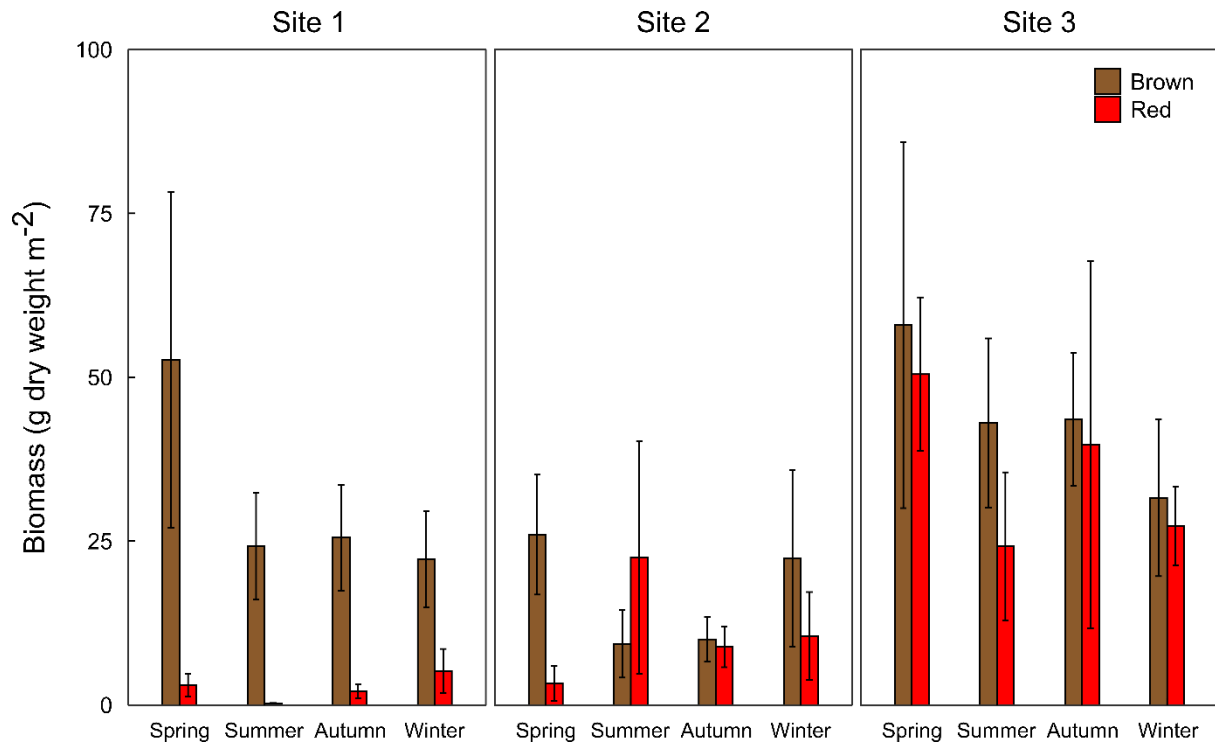


Figure 2.2: Biomass (g dry weight m⁻²) of understory seaweeds at each site each season. Brown bars refer to brown seaweeds (species pooled) and red bars refer to the red seaweeds (species pooled). Data is presented as means \pm standard error.

Spatial and seasonal variation in nutritional quality of red and brown seaweeds

The Principal Coordinates Analysis (PCoA) showed a clear separation of the red and brown seaweeds based on their fatty acid profiles (Figure 2.3). The browns clustered into one distinct group regardless of site or season, except for *Z. turneriana* which formed its own grouping (Figure 2.3). The reds separated into two distinct groups with the species from site 2 forming one group and the species from site 3 forming the other (Figure 2.3). Separate PERMANOVA models for each group detected significant 2-way interactions between “Site” and “Season” for both the browns and reds (browns: PERMANOVA: Pseudo- $F_{(6,137)} = 1.98$, $p = 0.006$, reds: PERMANOVA: Pseudo- $F_{(3,48)} = 4.23$, $p = 0.0006$). Pairwise tests indicated that for the browns at site 1 only spring and winter were significantly different and at site 2 there were no significant differences between seasons. At site 3, summer was significantly different to all other seasons, while spring and autumn were also significantly different. For the reds at site 2, all seasons were significantly different except for autumn and winter ($p = 0.07$). At site

3 all seasons were significantly different. The variance components indicated that for the browns the residual variation accounted for most of the variation (65.99 %) followed by Site (26.16 %), while Season and the Site \times Season interaction accounted for only a small proportion of the variability (2.01 % and 5.84 % respectively). In contrast, most of the variance in the reds was explained by Site (64.02 %), followed by residual variation (15.74 %), with Season and the Site \times Season interaction explaining the least of the variation (11.12 % and 9.12 % respectively).

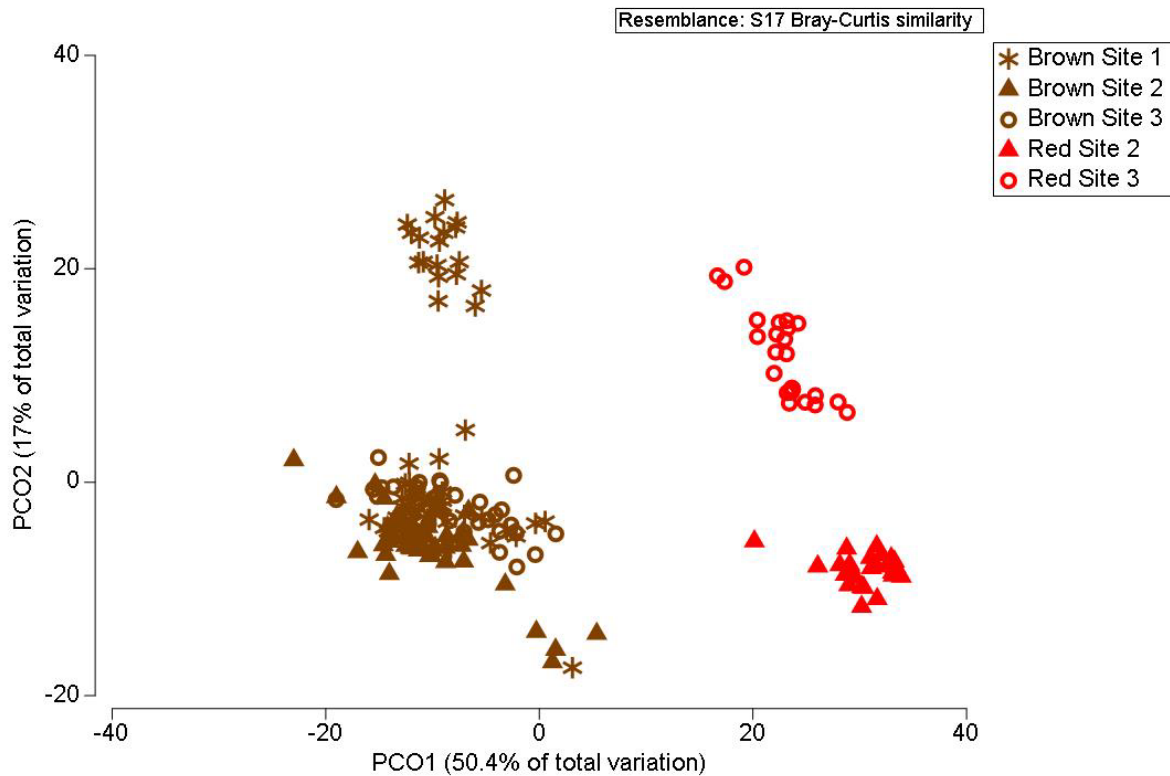


Figure 2.3: Principal Coordinates Analysis (PCoA) of fatty acids that were on average at least 1 % of total fatty acids (TFA). The PCoA is based on a resemblance matrix using the Bray-Curtis Similarity measure. Brown symbols refer to brown seaweeds (species pooled) and red symbols refer to the red seaweeds (species pooled). Stars refer to samples from site 1, filled triangles refer to samples from site 2, and open circles refer to samples from site 3.

Overview of nutritionally important compounds in the reds and browns

The following values are given as means \pm standard deviation of each group unless stated otherwise. An overview of nutritionally important compounds for each species, pooled across sites and seasons can be viewed in the supplementary material (Appendix 2.9). ARA was higher in the reds at site 2: $33.65\% \pm 5.45$ compared to site 3: $19.62\% \pm 6.62$ (Figure 2.4), while in the browns ARA was similar across sites: site 1 = $15.54\% \pm 3.92$, site 2 = $19.33\% \pm 2.85$, site 3 = $17.15\% \pm 3.81$ (Figure 2.4). ARA remained stable in the browns across seasons at all sites, while in the reds the seasonal variation in ARA content differed between sites: at site 2 ARA decreased from spring and summer into autumn and winter, whereas at site 3 ARA increased from spring into winter. EPA was only present in trace amounts in the reds at site 2 ($0.82\% \pm 0.68$) but was in high abundance in reds at site 3 ($15.88\% \pm 4.50$), while the browns had similar amounts of EPA at all three sites, site 1 = $8.18\% \pm 3.12$, site 2 = $6.29\% \pm 2.20$, site 3 = $8.41\% \pm 1.81$. EPA in the reds at site 3 displayed a seasonal trend of an increase from spring until winter (Figure 2.4). There were no seasonal trends in EPA in the reds at site 2 or the browns at site 2 or 3 (Figure 2.4). In contrast, EPA declined from spring through winter in the browns at site 1 (Figure 2.4). The red species had only trace amounts of C₁₈ n-3 PUFA: site 2 = $0.56\% \pm 0.29$, site 3 = $0.88\% \pm 0.72$ (Figure 2.5), whereas these fatty acids were in high abundance in the browns at all three sites – site 1 = $14.78\% \pm 5.64$, site 2 = $21.54\% \pm 5.03$, and site 3 = $20.39\% \pm 7.28$ (Figure 2.5).

% N was typically higher in the reds than the browns: for the reds, site 2 = $3.43\% \pm 0.71$, site 3 = $3.48\% \pm 0.47$, whereas for the browns, site 1 = $1.65\% \pm 0.35$, site 2 = $1.57\% \pm 0.26$, and site 3 = $1.61\% \pm 0.47$ (Figure 2.5). The browns displayed minimal seasonal variation in % N at sites 1 and 2 whereas the reds had higher % N in autumn and winter at site 2 relative to spring and summer. At site 3, the browns had slightly higher % N in spring than in the other seasons, whereas the reds had high % N in all seasons with a slight decrease in summer.

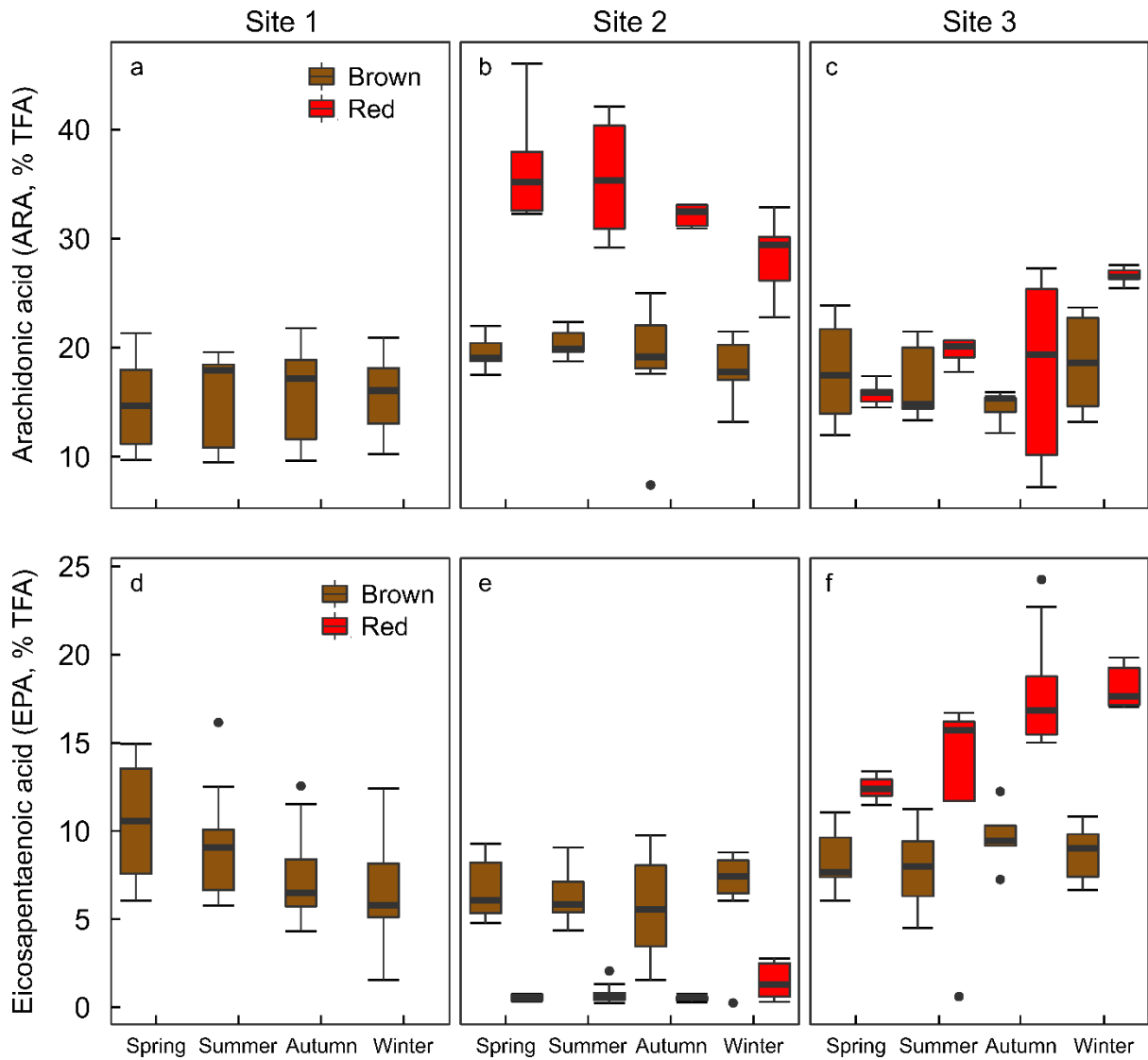


Figure 2.4: Boxplots of the nutritionally important fatty acids arachidonic acid (ARA, % dry weight, a, b, c) and eicosapentaenoic acid (EPA, % TFA, d, e, f) at each site in each season for the red (red boxes) and brown (brown boxes) seaweeds sampled. The black lines display the median, boxes cover interquartile range and error bars display the maximum and minimum values. Outliers are displayed as points. No red species were sampled for biochemical composition at site 1.

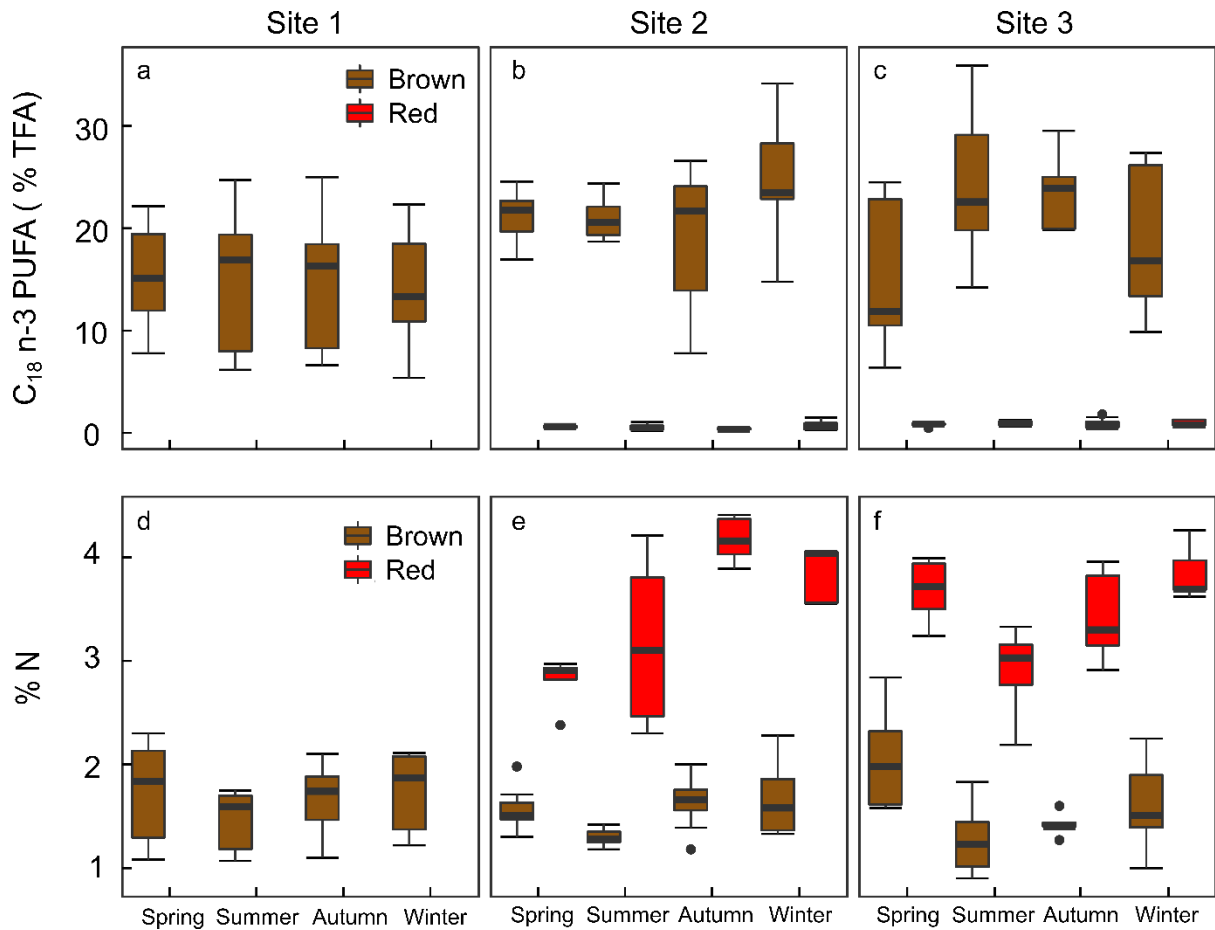


Figure 2.5: Boxplots of the nutritionally important fatty acid group C_{18} n-3 PUFA (% TFA, a, b, c) and percentage nitrogen (d, e, f) at each site in each season for the red (red boxes) and brown (brown boxes) seaweeds sampled. The black lines display the median, boxes cover interquartile range and error bars display the maximum and minimum values. Outliers are displayed as points. No red species were sampled for biochemical composition at site 1.

Seasonal variation in fatty acids at the species level

Site 1

Clear seasonal trends were observed in SFA and PUFA for all three dominant species. SFA levels differed significantly between seasons and this pattern was the same for all three species, with no 2-way interaction detected (Figure 2.6, Table 2.1). All species displayed a trend of an increase in SFA from spring/summer to winter with levels of SFA significantly higher in winter than in all other seasons (THSD, $p < 0.05$; Figure 2.6, 19 % higher than spring and summer, 11 % higher than autumn). Levels of PUFA displayed the opposite trend to SFA and decreased from spring/summer to winter (Figure 2.6). This pattern was the same for all species with a significant effect of Season detected in the overall ANOVA, with no significant interaction (Table 2.1). PUFA levels in winter were significantly lower than in spring and summer (16 and 13 %, respectively) (THSD, $p < 0.05$). Levels of PUFA were also significantly lower in autumn relative to spring (9 % lower, THSD, $p < 0.05$).

Site 2

Seasonal trends in both SFA and PUFA for the three dominant understory species were less clear than at site 1. A significant interaction was detected between season and species for both SFA and PUFA (Appendix 2.10) and as such, separate ANOVAs were conducted for each species. Levels of SFA in *E. radiata* were lower in winter relative to the other seasons (Figure 2.6) but this difference was only significantly lower compared to autumn (13 % lower, Table 2.1), while the difference between winter and spring was not significant (10 % lower, $p = 0.057$). *P. comosa* displayed a trend of a decrease in SFA from spring to autumn, followed by a sharp increase in winter (Figure 2.6). The only significant differences were between autumn and winter with *P. comosa* having 30 % higher SFA in winter. SFA was 20 % higher in spring relative to autumn but this was not significant ($p = 0.051$). There were no significant effects of season on SFA levels detected in *P. novaehollandiae* (Figure 2.6, Table

2.1). PUFA was significantly higher in winter in *E. radiata* compared to all other seasons (11 % higher on average, Table 2.1, Figure 2.6). For *P. comosa*, levels of PUFA displayed a trend of an increase from spring to autumn, followed by a decrease in winter (Table 2.1, Figure 2.6). Significant differences in PUFA were found between autumn and winter (12 % lower in winter). No significant differences in PUFA were detected between seasons for *P. novaehollandiae* (Table 2.1, Figure 2.6).

Site 3

A strong seasonal trend in SFA and PUFA was observed for the dominant understory red (*P. angustum*), but not for the dominant understory brown (*Sargassum spp*) (Figure 2.6). A significant interaction was detected between season and species for both SFA and PUFA (Appendix 2.11) and separate ANOVAs were conducted for each species. SFA in *P. angustum* displayed a decreasing trend from spring to winter, with average SFA levels in spring and summer being significantly higher than in autumn and winter (31 % higher, Table 2.1). The opposite trend was observed for PUFA in *P. angustum*, with significantly lower values of PUFA in spring and summer compared to autumn and winter (24 % lower, Table 2.1). *P. angustum* was the only species across all sites to show a trend of declining SFA and increasing PUFA from spring to winter. There were no significant effects of season on either SFA or PUFA in *Sargassum spp*. (Table 2.1, Figure 2.6).

Table 2.1: Analysis of Variance (ANOVA) table showing degrees of freedom (df), F – values and *p* – values for seasonal differences in polyunsaturated fatty acids (PUFA) and saturated fatty acids (SFA). For site 1, there was no significant interaction between season and species detected in the 2-way ANOVAs for PUFA or SFA and as such when the main effect of season was significant at $\alpha = 0.05$, differences between season were assessed across all species using Tukey’s Honestly Significant Different (THSD) post-hoc tests. For sites 2 and 3 a significant interaction between site and season were detected and as such, all species were analysed separately within each site. When these ANOVAs detected significant differences at $\alpha = 0.05$, *p*-values are displayed in bold and THSD post-hoc tests were conducted. Significant differences ($\alpha = 0.05$) between seasons detected in THSD post-hoc tests are displayed, and abbreviations of seasons are given: Sp = spring, Su = summer, Au = autumn and Wi = winter.

Site	Species	Variable	df	F - value	p-value	THSD differences
1	<i>E. radiata</i> , <i>P. comosa</i> and <i>Z. turneriana</i>	SFA	3, 43	10.61	< 0.0001	Wi > Sp, Su, Au
	<i>E. radiata</i> , <i>P. comosa</i> and <i>Z. turneriana</i>	PUFA	3, 43	10.08	< 0.0001	Sp, Su > Wi Sp > Au
2	<i>E. radiata</i>	SFA	3, 16	5.00	0.012	Au > Wi
		PUFA	3, 16	7.70	0.002	
	<i>P. comosa</i>	SFA	3, 16	3.67	0.035	Au < Wi
		PUFA	3, 16	3.59	0.037	Au > Wi
	<i>P. novaehollandiae</i>	SFA	2, 12	2.94	0.091	-
		PUFA	2,12	3.32	0.071	-
3	<i>P. angustum</i>	SFA	3, 15	32.42	< 0.0001	Sp, Su > Au, Wi
		PUFA	3, 15	27.79	< 0.0001	Sp, Su > Au, Wi
	<i>Sargassum spp.</i>	SFA	3, 16	0.78	0.523	-
		PUFA	3,16	0.49	0.696	-

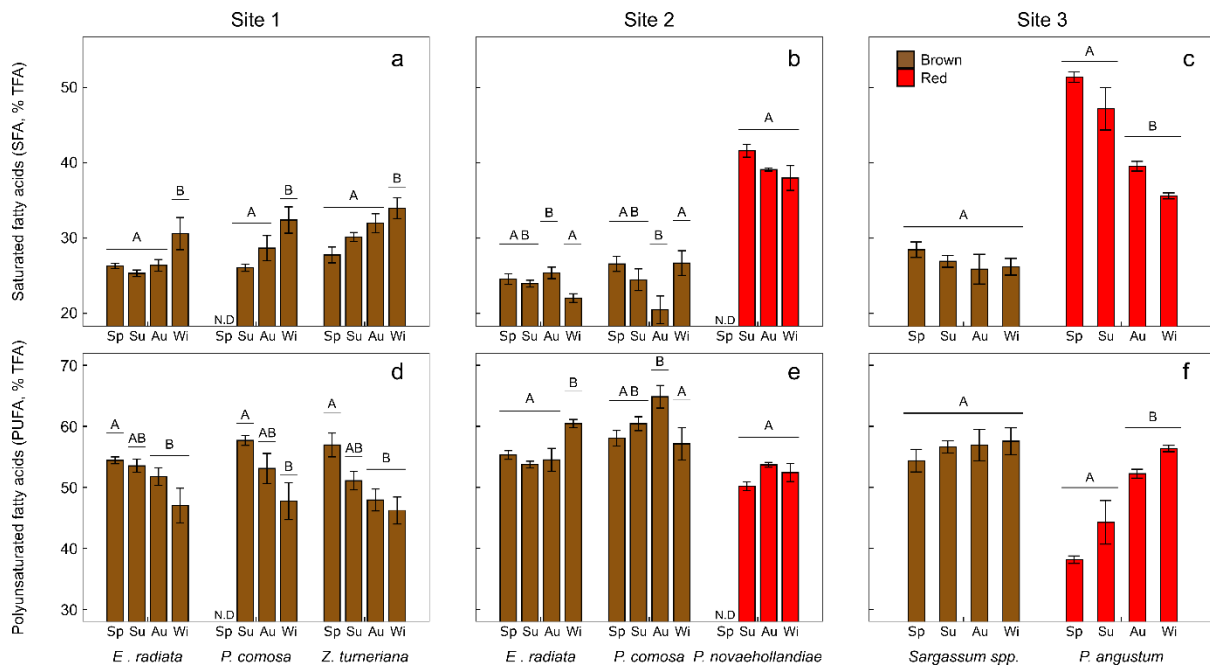


Figure 2.6: Levels of saturated fatty acids (SFA, % TFA) and polyunsaturated fatty acids (PUFA % TFA) for understory species sampled in at least 3 seasons at site 1 (a, d), site 2 (b, e), and site 3 (c, f). Seasons sharing the same letter were not found to be significantly different in THSD post-hoc tests. Differences in SFA and PUFA were compared across seasons in site 1 on pooled data for all species as no significant interactions between site and species were detected in the two-way ANOVA. All other sites had SFA and PUFA content compared across seasons separately for each species with one-way ANOVAs as a significant interaction between site and species was detected in the 2-way ANOVAs. Brown seaweeds are coloured brown and red seaweeds are coloured red. N.D. refers to no data for a species in that season and site combination (*P. comosa* in spring at site 1 and *P. novaehollandiae* at site 2 in spring). Seasons are abbreviated: Sp = spring, Su = summer, Au = autumn, Wi = winter. Data is presented as means \pm standard error.

Discussion

Our findings show that the fatty acid composition and nitrogen content of ecologically dominant understory seaweeds vary between sites, seasons and phyla in Tasmania, Australia. Each of the three sites, which were located along a latitudinal gradient, had unique understory compositions and differing amounts of nutritional compounds. This variation in nutritional quality was driven by differences in the biomass of, and biochemical composition within, the brown and red seaweeds. The biomass of understory browns was similar across all three sites, with slightly lower biomass detected at site 2 relative to site 3. In general, the proportion of nutritional compounds in the browns (EPA, ARA, C18 n-3 PUFA, PUFA and % N) were similar across sites, but seasonal patterns within sites differed: there were strong seasonal patterns in the PUFA, SFA and EPA content of browns at the northern site while no seasonal patterns were present in the southern sites. The biomass of the red seaweeds differed between sites: there was a low biomass of understory reds at the northern site (site 1), with ~ 4- and 13-times higher biomass at site 2 and site 3 respectively. In contrast to the browns, the proportion of nutritional compounds in the reds was substantially different between sites. These differences were possibly driven by differences in species composition, with different abundant reds present at each site. Seasonal patterns in the concentrations of PUFA, SFA and nutritional compounds in the reds varied across sites and they were generally more nutritious than the browns (high nitrogen content and high levels of EPA or ARA). The high variability in the nutritional quality of the reds suggests that in Tasmania, variation in the quality of seaweed assemblages as a food source for grazers is driven primarily by the presence/absence of red species. The increasing biomass of nutritious reds from the northern to southern sites is consistent with regional differences in productivity of commercially valuable abalone in Tasmania, and thus nutritional quality and biomass of seaweeds may be a key driver of invertebrate grazer populations on these reefs.

Differences in the nutritional quality between sites is driven by the red seaweeds

Fatty acids are strong taxonomic markers and seaweeds exhibit similar fatty acid profiles between species within their respective phyla (Galloway et al., 2012). In our study, the reds and browns were clearly distinguishable from each other in multivariate space supporting earlier work from southern Australia (Guest et al., 2010; Guest et al., 2008; Schmid et al., 2018), and the USA (Galloway et al., 2012). The red species formed two distinct groups, with most of the variability in fatty acid composition explained by site; this trend of higher variability between sites and seasons was also apparent when undertaking univariate analysis of the nutritionally important PUFA (C₁₈ n-3 PUFA, ARA and EPA) and nitrogen content. In contrast, the browns had similar fatty acid profiles and nitrogen content across sites and seasons. Our results for *E. radiata* and *P. comosa* are consistent with a previous study from Tasmania, in which higher variability in fatty acid profiles was found to occur between replicate samples than across sites for both *E. radiata* and *P. comosa* (Guest et al., 2010). Together, these studies suggest that minimal spatial variation in fatty acid composition of the browns is common trait in this region. The biomass of the reds was highly variable across sites, with up to an 13-fold increase in the biomass of red species from our most northern to our most southern site. This again contrasted with the browns, with biomass being much more similar across sites for this group (although site 2 had slightly lower biomass than site 3). Both the high variability in biomass and nutritional quality in the reds, coupled with the relative lack of variation at these scales in the browns suggest that variation in the quality of food available to grazers at different sites and seasons is driven primarily by the red species.

The high variability in fatty acid composition in the reds between sites may have been driven by site-specific factors or differences in the composition of abundant species. For example, the amount of ARA and EPA, which are both nutritionally important (Bell and Tocher 2009; Brett and Müller-Navarra 1997), in the reds was highly variable across sites: species at site 2 had high levels of ARA and trace amounts of EPA, whereas the species at site 3 had high

levels of EPA and moderate amounts of ARA. However, the abundant reds at site 2 were not found in abundance at site 3 and vice versa. As such, we are unable to separate the confounding effects of site and species in driving the differences in the nutritional quality of the red seaweeds. It is likely a combination of the two factors that drive these differences. Seaweed species generally have similar fatty acid profiles to others within their phylum (Galloway et al., 2012; Schmid et al., 2018). As such, differences in species composition within a phylum is likely to be less important than changes in the proportion each phylum contributes to the overall biomass. While it was not our aim to determine what was driving the variability in species composition, spatial and temporal variation in abundance and composition of understory seaweeds is influenced by a range of environmental variables such as temperature, light, nutrient concentrations and wave exposure (Breda and Foster 1985; Goldberg 2005; Wernberg and Goldberg 2008). Given that the magnitude and frequency of many of these variables have been and will continue to be altered under climate change in southeastern Australia (Johnson et al., 2011; Oliver et al., 2018; Ridgway 2007), determining the major drivers of species composition and abundance of understory seaweeds in this region requires ongoing investigation. Doing so may allow us to predict how the food quality of reef systems in this area will change in a future ocean and provide critical information for management.

Implications of variability in the nutritional quality of red seaweeds for commercial fisheries

The commercially valuable blacklip abalone (*H. rubra*) is highly productive in southern Tasmania despite temperatures being low and sub-optimal for growth (Gilroy and Edwards 1998). A substantially high proportion of the total catch comes from the region adjacent to our most southern site (site 3), with a comparatively small and declining proportion of catch harvested adjacent to the northern site (site 1, Mundy and McAllister 2019). While factors such as harvest intensity, habitat quality and predation rates may be responsible for the

regional variation in productivity of *H. rubra* across the study sites, this variation may also be partly explained by differences in the biomass and nutritional quality of the red seaweeds observed here. In general, the reds were more nutritious (higher levels of ARA or EPA and high nitrogen content) and all these compounds are known to be important for growth in abalone (Fleming 1995a; Mai et al., 1996; McShane et al., 1994; Nelson et al., 2002a). It is possible that the high productivity of *H. rubra* in the southern region is partly driven by the higher biomass of nutritious reds. This link is speculative however and serves to pose questions rather than answer specific hypotheses. Future studies should attempt to examine the drivers of variability in nutritional compounds over multiple spatial scales using a hierarchical sampling design with a correlative analysis of multiple environmental conditions.

Our study describes the differences in the nutritional quality of seaweeds available to grazers, but not whether these differences have flow on effects to *H. rubra*. This will depend on both the proportion of the diet that is made up of red species and the relative energetic costs of extracting nutritional compounds from each group (Angell et al., 2012). Studies on the dietary components of *H. rubra* have been inconclusive with inherent biases associated with traditional methods limiting their reliability: red seaweeds are more easily digested than browns resulting in an underestimation of reds in the diet (Foale and Day 1992), while feeding trials may introduce artefacts that influence feeding behaviour (Guest et al., 2008). A study using combined fatty acid and stable isotope analysis found that the major components of the diet were brown algae and detritus (Guest et al., 2008). However, Guest et al. (2008) conducted their study on the mid-east coast of Tasmania, which was likely most similar to site 1 in our study. This raises the question of whether *H. rubra* in their study were consuming browns as a preference or because they were most widely available. The relative energetic cost of extracting nutritionally important compounds from each group is unclear, but the high digestibility of the reds (Foale and Day 1992), coupled with the high levels of phenolic and the physical ‘toughness’ of the browns (Fleming 1995b) may make reds more

palatable and likely more digestible for *H. rubra*. Future research should not only attempt to determine the site-specific differences in the nutritional quality of seaweed assemblages over multiple spatial scales, but also whether these differences are reflected in the tissue of commercially important grazers.

Seasonal variability in fatty acids at the species level

A common trend in fatty acid composition in seaweeds is for PUFA to increase and SFA to decrease from spring/summer into autumn/winter (Schmid et al., 2014, 2017a). This is likely a mechanism that allows seaweeds to maintain optimum membrane fluidity at a range of temperatures (Los and Murata 2004). This trend was only displayed in the red seaweed *P. angustum* at site 3, while at site 2, *E. radiata* and *P. comosa* displayed slight variations on this trend. An explanation for the lack of consistent temperature driven changes in fatty acids that have been previously reported in seaweeds, is that most seasonal studies on fatty acid composition have been conducted in the intertidal (Kendel et al., 2013; Kim et al., 1996; Schmid et al., 2014, 2017a; Schmid et al., 2017b; Venkatesalu et al., 2012) or shallow (< 2 m depth) subtidal (Gaitán-Espitia et al., 2014; Gerasimenko et al., 2011; Gosch et al., 2015a). In these habitats temperature fluctuations are typically much larger than at the depth we conducted our study (7 m). As such, it is possible that given the small temperature range (~12 – 20 °C, Appendix 2.6 – 2.8), adjustments in fatty acid composition to maintain optimum membrane fluidity are either not required for all species, or adjustments are small and difficult to detect. Other environmental factors such as irradiance and nitrogen availability, within-species variability (Gosch et al., 2015a) or interactions between drivers may exert a greater influence on fatty acid composition in seaweeds than temperature in this system.

The effect of environmental conditions on fatty acid composition in seaweeds has only been studied extensively for temperature (Floreto et al., 1993; Floreto and Teshima 1998; Gómez Pinchetti et al., 1998; Gordillo et al., 2001; Gosch et al., 2015a; Hotimchenko 2002;

Khotimchenko and Yakovleva 2005; Kumari et al., 2013), with relatively little information on the effects of irradiance and nitrogen. Both seawater nitrogen concentrations and irradiance vary seasonally in temperate regions with higher irradiance, longer daylight hours and reduced nitrogen availability in summer and the opposite in winter (Fairhead and Cheshire 2004; Flukes et al., 2015). However, these seasonal trends in irradiance and nitrogen would be expected to exacerbate the effects of temperature on fatty acid composition in seaweeds: both high irradiance and nitrogen limitation can result in an accumulation of storage lipids such as triacylglycerols (TAG) and these are typically low in PUFA and high in SFA (Guihéneuf et al., 2009; Khotimchenko and Yakovleva 2005; Kim et al., 1996). Given that these patterns were not widespread in our study, it appears that factors other than light or nitrogen concentrations were driving the responses at these sites. In order to better understand how environmental conditions regulate fatty acid composition in seaweeds and explain the responses observed in our study, targeted laboratory experiments to identify the individual and interactive effects of environmental drivers are required.

Implications of species and site-specific variability in fatty acids for commercial exploitation of seaweeds

Seaweeds in Tasmania are a promising source of n-3 PUFA and n-3 LC-PUFA, with many species having a favourable ratio of n-6:n-3 PUFA of ~ 1, which is ideal for human diets (Schmid et al., 2018). The lack of consistency in seasonal patterns of fatty acid composition across the species examined and the site-specific differences in fatty acids within *E. radiata* and *P. comosa* has important implications for potential commercial exploitation of seaweeds in this region. Any attempts to extrapolate patterns in fatty acid composition in seaweeds from one site or species to another for commercial uses should exercise caution, as seasonal and species-specific patterns appear to be localised. The timing of harvest of wild seaweeds for functional foods, nutraceuticals or for use in feedstock applications will be highly dependent on both the seasonal and spatial availability of nutritionally important compounds

in the seaweeds and this will differ between species. For example, both *P. angustum* and *Sargassum spp.* at site 3 had low n-6:n-3 ratio. However, seasonal variability in PUFA content was only observed in *P. angustum*. As such, the timing of harvest of these species would be critical for *P. angustum* to ensure maximum PUFA content, whereas *Sargassum spp.* could be harvested year-round. Knowledge of seasonal, site and species-specific variability in biochemical composition is therefore essential. Additionally, seasonal changes in abundance or biomass of species must also be considered as the highest concentration of a favourable compound may not necessarily coincide with periods of high biomass or abundance requiring a trade-off between quality and quantity.

Summary

This study provides evidence that variability in food quality of understory seaweeds between sites and seasons in eastern Tasmania appears to be driven primarily by changes in the biomass and biochemical composition of the red species. The reds were generally more nutritious, and there was high variability in the proportions of nutritional compounds in the reds across sites and seasons. This contrasted with the browns, which had much less variability in the amount of nutritional compounds between sites, but had differing seasonal patterns in PUFA, SFA and EPA within sites. The biomass of the browns was similar across sites whereas the biomass of the reds increased from the northern to southern sites. This increase in biomass of the nutritious reds may be an important driver of regional differences in productivity of commercially valuable abalone in Tasmania. At the species level, seasonal variability was both species- and site-specific and did not follow expected patterns if temperature, light or seawater nitrogen concentrations were the primary drivers. This suggests seasonal patterns in fatty acid composition in this system are likely driven by a complex combination of environmental drivers and species-specific responses. This finding has implications for the commercial exploitation of seaweeds for use in functional foods or nutraceuticals as seasonal variability in fatty acids observed in one species at a site may not

be the same at another site or for another species. Future studies should aim to investigate whether the spatial patterns in nutritional quality presented here are widespread by examining a greater proportion of sites at multiple spatial scales. Moreover, studies should investigate whether differences in the nutritional quality and species composition of seaweed assemblages between sites affect the performance of commercially important grazers.

Acknowledgements

We thank David Faloon, Jane Ruckert, Kylie Cahill, Sarah Pyke, Ruari Colquhoun, Jaime McAllister, Ellie Paine and Kathryn Willis for assistance in the field and for providing valuable insights into the study, and Toby Bolton for his expert support. DB was supported by a University of Tasmania, Australian Postgraduate Award. The research was funded by a grant from the Tasmanian Abalone Council (UTAS 113626), matched by the Institute for Marine and Antarctic Studies. MS was funded by the Deutsche Forschungsgemeinschaft (DFG, grant ID: SCHM 3335/1-1).

References

- Al-Hasan, R.H., Hantash, F.M., and Radwan, S.S. 1991. Enriching marine macroalgae with eicosatetraenoic (arachidonic) and eicosapentaenoic acids by chilling. *Applied Microbiology and Biotechnology* 35 (4):530-535. doi:10.1007/BF00169763
- Anderson, M.J. 2001. A new method for non-parametric multivariate analysis of variance. *Austral Ecology* 26 (1):32-46. doi:10.1111/j.1442-9993.2001.01070.pp.x
- Angell, A.R, Mata, L., de Nys, R., and Paul, N.A. 2016. The protein content of seaweeds: a universal nitrogen-to-protein conversion factor of five. *Journal of Applied Phycology* 28 (1):511-524. doi:10.1007/s10811-015-0650-1
- Angell, A. R., Pirozzi, I., de Nys, R., and Paul, N. A. 2012. Feeding preferences and the nutritional value of tropical algae for the abalone *Haliotis asinina*. *PLoS ONE*, 7: e38857.
- Banzon, V., Smith, T. M., Chin, T. M., Liu, C., and Hankins, W. 2016. A long-term record of blended satellite and in situ sea-surface temperature for climate monitoring, modelling and

environmental studies. *Earth System Science Data*, 8(1), 165-176. doi:10.5194/essd-8-165-2016

Bell M.V., and Tocher D.R. (2009) Biosynthesis of polyunsaturated fatty acids in aquatic ecosystems: general pathways and new directions. In: Kainz M., Brett M., Arts M. (eds) *Lipids in Aquatic Ecosystems*. Springer, New York, NY. https://doi.org/10.1007/978-0-387-89366-2_9

Bennett, S., Wernberg, T., Connell, S.D., Hobday, A.J., Johnson, C.R., and Poloczanska, E.S. 2015. The ‘Great Southern Reef’: social, ecological and economic value of Australia’s neglected kelp forests. *Marine and Freshwater Research* 67 (1):47-56

Box, G. E., and Cox, D. R. 1964. An analysis of transformations. *Journal of the Royal Statistical Society: Series B (Methodological)*, 26: 211–243

Breda, V.A., and Foster, M.S. 1985. Composition, abundance, and phenology of foliose red algae associated with two central California kelp forests. *Journal of Experimental Marine Biology and Ecology* 94 (1):115-130. doi:[http://dx.doi.org/10.1016/0022-0981\(85\)90053-X](http://dx.doi.org/10.1016/0022-0981(85)90053-X)

Brett, M., and Müller-Navarra, D. 1997. The role of highly unsaturated fatty acids in aquatic foodweb processes. *Freshwater Biology* 38 (3):483-499. doi:10.1046/j.1365-2427.1997.00220.x

Britton, D., Mundy, C.N., McGraw, C.M., Revill, A.T., and Hurd, C.L. 2019. Responses of seaweeds that use CO₂ as their sole inorganic carbon source to ocean acidification: differential effects of fluctuating pH but little benefit of CO₂ enrichment. *ICES Journal of Marine Science*

Britton, D., Schmid, M., Noisette, F., Havenhand, J. N., Paine, E. R., McGraw, C. M., Revill, A. T., *et al.* 2020. Adjustments in fatty acid composition is a mechanism that can explain resilience to marine heatwaves and future ocean conditions in the habitat-forming seaweed *Phyllospora comosa* (Labillardière) C.Agardh. *Global Change Biology*, 26:3512-3524. <https://doi.org/10.1111/gcb.15052>

Brown, M. T., Nyman, M. A., Keogh, J. A., and Chin, N. K. M. 1997. Seasonal growth of the giant kelp *Macrocystis pyrifera* in New Zealand. *Marine Biology*, 129: 417-424.

Cook, P. 2016. Recent trends in worldwide abalone production. *Journal of Shellfish Research*, 35: 581-583.

Cottin, S. C., Sanders, T. A., and Hall, W. L. 2011. The differential effects of EPA and DHA on cardiovascular risk factors. *Proceedings of the Nutrition Society*, 70: 215-231.

Fairhead, V. A., and Cheshire, A. C. 2004. Seasonal and depth related variation in the photosynthesis–irradiance response of *Ecklonia radiata* (Phaeophyta, Laminariales) at West Island, South Australia. *Marine Biology*, 145: 415-426.

Falkenberg, L. J., Russell, B. D., and Connell, S. D. 2013. Future herbivory: The indirect effects of enriched CO₂ may rival its direct effects. *Marine Ecology Progress Series*, 492: 85-95.

- Fleming, A. E. 1995a. Digestive efficiency of the Australian abalone *Haliotis rubra* in relation to growth and feed preference. *Aquaculture*, 134: 279-293.
- Fleming, A. E. 1995b. Growth, intake, feed conversion efficiency and chemosensory preference of the Australian abalone, *Haliotis rubra*. *Aquaculture*, 132: 297-311.
- Floreto, E. A. T., Hirata, H., Ando, S., and Yamasaki, S. 1993. Effects of temperature, light intensity, salinity and source of nitrogen on the growth, total lipid and fatty acid composition of *Ulva pertusa* Kjellman (Chlorophyta). *Botanica Marina*, 36:149-158.
- Floreto, E. A. T., and Teshima, S. 1998. The fatty acid composition of seaweeds exposed to different levels of light intensity and salinity. *Botanica Marina*, 41:467-481.
- Flukes, E., T. Wright, J., and Johnson, C. 2015. Phenotypic plasticity and biogeographic variation in physiology of habitat-forming seaweed: response to temperature and nitrate. *Journal of Phycology*, 51: 896-909.
- Foale, S., and Day, R. 1992. Recognizability of algae ingested by abalone. *Marine and Freshwater Research*, 43: 1331-1338.
- Gaitán-Espitia, J. D., Hancock, J. R., Padilla-Gamiño, J. L., Rivest, E. B., Blanchette, C. A., Reed, D. C., and Hofmann, G. E. 2014. Interactive effects of elevated temperature and pCO₂ on early-life-history stages of the giant kelp *Macrocystis pyrifera*. *Journal of Experimental Marine Biology and Ecology*, 457: 51-58.
- Galloway, A. W. E., Britton-Simmons, K. H., Duggins, D. O., Gabrielson, P. W., and Brett, M. T. 2012. Fatty acid signatures differentiate marine macrophytes at ordinal and family ranks. *Journal of Phycology* 48 (4):956-965. doi:10.1111/j.1529-8817.2012.01173.x
- Gerasimenko, N. I., Skriptsova, A. V., Busarova, N. G., and Moiseenko, O. P. 2011. Effects of the season and growth stage on the contents of lipids and photosynthetic pigments in brown alga *Undaria pinnatifida*. *Russian Journal of Plant Physiology*, 58: 885-891.
- Gilroy, A., and Edwards, S. J. 1998. Optimum temperature for growth of Australian abalone: preferred temperature and critical thermal maximum for blacklip abalone, *Haliotis rubra* (Leach), and greenlip abalone, *Haliotis laevigata* (Leach). *Aquaculture Research*, 29: 481-485.
- Goldberg, N. 2005. Temporal variation in subtidal macroalgal assemblages at Black Island, Recherche Archipelago. *Journal of the Royal Society of Western Australia*, 88: 65-71.
- Pinchetti, J. L.G., del Campo Fernández, E.d.C., Díez, P.M., and Garcia-Reina, G.. 1998. Nitrogen availability influences the biochemical composition and photosynthesis of tank-cultivated *Ulva rigida* (Chlorophyta). *Journal of Applied Phycology*, 10:383:389.
- Gordillo, F., Jiménez, C., Goutx, M., and Niell, X. 2001. Effects of CO₂ and nitrogen supply on the biochemical composition of *Ulva rigida* with especial emphasis on lipid class analysis. *Journal of Plant Physiology*, 158: 367-373.
- Gosch, B. J., Lawton, R. J., Paul, N. A., de Nys, R., and Magnusson, M. 2015a. Environmental effects on growth and fatty acids in three isolates of *Derbesia tenuissima* (Bryopsidales, Chlorophyta). *Algal Research*, 9: 82-93.

- Gosch, B. J., Magnusson, M., Paul, N. A., and de Nys, R. 2012. Total lipid and fatty acid composition of seaweeds for the selection of species for oil-based biofuel and bioproducts. *GCB Bioenergy*, 4: 919-930.
- Gosch, B. J., Paul, N. A., de Nys, R., and Magnusson, M. 2015b. Spatial, seasonal, and within-plant variation in total fatty acid content and composition in the brown seaweeds *Dictyota bartayresii* and *Dictyopteris australis* (Dictyotales, Phaeophyceae). *Journal of Applied Phycology*, 27: 1607-1622.
- Guest, M. A., Hirst, A. J., Nichols, P. D., and Frusher, S. D. 2010. Multi-scale spatial variation in stable isotope and fatty acid profiles amongst temperate reef species: Implications for design and interpretation of trophic studies. *Marine Ecology Progress Series*, 410: 25-41.
- Guest, M. A., Nichols, P. D., Frusher, S. D., and Hirst, A. J. 2008. Evidence of abalone (*Haliotis rubra*) diet from combined fatty acid and stable isotope analyses. *Marine Biology*, 153: 579-588.
- Guihéneuf, F., Mimouni, V., Ulmann, L., and Tremblin, G. 2009. Combined effects of irradiance level and carbon source on fatty acid and lipid class composition in the microalga *Pavlova lutheri* commonly used in mariculture. *Journal of Experimental Marine Biology and Ecology*, 369: 136-143.
- Hotimchenko, S. V. 2002. Fatty acid composition of algae from habitats with varying amounts of illumination. *Russian Journal of Marine Biology*, 28: 218-220.
- Hurd, C. L., Harrison, P. J., Bischof, K., and Lobban, C. S. 2014. *Seaweed ecology and physiology*, Cambridge University Press, Cambridge.
- Johnson, C. R., Banks, S. C., Barrett, N. S., Cazassus, F., Dunstan, P. K., Edgar, G. J., Frusher, S. D., et al. 2011. Climate change cascades: shifts in oceanography, species' ranges and subtidal marine community dynamics in eastern Tasmania. *Journal of Experimental Marine Biology and Ecology*, 400: 17-32.
- Kendel, M., Couzinet-Mossion, A., Viau, M., Fleurence, J., Barnathan, G., and Wielgosz-Collin, G. 2013. Seasonal composition of lipids, fatty acids, and sterols in the edible red alga *Grateloupia turuturu*. *Journal of Applied Phycology*, 25: 425-432.
- Khotimchenko, S. V., and Yakovleva, I. M. 2005. Lipid composition of the red alga *Tichocarpus crinitus* exposed to different levels of photon irradiance. *Phytochemistry*, 66: 73-79.
- Kim, M.-K., Dubacq, J.-P., Thomas, J.-C., and Giraud, G. 1996. Seasonal variations of triacylglycerols and fatty acids in *Fucus serratus*. *Phytochemistry*, 43:49-55.
- Kumar, M., Kumari, P., Gupta, V., Reddy, C. R. K., and Jha, B. 2010. Biochemical responses of red alga *Gracilaria corticata* (Gracilariales, Rhodophyta) to salinity induced oxidative stress. *Journal of Experimental Marine Biology and Ecology*, 391:27-34.
- Kumari, P., Kumar, M., Reddy, C. R. K., and Jha, B. 2013. Nitrate and phosphate regimes induced lipidomic and biochemical changes in the intertidal macroalga *Ulva lactuca* (Ulvophyceae, Chlorophyta). *Plant and Cell Physiology*, 55:52-63.

- Los, D. A., and Murata, N. 2004. Membrane fluidity and its roles in the perception of environmental signals. *Biochimica et Biophysica Acta (BBA) - Biomembranes*, 1666: 142-157.
- Mai, K., Mercer, J. P., and Donlon, J. 1996. Comparative studies on the nutrition of two species of abalone, *Haliotis tuberculata* L. and *Haliotis discus hannai* Ino. V. The role of polyunsaturated fatty acids of macroalgae in abalone nutrition. *Aquaculture*, 139: 77-89.
- McShane, P. E., Gorfine, H. K., and Knuckey, I. A. 1994. Factors influencing food selection in the abalone *Haliotis rubra* (Mollusca: Gastropoda). *Journal of Experimental Marine Biology and Ecology*, 176: 27-37.
- Mundy C.M., and Jones, H.J. 2016. Tasmanian abalone fishery assessment 2015. Institute for Marine and Antarctic Studies (IMAS), University of Tasmania.
- Mundy C.M., and McAllister, J.D., 2019. Tasmanian abalone fishery assessment 2018. Institute for Marine and Antarctic Studies (IMAS), University of Tasmania.
- Nelson, M. M., Leighton, D. L., Phleger, C. F., and Nichols, P. D. 2002a. Comparison of growth and lipid composition in the green abalone, *Haliotis fulgens*, provided specific macroalgal diets. *Comp Biochem Physiol B Biochem Mol Biol*, 131: 695-712.
- Nelson, M. M., Phleger, C. F., and Nichols, P. D. 2002b. Seasonal lipid composition in macroalgae of the northeastern pacific ocean. *Botanica Marina*, p. 58.
- Oliver, E. C. J., Lago, V., Hobday, A. J., Holbrook, N. J., Ling, S. D., and Mundy, C. N. 2018. Marine heatwaves off eastern Tasmania: trends, interannual variability, and predictability. *Progress in Oceanography*, 161: 116-130.
- Parrish, C. C., Nichols, P. D., Pethybridge, H., and Young, J. W. 2015. Direct determination of fatty acids in fish tissues: quantifying top predator trophic connections. *Oecologia*, 177: 85-95.
- Poore, A. G. B., Graba-Landry, A., Favret, M., Sheppard Brennand, H., Byrne, M., and Dworjanyn, S. A. 2013. Direct and indirect effects of ocean acidification and warming on a marine plant-herbivore interaction. *Oecologia*, 173: 1113-1124.
- R Core Team. 2019. R: A language and environment for statistical computing. R Foundation for Statistical Computing, Vienna, Austria. URL: <https://www.R-project.org/>
- Ridgway, K. R. 2007. Long-term trend and decadal variability of the southward penetration of the East Australian Current. *Geophysical Research Letters*, 34:L13613.
- Roberts, R. 2001. A review of settlement cues for larval abalone (*Haliotis spp.*). *Journal of Shellfish Research*, 20: 571-586.
- Roberts, R. D., Barker, M. F., and Mladenov, P. 2010. Is settlement of *Haliotis iris* larvae on coralline algae triggered by the alga or its surface biofilm? *Journal of Shellfish Research*, 29: 671-678.

- Schmid, M., Guihéneuf, F., and Stengel, D. B. 2014. Fatty acid contents and profiles of 16 macroalgae collected from the Irish Coast at two seasons. *Journal of Applied Phycology*, 26: 451-463.
- Schmid, M., Guihéneuf, F., and Stengel, D. B. 2017a. Ecological and commercial implications of temporal and spatial variability in the composition of pigments and fatty acids in five Irish macroalgae. *Marine Biology*, 164: 158.
- Schmid, M., Guihéneuf, F., and Stengel, D. B. 2017b. Plasticity and remodelling of lipids support acclimation potential in two species of low-intertidal macroalgae, *Fucus serratus* (Phaeophyceae) and *Palmaria palmata* (Rhodophyta). *Algal Research*, 26: 104-114.
- Schmid, M., Kraft, L. G. K., van der Loos, L. M., Kraft, G. T., Virtue, P., Nichols, P. D., and Hurd, C. L. 2018. Southern Australian seaweeds: a promising resource for omega-3 fatty acids. *Food Chemistry*, 265: 70-77.
- Steneck, R. S., Graham, M. H., Bourque, B. J., Corbett, D., Erlandson, J. M., Estes, J. A., and Tegner, M. J. 2002. Kelp forest ecosystems: biodiversity, stability, resilience and future. *Environmental Conservation*, 29: 436-459.
- Venkatesalu, V., Sundaramoorthy, P., Anantharaj, M., Chandrasekaran, M., and Senthilkumar, A. 2012. Seasonal variation on fatty acid composition of some marine macroalgae from Gulf of Mannar Marine Biosphere Reserve, southeast coast of India. *Indian Journal of Marine Sciences*, 41: 442-450.
- Waters, J. M., Wernberg, T., Connell, S. D., Thomsen, M. S., Zuccarello, G. C., Kraft, G. T., Sanderson, J. C., et al. 2010. Australia's marine biogeography revisited: back to the future? *Austral Ecology*, 35: 988-992.
- Wells, M. L., Potin, P., Craigie, J. S., Raven, J. A., Merchant, S. S., Helliwell, K. E., Smith, A. G., et al. 2017. Algae as nutritional and functional food sources: revisiting our understanding. *Journal of Applied Phycology*, 29: 949-982.
- Wernberg, T., and Goldberg, N. 2008. Short-term temporal dynamics of algal species in a subtidal kelp bed in relation to changes in environmental conditions and canopy biomass. *Estuarine, Coastal and Shelf Science*, 76: 265-272.
- Wernberg, T., Thomsen, M. S., Connell, S. D., Russell, B. D., Waters, J. M., Zuccarello, G. C., Kraft, G. T., et al. 2013. The footprint of continental-scale ocean currents on the biogeography of seaweeds. *PLoS ONE*, 8: e80168.
- White, C. A., Bannister, R. J., Dworjanyn, S. A., Husa, V., Nichols, P. D., Kutti, T., and Dempster, T. 2017. Consumption of aquaculture waste affects the fatty acid metabolism of a benthic invertebrate. *Sci Total Environ*, 586: 1170-1181.

Appendices

Appendix 2.1: Dates of sampling for biomass and biochemical composition for each site every season.

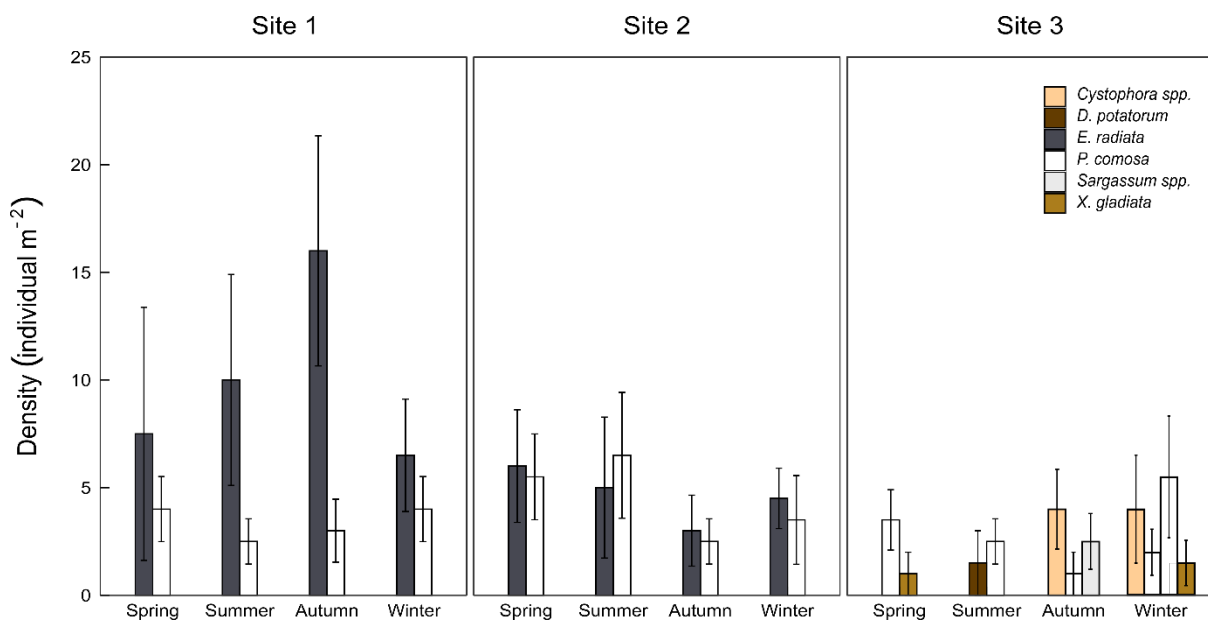
	Season			
	Spring	Summer	Autumn	Winter
Site 1	16/11/2017	15/02/2018	21/05/2018	13/08/2018
Site 2	24/11/2017	27/02/2018	21/06/2018	04/09/2018
Site 3	21/11/2017	13/02/2018	15/06/2018	15/08/2018

Appendix 2.2: Permutational Multivariate Analysis of Variance (PERMANOVA) table for a 3-way PERMANOVA examining fatty acid composition of red and brown seaweed species. Results are shown for the fixed factors Site (2 levels: site 2 and 3), Season (4 levels: Spring, Summer, Autumn and Winter), Group (2 levels: Red and Brown) and all interactions. The table displays degrees of freedom (df), Pseudo F - values and *p* – values.. Significant differences at $\alpha = 0.05$ have *p* – values displayed in bold. The PERMANOVA was conducted on resemblance matrices based on the Bray – Curtis dissimilarity measure. Only fatty acids that were on average 1 % of total fatty acids were included in the analysis.

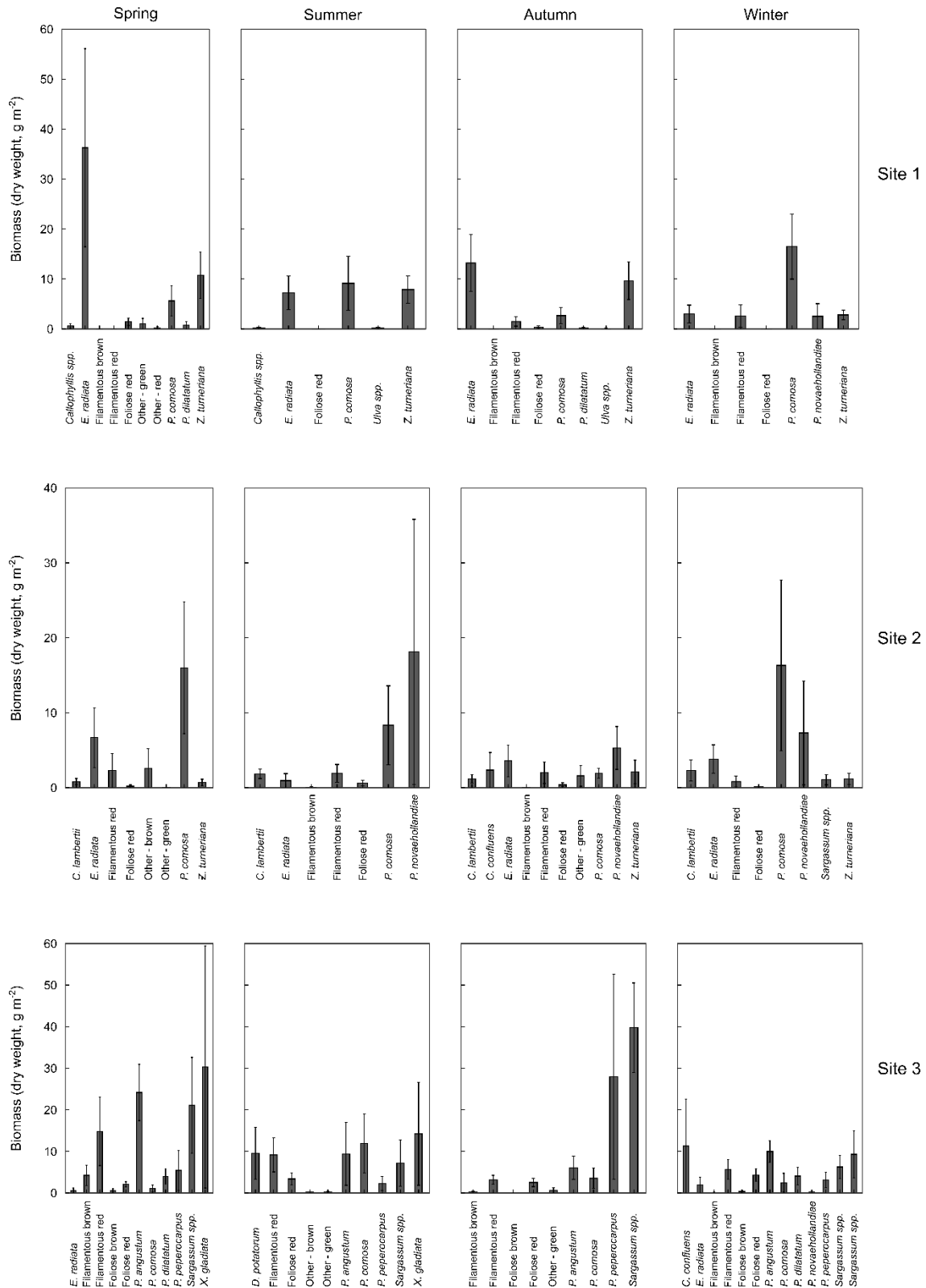
Source	df	Pseudo F - value	<i>p</i> - value (permuted)	Unique permutations
Group	1	254.93	0.0001	9957
Site	1	51.558	0.0001	9953
Season	3	6.2882	0.0001	9923
Group × Site	1	34.615	0.0001	9942
Group × Season	3	6.0385	0.0001	9919
Site × Season	3	4.4625	0.0001	9934
Group × Site × Season	3	2.128	0.0365	9930
Residuals	102			

Appendix 2.3: Analysis of Variance (ANOVA) table for a 3-way ANOVA examining biomass of red and brown seaweed species. Results are shown for the fixed factors Site (3 levels: Site 1, 2 and 3), Season (4 levels: Spring, Summer, Autumn and Winter), Group (2 levels: Red and Brown) and all interactions. The table displays degrees of freedom (df), Sums of Squares (SS), Mean Square (MS), F – values and *p* – values. Significant differences at $\alpha = 0.05$ have *p* – values displayed in bold.

Factor	df	SS	MS	F – value	<i>p</i> – value
Site	2	20.89	10.44	20.71	< 0.0001
Season	3	1.37	0.46	0.90	0.44
Group	1	7.10	7.10	14.08	< 0.001
Site × Season	6	0.94	0.16	0.31	0.93
Site × Group	2	8.45	4.23	8.38	< 0.001
Season × Group	3	0.83	0.28	0.55	0.65
Site × Season × Group	6	4.33	0.72	1.43	0.21
Residuals	168	84.73	0.50		

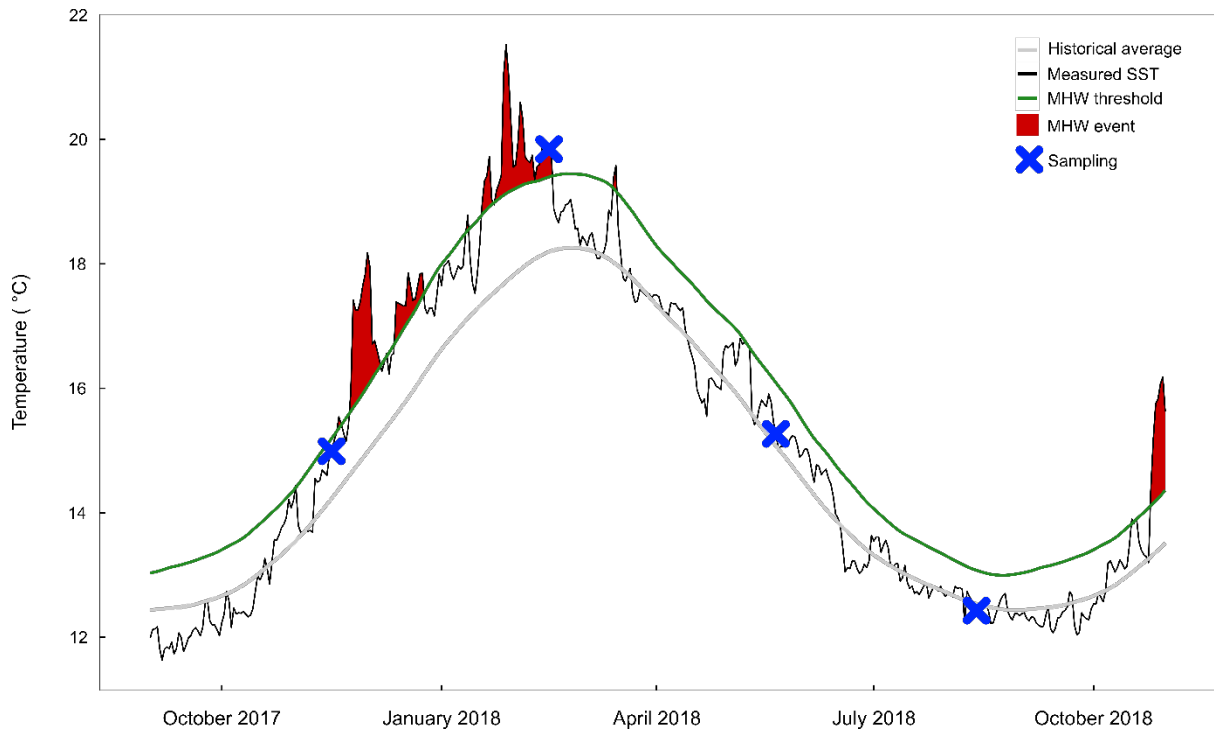


Appendix 2.4: Density of overstory canopy (individuals > 50 cm high m⁻²) at site 1 (left panel), site 2 (middle panel) and site 3 (right panel). Densities are given separately for each species in each season.

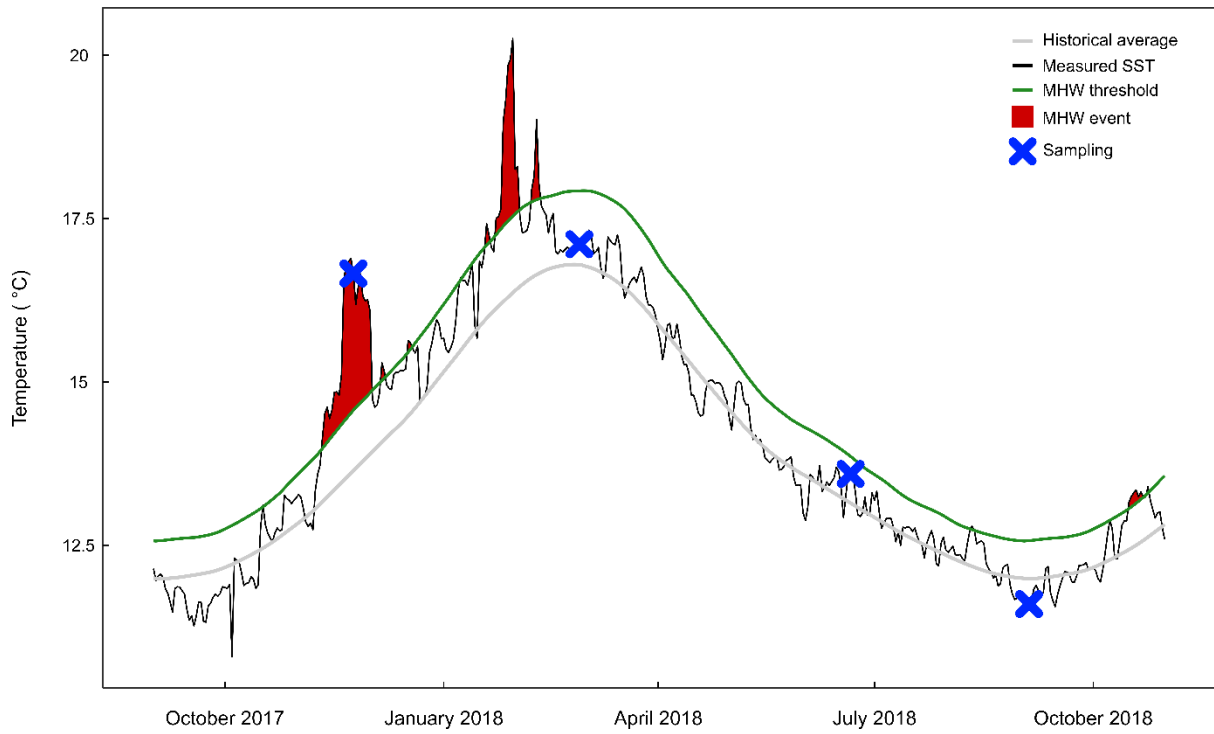


Appendix 2.5: Biomass (dry weight, g m⁻²) of understory species in each season at site 1 (top row), site 2 (middle row) and site 3 (bottom row). Abundant species were identified to species level and if this was not possible then they were identified to genus. Species of low abundance were pooled into

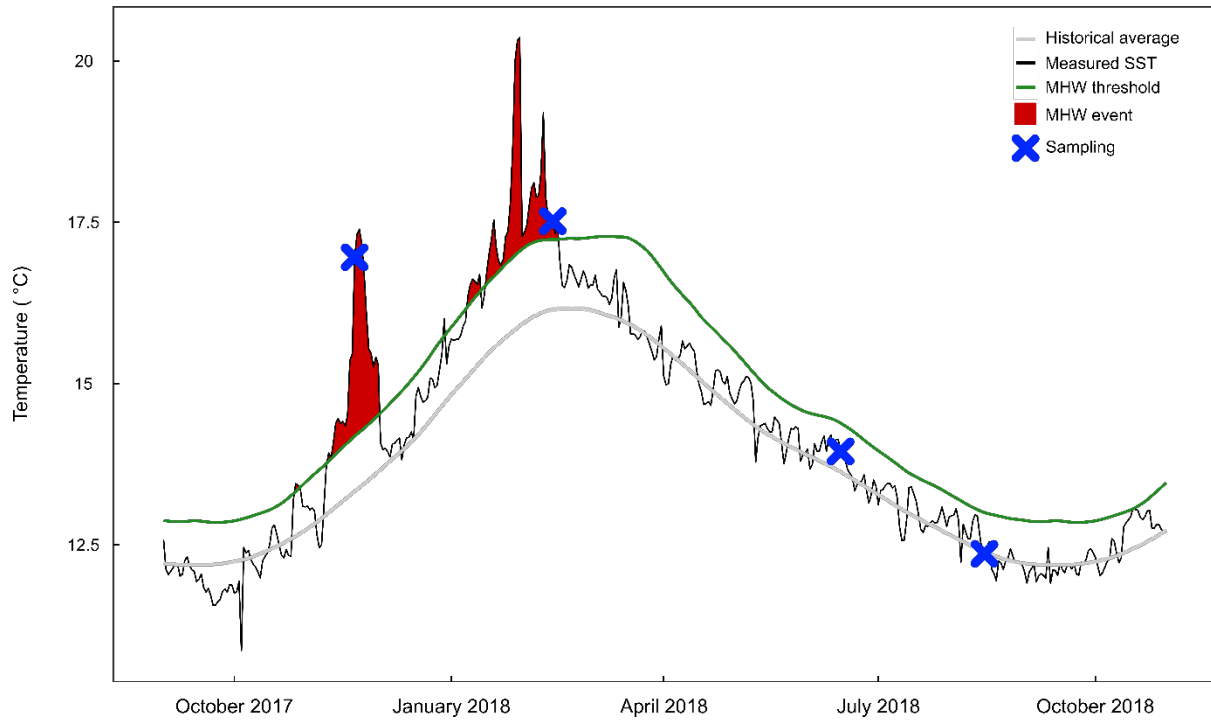
functional groups of: 'filamentous reds', 'foliose reds', 'filamentous browns', 'foliose browns', 'other – green' and 'other – brown'.



Appendix 2.6: Time series of measured sea surface temperature (Measured SST, black line), historical average SST (Historical average, grey line) and threshold temperature for marine heatwave (MHW) events (MHW threshold, green line) at site 1 throughout the study period. Red fill indicates a MHW event as defined by Hobday et al (2016). Blue crosses indicate sampling points.



Appendix 2.7: Time series of measured sea surface temperature (Measured SST, black line), historical average SST (Historical average, grey line) and threshold temperature for marine heatwave (MHW) events (MHW threshold, green line) at site 2 throughout the study period. Red fill indicates a MHW event as defined by Hobday et al (2016). Blue crosses indicate sampling points.



Appendix 2.8: Time series of measured sea surface temperature (Measured SST, black line), historical average SST (Historical average, grey line) and threshold temperature for marine heatwave (MHW) events (MHW threshold, green line) at site 3 throughout the study period. Red fill indicates a MHW event as defined by Hobday et al (2016). Blue crosses indicate sampling points.

Appendix 2.9: Summary of the biochemical composition of main understory species, pooled across all sites and seasons sampled and whether each species was classified as CCM or non-CCM according to Cornwall, Revill and Hurd (2015). Values represent the range of values detected in each species for a compound. Abbreviations: TFA = total fatty acids (% dry weight), SFA = saturated fatty acids (% TFA), PUFA = polyunsaturated fatty acids (% TFA), MUFA = monounsaturated fatty acids (% TFA), n-6:n-3 = ratio of n-6 PUFA to n-3 PUFA, ARA = arachidonic acid (% TFA), EPA = eicosapentaenoic acid (% TFA), C₁₈ n-3 PUFA = 18 carbon chain n-3 polyunsaturated fatty acids, % N = percentage tissue nitrogen. *E. radiata*, *P. comosa* and *Sargassum spp.* were all sampled in one less season for % N relative to fatty acids.

Group	Species	Seasons/sites sampled	TFA	SFA	PUFA	MUFA	n-6: n-3	ARA	EPA	C ₁₈ n-3 PUFA	% N	CCM/ non-CCM
Brown	<i>C. confluens</i>	1	0.70 – 0.87	30.6 – 33.7	42.4 – 47.2	21.9 – 23.9	1.59 – 2.19	17.6 – 20.0	1.55 – 2.85	7.78 – 11.6	1.18 – 1.63	CCM
	<i>D. potatorum</i>	1	1.46 – 2.22	23.3 – 29.1	56.5 – 63.1	12.6 – 14.5	0.44 – 0.60	13.4 – 15.3	6.04 – 7.97	27.8 – 35.9	1.24 – 1.83	CCM
	<i>E. radiata</i>	8	0.98 – 2.17	20.3 – 36.0	40.3 – 62.2	16.4 – 24.9	0.44 – 1.14	7.41 – 21.5	4.32 – 9.81	12.9 – 34.2	1.08 – 2.28	CCM
	<i>P. comosa</i>	8	0.76 – 2.04	13.2 – 37.8	37.8 – 72.0	14.1 – 24.4	0.74 – 1.85	13.2 – 25.0	0.25 – 10.26	9.71 – 26.5	0.90 – 1.60	CCM
	<i>Sargassum spp.</i>	4	1.55 – 2.40	18.1 – 32.2	47.8 – 65.9	14.6 – 20.9	0.43 – 1.05	12.0 – 16.1	7.25 – 12.24	12.8 – 29.5	1.27 – 1.76	CCM
	<i>X. gladiata</i>	2	0.68 – 1.24	27.2 – 31.4	43.8 – 54.3	18.4 – 25.8	1.17 – 2.20	18.8 – 23.9	6.06 – 9.24	6.39 – 14.2	1.00 – 2.84	CCM
	<i>Z. turneriana</i>	4	0.74 – 2.12	25.4 – 37.3	41.0 – 60.2	13.3 – 22.5	0.52 – 2.30	9.51 – 20.9	1.56 – 16.15	5.38 – 12.5	1.55 – 2.33	CCM
Red	<i>C. lambertii</i>	2	0.44 – 0.56	37.8 – 48.5	38.1 – 50.7	11.5 – 14.4	0.10 – 0.28	132.3 – 46.1	0.31 – 2.06	0.41 – 1.04	2.30 – 2.97	non-CCM
	<i>P. angustum</i>	4	0.43 – 1.11	34.7 – 55.4	33.7 – 58.0	5.80 – 11.4	1.53 – 7.54	14.5 – 27.6	0.61 – 19.8	0.48 – 1.29	2.19 – 4.26	non-CCM
	<i>P. novaehollandiae</i>	3	0.81 – 1.21	34.1 – 44.8	47.6 – 57.7	6.04 – 13.5	0.05 – 33.0	22.8 – 33.1	0.24 – 2.78	0.19 – 1.48	3.51 – 4.41	unknown
	<i>P. peperocarpus</i>	1	0.38 – 0.80	40.5 – 50.7	31.0 – 42.9	14.6 – 24.3	0.36 – 0.85	7.23 – 14.0	17.6 – 24.3	0.45 – 1.80	3.13 – 3.62	non-CCM

Appendix 2.10: Analysis of Variance (ANOVA) tables for 2-way ANOVAs examining seasonal variation in both saturated fatty acid (SFA) and polyunsaturated fatty acids (PUFA) in multiple seaweed species at site 2. Results are shown for the fixed factors Season (4 levels: Spring, Summer, Autumn and Winter), Species (3 levels: *E. radiata*, *P. comosa* and *P. novaehollandiae*) and the two-way interaction. The tables display degrees of freedom (df), Sums of Squares (SS), Mean Square (MS), F – values and *p* – values. Significant differences at $\alpha = 0.05$ have *p* – values displayed in bold.

Variable	Factor	df	SS	MS	F – value	<i>p</i> – value
SFA	Season	3	123.27	41.09	6.31	0.001
	Species	2	2481.36	1240.78	190.51	< 0.0001
	Season × species	5	146.94	29.39	4.51	0.002
	Residuals	44	285.56	6.51		
PUFA	Season	3	66.16	22.05	2.32	0.088
	Species	2	581.03	290.52	30.60	< 0.0001
	Season × species	5	257.33	51.47	5.42	< 0.001
	Residuals	44	417.78	9.50		

Appendix 2.11: Analysis of Variance (ANOVA) tables for 2-way ANOVAs examining seasonal variation in both saturated fatty acid (SFA) and polyunsaturated fatty acids (PUFA) in multiple seaweed species at site 3. Results are shown for the fixed factors Season (4 levels: Spring, Summer, Autumn and Winter), Species (2 levels: *P. angustum* and *Sargassum spp.*) and the two-way interaction. The tables display degrees of freedom (df), Sums of Squares (SS), Mean Square (MS), F – values and *p* – values. Significant differences at $\alpha = 0.05$ have *p* – values displayed in bold.

Variable	Factor	df	SS	MS	F – value	<i>p</i> – value
SFA	Season	3	470.21	156.74	19.21	< 0.0001
	Species	1	2639.36	2639.36	323.44	< 0.0001
	Season × species	3	280.50	93.50	11.46	< 0.0001
	Residuals	31	252.97	8.16		
PUFA	Season	3	646.02	215.34	13.54	< 0.0001
	Species	1	703.32	703.32	44.21	< 0.0001
	Season × species	3	351.51	117.17	7.37	< 0.001
	Residuals	31	493.13	15.91		

References

- Cornwall, C. E., Revill, A. T., & Hurd, C. L. (2015). High prevalence of diffusive uptake of CO₂ by macroalgae in a temperate subtidal ecosystem. *Photosynthesis Research*, 124(2), 181-190. doi:10.1007/s11120-015-0114-0
- Hobday, A.J., Alexander, L.V., Perkins, S.E., Smale, D.A., Straub, S.C., Oliver, E.C.J. et al. (2016). A hierarchical approach to defining marine heatwaves. *Progress in Oceanography*, 141, 227-238.

Chapter 3. Responses of seaweeds that use CO₂ as their sole inorganic carbon source to ocean acidification: differential effects of fluctuating pH but little benefit of CO₂ enrichment.

Damon Britton, Craig N. Mundy, Christina M. McGraw, Andrew T. Revill, Catriona L. Hurd

A version of this paper has been published as:

Britton, D., Mundy, C. N., McGraw, C. M., Revill, A. T., & Hurd, C. L. (2019). Responses of seaweeds that use CO₂ as their sole inorganic carbon source to ocean acidification: differential effects of fluctuating pH but little benefit of CO₂ enrichment. ICES Journal of Marine Science. doi:10.1093/icesjms/fsz070.

Abstract

Laboratory studies that test the responses of coastal organisms to ocean acidification (OA) typically use constant pH regimes which do not reflect coastal systems, such as seaweed beds, where pH fluctuates on diel cycles. Seaweeds that use CO₂ as their sole inorganic carbon source (non-CCM species) are predicted to benefit from OA as concentrations of dissolved CO₂ increase, yet this prediction has rarely been tested, and no studies have tested the effect of pH fluctuations on non-CCM seaweeds. We conducted a laboratory experiment in which two ecologically dominant non-CCM red seaweeds (*Callophyllis lambertii* and *Plocamium dilatatum*) were exposed to four pH treatments: two static, pH_T 8.0 and pH_T 7.7 and two fluctuating, pH_T 8.0 ± 0.3 and pH_T 7.7 ± 0.3. Fluctuating pH reduced growth and net photosynthesis in *C. lambertii*, while *P. dilatatum* was unaffected. OA did not benefit *P. dilatatum*, while *C. lambertii* displayed elevated net photosynthetic rates. We provide evidence that carbon uptake strategy alone cannot be used as a predictor of seaweed responses to OA and highlight the importance of species-specific sensitivity to [H⁺]. We

also emphasise the importance of including realistic pH fluctuations in experimental studies on coastal organisms.

Introduction

Anthropogenic greenhouse gas emissions have increased atmospheric CO₂ concentrations from ~ 280 p.p.m since the 1850s to ~ 400 p.p.m in 2018, and they are projected to reach ~ 850 p.p.m by 2100 under the Representative Concentration Pathway (RCP) 6.0 scenario (IPCC, 2014; Hurd et al., 2018). The oceans have absorbed ~ 30% of this emitted CO₂ causing a suite of chemical changes to the seawater carbonate system, termed ocean acidification (OA, Doney et al., 2009). By the year 2100, pH is projected to decline by ~ 0.3 units from current levels (~ pH 8), corresponding to a respective increase in the concentrations of H⁺, CO₂ and HCO₃⁻ of ~ 100 %, 200 % and 14 % (Hurd et al., 2009; IPCC, 2014). Substantial international research effort has been undertaken to examine how marine taxa will respond to OA (Gattuso et al., 2015; Hurd et al., 2018). However, as methods for investigating responses and our understanding evolve, further questions arise such as the relative importance of elevated CO₂ and H⁺ in influencing the response of organisms to OA (van der Loos et al., 2019).

The majority of experimental studies on the responses of coastal organisms to OA have maintained a constant pH regime for the duration of the experiment (Britton et al., 2016; Wahl et al., 2016; Hurd et al., 2018). Such an approach is representative of the open ocean but does not reflect the dynamic nature of coastal systems where local biological (invertebrate and algal metabolism) and physical (e.g. upwelling events) factors alter carbonate chemistry (Hofmann et al., 2011; Baumann and Smith, 2018). In seaweed dominated systems, pH fluctuates on diel cycles as dissolved inorganic carbon (DIC) uptake by seaweeds causes an increase in daytime pH, and release of CO₂ overnight via respiration causes pH to decline (Delille et al., 2009; Hofmann et al., 2011; Cornwall et al., 2013). Organisms in these habitats are subjected to highly variable pH and CO₂ concentrations that can be of a similar magnitude to the changes expected to occur due to OA (Hurd et al., 2011;

Hurd, 2015). Furthermore, it is likely that organisms will respond differently to OA when pH variability is superimposed on the projected pH in 2100 (Cornwall et al., 2013; Roleda et al., 2015; Britton et al., 2016; Wahl et al., 2016).

Seaweeds are important primary producers that support diverse and productive communities in temperate coastal waters through provision of habitat (Dayton, 1985; Steneck et al., 2002; Hurd et al., 2014), as a settlement substratum for invertebrate larvae (Roberts, 2001; Steneck et al., 2002; Nelson, 2009), and as a food source for herbivores (Steneck et al., 2002; Hurd et al., 2014). Calcifying seaweeds (e.g. coralline algae) are thought to respond negatively to OA as their calcium carbonate skeletons are more costly to maintain under reduced pH (McCoy and Kamenos, 2014; Fabricius et al., 2015; Cornwall et al., 2017a). However, the response of non-calcifying (fleshy) seaweeds to OA has received far less attention (Koch et al., 2013; Kroeker et al., 2013; van der Loos et al., 2019). The meta-analysis of Kroeker et al. (2013) suggests that fleshy seaweeds will respond positively to OA, as they will benefit from the projected increase in dissolved CO₂. However, a more recent analysis of the literature suggests that the response of fleshy seaweeds to elevated CO₂ is variable, and partly regulated by their carbon uptake mechanisms and/or their sensitivity to [H⁺] (van der Loos et al., 2019). In addition, most of the studies in the meta-analysis of Kroeker et al. (2013) used constant pH conditions, which does not mimic the natural environment.

Fleshy seaweeds possess a range of carbon acquisition strategies, making predictions of how they will respond to OA difficult (Cornwall et al., 2017; Hepburn et al., 2011; van der Loos et al., 2019). Around 65 % of seaweed species are able to utilise HCO₃⁻ (the most abundant form of DIC in seawater) via a carbon-dioxide concentrating mechanism(s) (CCM), whereas ~ 35 % rely solely on CO₂ which is taken up by passive diffusion (Raven et al., 2005; Kübler and Dudgeon, 2015). To date, the majority (95 %) of studies on fleshy seaweed responses to

OA have focused on CCM-species and generally have found positive responses or no effects (Cornwall et al., 2012; Koch et al., 2013; Kroeker et al., 2013; van der Loos et al., 2019).

Non-CCM species are predicted to benefit from OA, with the additional CO₂ suggested to act as a ‘fertiliser’ by increasing the availability of CO₂ at the site of RuBisCO (Hepburn et al., 2011; Raven, 2011; Cornwall et al., 2015; Kübler and Dudgeon, 2015). However, the response of non-CCM species to OA in multi-day growth experiments has been studied for only three species, with contrasting results: a positive response for 1 species and no effect for 2 species (Kübler et al., 1999; Ho and Carpenter, 2017; van der Loos et al., 2019). Expanding this knowledge is critical for understanding how seaweed assemblages may respond to a future higher CO₂ ocean because up to 90% of some seaweed communities can be comprised of non-CCM species (Cornwall et al., 2015).

The response of photosynthetic organisms to fluctuating pH has been investigated for only 14 species with half of these studies on corals which either benefit or are unaffected by pH fluctuations (Dufault et al., 2012; Comeau et al., 2014; Camp et al., 2016; Chan and Eggins, 2017; Cornwall et al., 2018; Enochs et al., 2018). Rates of growth and photosynthesis are generally reduced under fluctuating pH in coralline algae (Cornwall et al., 2013; Johnson et al., 2014; Roleda et al., 2015), although calcification rates in *Hydrolithon reinboldii* are increased (Cornwall et al 2018) and unaffected in *Porolithon onkodes* (Johnson et al., 2014). Growth and photosynthesis in coastal species of diatoms are unaffected by pH fluctuations whereas oceanic species are negatively affected (Li et al., 2016). The effect of pH fluctuations on fleshy seaweed has been studied for only two species, both known to operate CCMs: the brown seaweed *Ecklonia radiata* (Britton et al., 2016) and the red *Gracillaria lemaneiformis* (Qu et al., 2017). *E. radiata* growth and photosynthetic rates were elevated in fluctuating pH under current pH levels, but under OA conditions growth was unaffected and photosynthetic rates were reduced. *G. lemaneiformis* displayed reduced rates of growth and photosynthesis in fluctuating pH at current pH levels and was unaffected by fluctuations

under OA conditions. There have been no studies on the responses of non-CCM seaweeds to pH fluctuations but their reliance on CO₂ as their inorganic carbon source may make them susceptible to DIC limitation (assuming they are not light-limited) during diel pH cycles because as pH increases during the day, only ~ 0.5 % is present as CO₂ (pH_T 8.2). In the context of OA, pH variability is important as the effect of diel fluctuations in pH on a species can be different when the mean pH is at current day levels or the mean pH expected under OA (Johnson et al., 2014; Britton et al., 2016; Qu et al., 2017).

In this study, we address the knowledge gap on the responses of non-CCM seaweeds to fluctuating pH and OA in a laboratory experiment using two highly abundant sympatric red seaweeds (*Callophyllis lambertii* and *Plocamium dilatatum*), known to be non-CCM species, from southeastern Australia (Cornwall et al., 2015). We hypothesised that 1) diel fluctuating pH would cause reduced rates of both growth and photosynthesis under current ocean conditions due to lower concentrations of CO₂ during the day and this reduction would be ameliorated under future ocean conditions, and 2) both species would have elevated growth and photosynthetic rates under future ocean conditions as the additional CO₂ would alleviate DIC limitation at today's concentrations in both static and fluctuating pH.

Methods

Seaweed collection

Approximately 50 mature individuals of both *Callophyllis lambertii* and *Plocamium dilatatum* were collected by divers using SCUBA at 8 – 10 m depth on the 6th June 2017 at Coal Point, Bruny Island, Tasmania (43.335287° S, 147.324707° E). Individuals were placed in zip-lock bags with enough seawater to prevent desiccation and kept cool in an insulated container during transport to the laboratory 2 hours away.

Pre-experimental treatment

To acclimate individuals to experimental conditions they were cut to experimental size (~ 1.0 g). Each species was subsequently placed in separate 60 L containers with UV-sterilised seawater filtered to 1 μm under constant aeration at 14 °C, which was refreshed daily. Light levels were 80 $\mu\text{mol photons m}^{-2} \text{s}^{-1}$ (similar to light levels at the collection site, Appendix 3.1) on a 12:12 light:dark cycle for 72 hours.

Experimental culture conditions

Experiments were conducted in an automated culture system described in van der Loos et al. (2019), with minor modifications. The seawater in each of 48 culture chambers was replaced every four hours with pH-adjusted seawater. Target pH_T was achieved using mass flow controllers (FMA5418A and FMA5402A, Omega Engineering, USA) to control the ratio of air and CO_2 in a mixed gas that was exposed to the incoming seawater from a single header tank using membrane contactors (3M™ Liqui-Cel™ MM-1×5.5 Series). The culture system was located in a walk-in temperature-controlled room set to experimental conditions of 14 °C, with overhead lighting providing 80 $\mu\text{mol photons m}^{-2} \text{s}^{-1}$ as this was similar to light levels measured at the collection site (Appendix 3.1). Culture chamber seawater was maintained at $13.98 \text{ °C} \pm 0.05$. An automated spectrophotometric pH_T system (McGraw et al., 2010) was integrated into a feedback system for the mass flow controllers to ensure incoming seawater was within 0.03 pH_T from the target value. Although pH_T was measured between 20.95 °C and 23.44 °C, values in this manuscript are reported at the experimental temperature (14 °C). These calculations were conducted in CO2calc (Robbins et al., 2010) using the dissociation constants of Mehrbach et al. (1973), refit by Dickson and Millero (1987) and the known alkalinity, temperature and salinity of the seawater.

Experimental treatments

On day 1 of the 14-day experiment, 24 individuals of each species were added to individual culture chambers. Each individual chamber was exposed to one of four treatments ($n = 6$ replicates for each treatment and species combination): current static ($\text{pH}_T = 8.0$), current fluctuating ($\text{pH}_T = 8.0 \pm 0.3$), future static ($\text{pH}_T = 7.7$) and future fluctuating ($\text{pH}_T = 7.7 \pm 0.3$). The range of pH variability for the fluctuating treatments was informed by measurements of pH *in situ* (range of 0.3 – 0.5, Britton et al., 2016). Static treatments consisted of a constant pH_T over 24 hours; pH_T in fluctuating treatments increased incrementally by 0.2 units every 4 hours in the light and decreased incrementally by 0.2 units every 4 hours in the dark.

To assess how the algae modified the chemical conditions of the seawater within the culture chambers during the four-hour water cycle, additional pH_T measurements were made within randomly selected culture chambers for each treatment 3 h 20 min (measurements of pH_T for each treatment: $n = 72 - 160$) after the seawater was replaced. Seawater samples for nutrient analysis were taken from the header tank ($n = 4$) and in a random subset of chambers for both species at the end of a water cycle (*C. lambertii*: $n = 12$ and *P. dilatatum*: $n = 16$). Samples were filtered with glass microfiber filters (pore size 1.6 μm , Whatman®) and frozen at -20°C in 12 mL polyethylene nutrient tubes. Samples were subsequently thawed and ammonium and nitrate concentrations were determined using a QuickChem® 8000 Automated Ion Analyser (LaChat Instruments).

Seawater samples for DIC measurements were taken on day 13 in a random subset of culture chambers across both fluctuating static treatments ($n = 4$), at the approximate mean pH_T of the current and OA scenarios. Measurements were made when the pH_T of the fluctuating treatments was the same as the static treatments ($\text{pH}_T 8.01$ and $\text{pH}_T 7.64$ at the time of

measurements). Samples were immediately poisoned with HgCl_2 and stored in darkness until later analysis. Measurements were made with a DIC analyser (Apollo SciTech DIC analyser model AS-C3) with an inbuilt CO_2 analyser (LI-COR LI-7000 $\text{CO}_2/\text{H}_2\text{O}$ analyser). The CO_2 analyser was calibrated with a certified reference material provided by Andrew Dickson, Scripps Institute for Oceanography, San Diego, USA. A_T and DIC at the mean pH_T for each treatment was calculated in CO2calc (Robbins et al., 2010) using the constants described above and the known DIC, pH_T , temperature and salinity of the incoming seawater at pH 8.01 and 7.64).

Biotic responses

Relative growth rates (wet weight)

Individuals were blotted dry to remove surface water and weighed immediately prior to, and at the end, of the experiment. Relative growth rates (RGR) were calculated according to Kain (1982).

Photosynthetic and respiration rates

On day 13, oxygen evolution (i.e. net photosynthesis) was measured within each culture chamber at random over 2 hours under the experimental irradiance; oxygen consumption (i.e. respiration) was measured for 1 hour in the dark. All net photosynthesis measurements were made between 10:00 and 16:00 and respiration measurements between 20:00 and 23:00. Dissolved oxygen measurements were made with a portable oxygen meter and optical probe (Hach®, HQ40D Portable Multi Meter and LDO™ probe). Net photosynthetic rates and respiration rates were expressed as $\mu\text{mol O}_2 \text{ g}^{-1} \text{ h}^{-1}$ released or consumed, respectively.

Pigment content, tissue C and N and stable C isotopes

At the end of the experiment, tissue was cut (~ 800 mg) and immediately frozen at -20 °C, then freeze-dried the following day (Labconco® FreezeZone® 4.5). Samples were stored frozen at -20 °C until analysis for chlorophyll *a*, phycocyanin, phycoerythrin, % C, % N and stable C isotopes.

Chlorophyll *a* content was calculated by adding 20 mg of freeze-dried tissue to 4 mL of ethanol and incubating for 24 hours at 4 °C, shaking occasionally (Pritchard et al., 2013). Following incubation samples were centrifuged at 15 000 g for 20 min at 4 °C (Pro-Research, Centurion Scientific Ltd) and the absorbance of aliquots was read at 649 and 665 nm with a UV-VIS spectrophotometer (Dynamica Scientific Ltd. Halo RB-10 UV-VIS ratio beam spectrophotometer). The concentration of chlorophyll *a* in extracts were calculated using the equations of Ritchie (2006) and expressed as mg g⁻¹ dry weight.

For phycocyanin and phycoerythrin, 20 mg of freeze-dried algal tissue was ground with a mortar and pestle and incubated in 5 mL of 0.1M phosphate buffer for 24 hours at 4 °C and shaken occasionally (Pritchard et al., 2013). Following incubation, samples were centrifuged at 15 000 g for 20 min. Aliquots were decanted, and absorbance was read at 564, 592, 455, 618 and 645 nm. The pellet was resuspended in 3 mL of the phosphate buffer and incubated for a further 24 hours at 4 °C. Samples were centrifuged at 15 000 g for 20 min at 4 °C and the absorbance of aliquots were read the same as in the first extraction. The concentration of phycocyanin and phycoxanthin in the extracts were calculated using the equations of Beer and Eshel (1985) and expressed as mg g⁻¹ dry weight.

% C, % N, C:N and $\delta^{13}\text{C}$ were determined using the methods outlined in (Britton et al., 2016). Known amounts (~ 5 mg) of freeze-dried samples were weighed into tin cups (Sercon,

U.K.) and analysed using a NA1500 elemental analyser coupled to a Thermo Scientific Delta V Plus via a ConFlo IV. Combustion and reduction were achieved at 1020 °C and 650 °C respectively. Isotope values were normalised to the VPDB scale via a 3-point calibration using certified reference material and both precision and accuracy were ± 0.1 % (1 SD). % C and N composition for C:N values were calculated by comparison of mass spectrometer peak areas to those of standards with known concentrations.

Statistical analysis

All analyses were conducted in the statistical software R v. 3.5.0. (R Core Team, 2017). Two-way factorial ANOVAs were used to assess whether there were differences between treatments for all response variables with the fixed factors: ‘Type’ (2 levels: fluctuating and static) and ‘Era’ (2 levels: current and future) and the Type \times Era interaction. When a significant interaction was detected (at $\alpha = 0.05$), separate one-way ANOVAs were used to determine differences between ‘Type’ at each level of ‘Era.’ All model fits were inspected to ensure they conformed to the assumptions of the ANOVA model (homogeneity of variances and normality of residuals) using residual vs. fitted plots and normal Q-Q plots. When inspections of the model fit suggested the assumptions were not met, the Box-Cox method (Box and Cox, 1964) was used to determine an appropriate transformation (see Table 3.1). The Box-Cox method suggested drastic transformations for three response variables (C:N, % C and $\delta^{13}\text{C}$ in *C. lambertii*) of Y^{-8} , Y^8 , Y^{-20} respectively. As these transformations were extreme and did not change the interpretation of the model (i.e. no change to significance), we present the results from the untransformed data for these three responses. The ANOVA tables for the transformed data of C:N, % C and $\delta^{13}\text{C}$ can be seen in Appendix 3.2. Three individuals became necrotic within a week of starting the experiment, (future fluctuating: 1 *P. dilatatum* individual, future fluctuating: 2 *C. lambertii* individuals), and were excluded from all analyses.

Results

Experimental culture conditions

pH_T levels were maintained close to target values. The mean pH_T (with standard error in parentheses) of each treatment was as follows: current static = 8.01 (± 0.004), future static = 7.71 (± 0.009), current fluctuating = 8.10 (± 0.013) and future fluctuating = 7.59 (± 0.018). Note that fluctuating treatments have inherently more variability around the mean pH_T. A summary of the carbonate system parameters is shown in Table 3.2. The mean pH_T of seawater entering the culture chambers at the beginning of each 4-hourly cycle is shown in Figure 3.1. The average change in pH_T for each treatment at each water cycle is shown in Appendix 3.3. Average concentrations of ammonium and nitrate at the beginning of each water cycle were $1 \pm 0.05 \mu\text{M}$ and $3.01 \pm 0.07 \mu\text{M}$, respectively. Final concentrations at the end of the water cycle were $1.13 \pm 0.04 \mu\text{M}$ for ammonium and $1.04 \pm 0.07 \mu\text{M}$ for nitrate.

Biotic responses

Relative growth rates (wet weight)

Relative growth rates of *C. lambertii* were 59 % higher on average under static pH relative to fluctuating pH in both current and future ocean conditions (Figure 3.2, Table 3.1). There were no significant differences in the relative growth rates of *P. dilatatum* between treatments (Figure 3.2, Table 3.1).

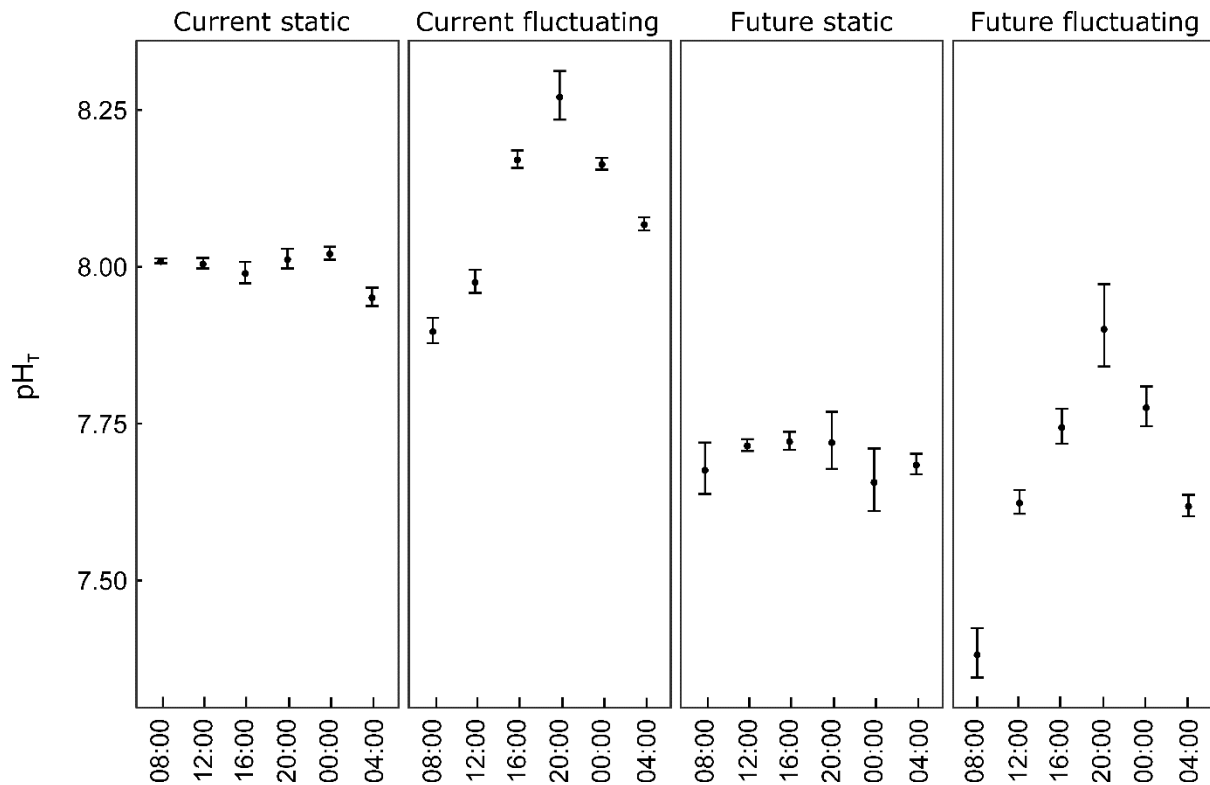


Figure 3.1: Average pH_T of seawater for each treatment following a seawater refresh of the culture chambers (4-hour intervals), error bars are standard error (measurements of pH_T for each treatment: n = 144 – 153).

Photosynthetic and respiration rates

Net photosynthetic rates were 56 % higher for *C. lambertii* cultured under static pH relative to fluctuating pH treatments (pooled means of current and future ocean conditions, interaction non-significant, Figure 3.2, Table 3.1). *C. lambertii* also had 41 % higher net photosynthetic rates when cultured under future ocean conditions relative to current conditions (pooled means of static and fluctuating treatments, interaction non-significant, Figure 3.2, Table 3.1). No differences in the net photosynthetic rates of *P. dilatatum* were observed between treatments (Figure 3.2, Table 3.1). Respiration rates were 470 % higher on average in *C. lambertii* and 194 % higher on average in *P. dilatatum* grown under future ocean conditions relative to current conditions regardless of whether pH was static or fluctuating (Figure 3.2, Table 3.1).

Pigment content, tissue C and N, stable C isotopes,

No significant differences in chlorophyll *a* content was observed between treatments for either species (Table 3.1). Phycocyanin content was, on average, 37% higher for *P. dilatatum* cultured under current ocean conditions relative to future conditions, regardless of whether pH was static or fluctuating (Table 3.1) whereas phycocyanin content did not vary significantly between treatments for *C. lambertii* (Table 3.1). Phycoerythrin was undetectable in both species.

C:N ratios were 7 % higher on average for *C. lambertii* cultured under static pH relative to fluctuating pH (Figure 3.3, Table 3.1), while *P. dilatatum* had 6 % higher C:N ratios on average under fluctuating pH relative to static pH (Figure 3.3, Table 3.1). There was a significant interaction between ‘Type’ and ‘Era’ for % C (Figure 3.3, Table 3.1) and % N in *C. lambertii* (Figure 3.3, Table 3.1). The interaction for % C was caused by % C being lower in individuals cultured under fluctuating pH, but only under future ocean conditions. The interaction for % N was driven by % N content being higher in individuals cultured under fluctuating pH in current ocean conditions while no differences were detected under future ocean conditions. The % C of *P. dilatatum* was not significantly different between treatments (Figure 3.3, Table 3.1) while the % N values were 0.16 % (actual value) higher in individuals cultured under static pH relative to individuals cultured under fluctuating pH (Figure 3.3, Table 3.1). $\delta^{13}\text{C}$ values were unaffected by treatment in *C. lambertii*, while *P. dilatatum* had on average more negative $\delta^{13}\text{C}$ values under future ocean conditions (Table 3.1). Both species had $\delta^{13}\text{C}$ values lower than -30 (*C. lambertii*: -35.49 ± 0.14 on average across treatments, *P. dilatatum*: -32.66 ± 0.19 on average across treatments) indicating that both species were non-CCM species.

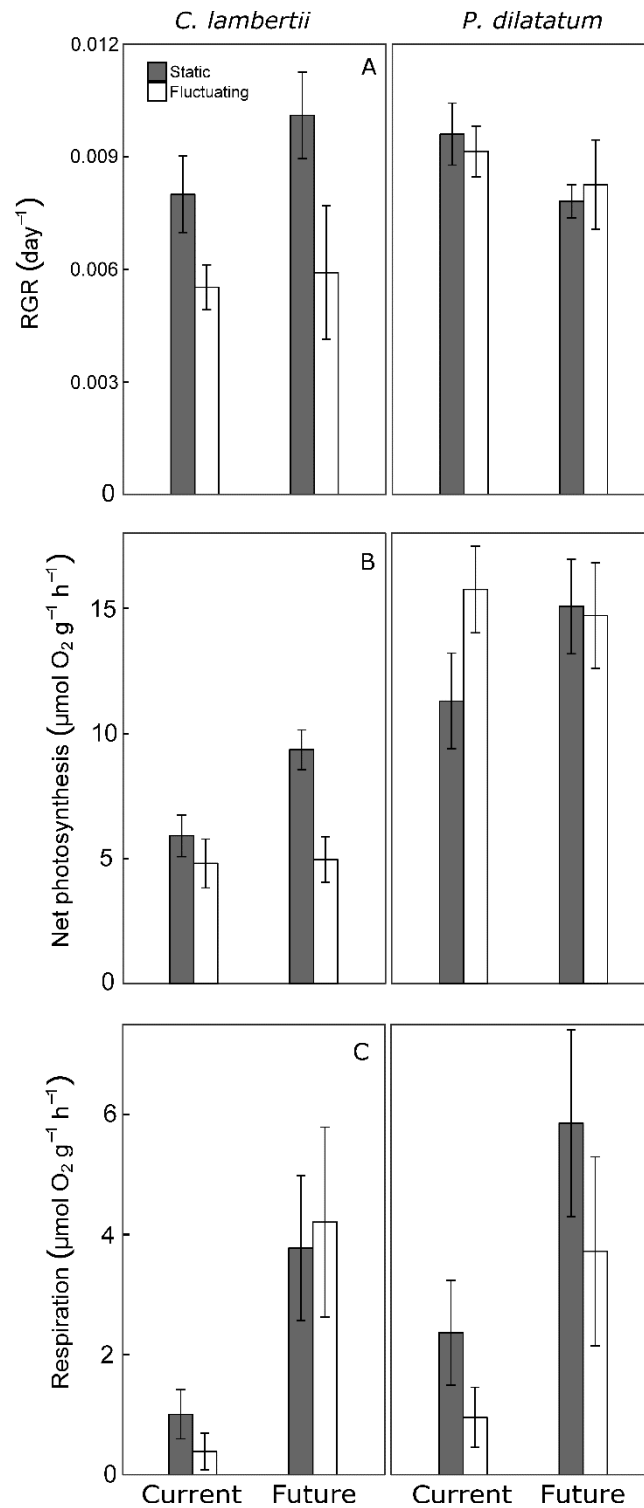


Figure 3.2: Responses of *C. lambertii* (left) and *P. dilatatum* (right) to current and future ocean pH after 14 days in culture. Shaded bars refer to treatments where pH was static and white bars refer to treatments where pH was fluctuating. Response variables and significant differences are as follows: a) Relative growth rates (RGR, day⁻¹), *C. lambertii*: Static > Fluctuating ($p = 0.007$), *P. dilatatum*: no significant differences; b) Net photosynthesis (μmol O₂ g⁻¹ h⁻¹), *C. lambertii*: Static > Fluctuating ($p = 0.007$), Future > Current ($p = 0.041$), *P. dilatatum*: no significant differences, and; c) Respiration (μmol O₂ g⁻¹ h⁻¹) *C. lambertii*: Future > Current ($p = 0.0008$), *P. dilatatum*: Future > Current ($p = 0.013$). Data are presented as means ± standard error, $n = 4 - 6$. All rates are calculated on a wet weight basis.

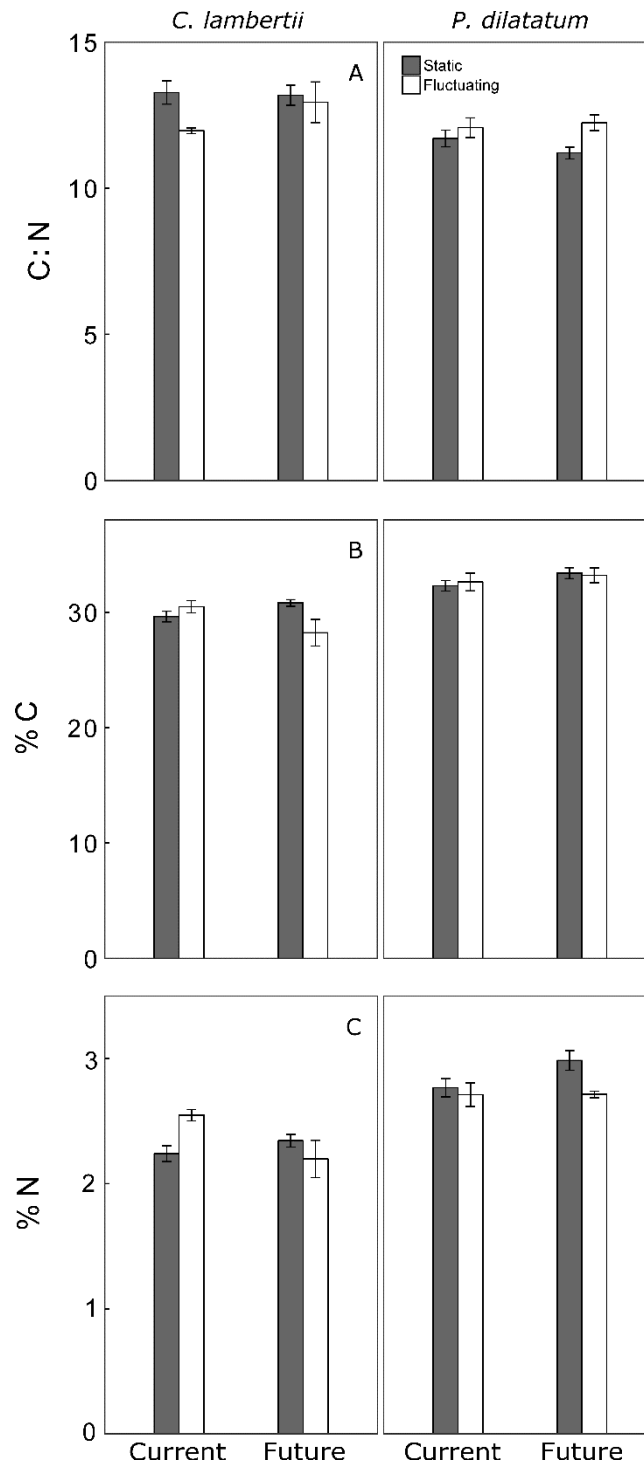


Figure 3.3: Responses of *C. lambertii* (left) and *P. dilatatum* (right) to current and future ocean pH after 14 days in culture. Shaded bars refer to treatments where pH was static and white bars refer to treatments where pH was fluctuating. Response variables and significant differences are as follows: a) C:N ratios, *C. lambertii*: Static > Fluctuating ($p = 0.035$), *P. dilatatum*: Fluctuating > Static ($p = 0.022$); b) % C, *C. lambertii*: Interaction ($p = 0.009$), *P. dilatatum*: no significant differences, and; c) % N, *C. lambertii*: Interaction ($p = 0.008$), *P. dilatatum*: Static > Fluctuating ($p = 0.043$). Data are presented as means \pm standard error, $n = 4 - 6$.

Table 3.1: Analysis of Variance (ANOVA) table for all response variables. The table displays p -values, transformations and the nature of differences for both *C. lambertii* and *P. dilatatum*. Significant effects ($\alpha = 0.05$) have p -values displayed in bold. For differences in main effects ‘Type’ (Two levels: static and fluctuating pH) and ‘Era’ (Two levels: Current and Future), acronyms are displayed: F = future, C = current, S = static and FL = fluctuating. For significant interactions, differences between ‘Type’ are displayed in bold when differences were significant at $\alpha = 0.05$ using separate one-way ANOVAs at each level of ‘Era’. Treatment acronyms: CF = current fluctuating, CS = current static, FF = future fluctuating, FS = future static. Degrees of Freedom = 1 for main effects and the interaction and 17 - 18 for residuals.

Species	Response	Differences	p -value			Transformation
			Type	Era	Type*Era	
<i>C. lambertii</i>	RGR	S > FL	0.007	0.24	0.45	
	Net PS	S > FL, F > C	0.007	0.041	0.086	
	Respiration	F > C	0.44	0.0008	0.37	Y ^{0.4}
	C:N	S > FL	0.035	0.34	0.18	
	% N	CF > CS , FF = FS	0.07	0.19	0.008	
	% C	CF = CS, FF < FS	0.28	0.55	0.009	
	$\delta^{13}\text{C}$	-	0.13	0.25	0.29	
	Chlorophyll	-	0.69	0.075	0.52	log _e Y
	Phycocyanin	-	0.79	0.7	0.13	Y ^{-0.6}
<i>P. dilatatum</i>	RGR	-	0.96	0.1	0.58	
	Net PS	-	0.29	0.45	0.22	
	Respiration	F > C	0.089	0.013	0.99	
	C:N	FL > S	0.022	0.53	0.25	
	% C	-	0.94	0.18	0.67	
	% N	S > FL	0.043	0.14	0.17	
	$\delta^{13}\text{C}$	F < C	0.75	0.0007	0.1	
	Chlorophyll	-	0.3	0.99	0.3	
	Phycocyanin	C > F	0.76	0.046	0.09	Y ⁻¹

Table 3.2: Carbonate system parameters at the mean pH_T of each treatment. pH_T , and salinity were measured while A_T , DIC at mean treatment pH_T , CO_2 and $[H^+]$ were calculated at the mean pH_T of each treatment using the program CO2Calc (Robbins et al., 2010) from the DIC samples measured at pH_T 8.01 and 7.64 and the known salinity, pH_T and temperature of the seawater.

Treatment	pH_T (14 °C)	Salinity (PSU)	DIC ($\mu\text{mol kg}^{-1}$)	A_T ($\mu\text{mol kg}^{-1}$)	CO_2 ($\mu\text{mol kg}^{-1}$)	$[H^+]$ (mol L^{-1})
Current static	8.01	36	2169	2375	17.15	9.77×10^{-9}
Current fluctuating	8.11	36	2119	2375	13.18	7.76×10^{-9}
Future static	7.71	36	2338	2422	38.13	1.95×10^{-8}
Future fluctuating	7.59	36	2378	2422	51.32	2.57×10^{-8}

Discussion

Experimental treatments simulating diel fluctuations in the seawater carbonate system (i.e. pH/H^+ , CO_2 , HCO_3^-) and OA differentially affected two ecologically dominant, temperate non-CCM seaweeds. We hypothesised that both species would have reduced growth and photosynthetic rates in fluctuating pH under current ocean conditions and that these reductions would be ameliorated under future ocean pH. These hypotheses were unsupported, with *C. lambertii* having reduced growth and photosynthetic rates in fluctuating pH regardless of the mean pH (current or future) while those of *P. dilatatum* were unaffected by pH fluctuations. We also hypothesised that elevated CO_2 under OA scenarios would act as a ‘fertiliser’ to benefit both species. There was weak evidence to support this hypothesis for *C. lambertii*, which displayed elevated net photosynthetic rates under the future scenario but no effect on growth. However, there was no evidence of a fertilisation effect for *P. dilatatum* in any OA treatment. Both species are obligate CO_2 -using species and the differential responses indicate that factors other than their passive inorganic carbon uptake strategy (*cf*

Hepburn et al., 2011) are responsible for their response to OA: this finding supports that of van der Loos et al. (2019) who suggest that inorganic carbon uptake strategy alone is not sufficient to predict the responses of fleshy seaweeds to OA. We detected interactive effects of mean pH and pH fluctuations, highlighting the need to incorporate fluctuating pH into experimental treatments when the study organism occurs in naturally fluctuating pH environments such as seaweed beds. Failure to include relevant pH fluctuations that are representative of the natural environment as part of experimental treatments may result in false conclusions being drawn when assessing the response of coastal species to OA.

Responses to fluctuating pH

The contrasting responses of these functionally similar, sympatric seaweeds to fluctuating pH supports the trend in research outcomes demonstrating species-specific responses of photosynthetic organisms to pH fluctuations. To date, the effect of fluctuating pH on photosynthetic organisms has been tested for 16 species and the results have been varied: Table 3.3 displays the growth, photosynthetic, respiration and calcification responses of photosynthetic organisms to fluctuating pH under both current and future ocean pH (see references therein). While there are some general trends such as corals either benefitting or being unaffected and coralline algae being negatively affected (Table 3.3, but see Cornwall et al., 2018), responses are typically species-specific and can even vary within a species e.g. *H. reinboldii* responds differently depending on the collection habitat (Cornwall et al., 2018). Furthermore, as in this study, commonalities between species (e.g. functional group or carbon uptake strategy) do not appear to explain the differential responses to fluctuations: four species of fleshy seaweeds have been tested (including the two in this study) with positive, negative and neutral responses observed (Table 3.3).

We predicted that both species in this study would be negatively affected by fluctuating pH under current ocean conditions due to DIC limitation during periods of high pH in daylight and that this negative effect would be alleviated under future ocean conditions due to increased DIC availability. While this hypothesis held true for *C. lambertii* under current ocean conditions, it was also negatively affected by fluctuating pH in the OA scenario. This suggests that DIC limitation was unlikely to be the driver of the negative response to fluctuating pH. Furthermore, the symmetrical nature of the pH fluctuations in this study (see Figure 3.1) resulted in the total DIC in daylight being similar to that of night time (Appendix 3.4). Additionally, total DIC in static and fluctuating treatments were nearly identical (when compared at current and future mean pH) and only the variability in DIC was different (Appendix 3.4). Therefore, DIC was higher in the fluctuating treatments during the morning and decreased throughout the day. Seaweeds are known to have diurnal cycles in photosynthetic rates independent of light levels (e.g. Mishkind et al., 1979), and differences in the natural circadian rhythms of these species could have contributed to the observed responses in net photosynthesis. For example, if *C. lambertii* had elevated photosynthetic rates towards the end of the day then the reduced DIC availability at this point could have contributed to the negative effect of fluctuating pH. In contrast, *P. dilatatum* may have maximal photosynthetic rates around midday and hence there would have been no differences in DIC availability at this time between static and fluctuating treatments. This may explain why *P. dilatatum* was relatively unaffected by fluctuating pH compared to *C. lambertii*, but any interactive effects of circadian rhythms in photosynthesis and pH fluctuations require testing.

Fluctuations in pH are actually fluctuations in $[H^+]$. Species-specific sensitivity to elevated $[H^+]$ has recently been suggested as a predictor of the response of algae to OA (Bach et al.,

2013; van der Loos et al., 2019) and this may explain, in part, the differential responses of *C. lambertii* and *P. dilatatum* to fluctuating pH. Seaweed must maintain intracellular pH within relatively narrow limits with intracellular pH of photosynthetic organisms varying ~ 0.1 pH units per unit decrease in external pH (Raven, 2011; Raven, 2013) and this likely comes at an energetic cost. As such, energetic demands may be increased in highly variable $[H^+]$ conditions such as those in seaweed beds, which were simulated in this experiment, and these demands may differ between species. Reductions in seawater pH can impair the ability of some phytoplankton to remove excess H^+ from the cell (Taylor et al., 2012), and it is possible this may occur in some seaweed species. Whether or not variability in $[H^+]$ would have similar effects to continually high $[H^+]$ remains unclear however, as no study has tested the effect of variable $[H^+]$ independent of variable DIC. Furthermore, the mechanisms of intracellular pH regulation in seaweeds has only been examined in a few species (Raven and Smith, 1980; Kirst and Bisson, 1982; Gibbon and Kropf, 1993). Studies also employ different experimental methods to achieve fluctuations (see discussion below) and measure different response variables (see Table 3.3). As such, it is difficult to elucidate what changes in the seawater carbonate system are affecting species responses. Further research to separate the effects of variability in DIC and $[H^+]$ and elucidate physiological, biochemical and molecular mechanisms are required if we are to understand why photosynthetic organisms display such varied and unpredictable responses to pH fluctuations. Doing so will allow researchers to understand why different responses to OA are often observed when using static pH treatments compared to the more environmentally relevant fluctuating pH treatments (e.g. Britton et al., 2016; Johnson et al., 2014).

Comparing studies that use different methods to fluctuate pH

For seaweeds, the method used to create diel fluctuations in pH in the laboratory may affect the response of species to the variability in pH. In this study, we used a ‘6-step method’ to create diel fluctuations in which the pH was altered 6 times over 24 h. For seaweeds most studies have used a simple regime consisting of high pH during the day and low pH during the night (hereafter day/night regime, Table 3.3). Exceptions are Cornwall et al. (2018) who used an intermediate change in pH at midday (i.e. 4 steps over 24 hours, hereafter 4-step method) and Qu et al. (2017) who achieved diel fluctuations in pH by increasing the density of cultivated seaweed. For corals and diatoms a range of methods have been employed including continual changes (Li et al., 2016; Enochs et al., 2018), the day/night regime (Dufault et al., 2012; Comeau et al., 2014), the 4-step method (Cornwall et al., 2018), and pumping water into culture chambers directly from mesocosms where biological activity alters carbonate chemistry (Camp et al., 2016; Chan and Eggins, 2017).

While all methods listed above mimic natural fluctuations to some extent, there are inherent differences in the chemistry of each method and comparisons between studies with different methods may be limited. For example the day/night regime results in substantially lower DIC and $\text{CO}_2\text{:HCO}_3^-$ ratios during the day compared to at night and abrupt changes in pH occur between day and night. Conversely, the 4 and 6-step methods have far less abrupt changes in pH and if fluctuations are symmetrical, nearly identical DIC availability and $\text{CO}_2\text{:HCO}_3^-$ ratios between day and night. This distinction is important because photosynthesis by non-CCM species may become more limited by CO_2 availability while photosynthesis is occurring in the day/night regime relative to the 4 or 6-step methods, whereas CCM species grown under a day/night regime may be forced to utilise the more energetically expensive HCO_3^- ; for both uptake strategies the biological responses recorded may be an artefact of the methodology rather than the phenomenon being tested. Furthermore, the relative energetic costs associated with 2 abrupt changes in $[\text{H}^+]$ over 24 hours versus 6 smaller changes or

continual changes remain unknown but are likely to differ. Currently it is difficult to determine whether different methods of achieving diel fluctuations in pH are having substantial impacts on responses due to confounding factors such as type of organism studied (e.g. calcified vs fleshy seaweeds are likely to respond differently), and the response variables measured (see Table 3.3). However, as pH fluctuations do affect the outcomes of experiments, studies should aim to mimic the gradual changes in pH that occur naturally in the field as closely as possible.

Table 3.3: Published responses of photosynthetic organisms to diel fluctuations in pH under ambient and OA conditions. All responses are relative to static pH at the mean pH of the respective scenario (i.e. ~ pH 8.0 and ~ pH 7.7). G = growth, PS = photosynthesis, R = respiration and C = calcification. ‘–’ refers to no effect and blank spaces indicate the variable was not measured or not tested by the authors. The calcification response of *H. reinboldii* under ambient pH from Cornwall et al. (2018) was dependent on the location individuals were collected from. Individuals collected at a site with high pH variability responded positively to fluctuating pH, while those from a site with low pH variability were unaffected.

Organism	Effect of fluctuating pH								Study
	Ambient				OA				
	G	PS	R	C	G	PS	R	C	
Coralline (<i>A. corymbosa</i>)	↓	—			↓	—			Cornwall et al. (2013)
Coralline (<i>A. corymbosa</i> recruits)	↓				↓				Roleda et al. (2015)
Coralline (<i>P. onkodes</i>)		↓		—		—		—	Johnson et al. (2014)
Coralline (<i>H. reinboldii</i>)		—	—	↑/—		—	—	—	Cornwall et al. (2018)
Kelp (<i>E. radiata</i>)	↑	↑			—	↓			Britton et al. (2016)
Red seaweed (<i>G. lemaneiformis</i>)	↓	↓			—	—			Qu et al. (2017)
Red algae (<i>C. lambertii</i>)	↓	↓	—		↓	↓	—		This study
Red algae (<i>P. dilatatum</i>)	—	—	—		—	—	—		This study
Diatom (<i>T. oceanica</i>)	—	↓	↑		↓	—	—		Li et al. (2016)
Diatom (<i>T. weissflogii</i>)	—	—	—		—	—	—		Li et al. (2016)
Coral (<i>S. caliendrum</i>)	↑				↑				Dufault et al. (2012)
Coral (<i>A. hyacinthus</i>)				—				↑	Comeau et al. (2014)
Coral (<i>A. cervicornis</i>)				↑				—	Enochs et al. (2018)
Coral (<i>A. formosa</i>)				↑					Chan and Eggins (2017)
Coral (<i>A. palmata</i>)		—	—	—		—	—	—	Camp et al. (2016)
Coral (<i>A. astreoides</i>)		—	—	—		—	—	—	Camp et al. (2016)
Coral (<i>Goniopora</i> sp.)		—	—	—		—	—	—	Cornwall et al. (2018)

Responses to OA

We predicted that elevated CO₂ would have a ‘fertilisation’ effect and increase the growth and photosynthetic rates of both species. *P. dilatatum* displayed no evidence of an increase in either photosynthesis or growth, while *C. lambertii* showed an increase only in photosynthetic rates. While modelling and theoretical work suggests that non-CCM species should benefit from elevated CO₂ concentrations (Hepburn et al., 2011; Raven, 2011; Cornwall et al., 2015; Kübler and Dudgeon, 2015), experimental work suggests this may not be the case. Of the five non-CCM species tested (including the two in this study) only one has shown an increase in growth rates (Kübler et al., 1999) while the other four species have shown no responses (Ho and Carpenter, 2017; van der Loos et al., 2019; this study). Photosynthetic rates of non-CCM species have not typically been higher under elevated CO₂ (Cornwall et al., 2012; van der Loos et al., 2019; *P. dilatatum* – this study), with the exception of *C. lambertii* in this study. Thus, on current evidence, a lack of a CCM is not a good indicator that a species will benefit from OA.

Species-specific differences in the amount, maximal RuBisCO activity (V_{\max}) and affinity of RuBisCO for CO₂ (K_m) may exist between non-CCM species (Israel and Hophy, 2002; van der Loos et al., 2019) and this could explain why *C. lambertii* had increased photosynthetic rates under future ocean conditions while *P. dilatatum* did not. For example, if the V_{\max} of *C. lambertii* is higher than what can be reached under current CO₂ levels, if it is able to increase the amount of RuBisCO or it has a low K_m , then additional CO₂ may lead to elevated photosynthetic rates. In contrast, if *P. dilatatum* has a V_{\max} that is reached at current CO₂ levels, is unable to increase the amount of RuBisCO or has a high K_m value it may be unable to increase photosynthetic rates under elevated CO₂. Further work examining the species-specific RuBisCO kinetics of non-CCM species are required if we hope to predict the response of fleshy seaweed species and communities to OA.

Elevated $[H^+]$ may also act antagonistically to offset any benefit of elevated DIC. To date, there has only been one study that has assessed the response of seaweed to elevated $[H^+]$ in the context of OA (Roleda et al., 2012): they found a significant reduction in germination of *Macrocystis pyrifera* meiospores when seawater pH was reduced without a simultaneous increase in DIC, whereas, the addition of DIC to seawater with lowered pH ameliorated this reduction. Sensitivity to $[H^+]$ was proposed as an important factor to consider by van der Loos et al. (2019) and this could explain the lack of elevated growth rates for both these species under elevated DIC. Respiration rates were elevated for both species under OA conditions and this increase in metabolic rate was not allocated towards growth or storage as % N, % C and pigment content did not increase in either species and phycocyanin content was slightly reduced under OA conditions in *P. dilatatum*. This raises the possibility that energy was being allocated towards maintaining intracellular pH (Raven, 2011; Raven, 2013) in both species and the increased energy arising from elevated photosynthesis in *C. lambertii* was also allocated to regulation, leading to a lack of an increase in growth rates. However, as we did not explicitly test the mechanisms driving the observed responses, these suggestions are speculative and require experimental testing. Future studies that attempt to separate the relative importance of elevated DIC versus elevated $[H^+]$ are required if we are to predict how species will respond to OA. There is likely a complex interaction between the potential benefit of elevated DIC and the potential negative effects of elevated $[H^+]$ and that the relative importance of these factors may be species-specific (van der Loos et al., 2019).

Interactive effects of pH fluctuations and OA: important implications for interpretations of species and community responses to OA

We detected significant interactions between fluctuating pH and OA for both % N and % C content in *C. lambertii* and weak, non-significant evidence of an interaction for net photosynthesis in *C. lambertii* and phycocyanin content in *P. dilatatum*. The presence of interactive effects of fluctuations and OA has important implications for interpretations of

how coastal species and communities will respond to OA. Coastal species that exist in variable pH environments such as those within seaweed beds and coral reefs may respond differently to OA when pH is either static or fluctuating as in demonstrated in this study and in Table 3.3. For example, if we conducted our study using only static pH and compared the net photosynthetic response of *C. lambertii* between current pH and OA pH we would infer that this species would benefit from OA using a simple one-way ANOVA (see Appendix 3.5). However, if we conducted our study using only fluctuating pH we would infer that the photosynthetic rates of this species would be unaffected by OA (see Appendix 3.5). This simple example, along with the contrasting responses of multiple species to pH fluctuations under current or future ocean pH shown in Table 3.3, clearly demonstrates that research on species that occupy environments with inherent pH variability must incorporate this variability into experimental treatments where possible or we risk making misleading conclusions.

Acknowledgements

We thank Matthias Schmid, Ellie Paine and Fanny Noisette for assistance in the field and the laboratory and for providing valuable insights into the study, and Toby Bolton for his expert support.

Funding sources

DB was supported by a University of Tasmania, Australian Postgraduate Award

References

- Bach, L. T., Mackinder, L. C. M., Schulz, K. G., Wheeler, G., Schroeder, D. C., Brownlee, C., and Riebesell, U. 2013. Dissecting the impact of CO₂ and pH on the mechanisms of photosynthesis and calcification in the coccolithophore *Emiliana huxleyi*. *New Phytologist*, 199: 121-134.
- Baumann, H., and Smith, E. M. 2018. Quantifying metabolically driven pH and oxygen fluctuations in US nearshore habitats at diel to interannual time scales. *Estuaries and Coasts*, 41: 1102-1117.
- Beer, S., and Eshel, A. 1985. Determining phycoerythrin and phycocyanin concentrations in aqueous crude extracts of red algae. *Marine and Freshwater Research*, 36: 785-792.
- Box, G. E., and Cox, D. R. 1964. An analysis of transformations. *Journal of the Royal Statistical Society: Series B (Methodological)*, 26: 211-243.
- Britton, D., Cornwall, C. E., Revill, A. T., Hurd, C. L., and Johnson, C. R. 2016. Ocean acidification reverses the positive effects of seawater pH fluctuations on growth and photosynthesis of the habitat-forming kelp, *Ecklonia radiata*. *Scientific Reports*, 6.
- Britton, D., Schmid, M., Noisette, F., Havenhand, J.N., Paine, E.R., McGraw, C.M. et al. (2020). Adjustments in fatty acid composition is a mechanism that can explain resilience to marine heatwaves and future ocean conditions in the habitat-forming seaweed *Phyllospora comosa* (Labillardière) C.Agardh. *Global Change Biology*. <https://doi.org/10.1111/gcb.15052>
- Camp, E. F., Smith, D. J., Evenhuis, C., Enochs, I., Manzello, D., Woodcock, S., and Suggett, D. J. 2016. Acclimatization to high-variance habitats does not enhance physiological tolerance of two key Caribbean corals to future temperature and pH. *Proceedings of the Royal Society B: Biological Sciences*, 283.
- Chan, W. Y., and Eggins, S. M. 2017. Calcification responses to diurnal variation in seawater carbonate chemistry by the coral *Acropora formosa*. *Coral Reefs*, 36: 763-772.
- Comeau, S., Edmunds, P. J., Spindel, N. B., and Carpenter, R. C. 2014. Diel pCO₂ oscillations modulate the response of the coral *Acropora hyacinthus* to ocean acidification. *Marine Ecology Progress Series*, 501: 99-111.
- Cornwall, C. E., Comeau, S., DeCarlo, T. M., Moore, B., D'Alexis, Q., and McCulloch, M. T. 2018. Resistance of corals and coralline algae to ocean acidification: physiological control of calcification under natural pH variability. *Proceedings of the Royal Society B: Biological Sciences*, 285.
- Cornwall, C. E., Comeau, S., and McCulloch, M. T. 2017a. Coralline algae elevate pH at the site of calcification under ocean acidification. *Global Change Biology*, 23: 4245-4256.
- Cornwall, C. E., Hepburn, C. D., McGraw, C. M., Currie, K. I., Pilditch, C. A., Hunter, K. A., Boyd, P. W., et al. 2013. Diurnal fluctuations in seawater pH influence the response of a calcifying macroalga to ocean acidification. *Proceedings of the Royal Society B: Biological Sciences*, 280: 20132201.

Cornwall, C. E., Hepburn, C. D., Pritchard, D., Currie, K. I., McGraw, C. M., Hunter, K. A., and Hurd, C. L. 2012. Carbon-use strategies in macroalgae: differential responses to lowered pH and implications for ocean acidification. *Journal of Phycology*, 48: 137-144.

Cornwall, C. E., Revill, A. T., Hall-Spencer, J. M., Milazzo, M., Raven, J. A., and Hurd, C. L. 2017b. Inorganic carbon physiology underpins macroalgal responses to elevated CO₂. *Scientific Reports*, 7: 46297.

Cornwall, C. E., Revill, A. T., and Hurd, C. L. 2015. High prevalence of diffusive uptake of CO₂ by macroalgae in a temperate subtidal ecosystem. *Photosynthesis Research*, 124: 181-190.

Dayton, P. K. 1985. Ecology of kelp communities. *Annual review of ecology and systematics*, 16: 215-245.

Delille, B., Borges, A. V., and Delille, D. 2009. Influence of giant kelp beds (*Macrocystis pyrifera*) on diel cycles of pCO₂ and DIC in the Sub-Antarctic coastal area. *Estuarine, Coastal and Shelf Science*, 81: 114-122.

Dickson, A. G., and Millero, F. J. 1987. A comparison of the equilibrium constants for the dissociation of carbonic acid in seawater media. *Deep Sea Research Part A. Oceanographic Research Papers*, 34: 1733-1743.

Doney, S. C., Fabry, V. J., Feely, R. A., and Kleypas, J. A. 2009. Ocean acidification: the other CO₂ problem. *Annual Review of Marine Science*, 1: 169-192.

Dufault, A. M., Cumbo, V. R., Fan, T. Y., and Edmunds, P. J. 2012. Effects of diurnally oscillating pCO₂ on the calcification and survival of coral recruits. *Proceedings of the Royal Society B: Biological Sciences*, 279: 2951-2958.

Enochs, I. C., Manzello, D. P., Jones, P. J., Aguilar, C., Cohen, K., Valentino, L., Schopmeyer, S., et al. 2018. The influence of diel carbonate chemistry fluctuations on the calcification rate of *Acropora cervicornis* under present day and future acidification conditions. *Journal of Experimental Marine Biology and Ecology*, 506: 135-143.

Fabricius, K. E., Klubenschedl, A., Harrington, L., Noonan, S., and De'ath, G. 2015. *In situ* changes of tropical crustose coralline algae along carbon dioxide gradients. *Scientific Reports*, 5: 9537.

Gattuso, J. P., Magnan, A., Billé, R., Cheung, W. W. L., Howes, E. L., Joos, F., Allemand, D., et al. 2015. Contrasting futures for ocean and society from different anthropogenic CO₂ emissions scenarios. *Science*, 349.

Gibbon, B. C., and Kropf, D. L. 1993. Intracellular pH and its regulation in *Pelvetia* zygotes. *Developmental Biology*, 157: 259-268.

Hepburn, C. D., Pritchard, D. W., Cornwall, C. E., McLeod, R. J., Beardall, J., Raven, J. A., and Hurd, C. L. 2011. Diversity of carbon use strategies in a kelp forest community: implications for a high CO₂ ocean. *Global Change Biology*, 17: 2488-2497.

- Ho, M., and Carpenter, R. C. 2017. Differential growth responses to water flow and reduced pH in tropical marine macroalgae. *Journal of Experimental Marine Biology and Ecology*, 491: 58-65.
- Hofmann, G. E., Smith, J. E., Johnson, K. S., Send, U., Levin, L. A., Micheli, F., Paytan, A., et al. 2011. High-frequency dynamics of ocean pH: a multi-ecosystem comparison. *PLoS ONE*, 6: e28983.
- Hurd, C. L. 2015. Slow-flow habitats as refugia for coastal calcifiers from ocean acidification. *Journal of Phycology*, 51: 599-605.
- Hurd, C. L., Cornwall, C. E., Currie, K., Hepburn, C. D., McGraw, C. M., Hunter, K. A., and Boyd, P. W. 2011. Metabolically induced pH fluctuations by some coastal calcifiers exceed projected 22nd century ocean acidification: a mechanism for differential susceptibility? *Global Change Biology*, 17: 3254-3262.
- Hurd, C. L., Harrison, P. J., Bischof, K., and Lobban, C. S. 2014. *Seaweed ecology and physiology*, Cambridge University Press, Cambridge.
- Hurd, C. L., Hepburn, C. D., Currie, K. I., Raven, J. A., and Hunter, K. A. 2009. Testing the effects of ocean acidification on algal metabolism: considerations for experimental designs. *Journal of Phycology*, 45: 1236-1251.
- Hurd, C. L., Lenton, A., Tilbrook, B., and Boyd, P. W. 2018. Current understanding and challenges for oceans in a higher-CO₂ world. *Nature Climate Change*, 8: 686-694.
- IPCC. 2014. *Climate Change 2014: Synthesis Report. Contribution of Working Groups I, II and III to the Fifth Assessment Report of the Intergovernmental Panel on Climate Change* [Core Writing Team, R.K. Pachauri and L.A. Meyer (eds.)]. IPCC, Geneva, Switzerland. 151 pp.
- Israel, A., and Hophy, M. 2002. Growth, photosynthetic properties and RuBisCO activities and amounts of marine macroalgae grown under current and elevated seawater CO₂ concentrations. *Global Change Biology*, 8: 831-840.
- Johnson, M. D., Moriarty, V. W., and Carpenter, R. C. 2014. Acclimatization of the crustose coralline alga *Porolithon onkodes* to variable pCO₂. *PLoS ONE*, 9: e87678.
- Kain, J. M. 1982. Morphology and growth of the giant kelp *Macrocystis pyrifera* in New Zealand and California. *Marine Biology*, 67: 143-157.
- Kirst, G. O., and Bisson, M. A. 1982. Vacuolar and cytoplasmic pH, ion composition, and turgor pressure in *Lamprothamnium* as a function of external pH. *Planta*, 155: 287-295.
- Koch, M., Bowes, G., Ross, C., and Zhang, X.-H. 2013. Climate change and ocean acidification effects on seagrasses and marine macroalgae. *Global Change Biology*, 19: 103 - 132.
- Kroeker, K. J., Kordas, R. L., Crim, R., Hendriks, I. E., Ramajo, L., Singh, G. S., Duarte, C. M., et al. 2013. Impacts of ocean acidification on marine organisms: quantifying sensitivities and interaction with warming. *Global Change Biology*, 19: 1884-1896.

Kübler, J. E., and Dudgeon, S. R. 2015. Predicting effects of ocean acidification and warming on algae lacking carbon concentrating mechanisms. PLoS ONE, 10: e0132806.

Kübler, J. E., Johnston, A. M., and Raven, J. A. 1999. The effects of reduced and elevated CO₂ and O₂ on the seaweed *Lomentaria articulata*. Plant, Cell and Environment, 22: 1303-1310.

Li, F., Wu, Y., Hutchins, D. A., Fu, F., and Gao, K. 2016. Physiological responses of coastal and oceanic diatoms to diurnal fluctuations in seawater carbonate chemistry under two CO₂ concentrations. Biogeosciences, 13: 6247-6259.

Maberly, S., Raven, J., and Johnston, A. 1992. Discrimination between ¹²C and ¹³C by marine plants. Oecologia, 91: 481-492.

McCoy, S. J., and Kamenos, N. A. 2014. Coralline algae (Rhodophyta) in a changing world: integrating ecological, physiological, and geochemical responses to global change. Journal of Phycology, 51: 6-24.

McGraw, C. M., Cornwall, C. E., Reid, M. R., Currie, K. I., Hepburn, C. D., Boyd, P., Hurd, C. L., et al. 2010. An automated pH-controlled culture system for laboratory-based ocean acidification experiments. Limnology and Oceanography: Methods, 8: 686-694.

Mehrbach, C., Culberson, C. H., Hawley, J. E., and Pytkowicz, R. M. 1973. Measurement of the apparent dissociation constants of carbonic acid in seawater at atmospheric pressure. Limnology and Oceanography, 18: 897-907.

Mishkind, M., Mauzerall, D., and Beale, S. I. 1979. Diurnal variation *in situ* of photosynthetic capacity in *Ulva* is caused by a dark reaction. Plant Physiology, 64: 896.

Nelson, W. A. 2009. Calcified macroalgae critical to coastal ecosystems and vulnerable to change: a review. Marine and Freshwater Research, 60: 787-801.

Pritchard, D. W., Hurd, C. L., Beardall, J., and Hepburn, C. D. 2013. Survival in low light: Photosynthesis and growth of a red alga in relation to measured *in situ* irradiance. Journal of Phycology, 49: 867-879.

Qu, L., Xu, J., Sun, J., Li, X., and Gao, K. 2017. Diurnal pH fluctuations of seawater influence the responses of an economic red macroalga *Gracilaria lemaneiformis* to future CO₂-induced seawater acidification. Aquaculture, 473: 383-388.

R Core Team 2017. R: A language and environment for statistical computing. R Foundation for Statistical Computing, Vienna, Austria. URL: <https://www.R-project.org/>.

Raven, J. 2013. Half a century of pursuing the pervasive proton. In Progress in Botany, pp. 3-34. Ed. by U. Lüttge, W. Beyschlag, D. Francis, and J. Cushman. Springer Berlin Heidelberg.

Raven, J., and Smith, F. 1980. Intracellular pH regulation in the giant-celled marine alga *Chaetomorpha darwinii*. Journal of Experimental Botany, 31: 1357-1369.

Raven, J. A. 2011. Effects on marine algae of changed seawater chemistry with increasing atmospheric CO₂. Biology and Environment, 111: 1-17.

- Raven, J. A., Ball, L. A., Beardall, J., Giordano, M., and Maberly, S. C. 2005. Algae lacking carbon-concentrating mechanisms. *Canadian Journal of Botany*, 83: 879-890.
- Ritchie, R. J. 2006. Consistent sets of spectrophotometric chlorophyll equations for acetone, methanol and ethanol solvents. *Photosynthesis Research*, 89: 27-41.
- Robbins, L. L., Hansen, M. E., Kleypas, J. A., and Meylan, S. C. 2010. CO2calc—A user-friendly seawater carbon calculator for Windows, Max OS X, and iOS (iPhone). U.S. Geological Survey Open-File Report 2010, 1280: 17.
- Roberts, R. 2001. A review of settlement cues for larval abalone (*Haliotis spp.*). *Journal of Shellfish Research*, 20: 571-586.
- Roleda, M. Y., Cornwall, C. E., Feng, Y., McGraw, C. M., Smith, A. M., and Hurd, C. L. 2015. Effect of ocean acidification and pH fluctuations on the growth and development of coralline algal recruits, and an associated benthic algal assemblage. *PLoS ONE*, 10.
- Roleda, M. Y., Morris, J. N., McGraw, C. M., and Hurd, C. L. 2012. Ocean acidification and seaweed reproduction: Increased CO₂ ameliorates the negative effect of lowered pH on meiospore germination in the giant kelp *Macrocystis pyrifera* (Laminariales, Phaeophyceae). *Global Change Biology*, 18: 854-864.
- Steneck, R. S., Graham, M. H., Bourque, B. J., Corbett, D., Erlandson, J. M., Estes, J. A., and Tegner, M. J. 2002. Kelp forest ecosystems: biodiversity, stability, resilience and future. *Environmental Conservation*, 29: 436-459.
- Taylor, A. R., Brownlee, C., and Wheeler, G. L. 2012. Proton channels in algae: reasons to be excited. *Trends in Plant Science*, 17: 675-684.
- van der Loos, L. M., Schmid, M., Leal, P. P., McGraw, C. M., Britton, D., Revill, A. T., Virtue, P., et al. 2019. Responses of macroalgae to CO₂ enrichment cannot be inferred solely from their inorganic carbon uptake strategy *Ecology and Evolution*: 1-16.
- Wahl, M., Saderne, V., and Sawall, Y. 2016. How good are we at assessing the impact of ocean acidification in coastal systems? Limitations, omissions and strengths of commonly used experimental approaches with special emphasis on the neglected role of fluctuations. *Marine and Freshwater Research*, 67: 25-36.

Appendices

Appendix 3.1: Light levels (photosynthetically active radiation, PAR) measured at four depths during collection of *C. lambertii* and *P. dilatatum* individuals at Coal Point, Bruny Island, Tasmania, Australia (43.335287° S, 147.324707° E). Values represent the average PAR recorded over 2 min intervals at each depth.

Depth (m)	PAR ($\mu\text{mol photons m}^{-2} \text{ s}^{-1}$)
0	1329
2	210
4.5	151
9	50

Appendix 3.2: Analysis of Variance (ANOVA) table for transformed data of C:N ratios, % C and % N for *C. lambertii*. The table displays *p*-values, transformations, and the nature of differences. Significant effects ($\alpha = 0.05$) have *p*-values displayed in bold. There are no changes to significance ($\alpha = 0.05$) compared to the untransformed data presented in the main text. For differences in main effects acronyms are displayed: F = future, C = current, S = static and FL = fluctuating. For significant interactions, differences between 'Type' are displayed in bold when differences were significant at $\alpha = 0.05$ using separate one-way ANOVAs at each level of 'Era'. Treatment acronyms: CF = current fluctuating, CS = current static, FF = future fluctuating, FS = future static. Degrees of Freedom = 1 for main effects and the interaction and 18 for residuals.

Response	Differences	<i>p</i> -value			Transformation
		Type	Era	Type \times Era	
C:N	S > FL	0.004	0.23	0.13	Y ⁻⁸
% C	CF = CS, FF < FS	0.43	0.74	0.008	Y ⁸
$\delta^{13}\text{C}$	-	0.15	0.36	0.55	Y ⁻²⁰

Appendix 3.3: Average change in pH (upper and lower standard error in parentheses) within culture tanks 3 hours and 20 min after each seawater refresh for all treatments. N = 22 – 28.

Time	Δ pH					
	8am	12pm	4pm	8pm	12am	4am
Treatment						
Current static	0.02 (0.01, -0.01)	0.10 (0.03, -0.02)	0.05 (0.01, -0.01)	-0.05 (0.02, -0.02)	-0.08 (0.01, -0.01)	-0.04 (0.01, -0.01)
Current fluctuating	0.03 (0.06, -0.05)	0.05 (0.02, -0.02)	-0.02 (0.01, -0.01)	-0.02 (0.03, -0.03)	-0.02 (0.01, -0.01)	0.01 (0.02, -0.02)
Future static	0.03 (0.01, -0.01)	0.12 (0.01, -0.01)	0.12 (0.01, -0.01)	0.03 (0.01, -0.01)	0.07 (0.08, -0.07)	-0.01 (0.02, -0.02)
Future fluctuating	0.17 (0.02, -0.02)	0.11 (0.03, -0.03)	0.05 (0.04, -0.04)	-0.08 (0.03, -0.03)	-0.04 (0.03, -0.03)	0.02 (0.03, -0.02)

Appendix 3.4: average concentrations of seawater CO₂, HCO₃⁻ and dissolved inorganic carbon (DIC) in each treatment during daylight, night time and the average over 24 hours.

Treatment		CO₂ (μmol kg⁻¹)	HCO₃⁻ (μmol kg⁻¹)	DIC (μmol kg⁻¹)
Daylight	Current Fluctuating	14.2	1927	2132
	Current Static	16.7	2011	2185
	Future Fluctuating	43.4	2183	2314
	Future Static	35.4	2183	2306
Night time	Current Fluctuating	13.4	1913	2123
	Current Static	17.0	2015	2187
	Future Fluctuating	42.8	2179	2311
	Future Static	36.8	2189	2311
24 hours	Current Fluctuating	13.8	1920	2128
	Current Static	16.9	2013	2186
	Future Fluctuating	43.1	2181	2312
	Future Static	36.1	2186	2309

Appendix 3.5: Analysis of Variance (ANOVA) tables of one-way ANOVAs comparing net photosynthetic rates between ‘Era’ (current and future) for each pH regime (static and fluctuating). Df = degrees of freedom, SS = sums of squares, MS = mean square. Significant effects ($\alpha = 0.05$) have *p*-values displayed in bold.

pH regime	component	Df	SS	MS	F-value	<i>p</i> -value
Static	Era	1	35.47	35.47	8.916	0.0137
	Error	10	39.78	3.98		
Fluctuating	Era	1	0.06	0.058	0.012	0.915
	error	8	38.72	4.84		

Chapter 4. Adjustments in fatty acid composition is a mechanism that can explain resilience to marine heatwaves and future ocean conditions in the habitat-forming seaweed *Phyllospora comosa* (Labillardière) C.Agardh.

Damon Britton, Matthias Schmid, Fanny Noisette, Jonathan N. Havenhand, Ellie R. Paine, Christina M. McGraw, Andrew T. Revill, Patti Virtue, Peter D. Nichols, Craig N. Mundy, Catriona L. Hurd

A version of this chapter has been published as:

Britton, D., Schmid, M., Noisette, F., Havenhand, J.N., Paine, E.R., McGraw, C.M., Revill, A.T., Virtue, P., Nichols, P.D., Mundy, C.N. & Hurd, C.L., (2020). Adjustments in fatty acid composition is a mechanism that can explain resilience to marine heatwaves and future ocean conditions in the habitat-forming seaweed *Phyllospora comosa* (Labillardière) C.Agardh. *Global Change Biology*. 26: 3512– 3524. <https://doi.org/10.1111/gcb.15052>

Abstract

Marine heatwaves are extreme events that can have profound and lasting impacts on marine species. Field observations have shown seaweeds to be highly susceptible to marine heatwaves, but the physiological drivers of this susceptibility are poorly understood. Furthermore, the effects of marine heatwaves in conjunction with ocean warming and acidification are yet to be investigated. To address this knowledge gap, we conducted a laboratory culture experiment in which we tested the growth and physiological responses of

Phyllospora comosa juveniles from the southern extent of its range (43 - 31° S) to marine heatwaves, ocean warming and acidification. We used a “collapsed factorial design” in which marine heatwaves were superimposed on current (today’s pH and temperature) and future (pH and temperature projected by 2100) ocean conditions. Responses were tested both during the heatwaves, and after a seven-day recovery period. Heatwaves reduced net photosynthetic rates in both current and future conditions, while respiration rates were elevated under heatwaves in the current conditions only. Following the recovery period, there was little evidence of heatwaves having lasting negative effects on growth, photosynthesis or respiration. Exposure to heatwaves, future ocean conditions or both caused an increase in the degree of saturation of fatty acids. This adjustment may have counteracted negative effects of elevated temperatures by decreasing membrane fluidity, which increases at higher temperatures. Furthermore, *P. comosa* appeared to down-regulate the energetically expensive carbon dioxide concentrating mechanism (CCM) in the future conditions with a reduction in $\delta^{13}\text{C}$ values detected in these treatments. Any saved energy arising from this down-regulation was not invested in growth and was likely invested in the adjustment of fatty acid composition. This adjustment is a mechanism by which *P. comosa* and other seaweeds may tolerate the negative effects of ocean warming and marine heatwaves through benefits arising from ocean acidification.

Introduction

Anthropogenic greenhouse gas emissions have caused average global sea surface temperatures to increase by ~ 0.11 °C per decade since 1880 (IPCC, 2014). A further increase of ~ 1.5 °C is projected by 2100 under the *Representative Concentration Pathway* 6.0 scenario (RCP 6.0, IPCC, 2014), termed ocean warming. Concurrently, the sustained absorption of rising atmospheric CO₂ by the oceans has increased dissolved CO₂ concentrations and reduced ocean pH by around 0.1 unit (IPCC, 2014), termed ocean acidification. By the end of the century, seawater CO₂ concentrations are projected to increase by ~ 200 %, with a corresponding decline in pH of ~ 0.3 units (i.e. a 100 % increase in H⁺ concentration, RCP 6.0, IPCC, 2014). While climate change is often considered as the change in the mean value of factor such as temperature, it is becoming increasingly defined by the occurrence of extreme events which can drastically impact ecosystem function (Allen et al., 2010; Wernberg et al., 2016).

Marine heatwaves are extreme localised warming events which are predicted to increase in intensity and duration in the future (Frölicher et al., 2018; Oliver et al., 2018a; Oliver et al., 2018b). They are defined as a warming event of five or more days that is warmer than the 90th percentile of average seasonal temperatures over the previous 30 years (Hobday et al. 2016). Already marine heatwaves are having detrimental and lasting impacts on marine systems, causing mass mortality of macro invertebrates (Garrahou et al., 2009), the downturn of commercially important fisheries (Mills et al., 2013) and substantial loss of canopy-forming seaweeds (Smale & Wernberg, 2013; Thomsen et al., 2019; Wernberg et al., 2016). As such, marine heatwaves, in combination with ocean warming and ocean acidification, are likely to have profound effects on the structure and functioning of marine ecosystems in the future (Hurd et al., 2018; IPCC, 2014; Poloczanska et al., 2016; Smale et al., 2019).

Seaweed beds are some of the most diverse and productive ecosystems in the world and provide complex biogenic habitat for a variety of species (Hurd et al., 2014; Steneck et al., 2002); however, they are under threat from a range of anthropogenic stressors including eutrophication, over-harvesting of invertebrate predators, invasive species and climate change (Filbee-Dexter & Wernberg, 2018; Krumhansl et al., 2016; Ling et al., 2009; Mineur et al., 2015). Ocean warming has been implicated in the decline of seaweed beds globally (Filbee-Dexter et al., 2016; Johnson et al., 2011; Voerman et al., 2013), while marine heatwaves have caused localised die-back events and substantial canopy loss (Smale & Wernberg, 2013; Thomsen et al., 2019; Wernberg et al., 2016). The effects of ocean acidification on seaweeds are species-specific with some benefitting, others unaffected and some negatively affected (Britton et al., 2016; Cornwall et al., 2017; Hurd et al., 2018; van der Loos et al., 2019). Despite predictions that seaweeds will undergo substantial range contractions by the end of the century due to global ocean change (Martínez et al., 2018; Takao et al., 2015; Wilson et al., 2019), the physiological responses of many species remain poorly understood. To accurately predict the consequences of elevated temperature and CO₂ on seaweeds we need to identify how their physiological performance will be affected and detect any mechanisms through which they can acclimate to changing ocean conditions.

Temperature regulates rates of key metabolic processes in seaweeds such as photosynthesis and respiration, which in turn can affect growth rates (Davison, 1991; Raven & Geider, 1988). Each species has a thermal optimum above which rate processes such as photosynthesis and growth decline (Eggert, 2012), and both ocean warming and marine heatwaves may raise temperatures above thermal optima. However, this will depend on where a population exists within its thermal range and the magnitude of the temperature increase (Smale et al., 2019). Membrane fluidity increases with increasing temperature, which can ultimately lead to disintegration of lipid bi-layers surrounding cells and organelles (Los & Murata, 2004). Seaweeds can reduce this fluidity by adjusting the fatty acid

composition in the membranes. Decreasing the proportion of polyunsaturated fatty acids (PUFA) relative to saturated fatty acids (SFA) and chain length elongation both reduce membrane fluidity (Los & Murata, 2004). Such changes in fatty acid composition in response to elevated temperature have been observed in seaweeds in both the field (Schmid et al., 2017) and laboratory (Becker et al., 2010; Gosch et al., 2015). This response may therefore be a mechanism by which seaweeds are able to tolerate elevated temperatures predicted under ocean warming and marine heatwaves.

Physiological performance of seaweeds will also be affected by ocean acidification. In general, the response of fleshy seaweeds are species-specific and dependent upon their carbon uptake strategy. The majority (~ 65 %) of seaweeds can utilise bicarbonate (HCO_3^-), the most abundant form of dissolved inorganic carbon (DIC) in seawater as an inorganic carbon source for photosynthesis. HCO_3^- uptake is an active process mediated by energetically expensive carbon dioxide concentrating mechanisms (CCMs, Giordano et al., 2005; Kübler & Dudgeon, 2015). The response of species that have a CCM to ocean acidification will likely depend on whether they are able to down-regulate the CCM to rely more on passive uptake of CO_2 as an inorganic carbon source. Under ocean acidification, the relative proportion of CO_2 to HCO_3^- will increase and species that can down-regulate the use of the CCM may benefit, whereas those that are unable to down-regulate the CCM may be unaffected (Cornwall et al., 2017; Hepburn et al., 2011; van der Loos et al., 2019). Changes in CCM activity can be identified with stable carbon isotope ratios ($\delta^{13}\text{C}$, Maberly et al., 1992): CO_2 has less ^{13}C than HCO_3^- and, consequently, lower $\delta^{13}\text{C}$ values indicate a greater proportion of CO_2 uptake. Thus, a reduction in $\delta^{13}\text{C}$ values indicates CCM down-regulation.

Ocean warming and ocean acidification will not occur in isolation, and the response of a species to future conditions will be dependent on the combined effect of these two drivers,

and interactions with additional drivers. However, examining the effects of ocean warming, acidification and a third acute impact such as marine heatwaves in a factorial design can become overly complex and logistically difficult (Boyd et al., 2018; Boyd et al., 2016). A way to reduce this complexity is to use a “collapsed factorial design” where co-varying drivers such as ocean warming and ocean acidification are manipulated or “collapsed” together into “current” and “future” scenarios (Boyd et al., 2018; Boyd et al., 2016). These scenarios can then be used in factorial designs with another driver of interest such as marine heatwaves. This approach has the advantage that only environmentally relevant scenarios are examined and is more focused on predicting responses as opposed to understanding the relevant importance of individual drivers (Boyd et al., 2018; Boyd et al., 2016).

While seaweed species can be highly susceptible to marine heatwaves in the field (Smale & Wernberg, 2013; Thomsen et al., 2019; Wernberg et al., 2016, however see Straub et al., 2019 for examples of species tolerant to heatwaves), these studies primarily document impacts and few studies have examined the physiological effects of marine heatwaves on seaweeds in the laboratory (Burdett et al., 2019; Gouvêa et al., 2017; Wilson et al., 2015). Furthermore, none have assessed the effects of marine heatwaves in combination with ocean warming and acidification. The brown seaweed *Phyllospora comosa* (Order Fucales) is one of the most widespread and abundant habitat-forming seaweeds in eastern Australia. *P. comosa* is dominant in the shallow subtidal of wave-exposed locations and as such, likely encounters fluctuating temperatures over short time scales. This, along with its widespread distribution (latitudinal range ~ 1300 kms from 43 – 31° S) and the fact it experiences summer temperatures of ~ 23 °C at the northern extent of its range (Flukes et al., 2015), suggest it may be tolerant to heatwaves and ocean warming in the cooler southern region of Tasmania. However, the responses of a species to warming is dependent on the temperature regime experienced by a population (Bennett et al., 2015) and anomalously warm seawater is considered a likely cause of historical die-back of *P. comosa* in Tasmania (Valentine &

Johnson, 2004). These factors and the fact other subtidal fucoids distributed along similar latitudes are susceptible to both warming and heatwaves (Smale & Wernberg, 2013), suggest that *P. comosa* may also be susceptible. Given its ecological importance and the uncertainty surrounding its response, *P. comosa* is an ideal species to examine the physiological effects of marine heatwaves combined with ocean warming and acidification. To test these effects we conducted a laboratory experiment on juvenile *P. comosa* in which we simulated marine heatwaves, ocean warming and acidification in a collapsed factorial design. Juveniles were used as early life-history stages can be considered a bottleneck in the development of seaweed populations (Lotze et al., 2001). We assessed the effects during the heatwave and after a recovery period to determine any lasting effects. We hypothesised that *P. comosa* would be resilient to marine heatwaves under current ocean conditions as this temperature would be far below the maximum temperature experienced by *P. comosa* within its latitudinal range, but when the heatwaves were superimposed on future ocean conditions the additional temperature increase would impair growth and photosynthesis. We also hypothesised that ocean warming and acidification in the absence of a marine heatwave would not affect growth and photosynthesis in *P. comosa* as temperatures would not be high enough to cause negative effects, or that any negative effects of elevated temperature would be offset by the beneficial effects of elevated CO₂. Lastly, we hypothesised that changing the fatty acid composition of cellular membranes would be a mechanism by which *P. comosa* would be able to tolerate elevated temperatures.

Materials and methods

Field conditions

Deployment of two combined pH-temperature loggers (pHTempion, Envco, New Zealand) was undertaken by divers using SCUBA on two occasions in ~ 7 m depth at Coal Point, Bruny Island, Tasmania (43.3353° S, 147.3247° E). These deployments were undertaken to

assess natural variability in pH to inform experimental treatments. The first deployment was undertaken between 24th January 2018 and 9th February 2018 and the second between 27th February 2018 and 14th April 2018. A light and temperature logger (HOBO Pendant MX temp/light, Onset Computer Corporation, USA) was deployed next to one pH logger on both occasions. Details of the pH logger calibrations and post-collection data processing are given in the appendices. Data from one pH logger was lost during the second sampling period. As the light loggers measured in lux, a calibration between lux and Photosynthetically Active Radiation (PAR) was undertaken with a LI-COR LI-192 2π quantum sensor that measured PAR. Details of this calibration can be seen in the appendices.

Seaweed collection and pre-experimental treatment

Approximately 70 juvenile individuals of *P. comosa* ~ 5-10 cm length were collected by divers using SCUBA at 6-8 m depth on the 14th April 2018 at Coal Point. This site was located at the southern (coldest) extent of the species range. Individuals were placed in zip-lock bags with enough seawater to prevent desiccation and transported in an insulated container to the laboratory two hours away. Upon return to the laboratory, all seaweeds were placed in a 60 L container with UV-sterilised seawater filtered to 1 μm under constant aeration at 15.5 °C. This temperature was chosen as it was the average sea surface temperature during the period from 15th March to 15th April at the collection site between 1985- 2015 ($15.44\text{ }^{\circ}\text{C} \pm 0.03$, minimum = 9.97, maximum = 19.47, Banzon et al., 2016). The average temperature at the site in the two weeks prior to collection as measured by the light and temperature loggers was $16.42\text{ }^{\circ}\text{C} \pm 0.06$ (1 standard deviation). Seawater was refreshed daily and light levels were maintained at $50\text{ }\mu\text{mol photons m}^{-2}\text{ s}^{-1}$ (typical maximum light levels at the collection site were between 50-100 $\mu\text{mol photons m}^{-2}\text{ s}^{-1}$ – see appendices) on a 12:12 light:dark cycle. Seaweed were held in these conditions for 48 hours prior to experimentation.

Experimental culture conditions

Experiments were conducted in an automated culture system (Britton et al., 2019), with modifications that allowed temperature control in addition to pH control. Seawater in each of 48 chambers was replaced every four hours with pH and temperature-adjusted seawater. Target pH_T was achieved using mass flow controllers (FMA5418A and FMA5402A, Omega Engineering, USA) to adjust the ratio of CO_2 to air in a gas mix that was exposed to incoming seawater from a single header tank using membrane contactors (Liqui-Cel™ MM-1×5.5 Series, 3M, USA). All gas mix equilibrations were made prior to temperature adjustments but all pH measurements were made following the temperature adjustments. The seawater was then diverted through a set of water baths maintained at an appropriate temperature using aquarium heaters (Jager 3612, Eheim, Germany) to adjust seawater to the correct temperature for each treatment. Temperature in the culture chambers was maintained by circulating water from a second set of water baths through external water jackets around each culture chamber. The temperatures of the second set of water baths were maintained using aquarium heaters (Jager 3612, Eheim, Germany and Aqua One IPX8, Kongs Australia, Australia) and temperature controllers (Temperature Controller 7028/3, Tunze, Germany). All pH_T values are reported at the treatment temperatures. Temperature was measured with temperature loggers (HOBO Pendant MX temp/light, Onset Computer Corporation, USA and SE011 General Temperature Probe, Pico Technology, UK) that were placed in random culture chambers of each treatment ($n = 3 - 4$ for each treatment).

An automated spectrophotometric pH_T system (McGraw et al., 2010) was incorporated into a feedback system to ensure incoming seawater was within 0.03 pH_T units from target values. To calculate carbonate system parameters, samples for DIC analysis were collected from random culture chambers at pH_T values spanning the range of observed pH_T fluctuations (7.6 - 8.2). Samples were poisoned immediately with HgCl_2 and stored in darkness until analysis. DIC measurements were made with a DIC analyser (DIC analyser model AS-C3, Apollo

SciTech USA) with an inbuilt CO₂ analyser (LI-7000 CO₂/H₂O analyser, LI-COR USA). The CO₂ analyser was calibrated with Certified Reference Material (A. Dickson, Scripps Institute for Oceanography, San Diego, USA). A pH_T vs DIC relationship was constructed from these results to determine the DIC at each of the treatment means. A_T and [H⁺] were calculated in CO2calc (Robbins et al., 2010) using the constants of Mehrbach et al. (1973) refit by Lueker et al. (2000) and the known DIC, temperature and salinity (measured with an Orion VersaStar Advanced Electrochemistry Meter, ThermoFisher Scientific, USA) of the seawater. All pH_T values were measured between 15.96 °C and 18.21 °C.

Experimental treatments

On day 1 of the experiment, 48 individual juvenile *P. comosa* sporophytes were randomly allocated to one of four experimental treatments. Half of the individuals were sampled on the final day of the heatwaves (hereafter, first sampling) and the remaining following a seven-day recovery period (hereafter, final sampling). This resulted in n = 6 replicates for each treatment × sampling point. Treatments were as follows: “current baseline” (pH_T = 8.0, temperature = 15.50 °C), “current heatwave” (pH_T = 8.0, temperature = 15.50 °C + 3 °C heatwave), “future baseline” (pH_T = 7.7, temperature = 18.50 °C), “future heatwave” (pH_T = 7.7, temperature = 18.50 °C + 3 °C heatwave). To mimic the diel fluctuations of pH_T measured in the field, all treatments had pH_T increase incrementally by 0.15 units during the daylight every 4 hours and decrease by 0.15 units in the dark every 4 hours except for the final increase at the end of the day and the initial decrease at the beginning of the night which were 0.1 units. This resulted in the treatments having a target mean pH_T 8.0 (range: 7.8 – 8.2) and pH_T 7.7 (range: 7.5 – 7.9) in the current and future scenarios respectively.

Replicates from each treatment were assigned to one of four shelves (n = 3 for each treatment per shelf) in a randomised block design. Temperatures were maintained at baseline levels of

the respective scenario in all treatments from day 1 – 6 (“pre-heatwave period”). On day 6 heatwaves were applied by increasing the temperature over 3 hours to 3 °C higher than the current and future baseline temperatures respectively. Heatwaves were maintained until day 12 (6 days total, “heatwave period”), at which point the temperature was reduced over 3 hours to the original mean for the treatment. Prior to the end of the heatwave period, 6 randomly selected individuals from each treatment were removed on day 12 (first sampling, the shelves tanks were located on were not considered for this random selection). Biotic responses (see below) of these individuals were analysed to assess physiological performance during heatwave conditions. The remaining 6 replicates in each treatment were cultured under temperatures of each scenario prior to the heatwaves for a further 7 days (“recovery period”) and removed on day 19 (final sampling) and biotic responses analysed. Figure 4.1 displays a timeline of the treatment conditions and sampling times over the course of the experiment. Net photosynthesis and respiration were measured prior to removal of individuals from culture for all individuals.

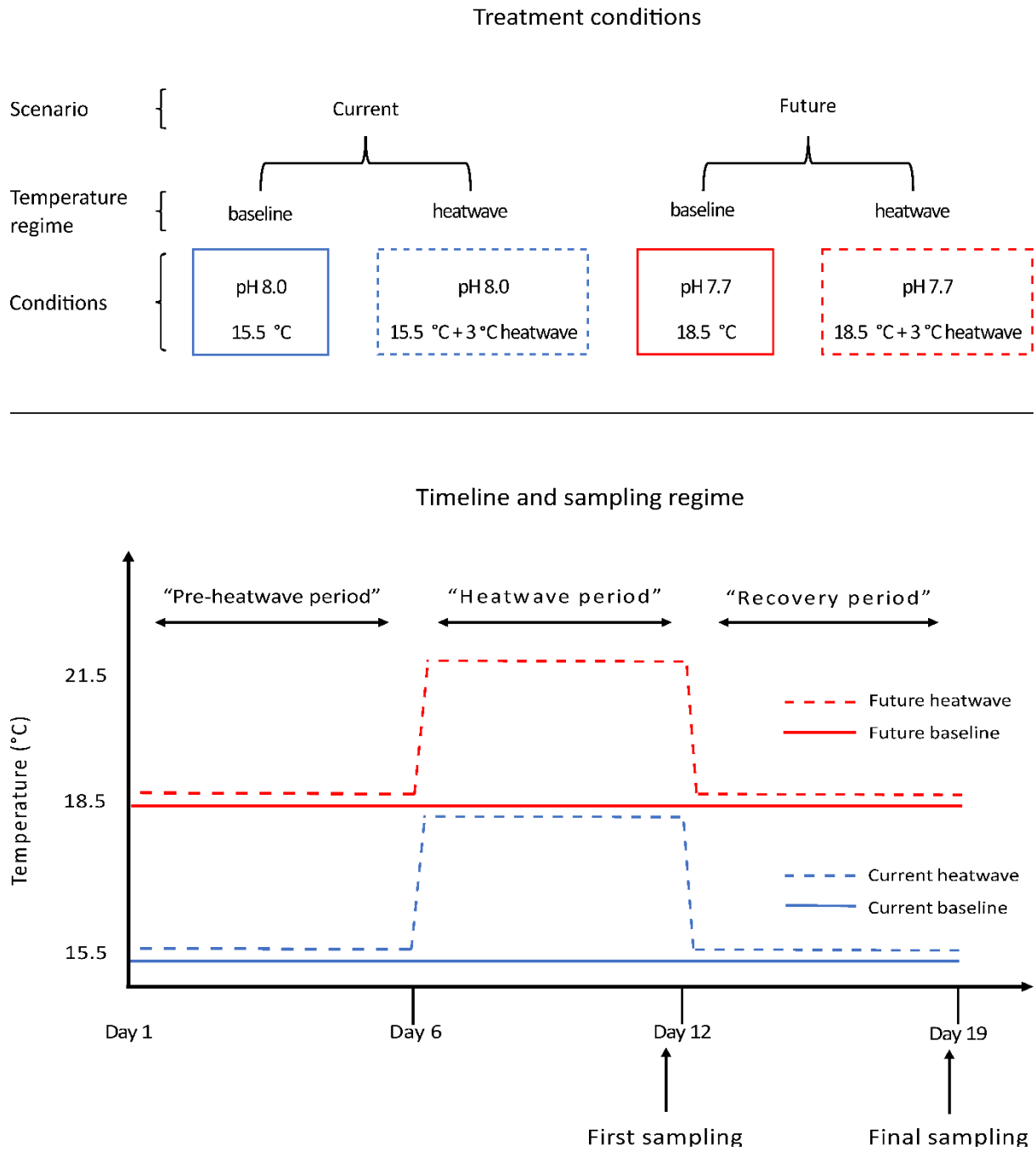


Figure 4.1: **Top panel:** pH and temperature conditions in each of the four experimental treatments. Blue boxes indicate the current scenario and red boxes the future scenario. Within each scenario, solid lines refer to baseline treatments in which temperature was constant for the duration of the experiment, whereas dashed lines refer to treatments in which a 6 day 3 °C heatwave was superimposed on the baseline temperature. **Bottom panel:** timeline of the sampling regime and the temperature levels in each treatment over the duration of the experiment. The first sampling was undertaken on the final day of the “heatwave period” and the final sampling was undertaken on the final day of the “recovery period.” For ease of visualisation overlapping lines are slightly offset despite having the same temperature. See results for precise temperature levels in each treatment.

Biotic responses

Relative growth rates (wet weight)

Individuals were blotted dry to remove surface water and weighed prior to, and upon removal from culture. Relative growth rates (RGR) as wet weight were calculated according to Kain (1982).

Photosynthetic and respiration rates

Oxygen consumption in the dark (respiration) and oxygen evolution (net photosynthesis) in experimental light were measured within culture chambers for 6 replicates in each treatment on days 11 and 12 respectively (final night and day of the heatwave period). The remaining 6 replicates in each treatment were measured on days 18 and 19 (final night and day of recovery period). Lights were turned off 1 hour prior to making any respiration measurements in order to measure dark adapted individuals. Respiration measurements were made between 15:15 and 20:30 and all photosynthesis measurements were made between 07:45 and 13:00. Chambers were sealed and oxygen measurements were made at the beginning and end of the incubation with a portable oxygen meter (Fibox 4, PreSens, Germany), coupled with a non-invasive oxygen sensor in each culture chamber (Oxygen Sensor Spot SP-PSt3-NAU, PreSens, Germany). Net photosynthesis and respiration are expressed as $\mu\text{mol O}_2 \text{ L}^{-1} \text{ g}^{-1} \text{ h}^{-1}$ produced or consumed respectively.

Pigment content, stable C isotopes, % tissue nitrogen and fatty acid profiles

For all samples, the entire thallus of each individual (~ 800 mg wet weight) was destructively sampled, tissue immediately frozen at -20 °C and freeze-dried the following day (FreezeZone 4.5, Labconco, USA). Freeze-dried samples remained frozen at -20 °C until analysis for

chlorophyll a, fucoxanthins, stable C isotopes, percentage tissue nitrogen and fatty acid profiles.

Chlorophyll a and fucoxanthin content were determined by adding ~ 10 mg of ground freeze-dried tissue to a solution of 4 ml dimethyl sulfoxide (DMSO) and 0.5 ml MilliQ water as outlined in Stephens & Hepburn (2014) and Wheeler (1980). Samples were incubated for 30 mins and the absorbance of the extract measured at 665, 631, 582 and 480 nm with a UV-VIS spectrophotometer (Halo RB-10 UV-VIS ratio beam spectrophotometer, Dynamica Scientific Ltd, UK). The content of each pigment in extracts were calculated using the equations of Seely et al. (1972) and expressed as mg g⁻¹ dry weight.

$\delta^{13}\text{C}$ isotopic ratios and % tissue nitrogen were determined using the methods outlined in Britton et al. (2019). Dried samples were weighed into tin cups (Sercon, UK) and analysed using an elemental analyser (NA1500, Fisons Instruments, UK) coupled to an isotope ratio mass spectrometer (Delta V Plus, ThermoFisher Scientific, USA) via a Universal Continuous Flow Interface (Conflo IV, ThermoFisher Scientific, USA). Combustion and reduction were achieved at 1020 °C and 650 °C respectively. Isotope values were normalised to the Vienna Pee Dee Belemnite scale via a 3-point calibration using certified reference material and both precision and accuracy were ± 0.1 % (one standard deviation). % N composition was determined by comparison of mass spectrometer peak areas to those of standards with known concentrations.

Fatty acids were extracted and analysed by the direct-transmethylation method described in Schmid et al (2018). A known amount (ca. 20 mg) of ground, freeze-dried biomass was transferred into borosilicate glass test tubes fitted with a polytetrafluoroethylene (PTFE) lined

screw cap. The samples were directly transmethylated using methanol: dichloromethane (DCM): concentrated hydrochloric acid (3 ml, 10:1:1 v/v/v) and placed in a heating block at 80 – 85 °C for two hours, after which samples were cooled to room temperature. Following cooling, 1 ml of Milli-Q water was added and fatty acid methyl esters (FAME) were extracted three times by addition of 2 ml of hexane/DCM (4:1, v/v). FAME samples were evaporated under nitrogen flow and re-dissolved in 0.5 ml of DCM containing a known amount of 23:0 added as an internal injection standard. Samples were analysed by gas chromatography (7890 GC, Agilent Technologies, USA) coupled with a flame ionisation detector with analytical conditions as described in Parrish et al. (2015). Individual fatty acids were confirmed by gas chromatography–mass spectrometry (1310 GC, ThermoFisher Scientific, USA) coupled with a TSQ triple quadrupole. Samples were injected using an auto sampler (TriPlus RSH, ThermoFisher Scientific, USA) with a non-polar HP-5 Ultra 2 bonded-phase column (50 m × 0.32 mm internal diameter × 0.17 µm film thickness). The system conditions were as described in White et al. (2017). Mass spectra data were acquired and processed with Xcalibur™ software (ThermoFisher Scientific, USA).

Statistical analysis

All analyses were conducted in the statistical software R v. 3.6.1 (R Core Team, 2019). To test responses during the heatwave and after the recovery period of the heatwave, a randomised block design was used to assess whether there were differences between biotic responses separately at each sampling time. Both models included the fixed factors “Scenario” (2 levels: current and future), “Temperature regime” (2 levels: baseline and heatwave) and the Scenario × Temperature regime interaction. The blocking factor “Shelf” (4 levels: 1 – 4) was included as a random factor. All model fits were made with the *lmer* function in the *lme4* package (Bates et al., 2015). Model fits were inspected using residual versus fitted and normal Q-Q plots. All models conformed to the assumptions of homogeneity of variances and normality of residuals. When significant interactions were

detected at $\alpha = 0.05$, Tukey's Honestly Significant Different (THSD) post-hoc tests were undertaken to compare all 6 pairwise combinations of treatments.

Results

Field pH and light measurements

Measurements of pH at the collection site displayed a clear diel pattern with pH increasing throughout the day and decreasing through the night (Appendix 4.1, Appendix 4.2). The range of pH_T values measured at the site were all between 7.85 and 8.40 units (Table 4.1). Maximum light levels were typically between 50 and 100 $\mu\text{mol photons m}^{-2} \text{s}^{-1}$ during both logger deployments (Appendix 4.3, Appendix 4.4). Average temperature at the site during both logger deployments as measured by the light loggers are shown in Table 4.1.

Table 4.1: Mean, minimum, maximum and range of pH_T values recorded by the pH loggers deployed at Coal Point over the two logger deployments. Deployment 1 consisted of two loggers between the 24th January to 9th February 2018 (Jan-Feb) and deployment 2 consisted of one logger between the 27th February and 14th April 2018 (Feb-April).

Deployment	Mean pH_T	Min pH_T	Max pH_T	Range pH_T	Temperature ($^{\circ}\text{C}$)
1 - Jan-Feb logger 1	8.24	7.95	8.40	0.45	17.83
1 - Jan-Feb logger 2	8.03	7.85	8.19	0.34	17.83
2 - Feb-April logger 1	8.11	7.87	8.26	0.39	16.82

Experimental culture conditions

Average temperatures (\pm standard deviation) in each treatment were as follows: current baseline, $15.88\text{ }^{\circ}\text{C} \pm 0.23$; current heatwave, $15.51\text{ }^{\circ}\text{C} \pm 0.05$ outside of the heatwave and $18.39\text{ }^{\circ}\text{C} \pm 0.07$ during the heatwave; future baseline, $18.48\text{ }^{\circ}\text{C} \pm 0.11$; future heatwave, $18.51\text{ }^{\circ}\text{C} \pm 0.09$ outside the heatwave and $21.57\text{ }^{\circ}\text{C} \pm 0.43$ during the heatwave (Table 4.2). pH_T increased incrementally throughout the day and decreased incrementally in the darkness (Appendix 4.5). Carbonate parameters at the mean pH_T of each treatment during and outside the heatwave are shown in Table 4.2.

Table 4.2: Mean pH_T , DIC, A_T and temperature (outside of and during the heatwaves) for each treatment. All pH values were measured, while DIC and A_T were calculated from the mean pH_T of each treatment and the relationship between pH_T and DIC. This relationship was constructed from the DIC values measured over pH_T values that spanned the range used in the experiment and the known salinity of the seawater.

	Treatment	pH_T	DIC ($\mu\text{mol kg}^{-1}$)	A_T ($\mu\text{mol kg}^{-1}$)	Temperature ($^{\circ}\text{C}$)
Outside heatwave period	Current baseline	8.05	2082	2311	15.83
	Current heatwave	8.06	2082	2311	15.51
	Future baseline	7.74	2201	2311	18.46
	Future heatwave	7.77	2189	2311	18.51
Heatwave Period	Current baseline	8.04	2086	2311	15.96
	Current heatwave	8.01	2082	2311	18.39
	Future baseline	7.74	2201	2311	18.48
	Future heatwave	7.72	2189	2311	21.57

Biotic responses

Relative growth rates (wet weight)

Relative growth rates (RGRs) of *P. comosa* did not differ significantly between experimental treatments at either sampling (Figure 4.2, Table 4.3). Mean RGRs were always lower under heatwaves, however high variability amongst replicates may have limited our capacity to detect differences statistically.

Photosynthetic and respiration rates

Heatwaves significantly reduced net photosynthetic rates irrespective of scenario at the first sampling (83 % lower in current scenario, 33 % lower in future scenario, Figure 4.2, Table 4.3). Additionally, the future scenario had higher net photosynthetic rates relative to the current scenario, irrespective of whether a heatwave was present or absent (70 % higher, pooled means of baseline and heatwave treatments, Figure 4.2, Table 4.3). There were no significant differences in net photosynthetic rates between treatments following the recovery period (Figure 4.2, Table 4.3). At the first sampling, respiration rates were 67 % higher in the heatwave treatment compared to the baseline treatment in the current scenario, while in the future scenario, the heatwave and baseline treatment had similar mean respiration (baseline: $7.65 \mu\text{mol O}_2 \text{ h}^{-1} \text{ g}^{-1}$, heatwave: $7.29 \mu\text{mol O}_2 \text{ h}^{-1} \text{ g}^{-1}$, Figure 4.2, Table 4.3). These responses resulted in a near significant interaction ($p = 0.059$, Figure 4.2, Table 4.3). Respiration rates were significantly lower in the future scenario relative to the current scenario at the final sampling (20 % lower, pooled means of baseline and heatwave treatments, Figure 4.2, Table 4.3), and no effects of heatwaves were detected.

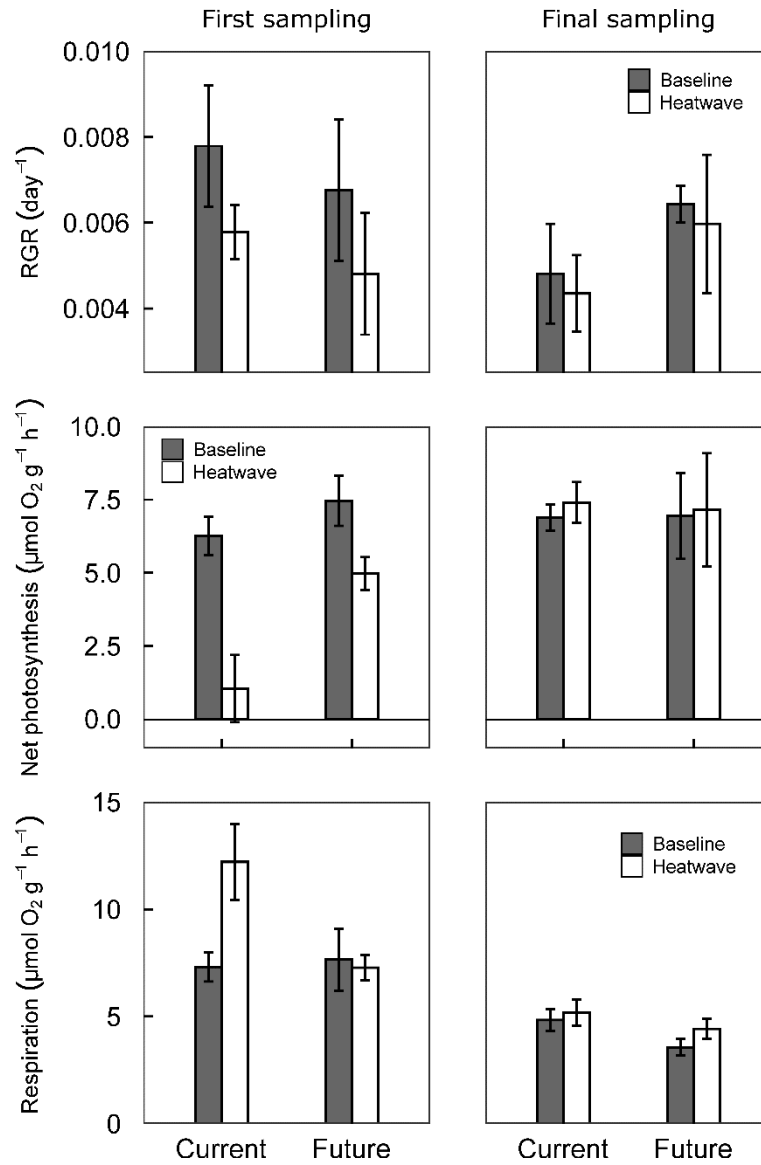


Figure 4.2: Responses of juvenile *Phyllospora comosa* at the end of the heatwave period (first sampling, left panels) and following the recovery period (final sampling, right panels). *P. comosa* juveniles were cultured in current (today's temperature and pH) and future (2100 temperature and pH projections) scenarios. Shaded bars refer to baseline temperature treatments and white bars refer to treatments where a 6 day 3 °C heatwave was superimposed on the baseline temperature in a given scenario. Response variables and significant differences are described for each panel. **Top row:** relative growth rates (RGR, day⁻¹); no significant differences at either sampling. **Middle row:** net photosynthesis (μmol O₂ L⁻¹ g⁻¹ h⁻¹); first sampling, future > current ($p = 0.006$), heatwave < baseline ($p = 0.0002$); final sampling, no significant differences. **Bottom row:** respiration (μmol O₂ L⁻¹ g⁻¹ h⁻¹); first sampling, interaction near significant ($p = 0.059$), final sampling, future < current ($p = 0.02$). Data are presented as means \pm standard error, $n = 6$ for all treatments at both sampling points excluding net photosynthesis in the future heatwave treatment at the first sampling ($n = 5$). All rates are calculated on a wet weight basis.

Pigment content, stable carbon isotopes and % tissue nitrogen

Chlorophyll a content did not differ significantly between treatments at the first sampling (Figure 4.3, Table 4.3). At the final sampling, chlorophyll a content was significantly lower in future scenario relative to the current scenario (17 % lower, pooled means of baseline and heatwave treatments, Figure 4.3, Table 4.3) and no effect of heatwaves were detected. There was a near significant trend of lower fucoxanthin content under heatwaves at the first sampling (15 % lower in the current scenario and 13 % lower in the future scenario; $p = 0.067$, Figure 4.3, Table 4.3). At the final sampling, fucoxanthin content was significantly lower in future scenario relative to the current scenario (14 % lower, pooled means of baseline and heatwave treatments, Figure 4.3, Table 4.3) and there was no detectable effect of heatwaves. $\delta^{13}\text{C}$ values did not differ significantly between treatments at the first sampling (Figure 4.3, Table 4.3), whereas at the final sampling $\delta^{13}\text{C}$ values were significantly lower in *P. comosa* grown under future scenarios (9 % lower, pooled means of baseline and heatwave treatments, Figure 4.3, Table 4.3). % tissue nitrogen was lower in the future scenario at both sampling points but this was only significant at the final sampling (first sampling: $p = 0.063$, Appendix 4.6, Table 4.3).

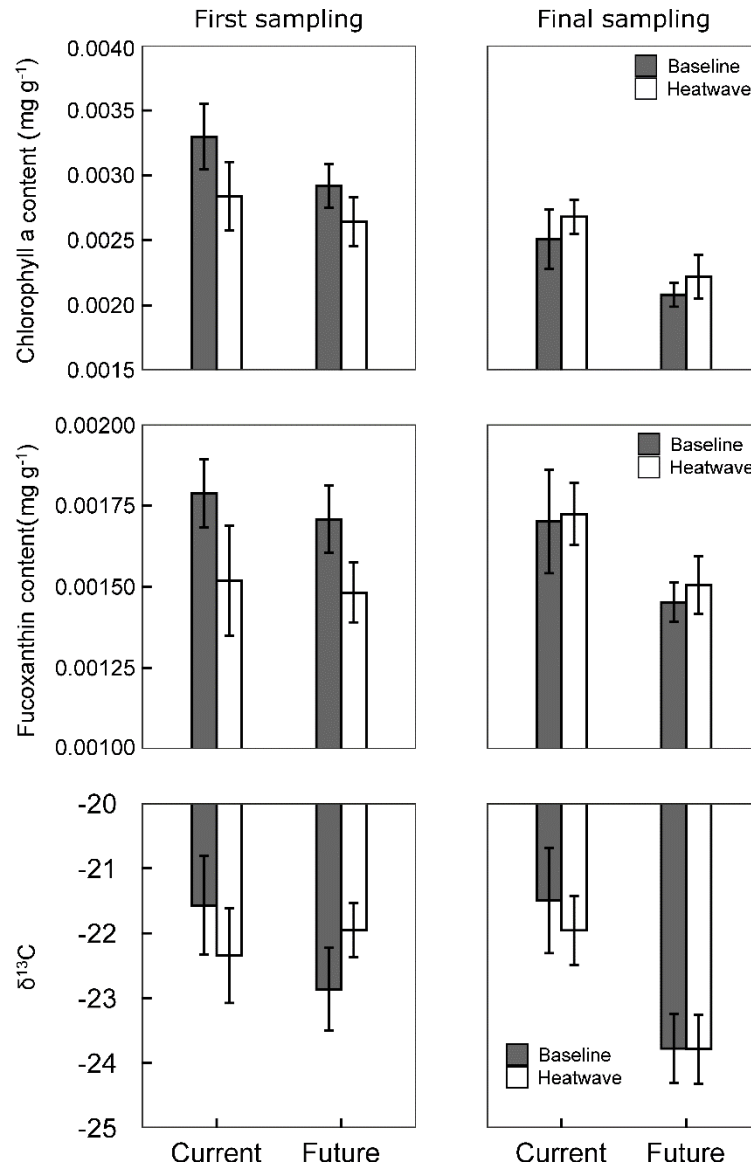


Figure 4.3: Responses of juvenile *Phyllospora comosa* at the end of the heatwave period (first sampling, left panels) and following the recovery period (final sampling, right panels). *P. comosa* juveniles were cultured in current (today's temperature and pH) and future (2100 temperature and pH projections) scenarios. Shaded bars refer to baseline temperature treatments, and white bars refer to treatments where a 6 day 3 °C heatwave was superimposed on the baseline temperature in a given scenario. Response variables and significant differences are described for each panel. **Top row:** chlorophyll a content (mg g⁻¹); first sampling, no significant differences, final sampling, future < current ($p = 0.013$). **Middle row:** fucoxanthin content (mg g⁻¹); first sampling, no significant differences; final sampling: future < current ($p = 0.042$). **Bottom row:** δ¹³C; first sampling, no significant differences, final sampling: future < current ($p = 0.002$). Data are presented as means ± standard error, $n = 6$ for all treatments at both sampling points excluding chlorophyll a and fucoxanthin content in the future baseline and future heatwave treatment at the first sampling ($n = 5$). Chlorophyll a and fucoxanthin content are calculated on a dry weight basis.

Fatty acid profiles

At the first sampling total fatty acid (TFA) content was similar in the heatwave and baseline treatment in the current scenario but was 21 % lower in the heatwave treatment relative to the baseline treatment in the future scenario (Figure 4.4). This result was near significant (interaction: $p = 0.065$, Table 4.3). At the final sampling, TFA content was higher in the heatwave treatment relative to the baseline treatment under current ocean conditions (14 % higher), while the opposite trend was observed in the future scenario (baseline 11 % higher than heatwave). This result lead to a significant interaction (Figure 4.4, Table 4.3). THSD post-hoc tests detected near significant differences between the current baseline treatment and both the current heatwave treatment ($p = 0.06$) and future baseline treatment ($p = 0.057$). At the first sampling, SFA content was significantly lower in the future scenarios relative to the current scenario (10 % lower, pooled means of baseline and heatwave treatments, Figure 4.4, Table 4.3), whereas PUFA content was significantly higher in the future scenario relative to the current scenario (9% higher, pooled means of baseline and heatwave treatments, Figure 4.4, Table 4.3). No significant effects of heatwaves on SFA and PUFA content were detected at the first sampling. At the final sampling, SFA content was higher in the heatwave treatment relative to the baseline treatment in the current scenario (12 % higher, Figure 4.4), while in the future scenario the baseline and heatwave treatment had similar values and both were higher than the current baseline treatment (18 % higher in future baseline and 11 % higher in future heatwave, Figure 4.4). This response resulted in a significant interaction and THSD post-hoc tests indicated that all treatments were significantly different to the current baseline treatment (Table 4.3). PUFA content was 6 % lower in the heatwave treatment relative to the baseline treatment in the current scenario whereas the baseline and heatwave treatments had similar values in the future scenario at the final sampling. Both the future baseline and future heatwave treatments had lower PUFA content than the current baseline treatment (9 % lower in future baseline and 5 % lower in future heatwave, Figure 4.4). This result caused the interaction to be significant and THSD post-hoc tests indicated a significant difference between the current baseline and the current heatwave and future baseline

treatments (Table 4.3). The difference between the current baseline treatment and the future heatwave treatment was not significant ($p = 0.097$, Table 4.3). The mean chain length of PUFA was not significantly different between treatments at either sampling (Table 4.3).

Table 4.3: Linear mixed model table for all response variables. The table displays p -values and the nature of differences at both sampling points. Significant effects ($\alpha = 0.05$) have p -values displayed in bold. Near significant differences ($\alpha < 0.1$) have p -values displayed in italics. For differences in the main effects of “Scenario” (Two levels: current and future) and “Temperature regime” (Two levels: baseline or heatwave), factor names are displayed showing the nature of differences. For significant interactions, significant differences ($\alpha < 0.05$) between treatments identified using THSD post-hoc tests are displayed. Near significant differences ($\alpha < 0.1$) between treatments detected in THSD post-hoc tests are displayed in italics with p -values displayed in parentheses. Response variables displayed as acronyms: RGR = relative growth rates, TFA = total fatty acids, SFA = saturated fatty acids, PUFA = polyunsaturated fatty acids. Treatment acronyms: CB = current baseline, CH = current heatwave, FB = future baseline, FH = future heatwave. Degrees of Freedom = 1 for main effects and the interaction and 17 - 20 for residuals.

Sampling	Response	Differences	p -values		
			Scenario	Temperature regime	Interaction
First sampling	RGR		0.447	0.167	0.939
	Net photosynthesis	future > current, heatwave < baseline	0.006	0.0002	0.119
	Respiration	heatwave > baseline,	<i>0.073</i>	0.046	<i>0.059</i>
	Chlorophyll α		0.231	0.131	0.702
	Fucoxanthins		0.650	<i>0.067</i>	0.863
	TFA		0.514	0.108	<i>0.065</i>
	SFA	future < current	0.022	0.287	0.454
	PUFA	future > current	0.028	0.769	0.825
	$\delta^{13}\text{C}$		0.406	0.844	0.167
	% N		<i>0.063</i>	0.740	0.509
	Mean PUFA chain length		0.805	0.743	0.198
Final sampling	RGR		0.159	0.682	0.998
	Net photosynthesis		0.940	0.765	0.898
	Respiration	future < current	0.020	0.208	0.588
	Chlorophyll α	future < current	0.013	0.311	0.971
	Fucoxanthins	future < current	0.042	0.703	0.868
	TFA	CB < CH ($p = 0.06$), CB < FB ($p = 0.057$)	0.688	0.732	0.003
	SFA	CB < CH, FB, FH	0.004	0.299	0.002
	PUFA	CB > CH, FB CB > FH ($p = 0.097$)	0.015	0.417	0.003
	$\delta^{13}\text{C}$	future < current	0.002	0.686	0.680
	% N	future < current	0.001	0.737	0.598
	Mean PUFA chain length		0.519	0.133	<i>0.068</i>

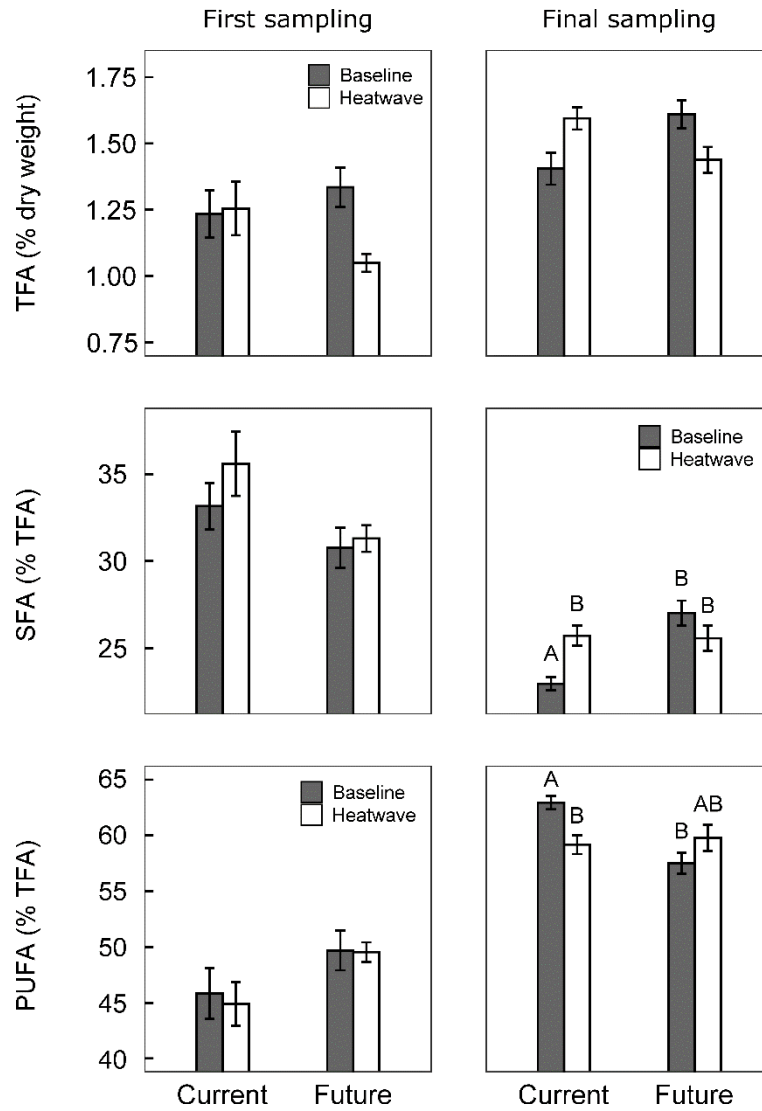


Figure 4.4: Responses of juvenile *Phyllospora comosa* at the end of the heatwave period (first sampling, left panels) and following the recovery period (final sampling, right panels). *P. comosa* juveniles were cultured in current (today's temperature and pH) and future (2100 temperature and pH projections) scenarios. Shaded bars refer to baseline temperature treatments, and white bars refer to treatments where a 6 day 3 °C heatwave was superimposed on the baseline temperature in a given scenario. Response variables and significant differences are described for each panel. **Top row:** total fatty acids (TFA, % dry weight); first sampling, no significant differences; final sampling, interaction significant ($p = 0.003$). **Middle row:** saturated fatty acids (SFA, % TFA); first sampling, future < current ($p = 0.022$); final sampling: interaction ($p = 0.002$). **Bottom row:** polyunsaturated fatty acids (PUFA, % TFA); first sampling, future > current ($p = 0.028$); final sampling, interaction significant ($p = 0.003$). Data are presented as means \pm standard error, $n = 6$. For significant interactions, treatments displaying the same letter were not significantly different in THSD post-hoc tests. TFA is calculated on a dry weight basis.

Discussion

We found that juveniles of the ecologically important habitat forming seaweed *Phyllospora comosa* is resilient to short-term marine heatwaves, under both current ocean conditions and those predicted by 2100. This is consistent with the lack of widespread mortality or bleaching of *P. comosa* observed in a recent marine heatwave of $\sim 3^{\circ}\text{C}$ in Tasmania (Oliver et al., 2017; Oliver et al., 2018b) and unsurprising given that *P. comosa* occupies the shallow subtidal where it is likely to experience large temperature fluctuations over short time-scales. However, we note that adults and juveniles may respond differently. We observed a temporary reduction in net photosynthetic rates during the heatwaves indicating that conditions were sub-optimal. However, this reduction did not persist following a seven-day recovery period. No significant adverse impacts of combined ocean warming and acidification on *P. comosa* growth and photosynthesis were detected. However, we observed an increase in the proportion of SFA and a decrease in the proportion of PUFA under heatwaves and in the future baseline treatment (noting that the decrease in PUFA was not significant in the future heatwave treatment). We suggest that this increase in the degree of fatty acid saturation is a mechanism by which *P. comosa* maintained growth and photosynthetic rates under future ocean warming, acidification and marine heatwaves.

P. comosa is known to operate a CCM and actively take up bicarbonate in addition to passive diffusion of CO_2 (Cornwall et al., 2015). The decrease in $\delta^{13}\text{C}$ values detected in the future scenario relative to the current scenario at the final sampling indicates a down-regulation of the CCM. This can provide energetic savings in seaweeds, as the use of CO_2 as an inorganic carbon source requires less energy than HCO_3^- (Cornwall et al., 2017; van der Loos et al., 2019). Any saved energy was not invested in growth (in contrast to that reported for a red seaweed by van der Loos et al., 2019), but instead could have been invested in the adjustment of fatty acid composition in response to elevated temperatures. We suggest that this is a mechanism by which *P. comosa* can tolerate elevated temperature via benefits arising from

ocean acidification i.e. saved energy arising from down-regulation of the CCM. Respiration rates were elevated at the first sampling in the current heatwave treatment but not in the future heatwave treatment. The lack of increase in respiration in the future heatwave treatment may also be related to CCM down-regulation. Elevated temperature can cause respiration to increase in seaweeds (Piñeiro-Corbeira et al., 2018) and it is possible that energetic savings due to CCM down-regulation counteracted such an increase in the future heatwave treatment. We did not detect the same reduction in $\delta^{13}\text{C}$ values in the first sampling however, and as such, we cannot be certain that the down-regulation of the CCM was occurring at this time. Although changes in $\delta^{13}\text{C}$ resulting from down-regulation of the CCM can be detected in less than 8 days in some brown seaweeds (Iñiguez et al., 2015), down-regulation will invariably occur before changes in $\delta^{13}\text{C}$ values of the tissue are detectable. Therefore, it is likely that down-regulation of the CCM was occurring during first 12 days of the experiment, but we were unable to detect the change.

There was some evidence of conditions being sub-optimal for photosynthesis during the heatwaves with a reduction in net photosynthesis detected in both heatwave treatments at the first sampling. This likely reflected a temporary reduction in photosynthetic activity rather than lasting damage to photosynthetic tissue, because it did not persist post-heatwaves and the temperature increases were relatively small ($\sim 3 - 6^\circ\text{C}$) compared to the changes of greater than 10°C frequently experienced by intertidal seaweeds (Hurd et al., 2014).

Inhibition of *de novo* synthesis of proteins to replace damaged ones can occur under elevated temperatures (Allakhverdiev et al., 2008) and this may have occurred in *P. comosa* in the heatwave treatments. Subsequent reductions in temperature following cessation of heatwaves may have then allowed *P. comosa* to replace damaged proteins, resulting in similar photosynthetic rates across treatments following the recovery period. Alternatively, this response may represent an energetic trade-off: to quickly respond to the temperature increase, *P. comosa* diverted energy away from photosynthesis towards temperature protection such as

the remodelling of fatty acids as we suggest, and other protective mechanisms such as the production of heat shock proteins (Eggert, 2012; Hurd et al., 2014).

During the first sampling, we detected a decrease in SFA and an increase in PUFA in the future scenario, which contrasted with the increase in SFA and decrease in PUFA observed at the final sampling. An explanation is that fatty acid adjustments in response to elevated temperatures may take longer than six days to detect in *P. comosa*. The time-scale at which seaweeds adjust fatty acid composition in response to changes in temperature has been generally understudied: elevated temperature induces changes in fatty acid composition in less than 7 days for a range of red, green and brown seaweed species (Al-Hasan et al., 1991) and in less than 3 days for *Macrocystis pyrifera* (Schmid et al. *in review*). However, changes in the fatty acid composition of land plants in response to elevated temperature can be ongoing after 11 days (Falcone et al., 2004) and it is possible that some seaweed species could take as long or longer to adjust fatty acid composition. The adjustment of fatty acid composition is a mechanism that may explain the resilience of some seaweeds to ocean warming. As such, a greater research focus on the time-scale at which seaweeds adjust their fatty acid composition in response to temperature is required if we are to understand the mechanisms by which seaweeds will be resilient to future ocean conditions.

Marine heatwaves are predicted to increase in duration in the future (Frölicher et al., 2018; Oliver et al., 2018a) and whether the acclimation mechanism presented here will be enough to mitigate any negative effects of longer heatwaves is unclear. Substantial tissue loss has been observed in *P. comosa* cultured at 22 °C (Flukes et al., 2015) and a recent modelling study projected the extinction of *P. comosa* in Australia by 2100 (Martínez et al., 2018). However, these papers considered temperature alone, whereas our work suggests that when combined with ocean acidification (i.e. elevated supply of CO₂) *P. comosa* may be more

resilient to ocean warming and marine heatwaves. The differing responses highlight the importance of considering co-occurring stressors: ocean warming and extreme events such as marine heatwaves are occurring simultaneously with ocean acidification, and all relevant factors need to be considered together when undertaking predictive studies on how species will respond in a future ocean.

Implications for management

P. comosa forms extensive beds over a large latitudinal range in eastern Australia (~ 1300 kms). Towards the northern (warmest) extent of its range, in Sydney, Australia, there is a substantial restoration program being undertaken (Campbell et al., 2014). This program aims to restore *P. comosa* forests in areas they were once abundant. A general focus is the importance of restoring populations that are able to persist in a future ocean (Wood et al., 2019). The responses presented here, which suggest that *P. comosa* may be resilient to future ocean conditions, indicate that these restoration efforts may remain successful in the future. However, this study was conducted on one population, which exists at the southern (coldest) extent of this species range. The response of other populations may differ and are likely to be dependent on the temperature regimes experienced by that population, interactions of warming with local environmental drivers, species interactions and genetic variability between populations. Future research should investigate whether the trends observed here are consistent across spatially separated populations to provide a clearer indication of how this species will respond over its entire range. Such research will assist in future-proofing restored populations of this species.

Funding sources

DB was supported by a University of Tasmania, Australian Postgraduate Award. FN was supported by the European Union's Horizon 2020 research and innovation programme under the Marie Skłodowska-Curie grant agreement (No. 701366). Matthias Schmid was supported by a grant of the Deutsche Forschungsgemeinschaft (DFG, grant ID: SCHM3335/1-1).

References

- Allakhverdiev, S. I., Kreslavski, V. D., Klimov, V. V., Los, D. A., Carpentier, R., & Mohanty, P. (2008). Heat stress: an overview of molecular responses in photosynthesis. *Photosynthesis Research*, 98, 541-550. doi:10.1007/s11120-008-9331-0
- Allen, C. D., Macalady, A. K., Chenchouni, H., Bachelet, D., McDowell, N., Vennetier, M., . . . Cobb, N. (2010). A global overview of drought and heat-induced tree mortality reveals emerging climate change risks for forests. *Forest Ecology and Management*, 259(4), 660-684. doi:<https://doi.org/10.1016/j.foreco.2009.09.001>
- Al-Hasan, R. H., Hantash, F. M., & Radwan, S. S. (1991). Enriching marine macroalgae with eicosatetraenoic (arachidonic) and eicosapentaenoic acids by chilling. *Applied Microbiology and Biotechnology*, 35(4), 530-535. doi:10.1007/BF00169763
- Banzon, V., Smith, T. M., Chin, T. M., Liu, C., & Hankins, W. (2016). A long-term record of blended satellite and in situ sea-surface temperature for climate monitoring, modeling and environmental studies. *Earth System Science Data*, 8(1), 165-176. doi:10.5194/essd-8-165-2016
- Bates, D., Mächler, M., Bolker, B., & Walker, S. (2015). Fitting linear mixed-effects models using lme4. *Journal of Statistical Software*; Vol 1, Issue 1 (2015). doi:10.18637/jss.v067.i01
- Becker, S., Graeve, M., & Bischof, K. (2010). Photosynthesis and lipid composition of the Antarctic endemic rhodophyte *Palmaria decipiens*: effects of changing light and temperature levels. *Polar Biology*, 33(7), 945-955. doi:10.1007/s00300-010-0772-5
- Bennett, S., Wernberg, T., Joy, B. A., De Bettignies, T., & Campbell, A. H. (2015). Central and rear-edge populations can be equally vulnerable to warming. *Nature Communications*, 6. doi:10.1038/ncomms10280
- Boyd, P. W., Dillingham, P. W., McGraw, C. M., Armstrong, E. A., Cornwall, C. E., Feng, Y. y., . . . Nunn, B. L. (2016). Physiological responses of a Southern Ocean diatom to complex future ocean conditions. *Nature Climate Change*, 6, 207. doi:10.1038/nclimate2811
- Boyd, P. W., Collins, S., Dupont, S., Fabricius, K., Gattuso, J. P., Havenhand, J., . . . Pörtner, H. O. (2018). Experimental strategies to assess the biological ramifications of multiple

drivers of global ocean change—A review. *Global Change Biology*, 24(6), 2239-2261. doi:10.1111/gcb.14102

Britton, D., Cornwall, C. E., Revill, A. T., Hurd, C. L., & Johnson, C. R. (2016). Ocean acidification reverses the positive effects of seawater pH fluctuations on growth and photosynthesis of the habitat-forming kelp, *Ecklonia radiata*. *Scientific Reports*, 6. doi:10.1038/srep26036

Britton, D., Mundy, C. N., McGraw, C. M., Revill, A. T., & Hurd, C. L. (2019). Responses of seaweeds that use CO₂ as their sole inorganic carbon source to ocean acidification: differential effects of fluctuating pH but little benefit of CO₂ enrichment. *ICES Journal of Marine Science*, fsz070. doi.org/10.1093/icesjms/fsz070

Burdett, H. L., Wright, H., & Smale, D. A. (2019). Photophysiological responses of canopy-forming kelp species to short-term acute warming. *Frontiers in Marine Science*, 6(516). doi:10.3389/fmars.2019.00516

Campbell, A. H., Marzinelli, E. M., Vergés, A., Coleman, M. A., & Steinberg, P. D. (2014). Towards restoration of missing underwater forests. *PLoS ONE*, 9(1), e84106. doi:10.1371/journal.pone.0084106

Cornwall, C. E., Revill, A. T., Hall-Spencer, J. M., Milazzo, M., Raven, J. A., & Hurd, C. L. (2017). Inorganic carbon physiology underpins macroalgal responses to elevated CO₂. *Scientific Reports*, 7, 46297. doi:10.1038/srep46297

Cornwall, C. E., Revill, A. T., & Hurd, C. L. (2015). High prevalence of diffusive uptake of CO₂ by macroalgae in a temperate subtidal ecosystem. *Photosynthesis Research*, 124(2), 181-190. doi:10.1007/s11120-015-0114-0

Davison, I. R. (1991). Environmental effects on algal photosynthesis: temperature. *Journal of Phycology*, 27(1), 2-8. doi:10.1111/j.0022-3646.1991.00002.x

Eggert, A. (2012). Seaweed responses to temperature. In C. Wiencke & K. Bischof (Eds.), *Seaweed biology: novel insights into ecophysiology, ecology and utilization* (pp. 47-66). Berlin, Heidelberg: Springer Berlin Heidelberg.

Falcone, D. L., Ogas, J. P., & Somerville, C. R. (2004). Regulation of membrane fatty acid composition by temperature in mutants of *Arabidopsis* with alterations in membrane lipid composition. *BMC Plant Biology*, 4(1), 17. doi:10.1186/1471-2229-4-17

Filbee-Dexter, K., Feehan, C. J., & Scheibling, R. E. (2016). Large-scale degradation of a kelp ecosystem in an ocean warming hotspot. *Marine Ecology Progress Series*, 543, 141-152. doi:10.3354/meps11554

Filbee-Dexter, K., & Wernberg, T. (2018). Rise of turfs: a new battlefield for globally declining kelp forests. *BioScience*, 68(2), 64-76. doi:10.1093/biosci/bix147

Flukes, E.B, Wright, J.T, & Johnson, C.R. (2015). Phenotypic plasticity and biogeographic variation in physiology of habitat-forming seaweed: response to temperature and nitrate. *Journal of Phycology*, 51. doi:10.1111/jpy.12330

- Frölicher, T. L., Fischer, E. M., & Gruber, N. (2018). Marine heatwaves under global warming. *Nature*, 560(7718), 360-364. doi:10.1038/s41586-018-0383-9
- Garrabou, J., Coma, R., Bensoussan, N., Bally, M., Chevaldonné, P., Cigliano, M., . . . Cerrano, C. (2009). Mass mortality in northwestern Mediterranean rocky benthic communities: effects of the 2003 heat wave. *Global Change Biology*, 15(5), 1090-1103. doi:10.1111/j.1365-2486.2008.01823.x
- Giordano, M., Beardall, J., & Raven, J. A. (2005). CO₂ concentrating mechanisms in algae: mechanisms, environmental modulation, and evolution. *Annual Review of Plant Biology*, 56, 99-131.
- Gosch, B. J., Lawton, R. J., Paul, N. A., de Nys, R., & Magnusson, M. (2015). Environmental effects on growth and fatty acids in three isolates of *Derbesia tenuissima* (Bryopsidales, Chlorophyta). *Algal Research*, 9, 82-93. doi:https://doi.org/10.1016/j.algal.2015.02.022
- Gouvêa, L. P., Schubert, N., Martins, C. D. L., Sissini, M., Ramlov, F., de Oliveira Rodrigues, E. R., . . . Simonassi, J. C. (2017). Interactive effects of marine heatwaves and eutrophication on the ecophysiology of a widespread and ecologically important macroalga. *Limnology and Oceanography*, 62(5), 2056-2075.
- Hepburn, C. D., Pritchard, D. W., Cornwall, C. E., McLeod, R. J., Beardall, J., Raven, J. A., & Hurd, C. L. (2011). Diversity of carbon use strategies in a kelp forest community: implications for a high CO₂ ocean. *Global Change Biology*, 17(7), 2488-2497.
- Hobday, A. J., Alexander, L. V., Perkins, S. E., Smale, D. A., Straub, S. C., Oliver, E. C. J., . . . Wernberg, T. (2016). A hierarchical approach to defining marine heatwaves. *Progress in Oceanography*, 141, 227-238. doi:https://doi.org/10.1016/j.pocean.2015.12.014
- Hurd, C. L., Harrison, P. J., Bischof, K., & Lobban, C. S. (2014). *Seaweed ecology and physiology* (2nd ed.). Cambridge: Cambridge University Press.
- Hurd, C. L., Lenton, A., Tilbrook, B., & Boyd, P. W. (2018). Current understanding and challenges for oceans in a higher-CO₂ world. *Nature Climate Change*, 8(8), 686-694. doi:10.1038/s41558-018-0211-0
- Iñiguez, C., Carmona, R., Lorenzo, M. R., Niell, F. X., Wiencke, C., & Gordillo, F. J. L. (2015). Increased CO₂ modifies the carbon balance and the photosynthetic yield of two common Arctic brown seaweeds: *Desmarestia aculeata* and *Alaria esculenta*. *Polar Biology*. doi:10.1007/s00300-015-1724-x
- IPCC. (2014). *Climate Change 2014: Synthesis Report. Contribution of Working Groups I, II and III to the Fifth Assessment Report of the Intergovernmental Panel on Climate Change* [Core Writing Team, R.K. Pachauri and L.A. Meyer (eds.)]. IPCC, Geneva, Switzerland.
- Johnson, C. R., Banks, S. C., Barrett, N. S., Cazassus, F., Dunstan, P. K., Edgar, G. J., . . . Taw, N. (2011). Climate change cascades: shifts in oceanography, species' ranges and subtidal marine community dynamics in eastern Tasmania. *Journal of Experimental Marine Biology and Ecology*, 400(1-2), 17-32. doi:http://dx.doi.org/10.1016/j.jembe.2011.02.032.
- Kain, J. M. (1982). Morphology and growth of the giant kelp *Macrocystis pyrifera* in New Zealand and California. *Marine Biology*, 67(2), 143-157.

- Krumhansl, K. A., Okamoto, D. K., Rassweiler, A., Novak, M., Bolton, J. J., Cavanaugh, K. C., . . . Byrnes, J. E. K. (2016). Global patterns of kelp forest change over the past half-century. *Proceedings of the National Academy of Sciences*, 113(48), 13785. doi:10.1073/pnas.1606102113
- Kübler, J. E., & Dudgeon, S. R. (2015). Predicting effects of ocean acidification and warming on algae lacking carbon concentrating mechanisms. *PLoS ONE*, 10(7), e0132806. doi:10.1371/journal.pone.0132806
- Ling, S. D., Johnson, C. R., Frusher, S. D., & Ridgway, K. R. (2009). Overfishing reduces resilience of kelp beds to climate-driven catastrophic phase shift. *Proceedings of the National Academy of Sciences of the United States of America*, 106(52), 22341-22345.
- Los, D. A., & Murata, N. (2004). Membrane fluidity and its roles in the perception of environmental signals. *Biochimica et Biophysica Acta (BBA) - Biomembranes*, 1666(1), 142-157. doi:https://doi.org/10.1016/j.bbamem.2004.08.002
- Lotze, H. K., Worm, B., & Sommer, U. (2001). Strong bottom-up and top-down control of early life stages of macroalgae. *Limnology and Oceanography*, 46(4), 749-757. doi:10.4319/lo.2001.46.4.0749
- Lueker, T. J., Dickson, A. G., & Keeling, C. D. (2000). Ocean pCO₂ calculated from dissolved inorganic carbon, alkalinity, and equations for K₁ and K₂: validation based on laboratory measurements of CO₂ in gas and seawater at equilibrium. *Marine Chemistry*, 70(1), 105-119. doi:https://doi.org/10.1016/S0304-4203(00)00022-0
- Maberly, S., Raven, J., & Johnston, A. (1992). Discrimination between ¹²C and ¹³C by marine plants. *Oecologia*, 91(4), 481-492.
- Martínez, B., Radford, B., Thomsen, M. S., Connell, S. D., Carreño, F., Bradshaw, C. J. A., . . . Wernberg, T. (2018). Distribution models predict large contractions of habitat-forming seaweeds in response to ocean warming. *Diversity and Distributions*, 24(10), 1350-1366. doi:10.1111/ddi.12767
- McGraw, C. M., Cornwall, C. E., Reid, M. R., Currie, K. I., Hepburn, C. D., Boyd, P., . . . Hunter, K. A. (2010). An automated pH-controlled culture system for laboratory-based ocean acidification experiments. *Limnology and Oceanography: Methods*, 8(12), 686-694. doi:doi:10.4319/lom.2010.8.0686
- Mehrbach, C., Culbertson, C. H., Hawley, J. E., & Pytkowicz, R. M. (1973). Measurement of the apparent dissociation constants of carbonic acid in seawater at atmospheric pressure. *Limnology and Oceanography*, 18(6), 897-907. doi:doi:10.4319/lo.1973.18.6.0897
- Mills, K. E., Pershing, A. J., Brown, C. J., Chen, Y., Chiang, F.-S., Holland, D. S., . . . Thomas, A. C. (2013). Fisheries management in a changing climate: lessons from the 2012 ocean heat wave in the Northwest Atlantic. *Oceanography*, 26(2), 191-195.
- Mineur, F., Arenas, F., Assis, J., Davies, A. J., Engelen, A. H., Fernandes, F., . . . De Clerck, O. (2015). European seaweeds under pressure: Consequences for communities and ecosystem functioning. *Journal of Sea Research*, 98, 91-108. doi:10.1016/j.seares.2014.11.004

- Oliver, E. C. J., Benthuyssen, J. A., Bindoff, N. L., Hobday, A. J., Holbrook, N. J., Mundy, C. N., & Perkins-Kirkpatrick, S. E. (2017). The unprecedented 2015/16 Tasman Sea marine heatwave. *Nature Communications* 8, 16101. doi:10.1038/ncomms16101
- Oliver, E. C. J., Donat, M. G., Burrows, M. T., Moore, P. J., Smale, D. A., Alexander, L. V., . . . Wernberg, T. (2018a). Longer and more frequent marine heatwaves over the past century. *Nature Communications*, 9(1). doi:10.1038/s41467-018-03732-9
- Oliver, E. C. J., Lago, V., Hobday, A. J., Holbrook, N. J., Ling, S. D., & Mundy, C. N. (2018b). Marine heatwaves off eastern Tasmania: trends, interannual variability, and predictability. *Progress in Oceanography*, 161, 116-130. doi:https://doi.org/10.1016/j.pocean.2018.02.007
- Parrish, C. C., Nichols, P. D., Pethybridge, H., & Young, J. W. (2015). Direct determination of fatty acids in fish tissues: quantifying top predator trophic connections. *Oecologia*, 177(1), 85-95. doi:10.1007/s00442-014-3131-3
- Piñeiro-Corbeira, C., Barreiro, R., Cremades, J., & Arenas, F. (2018). Seaweed assemblages under a climate change scenario: functional responses to temperature of eight intertidal seaweeds match recent abundance shifts. *Scientific Reports*, 8(1). doi:10.1038/s41598-018-31357-x
- Poloczanska, E. S., Burrows, M. T., Brown, C. J., Molinos, J. G., Halpern, B. S., Hoegh-Guldberg, O., . . . Sydeman, W. J. (2016). Responses of marine organisms to climate change across oceans. *Frontiers in Marine Science*, 3. doi:10.3389/fmars.2016.00062
- R Core Team. (2019). R: A language and environment for statistical computing. Vienna, Austria. URL: <https://www.R-project.org/>; R Foundation for Statistical Computing. Retrieved from <https://www.R-project.org/>
- Raven, J. A., & Geider, R. J. (1988). Temperature and algal growth. *New Phytologist*, 110(4), 441-461. doi:10.1111/j.1469-8137.1988.tb00282.x
- Robbins, L. L., Hansen, M. E., Kleypas, J. A., & Meylan, S. C. (2010). CO2calc—A user-friendly seawater carbon calculator for Windows, Mac OS X, and iOS (iPhone). U.S. Geological Survey Open-File Report 2010, 1280, 17.
- Schmid, M., Guihéneuf, F., & Stengel, D. B. (2017). Ecological and commercial implications of temporal and spatial variability in the composition of pigments and fatty acids in five Irish macroalgae. *Marine Biology*, 164(8), 158. doi:10.1007/s00227-017-3188-8
- Schmid, M., Kraft, L. G. K., van der Loos, L. M., Kraft, G. T., Virtue, P., Nichols, P. D., & Hurd, C. L. (2018). Southern Australian seaweeds: a promising resource for omega-3 fatty acids. *Food Chemistry*, 265, 70-77. doi:https://doi.org/10.1016/j.foodchem.2018.05.060
- Seely, G. R., Duncan, M. J., & Vidaver, W. E. (1972). Preparative and analytical extraction of pigments from brown algae with dimethyl sulfoxide. *Marine Biology*, 12(2), 184-188. doi:10.1007/BF00350754
- Smale, D. A., & Wernberg, T. (2013). Extreme climatic event drives range contraction of a habitat-forming species. *Proceedings of the Royal Society B: Biological Sciences*, 280(1754), 20122829. doi:10.1098/rspb.2012.2829

- Smale, D. A., Wernberg, T., Oliver, E. C. J., Thomsen, M., Harvey, B. P., Straub, S. C., . . . Moore, P. J. (2019). Marine heatwaves threaten global biodiversity and the provision of ecosystem services. *Nature Climate Change*, 9(4), 306-312. doi:10.1038/s41558-019-0412-1
- Steneck, R. S., Graham, M. H., Bourque, B. J., Corbett, D., Erlandson, J. M., Estes, J. A., & Tegner, M. J. (2002). Kelp forest ecosystems: biodiversity, stability, resilience and future. *Environmental Conservation*, 29(4), 436-459.
- Stephens, T., & Hepburn, C. (2014). Mass-transfer gradients across kelp beds influence *Macrocystis pyrifera* growth over small spatial scales. *Marine Ecology Progress Series*, 515, 97-109.
- Straub, S. C., Wernberg, T., Thomsen, M. S., Moore, P. J., Burrows, M. T., Harvey, B. P., & Smale, D. A. (2019). Resistance, extinction, and everything in between – The diverse responses of seaweeds to marine heatwaves. *Frontiers in Marine Science*, 6(763). doi:10.3389/fmars.2019.00763
- Takao, S., Kumagai, N. H., Yamano, H., Fujii, M., & Yamanaka, Y. (2015). Projecting the impacts of rising seawater temperatures on the distribution of seaweeds around Japan under multiple climate change scenarios. *Ecology and Evolution*, 5(1), 213-223. doi:10.1002/ece3.1358
- Thomsen, M. S., Mondardini, L., Alestra, T., Gerrity, S., Tait, L., South, P. M., . . . Schiel, D. R. (2019). Local extinction of bull kelp (*Durvillaea spp.*) due to a marine heatwave. *Frontiers in Marine Science*, 6. doi:10.3389/fmars.2019.00084
- Valentine, J. P., & Johnson, C. R. (2004). Establishment of the introduced kelp *Undaria pinnatifida* following dieback of the native macroalga *Phyllospora comosa* in Tasmania, Australia. *Marine and Freshwater Research*, 55(3), 223-230. doi:10.1071/MF03048
- van der Loos, L. M., Schmid, M., Leal, P. P., McGraw, C. M., Britton, D., Revill, A. T., . . . Hurd, C. L. (2019). Responses of macroalgae to CO₂ enrichment cannot be inferred solely from their inorganic carbon uptake strategy. *Ecology and Evolution*, 9(1), 125-140. doi:10.1002/ece3.4679
- Voerman, S. E., Llera, E., & Rico, J. M. (2013). Climate driven changes in subtidal kelp forest communities in NW Spain. *Marine Environmental Research*, 90, 119-127. doi:10.1016/j.marenvres.2013.06.006
- Wernberg, T., Bennett, S., Babcock, R. C., De Bettignies, T., Cure, K., Depczynski, M., . . . Wilson, S. (2016). Climate-driven regime shift of a temperate marine ecosystem. *Science*, 353(6295), 169-172. doi:10.1126/science.aad8745
- Wheeler, W. N. (1980). Pigment content and photosynthetic rate of the fronds of *Macrocystis pyrifera*. *Marine Biology*, 56(2), 97-102. doi:10.1007/BF00397127
- White, C. A., Bannister, R. J., Dworjanyn, S. A., Husa, V., Nichols, P. D., Kutti, T., & Dempster, T. (2017). Consumption of aquaculture waste affects the fatty acid metabolism of a benthic invertebrate. *Sci Total Environ*, 586, 1170-1181. doi:10.1016/j.scitotenv.2017.02.109

Wilson, K. L., Kay, L. M., Schmidt, A. L., & Lotze, H. K. (2015). Effects of increasing water temperatures on survival and growth of ecologically and economically important seaweeds in Atlantic Canada: implications for climate change. *Marine Biology*, 162(12), 2431-2444. doi:10.1007/s00227-015-2769-7

Wilson, K. L., Skinner, M. A., & Lotze, H. K. (2019). Projected 21st-century distribution of canopy-forming seaweeds in the northwest Atlantic with climate change. *Diversity and Distributions*, 25(4), 582-602. doi:10.1111/ddi.12897

Wood, G., Marzinelli, E. M., Coleman, M. A., Campbell, A. H., Santini, N. S., Kajlich, L., . . . Vergés, A. (2019). Restoring subtidal marine macrophytes in the Anthropocene: trajectories and future-proofing. *Marine and Freshwater Research*, 70(7), 936-951. doi:https://doi.org/10.1071/MF18226

Appendices

Supplementary methods – pH logger calibration

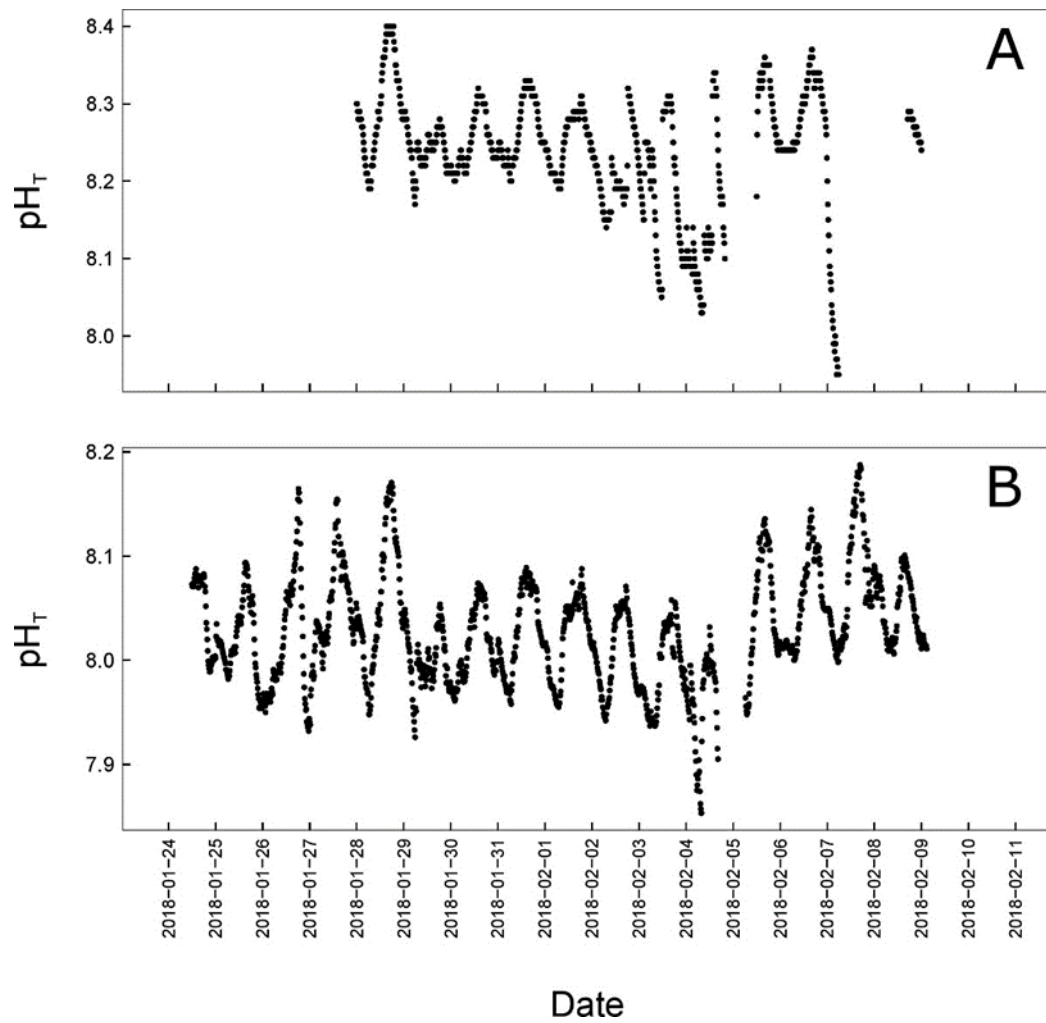
The pH loggers were calibrated against NBS pH buffers 4, 7 and 10 (Thermo Scientific) as well as homemade TRIS buffer (Dickson et al. 2007), at lab temperature (i.e. $21.2 \pm 0.2^\circ\text{C}$) before being immersed. Following collection, they were calibrated again to check and correct for any drift of the instruments. Values recorded by loggers in millivolts were converted into pH values on the total scale, following the SOP6a procedure of Dickson et al. 2007 using TRIS buffer. Occasionally during deployment, the loggers provided nonsensical data (highly variable, erratic measurements, possibly due to direct contact of the electrode with biological or abiotic material). During such instances the data was not included in any analysis or figures.

Dickson, A., Chris, S., and Christian, J. R. 2007. Guide to Best Practices for Ocean CO₂ Measurements. Guide to Best Practices for Ocean CO₂ Measurements, 3.

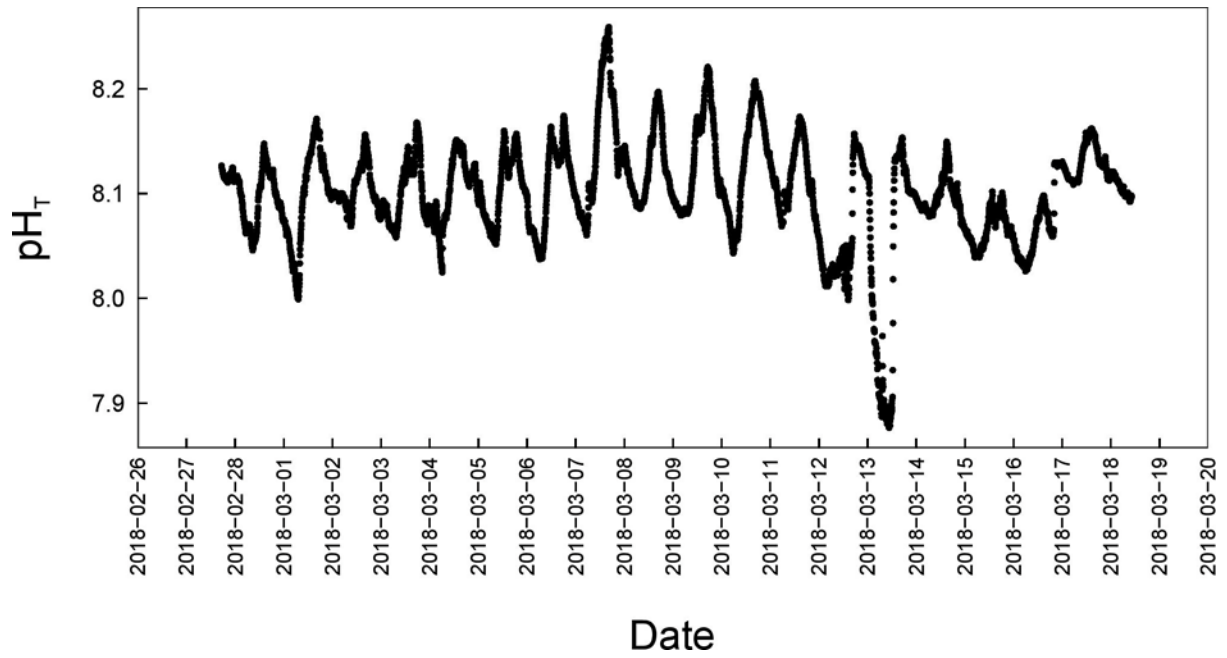
Supplementary methods – light logger calibration

The light and temperature logger (HOBO Pendant MX temp/light, Onset Computer Corporation, USA) measured light levels in lux. Measurements of lux were converted to Photosynthetically Active Radiation (PAR) with a relationship between PAR and lux we determined with a LI-COR LI-192 2π quantum sensor. This relationship was developed by measuring the average light intensity (lux) of the logger over a period of 15 seconds and comparing to the average PAR recorded by the LI-COR over the same time period. This comparison was made over a range of light intensities from $1106 \mu\text{mol photons m}^{-2} \text{s}^{-1}$ to $0 \mu\text{mol photons m}^{-2} \text{s}^{-1}$. The range of light intensities were achieved by lowering both the logger and the sensor off a wharf into the water and making measurements at different depths.

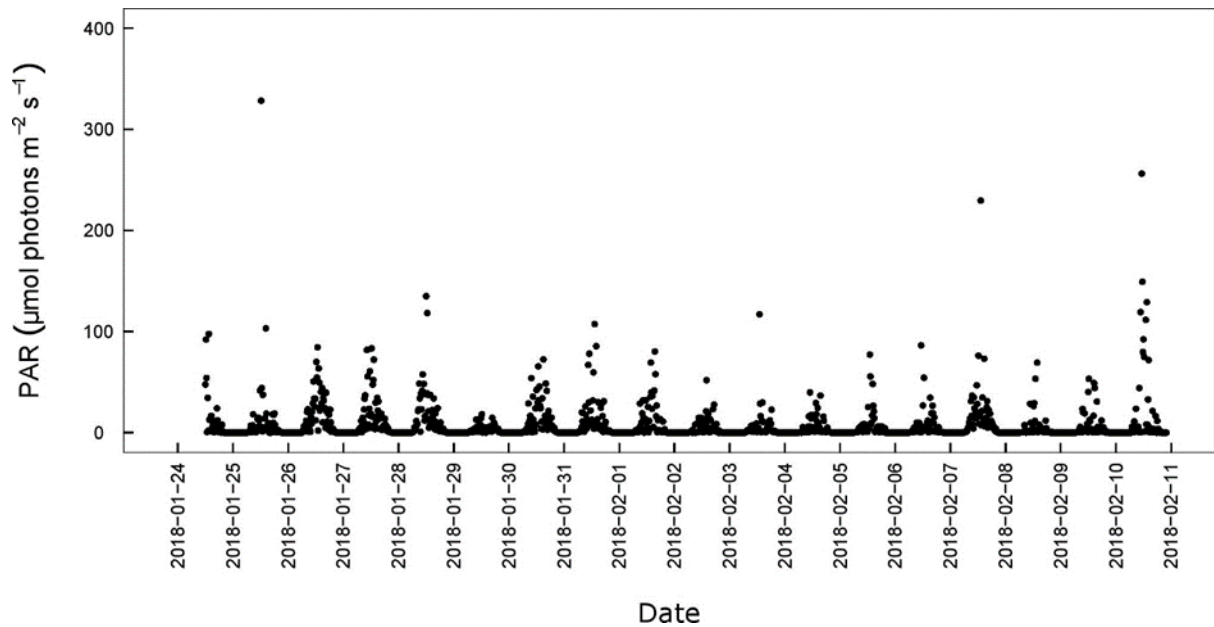
The calibration equation was: $\text{PAR} = 0.0166 \times \text{lux}$



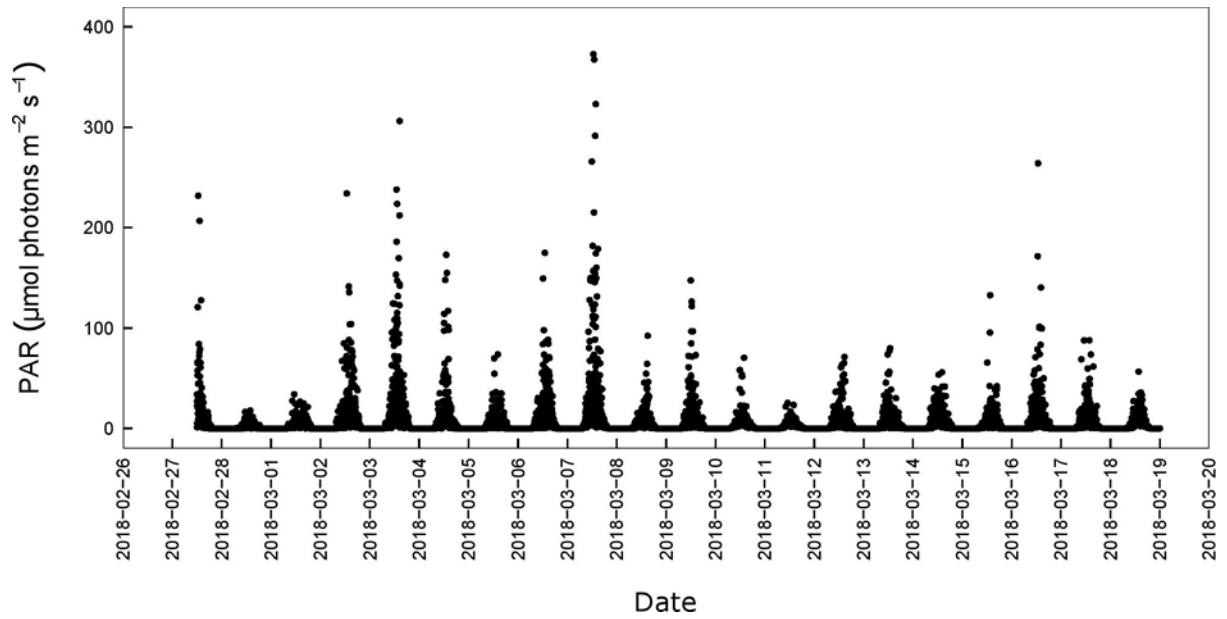
Appendix 4.1: Measurements of pH_T taken with two pH loggers (A: Logger 1, B: Logger 2) deployed at Coal Point, Bruny Island, Tasmania, Australia between 24th January 2018 and 2nd February 2018.



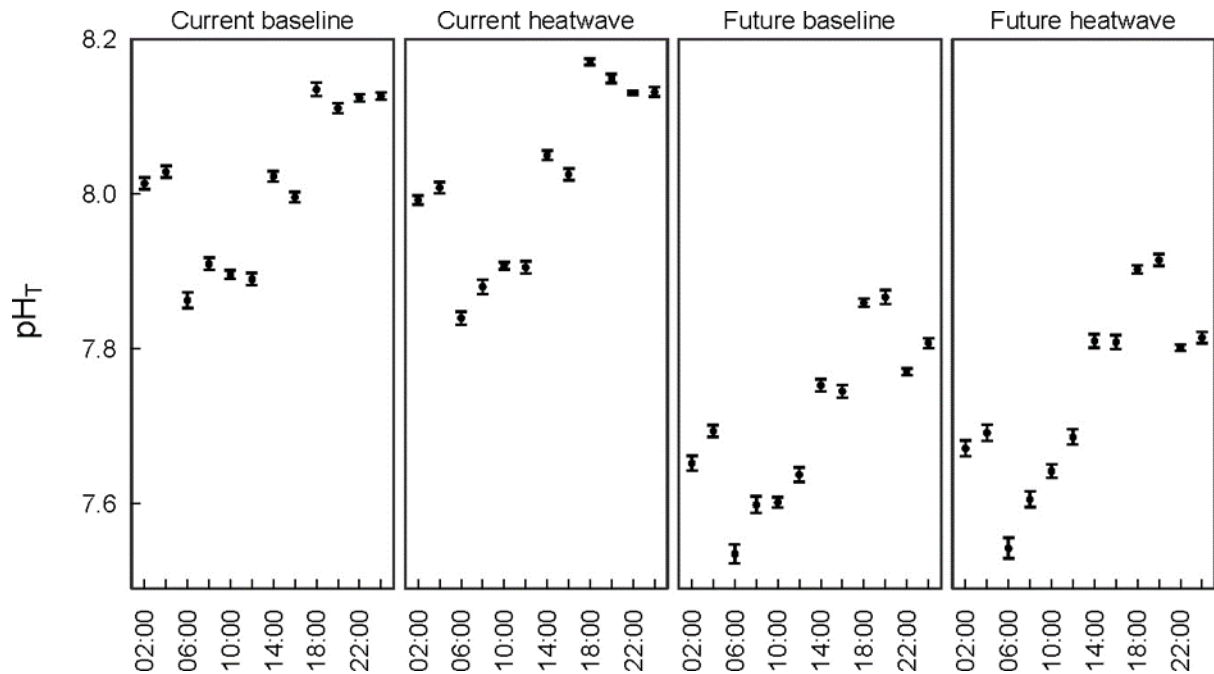
Appendix 4.2: Measurements of pH_T taken with a pH logger deployed at Coal Point, Bruny Island, Tasmania, Australia between 26th February 2018 and 20th March 2018.



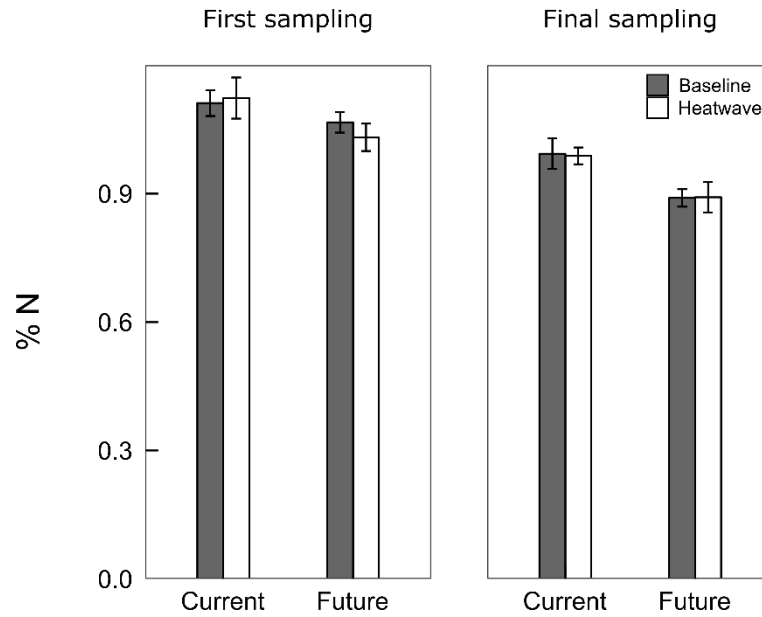
Appendix 4.3: Photosynthetically active radiation (PAR) measured at Coal Point, Bruny Island, Tasmania, Australia between 24th January 2018 and 2nd February 2018.



Appendix 4.4: Photosynthetically active radiation (PAR) measured at Coal Point, Bruny Island, Tasmania, Australia between 26th February 2018 and 20th March 2018.



Appendix 4.5: Mean pH_T of experimental treatments as measured in culture chambers over the course of the experiment at two-hour intervals. Error bars are \pm standard error, $n = 99-120$.



Appendix 4.6: Percentage tissue nitrogen content of juvenile *Phyllospora comosa* at the end of the heatwave period (first sampling, left panels) and following the recovery period (final sampling, right panels). *P. comosa* juveniles were cultured in current (today's temperature and pH) and future (2100 temperature and pH projections) scenarios. Shaded bars refer to baseline temperature treatments, and white bars refer to treatments where a 6 day 3 °C heatwave was superimposed on the baseline temperature in a given scenario. Significant differences are described for each panel. % N; first sampling, no significant differences (future < current, $p=0.063$); final sampling, future < current ($p = 0.001$). Data are presented as means \pm standard error, $n = 6$.

Chapter 5. Crustose coralline algae are sensitive to near future global ocean change scenarios.

Damon Britton, Craig N. Mundy, Fanny Noisette, Christina M. McGraw, Catriona L. Hurd

This chapter is currently in preparation for submission to a peer reviewed journal.

Abstract

Ocean warming and acidification are predicted to substantially impact crustose coralline algae (CCA), with potentially negative impacts on species that require CCA to induce metamorphosis. Most laboratory studies investigate the response of CCA to combined warming and acidification under the high emissions scenario (i.e. RCP 8.5), with few assessing responses to the low emissions scenario or near future conditions. To address this knowledge gap, we examined the responses of the temperate CCA *Sporolithon spp.* to combined warming and acidification in a laboratory experiment. CCA were exposed to conditions simulating today's pH and temperature and those projected under low, medium, and high emissions (RCP 2.6, 4.5, and 8.5). All RCP scenarios negatively affected CCA, with the greatest effects under RCP 8.5. The negative responses of CCA to both RCP 2.6 and 4.5 suggest that they may be adversely impacted by combined warming and acidification by 2030 if current emissions are sustained.

Introduction

Since the industrial revolution, anthropogenic greenhouse gas emissions have caused average global sea surface temperatures to rise by approximately 0.11 °C per decade (IPCC 2014, ocean warming). A further increase of between 2 – 3 °C is projected to occur by the end of this century depending on which Representative Concentration Pathway (RCP) emissions scenario is realised (IPCC, 2014). Concurrently with ocean warming, the sustained absorption of rising atmospheric CO₂ levels has caused ocean pH to decrease by ~ 0.1 unit and a further decrease of ~ 0.3 units is projected by 2100 under the RCP 8.5 scenario (IPCC 2014, ocean acidification). Ocean warming and ocean acidification are predicted to impact marine communities, with losses of canopy-forming seaweed species (Martínez et al., 2018) and subsequent effects on the commercial fisheries that depend on these habitat structuring species (Pinsky and Fogarty, 2012; Mills et al., 2013). Despite these impacts, the effects of combined warming and acidification on many ecologically important, but visually cryptic species remain unclear as researchers have tended to focus on visually dominant species such as corals and kelps, with smaller keystone species such as coralline algae receiving comparatively little attention (Cornwall et al., 2018).

One of the most crucial species in nearshore reef ecosystems globally are crustose coralline algae (CCA). CCA are species of calcified encrusting red macroalgae in the order Corallinales. These species play key ecological roles in temperate, tropical and polar ecosystems by creating and stabilising reefs (Nelson, 2009) and they provide settlement cues to a range of invertebrate larvae such as corals (Heyward and Negri, 1999; Doropoulos and Diaz-Pulido, 2013), sea urchins (Pearce and Scheibling, 1991) and abalone (Daume et al., 1999; Roberts, 2001; Roberts et al., 2010). CCA are highly susceptible to global ocean change, particularly ocean acidification. They generally respond negatively to ocean acidification (Hofmann and Bischof; Kroeker et al., 2013; McCoy, 2013; Fabricius et al.,

2015), because they precipitate a highly soluble form of calcium carbonate that is costly to maintain under reduced pH (Ries, 2011; Fabricius et al., 2015; McCoy and Kamenos, 2015; Cornwall et al., 2017). The effects of ocean warming on corallines has been less extensively studied than acidification and there is substantial species-specific variability in responses (Cornwall et al., 2019). The meta-analysis of Cornwall et al. (2019) found a net reduction in calcification under elevated temperatures; however, they noted that most studies have been conducted in European seas and the north Pacific Ocean, with very few studies in polar regions and the temperate regions of the southern hemisphere. The combined effects of warming and acidification on corallines have been examined in 23 studies and responses have been highly varied: in some species, the negative effects of OA are exacerbated by elevated temperature (Anthony et al., 2008; Martin and Gattuso, 2009; Martin et al., 2013; Ordoñez et al., 2017; Graba-Landry et al., 2018; Sordo et al., 2019), in others elevated temperature mitigates the effects of OA (Johnson and Carpenter, 2012; Huggett et al., 2018) and in some species, the drivers act independently or no effects are observed (Comeau et al., 2014; Comeau et al., 2016; Schoenrock et al., 2016; Vásquez-Elizondo and Enríquez, 2016; Vogel et al., 2016; Rich et al., 2018; Qui-Minet et al., 2019).

Most studies have focused on the responses of corallines to the most extreme emissions scenario i.e. RCP 8.5, with 73 % of studies using either temperature or pH levels projected under RCP 8.5 or worse in the future treatments. While this approach has highlighted the susceptibility of corallines to global ocean change and provides predictions of how species may respond in 2100, it makes it difficult to predict how species will respond to less extreme emissions scenarios or in the near future. Furthermore, only three studies have examined multiple scenarios of future temperature and pH simultaneously (Schoenrock et al., 2016; Vogel et al., 2016; Graba-Landry et al., 2018). Most studies assess the response to warming and acidification in a factorial design with one level of each driver (Martin and Gattuso, 2009; Martin et al., 2013; Schoenrock et al., 2016; Vásquez-Elizondo and Enríquez, 2016;

Legrand et al., 2017; Huggett et al., 2018; Legrand et al., 2018; Rich et al., 2018; Legrand et al., 2019; Marchini et al., 2019; Qui-Minet et al., 2019), or use multiple levels of either pH or temperature, crossed with one level of the other driver (Anthony et al., 2008; Diaz-Pulido et al., 2012; Johnson and Carpenter, 2012; Noisette et al., 2013; Comeau et al., 2014; Comeau et al., 2016; Sordo et al., 2019). While these approaches are useful in developing a mechanistic understanding of which driver is the primary influence and identify interactions, they can be limited in their predictive capabilities; both drivers are changing concurrently and scenarios such as a 4 °C temperature occurring alongside a 0.1 unit or no decrease in pH is unlikely to occur (excluding unique cases such as during marine heatwave events).

An alternative experimental design, that is more focused on predicting species responses under future ocean conditions, is to use a ‘scenario-based approach’ (Boyd et al., 2018). In this approach, future projections of co-occurring drivers (i.e. pH and temperature) are modified concurrently at levels projected to occur under different emissions scenarios (e.g. current versus RCP 2.6, 4.5 or 8.5 – for examples see Reyes-Nivia *et al.* 2014; Vogel *et al.* 2016) or timescales (e.g. current versus 2050 and 2100). This design, despite being unable to assess the effects of individual drivers independently, has the major benefit of being able to allocate resources towards undertaking predictions over multiple emissions scenarios. As such, these experiments can provide clear predictions, identify tipping points and the results may be easily interpreted by policy makers or industry. More scenario-based experiments are needed in order to assess the response of corallines to moderate emissions scenarios or near future conditions.

The Great Southern Reef is a diverse and productive reef system that spans 6000 kms along the temperate coastline of Australia (Bennett et al., 2015). The seaweeds in this region support highly productive fisheries including abalone and urchin fisheries, which rely on

CCA to provide settlement cues for metamorphosis (Pearce and Scheibling, 1991; Daume et al., 1999). Areas of the Great Southern Reef are under threat from climate change, with south-eastern Australia particularly susceptible (Johnson et al., 2011). Southeastern Australia is an ocean warming hotspot with warming occurring at a rate of 3 – 4 times the global average (Hobday and Pecl, 2014). The rapid warming coupled with ocean acidification and other environmental stressors such as marine heatwaves are likely to have impacts on the ecologically important CCA from this region. Despite this, there are no studies assessing the combined impacts of warming and acidification on CCA from temperate regions of Australia or the southern hemisphere (however see Huggett et al. (2018) for a study on the articulated coralline *Amphiroa gracilis*). To address this knowledge gap, we undertook a manipulative experiment assessing the growth, photosynthetic and calcification responses of the CCA *Sporolithon spp.* to combined warming and acidification. A scenario-based approach was used, in which the responses of CCA cultured under today's pH and temperature ($\text{pH}_T = 8.00$, 15°C) were compared to those projected to occur by 2100 under the RCP scenarios 2.6 ($\text{pH}_T = 7.90$, 16°C), 4.5 ($\text{pH}_T = 7.80$, 17°C) and 8.5 ($\text{pH}_T = 7.65$, 18.5°C). We hypothesised that the impacts of future ocean conditions on CCA growth, photosynthesis and calcification would be negative in all cases and the magnitude of the impacts would be greater with each successive scenario. We demonstrate that the negative impacts of combined warming and acidification on coralline algae are detectable even under moderate emissions scenarios. We highlight that if the RCP 8.5 scenario is realised then impacts are likely to be observable as soon as 2030, and severe by 2050. This will potentially have far reaching consequences for commercially important invertebrates that rely on them to induce settlement of larvae and provide habitat for the susceptible post-larval phase.

Materials and methods

Deployment and collection of settlement plates and in situ CCA cover estimates

Four acrylic plates measuring 15 cm × 15 cm were deployed by divers using SCUBA at Black Reef, Tasmania (43.5380° S, 146.9733° E) at a depth of 10 m on the 21 July 2017. The plates were attached with stainless steel bolts to larger (~ 50 cm diameter) acrylic plates that were secured directly to the reef. The surface of each plate was scratched with coarse sandpaper before deployment to promote settlement of CCA recruits. Plates remained in the field until 25 February 2019 at which stage, they had developed an advanced CCA community. During collection, plates were placed in individual zip-lock bags with seawater and were stored in an insulated container in darkness immediately upon return to the surface. The plates were kept in this container for ~ 5 hours until return to the laboratory. To provide an estimate of the percentage cover of CCA *in situ*, photo quadrats were taken at 7 m depth at three sites along the eastern coast of Tasmania, Australia following spring 2017, summer 2018 and winter 2018 (Appendix 5.1 contains coordinates of sites). Percentage cover of CCA was calculated using the online software CoralNet (Beijbom et al., 2015).

Pre-experimental treatment

Upon return to the laboratory each plate was placed in an individual 20 L container with seawater filtered to 1 µm under constant aeration at 15 °C. These conditions were maintained for 72 hours on a 12:12 light:dark cycle and light levels were kept at 10 µmol photons m⁻² s⁻¹. This irradiance was used as pilot studies indicated the CCA grew and remained unbleached for over 1 month at this irradiance in ambient seawater. After 72 hours, the plates were cut into smaller 4 cm × 4 cm squares and the CCA towards the edges of the plates were cleared with scalpel to allow space for growth. This step was undertaken as the larger plates would not fit in culture chambers and this size was needed to attach plates for settlement in the field. The smaller plates were then returned to the 20 L containers and maintained under the same

conditions for 12 days prior to the beginning of the experiment on the 13 March 2019.

Seawater was refreshed every 3 days.

Experimental culture conditions

Experiments were conducted in an automated culture system capable of modifying both pH and temperature. Every four hours, seawater in each of the 32 chambers was replaced with pH and temperature-adjusted seawater. Mass flow controllers (FMA5418A and FMA5402A, Omega Engineering, USA) were used to adjust the ratio of CO₂ to air in a gas mix and seawater from a universal header tank was equilibrated with this mix using membrane contactors (Liqui-Cel™ MM-1×5.5 Series, 3M, USA). Adjustments of pH were made prior to modifying the temperature and an automated spectrophotometric pH_T system (McGraw et al., 2010) was incorporated into a feedback loop. This system allowed incoming seawater to be within 0.03 pH_T units of target values. Following pH adjustments, seawater passed through one of four water baths maintained at the treatment temperatures using aquarium heaters (Jager 3612, Eheim, Germany). To maintain temperature in the culture chambers water from a second set of water baths was circulated around each culture chamber through external water jackets. This second set of water baths had temperature maintained using aquarium heaters (Jager 3612, Eheim, Germany and Aqua One IPX8, Kongs Australia, Australia) and temperature controllers (Temperature Controller 7028/3, Tunze, Germany). Temperature was measured with temperature loggers (HOBO Pendant MX temp/light, Onset Computer Corporation, USA) within random culture chambers of each treatment. Further detail on the culture system can be found in Britton et al. (2020).

Determination of carbonate chemistry

Measurements of pH within culture chambers were obtained independent of the main pH control system using a second automated spectrophotometric pH_T system and all pH_T values. Seawater samples (100 ml) for determination of total alkalinity (A_T) were collected at the mean pH and temperature of each treatment on day 27 and day 29. Samples were collected by gently filtering seawater through 0.7 μm glass microfibre filters (Grade GF/F, Whatman®, United Kingdom) into 100 ml Schott bottles. Samples were poisoned immediately with HgCl_2 (0.02 % vol/vol, Dickson et al., 2007) and stored in darkness until analysis. Total alkalinity was determined by 0.01 N HCl potentiometric titration (Dickson et al., 2007), using an automatic titrator (848 Titrino Plus, Metrohm, Herisau, Switzerland) at the University of Québec in Rimouski. The technical repeatability was 5 $\mu\text{mol kg}^{-1}$ seawater. Dissolved inorganic carbon DIC was calculated in CO2calc (Robbins et al., 2010) using the constants of Mehrbach et al. (1973) refit by Lueker et al. (2000) and the known pH_T , A_T , temperature and salinity of the seawater. All pH_T values were measured between 15.95 °C and 24.75 °C but are reported at the treatment temperatures.

Experimental treatments

On day one of the experiment, 32 of the smaller plates with unbleached CCA assemblages were randomly allocated to one of four experimental treatments; three treatments were based on projections of the RCP scenarios (IPCC, 2014), and one treatment simulated present day conditions, with $n = 8$ replicates for each treatment. The target values of pH_T and temperature for each treatment were : “Current” ($\text{pH}_T = 8.00$, temperature = 15 °C), “RCP 2.6” ($\text{pH}_T = 7.90$, temperature = 16 °C), “RCP 4.5” ($\text{pH}_T = 7.80$, temperature = 17 °C), “RCP 8.5” ($\text{pH}_T = 7.65$, temperature = 18.5 °C). To mimic the diel fluctuations of pH_T observed in a similar habitat to where the settlement plates were deployed (Britton et al., 2020), pH_T increased by 0.1 unit every 4 hours in the light (starting at 0.15 units below the mean as lights turned on at

06:00), and decreased by 0.1 unit every 4 hours in the dark (starting at 0.15 units above the mean as the lights turned off at 18:00). This resulted in the treatments having the mean pH_T described above with a range of ± 0.15 units around the mean (see Appendix 5.2 for target pH_T every 4 hours in each treatment). The CCA were cultured in the experimental treatments for a total of 29 days at which point they were removed, and biotic responses analysed. Light conditions were the same as in the pre-experimental treatment. Each week, CCA were briefly removed from culture and gently brushed with a soft toothbrush to prevent biofilm overgrowth.

Biotic responses

Relative growth rates (RGR) and percentage bleaching

Relative growth rates (RGR) were calculated from change in the surface area of CCA crusts measured on day 1 and day 29 and the equations of (Kain, 1982). Percentage of bleached tissue was measured by calculating the percentage of the total CCA area on each plate that had no pigmentation. The surface area and percentage of bleached tissue were measured in the image software Fiji (Schindelin et al., 2012).

Net photosynthesis

Oxygen evolution at experimental irradiance was measured in sealed chambers of seawater (260 mL, hereafter “oxygen chambers”) containing the CCA plates. The oxygen chambers were kept in water baths, maintained at the treatment temperatures and were placed on orbital shaker tables (OM7 Large Orbital Shaker, Ratek Instruments, Australia). Seawater for each treatment had pH adjusted to the mean pH_T of the treatment. Incubations were conducted for ~ 6 hours and measurements were made at the beginning and end of incubations. All oxygen measurements were made with a portable oxygen meter (Fibox 4, PreSens, Germany),

coupled with a non-invasive oxygen sensor in each oxygen chamber (Oxygen Sensor Spot SP-PSt3-NAU, PreSens, Germany). As we had only 16 oxygen chambers, measurements were made on 4 replicates for each treatment on day 27 and day 29. Net photosynthesis is expressed as $\mu\text{mol O}_2 \text{ L}^{-1} \text{ cm}^{-2} \text{ h}^{-1}$ produced.

Net calcification

To estimate net calcification rates of the CCA assemblages, seawater samples were taken for total alkalinity (A_T) on day 27 and 29 at the beginning and end of oxygen incubations. Initial samples were taken from the bulk seawater used to fill oxygen chambers with 3 replicate initial samples taken for each treatment on both days. Final measurements were taken in all oxygen chambers. Samples were taken and A_T determined as described above

(Determination of carbonate chemistry). Net calcification ($\mu\text{mol CaCO}_3 \text{ cm}^{-2} \text{ h}^{-1}$) rates were estimated using the alkalinity anomaly technique of Smith and Key (1975), in which a decrease in A_T of 2 moles corresponds to 1 mole of CaCO_3 precipitated (Wolf-Gladrow et al., 2007).

Statistical analysis

All statistical analyses were conducted statistical software R v. 3.6.1 (R Core Team, 2019). To test for differences in RGRs and % bleaching between treatments, a one-way Analysis of Variance (ANOVA) was conducted with the fixed factor “Treatment” (4 levels: “Current,” “RCP 2.6,” “RCP 4.5” and “RCP 8.5”). Differences in the net photosynthesis and net calcification were initially analysed with a two-way ANOVA, which in addition to the fixed factor of Treatment included the factor “Day” (2 levels: day 27 and day 29). Neither the factor Day nor its interaction with Treatment were significant for net photosynthesis or net calcification and as such, both days were pooled, and subsequent one-way ANOVAs were

conducted as for RGR and % bleaching. When significant effects were detected by the ANOVA models, three a-priori comparisons were conducted to independently compare each RCP scenario to the Current scenario. The three planned contrasts were as follows: planned comparison 1 = Current versus RCP 2.6, planned comparison 2 = Current versus RCP 4.5, and planned comparison 3 = Current versus RCP 8.5. A-priori comparisons were conducted using the *glht* function in the *multcomp* package (Hothorn et al., 2008) and *p*-values were adjusted for non-orthogonal comparisons. All model fits were checked to ensure they conformed to the assumptions of normality of residuals and homogeneity of variances using residual versus fitted and normal Q-Q plots and no transformations were required. One replicate in the RCP 2.6 treatment had substantially higher % bleaching than all others in that treatment (74.57 % versus 0 – 16.33 % for all other replicates). This outlier was removed from the bleaching analysis and figure, but the ANOVA table (Appendix 5.3) and figure (Appendix 5.4) with this outlier included can be viewed in the appendices. One replicate sample for determination of A_T for net calcification was lost during processing in each of the Current and RCP 8.5 treatments. Three replicates in the RCP 4.5 scenario had net calcification rates that were 7 – 11 times higher than the mean of the treatment with extreme values removed and twice that of the highest value for any other scenario. Furthermore, these replicates did not have erroneous values for any of the other metrics measured. As we considered it was likely that these values were an artefact of contamination or sampling error, we conducted the analysis with these outliers excluded. Both the ANOVA table (Appendix 5.5) and the figure (Appendix 5.6) with the values included are presented in the appendices.

Results

Percentage cover of CCA in situ

CCA cover was similar at sites 1 and 2 with average CCA cover \pm standard error (pooled across seasons) of $(35 \% \pm 3.83)$ and $(37 \% \pm 3.97)$ respectively. CCA cover at site 3 was around half that observed at the two northern sites $(19 \% \pm 2.43)$.

Experimental culture conditions

The observed pH_T of each treatment (mean, with the range of fluctuations in parentheses) were: Current = pH_T 8.01 (7.87 – 8.16), RCP 2.6 = pH_T 7.89 (7.75 – 8.01), RCP 4.5 = pH_T 7.80 (7.67 – 7.92) and RCP 8.5 = pH_T 7.66 (7.54 – 7.76). Average $\text{pH}_T \pm$ standard deviation of each treatment in 2-hour intervals are provided in Appendix 5.7. The mean temperatures of each treatment (\pm standard deviation) were: Current = $14.88\text{ }^\circ\text{C} \pm 0.34$, RCP 2.6 = $16.03\text{ }^\circ\text{C} \pm 0.20$, RCP 4.5 = $16.73\text{ }^\circ\text{C} \pm 0.61$ and RCP 8.5 = $18.40\text{ }^\circ\text{C} \pm 1.03$. Carbonate system parameters and temperature of each treatment can be seen in Table 5.1.

Table 5.1: Carbonate system parameters at the mean pH_T and temperature of each treatment. A_T , pH_T , temperature and salinity were measured and DIC was calculated in the program in CO2calc (Robbins, Hansen et al. 2010).

Treatment	$A_T \pm \text{Std. error}$ ($\mu\text{mol kg}^{-1}$)	DIC ($\mu\text{mol kg}^{-1}$)	pH_T $\pm \text{Std. error}$	Temperature ($^\circ\text{C}$)	Salinity (PSU)
Current	2422 ± 4	2223	8.01 ± 0.003	14.88	33
RCP 2.6	2412 ± 5	2258	7.89 ± 0.003	16.03	33
RCP 4.5	2398 ± 9	2276	7.80 ± 0.003	16.73	33
RCP 8.5	2407 ± 10	2331	7.66 ± 0.003	18.40	33

Biotic responses

Relative growth rates (RGR) and percentage bleaching

Mean RGRs of the CCA were positive for both the current and RCP 2.6 treatments, while CCA in the RCP 4.5 and 8.5 treatments displayed negative growth i.e. tissue loss (Figure 5.1 ANOVA: $F_{(3,28)} = 3.82$, $p = 0.021$). Planned comparisons indicated a significant reduction in RGRs of CCA in the RCP 8.5 treatment relative to the Current treatment. There was only a small proportion of bleaching in the Current, RCP 2.6 and the RCP 4.5 treatments and these differences were not significant (means: Current = 8.07 %, RCP 2.6 = 4.61 %, RCP 4.5 = 11.39 %, Figure 5.1). In contrast, bleaching was significantly greater in the RCP 8.5 treatment (mean = 33.98 %, Figure 5.1, ANOVA: $F_{(3,27)} = 11.36$, $p < 0.0001$).

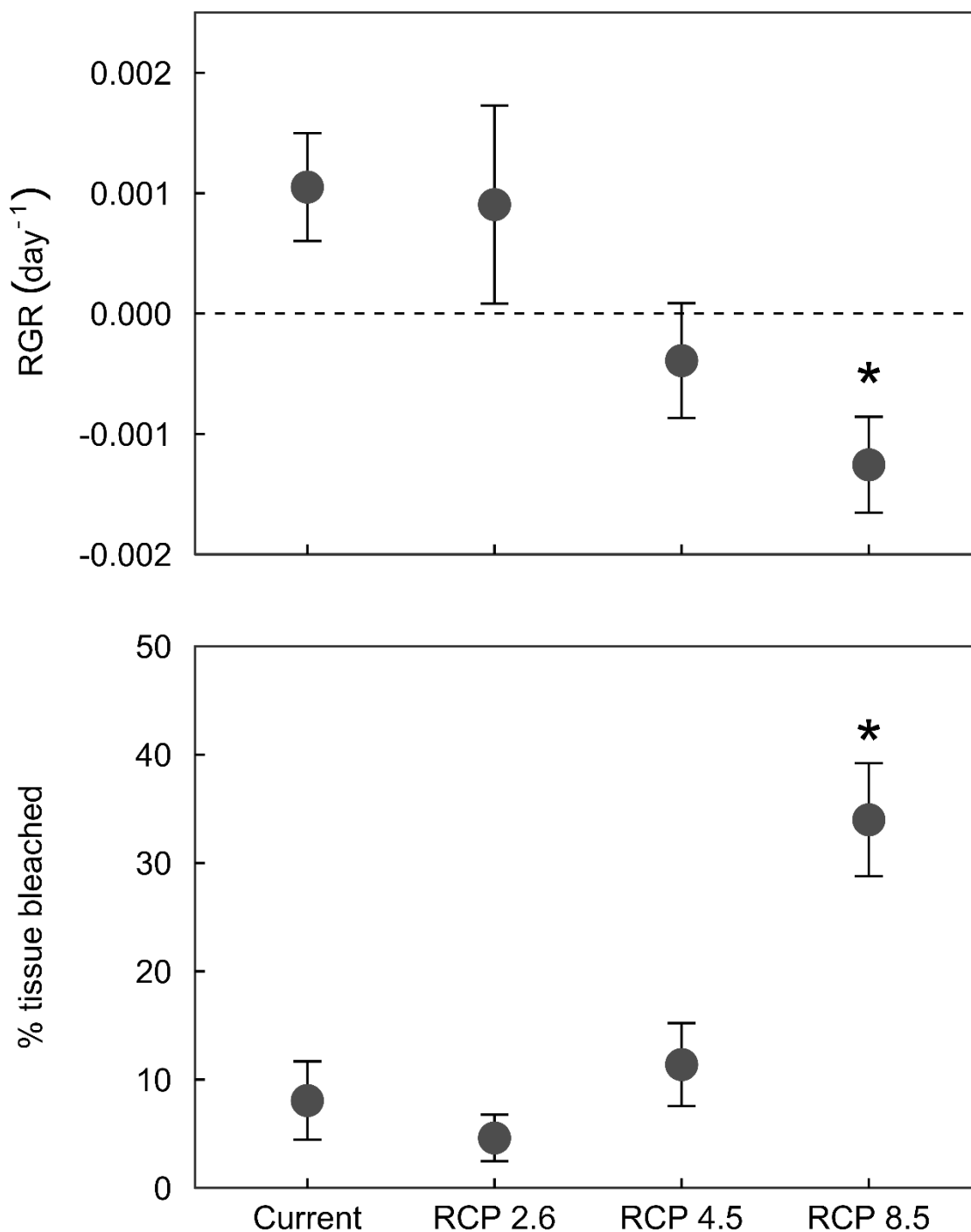


Figure 5.1: Relative growth rates (RGR, day^{-1} , top panel) and % tissue bleached (bottom panel) of crustose coralline algae (CCA) cultured for 29 days under current ocean pH and temperature and pH and temperature projected by 2100 under the RCP emission scenarios (low = RCP 2.6, medium = RCP 4.5, and high RCP 8.5, IPCC 2014). Treatments with an asterisk were significantly different from the Current scenario at $\alpha = 0.05$ in the a-priori planned comparisons. Data are presented as means \pm standard error, $n = 8$ for all treatments except for % tissue bleached in the RCP 2.6 treatment ($n = 7$).

Net photosynthesis

Positive net photosynthetic rates were detected under current ocean conditions, whereas net photosynthetic rates in the RCP 2.6 and 4.5 treatments were approximately zero (Figure 5.2). In contrast, CCA in the RCP 8.5 treatment had negative net photosynthetic rates (Figure 5.2, ANOVA: $F_{(3,28)} = 13.18$, $p < 0.0001$). The planned comparisons indicated net photosynthetic rates were significantly lower in all RCP scenarios relative to the Current scenario.

Calcification

Calcification rates were positive under current conditions. In contrast, the RCP 2.6, 4.5 and 8.5 scenarios had negative mean net calcification rates, i.e. net dissolution (Figure 5.2). A significant effect of treatment was detected (ANOVA: $F_{(3,23)} = 7.47$, $p < 0.001$, Figure 5.2), and planned comparisons indicated all RCP scenarios had significantly lower net calcification than in the Current scenario (Figure 5.2).

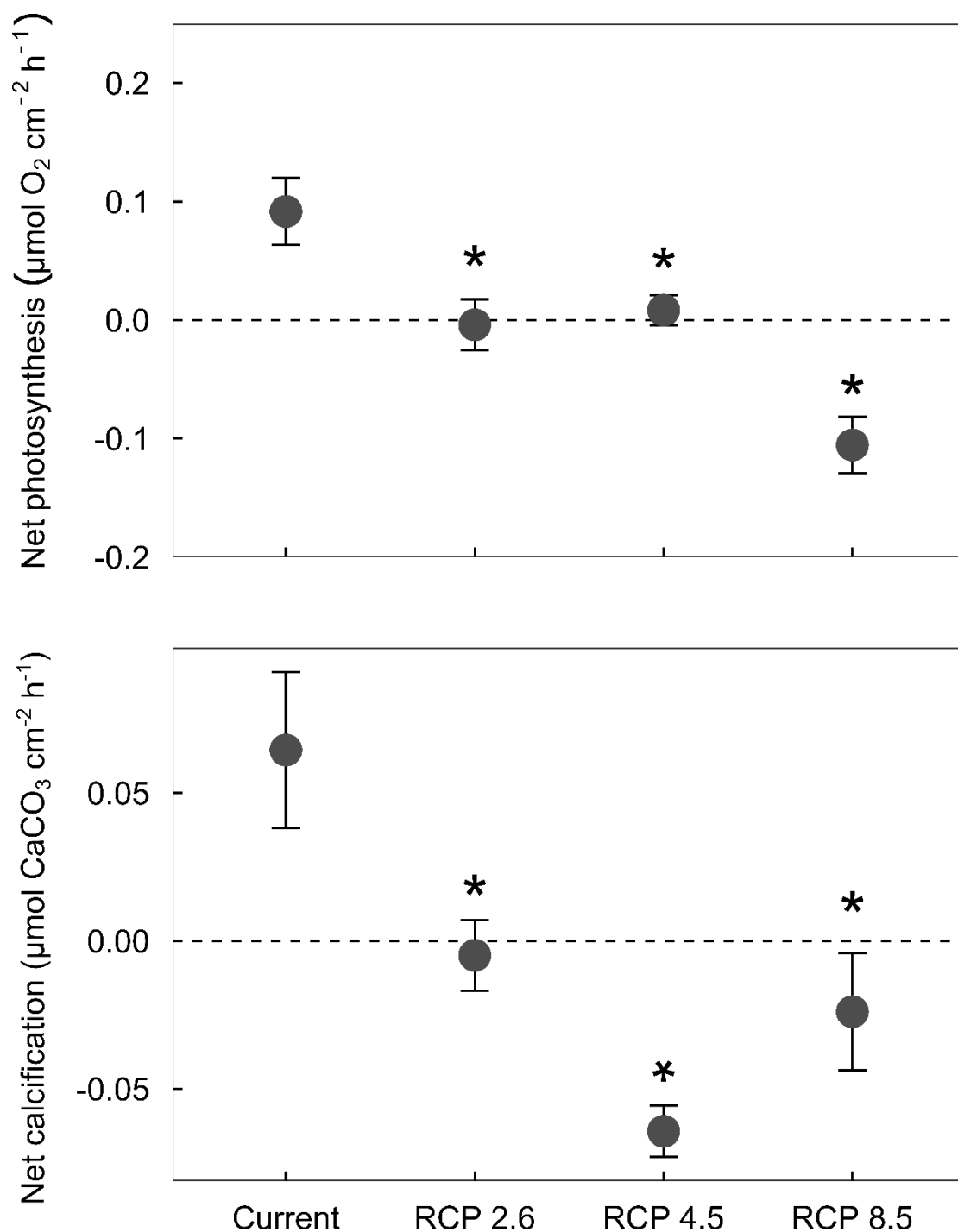


Figure 5.2: Net photosynthetic rates ($\mu\text{mol O}_2 \text{ cm}^{-2} \text{ h}^{-1}$, top panel) and net calcification rates ($\mu\text{mol CaCO}_3 \text{ cm}^{-2} \text{ h}^{-1}$, bottom panel) of crustose coralline algae (CCA) cultured for 29 days under current ocean pH and temperature and pH and temperature projected by 2100 under the RCP emission scenarios (low = RCP 2.6, medium = RCP 4.5, and high RCP 8.5, IPCC 2014). Treatments with an asterisk were significantly different from the current scenario at $\alpha = 0.05$ in the a-priori planned comparisons. Data are presented as means \pm standard error, $n = 8$ in all treatments for net photosynthesis, $n = 8$ in RCP 2.6, $n = 7$ in Current, RCP 8.5 and $n = 5$ in RCP 4.5.

Discussion

The responses presented here suggest that the functionally important temperate reef CCA (*Sporolithon spp*) is highly sensitive to combined warming and acidification. A reduction in net photosynthesis and calcification were detected even in the low emissions scenario (RCP 2.6) and severe negative effects were detected for all responses excluding bleaching in the medium emissions scenario (RCP 4.5). The most severe impacts were detected in the high emissions scenario (RCP 8.5) with all responses being negatively affected. The RCP 8.5 is likely unless emissions are rapidly reduced (Gattuso et al., 2015). As such, the negative impacts observed in the more moderate treatments (which double as near-future treatments under RCP 8.5) suggest impacts are likely to be detectable by as early as 2030 (Figure 5.3). By using a scenario-based approach, where we assessed responses to multiple scenarios, we are able to highlight that CCA are susceptible to near-future levels of warming and acidification, which given the short time frame, may impact their ability to adapt to these changes.

Most studies investigating the response of corallines to combined warming and acidification have been undertaken at conditions projected under RCP 8.5 or worse and generally they have found negative responses (Anthony et al., 2008; Martin and Gattuso, 2009; Diaz-Pulido et al., 2012; Johnson and Carpenter, 2012; Martin et al., 2013; Noisette et al., 2013; Reyes-Nivia et al., 2014; Comeau et al., 2016; Legrand et al., 2017; Graba-Landry et al., 2018; Huggett et al., 2018; Rich et al., 2018; Marchini et al., 2019; Qui-Minet et al., 2019; Sordo et al., 2019), although, there are notable exceptions (Comeau et al., 2014; Legrand et al., 2018). In this study, by assessing the response to multiple emissions scenarios, we demonstrate that negative impacts are likely under low and medium emissions (RCP 2.6 and 4.5) and become worse under more extreme scenarios. The RCP 2.6 scenario consisted of only a 0.1 unit reduction in pH and a 1 degree increase in temperature, which suggests that CCA from

Tasmania or this genus are particularly sensitive to combined warming and acidification. Furthermore, our treatments included realistic fluctuations in pH that simulated the conditions observed in the field (Britton et al., 2020). It has been suggested that the elevated pH during the day may provide refugia for calcifying species from ocean acidification (Hurd, 2015). However, the highly sensitive responses observed here provide little evidence that this is the case for *Sporolithon* spp. This finding supports earlier research in which greater impacts of acidification on CCA have been observed when cultured in fluctuating pH (Cornwall et al., 2013; Roleda et al., 2015).

It is difficult to determine whether most temperate CCA species are sensitive to moderate emissions scenarios as only one study looking at both moderate changes in temperature and pH on a temperate CCA species has been conducted. This study (on an intertidal CCA) found negative effects under RCP 4.5 (Kram et al., 2015). Tropical CCA have varied responses to moderate changes in temperature and pH with neutral (Reyes-Nivia et al., 2014; Schoenrock et al., 2016; Vogel et al., 2016) and negative responses observed (Vásquez-Elizondo and Enríquez, 2016; Ordoñez et al., 2017) and some species tolerant to high emissions scenarios (Comeau et al., 2014; Legrand et al., 2018). However, declines in CCA cover between 2010 – 2016 on the Great Barrier Reef are correlated with changes in carbonate chemistry due to ocean acidification (Smith et al., 2020), suggesting that impacts of global ocean change are already occurring. This, along with the negative responses of CCA to near future changes in our study highlight that more studies assessing the response to low and moderate scenarios are required as it is apparent that some CCA species are highly sensitive to low amounts of warming and acidification that are projected for the near future.

Rates of change: implications for adaptation

The RCP 8.5 scenario is likely to be realised unless drastic reductions in emissions occur almost immediately (Gattuso et al., 2015). If current emissions are sustained, then both the RCP 2.6 and 4.5 treatments can be considered as near and medium-term projections of ocean conditions under the RCP 8.5 scenario. Figure 5.3 is a conceptual diagram, based on the IPCC projections, which illustrates that under the RCP 8.5 scenario the conditions projected by 2100 under RCP 2.6 and 4.5 will occur as soon as 2030 and 2050 respectively (IPCC 2014, Figure 5.3). Therefore, the impacts on CCA that we detected in this study under the RCP 2.6 scenario are likely to be realised by 2030, and the impacts for the RCP 4.5 scenario by 2050. Furthermore, even if emissions are reduced to a scenario similar to that of RCP 4.5, the reductions in net photosynthesis and calcification detected in the RCP 2.6 scenario are likely to be detectable by 2050 (IPCC 2014, Figure 5.3).

The rate of change in ocean conditions is likely to influence the ability of species to adapt to climate change (Kamenos et al., 2013). A recent study by Cornwall et al. (2020) is the first to demonstrate that a CCA (*Hydrolithon reinboldii*) is capable of gaining tolerance to future levels of ocean acidification (reflecting RCP 8.5) within 6 generations. This finding suggests that CCA may be more tolerant than previously thought. However, whether different species and lineages of corallines are capable of gaining similar tolerances and whether the mechanisms of adaptation are sufficient to withstand the additional stressor of warming remains unclear. It is likely that more than 6 generations will have passed for *Sporolithon spp.* by the time impacts begin to occur (2030). However, species from *Sporolithon* appear highly sensitive to both acidification (Cornwall et al., 2017; Comeau et al., 2019) and combined warming and acidification (this study). This sensitivity may therefore increase the number of generations required to adapt to changes. Keeping emissions lower than RCP 8.5 and thus extending the time until conditions become detrimental (i.e. RCP 2.6 – 4.5), is likely to be critically important in mitigating the impacts on sensitive keystone species such as

Sporolithon spp. Urgent research is now required that assesses the impact of combined warming and acidification to near future climate change in multi-generation studies. Negative effects are likely to occur before 2100 and we need to understand the capacity of species to adapt to these near future conditions if we are to mitigate any impacts through methods such as assisted evolution (van Oppen et al., 2015).

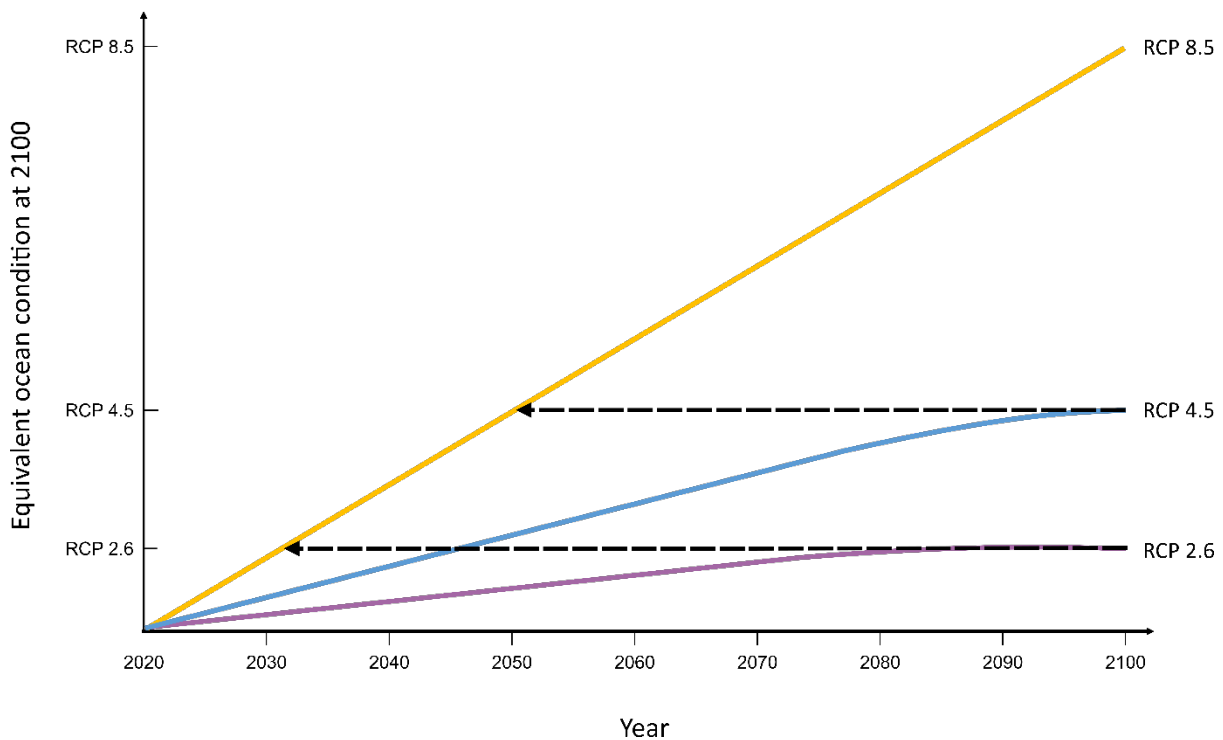


Figure 5.3: Conceptual diagram displaying the change in ocean conditions until 2100 according to the IPCC *Representative Concentration Pathways* (RCP) emission scenarios 2.6 (low emissions), 4.5 (medium emissions), and 8.5 (high emissions). The y-axis displays the ocean conditions projected in 2100 under each emission scenario. Arrows mark the year when the conditions projected to occur in 2100 under the RCP 2.6 and 4.5 scenarios will occur in the high emissions RCP 8.5 scenario. Under the RCP 8.5 scenario the impacts detected in this study in the RCP 2.6 scenario will occur ~ 2030 and the impacts detected in the RCP 4.5 scenario will occur ~ 2050. The “Equivalent ocean condition at 2100” scale is approximate and is for conceptual purposes only.

Ecological considerations

CCA play critical roles in maintaining ecosystem function by creating and stabilising reefs (Nelson, 2009), and providing chemical cues to induce settlement and metamorphosis of invertebrate larvae (Pearce and Scheibling, 1991; Heyward and Negri, 1999; Roberts, 2001). In many cases these invertebrates form the basis of valuable fisheries. For example, in temperate Australasia, settlement of the three commercially important abalone *Haliotis rubra*, *Haliotis laevis* and *Haliotis iris* are induced by CCA assemblages (Daume et al., 1999; Huggett et al., 2005; Roberts et al., 2010) and collectively these fisheries account for ~ 42 % of the global harvest of wild caught abalone (Cook 2016; Mundy and Jones 2016; Fisheries New Zealand, 2020). As such, any impacts on CCA would likely to have significant flow on effects to abalone populations and the commercial fisheries they support. One mechanism through which impacts on CCA could impact abalone populations is via the loss of CCA cover (as a result of bleaching or reduced growth rates). Any loss of cover would directly reduce the physical area of reef covered by CCA that can induce larval settlement. For example, the rate of bleaching observed in the RCP 8.5 scenario over 29 days equates to ~ 1 % a day. This rate of bleaching, if maintained, would result in 100 % bleaching of CCA in 100 days, unless adaptation is possible. Considering that bleaching of CCA often leads to necrosis and death (Martone et al., 2010), this could result in a catastrophic reduction in the proportion of substrate capable of promoting settlement of invertebrate larvae. Identifying tipping points of when conditions become too stressful for adaptation to compensate should be a priority of future research.

Warming and acidification may reduce the capacity of the CCA assemblage to induce settlement or disrupt direct interactions such as post-larval grazing between the CCA assemblage and invertebrate larvae (Daume et al., 1997; Webster et al., 2011; Doropoulos et al., 2012; Espinel-Velasco et al., 2018). The effects of combined warming and acidification on the ability of coralline assemblages to induce invertebrate larval settlement have only been

studied once, in which settlement rates of sea urchin larvae were reduced (Huggett et al., 2018). However, the individual effects of each driver have been studied more extensively: ocean acidification typically reduces the ability of corallines to induce settlement of corals (Doropoulos et al., 2012; Webster et al., 2013; Espinel-Velasco et al., 2018) and sea stars (Uthicke et al., 2013), while warming can reduce rates of settlement induction in corals (Webster et al., 2011) or increase rates in sponges (Whalan and Webster, 2014). For abalone, the impacts on the ability of corallines to induce larval settlement has only been assessed for ocean acidification, with one study finding no effects (O'Leary et al., 2017) and the other finding reduced settlement (Tahil and Dy, 2015). Clearly more research is required that investigates the effects of combined warming and acidification on the ability of corallines to induce settlement and support post-larval grazing by abalone and other benthic invertebrate larvae. The early post-settlement period is frequently associated with high levels of mortality in marine invertebrates (Hunt and Scheibling, 1997). Further degradation of supporting environments, in addition to the direct effects of warming and acidification on larvae and post-larvae, has the potential to exacerbate an already challenging life-history phase.

The results presented here provide the first information on how CCA in the southern hemisphere will respond to combined warming and acidification. The observed physiological responses suggest that the ecologically important CCA *Sporolithon spp.* in Tasmania, Australia will be significantly impacted by projected future levels of temperature and pH and that these effects are likely to occur as soon as 2030 if the RCP 8.5 emissions scenario is realised. Given the crucial role CCA play in maintaining ecosystem function in habitats ranging from the tropics to the poles, reef ecosystems globally are likely to be negatively impacted unless rapid adaptation is possible.

Acknowledgments

We thank Camille White for assistance in the field and Ellie Paine and Matthias Schmid for assistance in the laboratory and for providing valuable insights into the study. We also thank Toby Bolton for his expert support. DB was supported by a University of Tasmania, Australian Postgraduate Award. FN was supported by the European Union's Horizon 2020 research and innovation programme under the Marie Skłodowska-Curie grant agreement (No. 701366).

References

- Anthony, K. R. N., Kline, D. I., Diaz-Pulido, G., Dove, S., and Hoegh-Guldberg, O. 2008. Ocean acidification causes bleaching and productivity loss in coral reef builders. *Proceedings of the National Academy of Sciences*, 105: 17442.
- Beijbom, O., Edmunds, P. J., Roelfsema, C., Smith, J., Kline, D. I., Neal, B. P., Dunlap, M. J., et al. 2015. Towards automated annotation of benthic survey images: variability of human experts and operational modes of automation. *PLoS ONE*, 10: e0130312.
- Bennett, S., Wernberg, T., Connell, S. D., Hobday, A. J., Johnson, C. R., and Poloczanska, E. S. 2015. The 'Great Southern Reef': social, ecological and economic value of Australia's neglected kelp forests. *Marine and Freshwater Research*, 67: 47-56.
- Boyd, P. W., Collins, S., Dupont, S., Fabricius, K., Gattuso, J.-P., Havenhand, J., Hutchins, D. A., et al. 2018. Experimental strategies to assess the biological ramifications of multiple drivers of global ocean change—A review. *Global Change Biology*, 24: 2239-2261.
- Britton, D., Schmid, M., Noisette, F., Havenhand, J. N., Paine, E. R., McGraw, C. M., Revill, A. T., et al. 2020. Adjustments in fatty acid composition is a mechanism that can explain resilience to marine heatwaves and future ocean conditions in the habitat-forming seaweed *Phyllospora comosa* (Labillardière) C. Agardh. *Global Change Biology*, 26: 3512-3524..
- Comeau, S., Carpenter, R. C., and Edmunds, P. J. 2014. Effects of irradiance on the response of the coral *Acropora pulchra* and the calcifying alga *Hydrolithon reinboldii* to temperature elevation and ocean acidification. *Journal of Experimental Marine Biology and Ecology*, 453: 28-35.
- Comeau, S., Carpenter, R. C., Lantz, C. A., and Edmunds, P. J. 2016. Parameterization of the response of calcification to temperature and pCO₂ in the coral *Acropora pulchra* and the alga *Lithophyllum kotschyannum*. *Coral Reefs*, 35: 929-939.

Comeau, S., Cornwall, C. E., Pupier, C. A., DeCarlo, T. M., Alessi, C., Trehern, R., and McCulloch, M. T. 2019. Flow-driven micro-scale pH variability affects the physiology of corals and coralline algae under ocean acidification. *Scientific Reports*, 9: 12829.

Cook, P. 2016. Recent trends in worldwide abalone production. *Journal of Shellfish Research*, 35: 581-583.

Cornwall, C. E., Comeau, S., DeCarlo, T. M., Larcombe, E., Moore, B., Giltrow, K., Puerzer, F., et al. 2020. A coralline alga gains tolerance to ocean acidification over multiple generations of exposure. *Nature Climate Change*. 10:143–146.
<https://doi.org/10.1038/s41558-019-0681-8>

Cornwall, C. E., Comeau, S., DeCarlo, T. M., Moore, B., D'Alexis, Q., and McCulloch, M. T. 2018. Resistance of corals and coralline algae to ocean acidification: physiological control of calcification under natural pH variability. *Proceedings of the Royal Society B: Biological Sciences*, 285: 20181168.

Cornwall, C. E., Comeau, S., and McCulloch, M. T. 2017. Coralline algae elevate pH at the site of calcification under ocean acidification. *Global Change Biology*, 23: 4245-4256.

Cornwall, C. E., Diaz-Pulido, G., and Comeau, S. 2019. Impacts of ocean warming on coralline algal calcification: Meta-analysis, knowledge gaps, and key recommendations for future research. *Frontiers in Marine Science*, 6: 186.

Cornwall, C. E., Hepburn, C. D., McGraw, C. M., Currie, K. I., Pilditch, C. A., Hunter, K. A., Boyd, P. W., et al. 2013. Diurnal fluctuations in seawater pH influence the response of a calcifying macroalga to ocean acidification. *Proceedings of the Royal Society B: Biological Sciences*, 280: 20132201.

Daume, S., Brand-Gardner, S., and Woelkerling, W. J. 1999. Preferential settlement of abalone larvae: diatom films vs. non-geniculate coralline red algae. *Aquaculture*, 174: 243-254.

Daume, S., Brand, S., and Woelkerling, J. 1997. Effects of post-larval abalone (*Haliotis rubra*) grazing on the epiphytic diatom assemblage of coralline red algae. *Molluscan Research*, 18: 119-130.

Diaz-Pulido, G., Anthony, K. R. N., Kline, D. I., Dove, S., and Hoegh-Guldberg, O. 2012. Interactions between ocean acidification and warming on the mortality and dissolution of coralline algae. *Journal of Phycology*, 48: 32-39.

Dickson, A., Chris, S., and Christian, J. R. 2007. Guide to Best Practices for Ocean CO₂ Measurements. Guide to Best Practices for Ocean CO₂ Measurements, PICES Special Publication 3, 191 pp..

Doropoulos, C., and Diaz-Pulido, G. 2013. High CO₂ reduces the settlement of a spawning coral on three common species of crustose coralline algae. *Marine Ecology Progress Series*, 475: 93-99.

Doropoulos, C., Ward, S., Diaz-Pulido, G., Hoegh-Guldberg, O., and Mumby, P. J. 2012. Ocean acidification reduces coral recruitment by disrupting intimate larval-algal settlement interactions. *Ecology Letters*, 15: 338-346.

- Espinel-Velasco, N., Hoffmann, L., Agüera, A., Byrne, M., Dupont, S., Uthicke, S., Webster, N. S., et al. 2018. Effects of ocean acidification on the settlement and metamorphosis of marine invertebrate and fish larvae: a review. *Marine Ecology Progress Series*, 606: 237-257.
- Fabrizius, K. E., Kluibenschedl, A., Harrington, L., Noonan, S., and De'ath, G. 2015. *In situ* changes of tropical crustose coralline algae along carbon dioxide gradients. *Scientific Reports*, 5: 9537.
- Fisheries New Zealand. 2020. Black Paua & Yellowfoot Paua (PAU) – Catch 2015. <https://fs.fish.govt.nz/Page.aspx?pk=7&sc=PAU&ey=2015>. Accessed 24/03/20.
- Frölicher, T. L., Fischer, E. M., and Gruber, N. 2018. Marine heatwaves under global warming. *Nature*, 560: 360-364.
- Gattuso, J. P., Magnan, A., Billé, R., Cheung, W. W. L., Howes, E. L., Joos, F., Allemand, D., et al. 2015. Contrasting futures for ocean and society from different anthropogenic CO₂ emissions scenarios. *Science*, 349: aac4722.
- Graba-Landry, A., Hoey, A. S., Matley, J. K., Sheppard-Brennand, H., Poore, A. G. B., Byrne, M., and Dworjanyn, S. A. 2018. Ocean warming has greater and more consistent negative effects than ocean acidification on the growth and health of subtropical macroalgae. *Marine Ecology Progress Series*, 595: 55-69.
- Heyward, A. J., and Negri, A. P. 1999. Natural inducers for coral larval metamorphosis. *Coral Reefs*, 18: 273-279.
- Hobday, A. J., and Pecl, G. T. 2014. Identification of global marine hotspots: sentinels for change and vanguards for adaptation action. *Reviews in Fish Biology and Fisheries*, 24: 415-425.
- Hofmann, L. C., and Bischof, K. 2014. Ocean acidification effects on calcifying macroalgae. *Aquatic Biology*, 22: 261-279.
- Hothorn, T., Bretz, F., and Westfall, P. 2008. Simultaneous inference in general parametric models. *Biometrical Journal*, 50: 346-363.
- Huggett, M. J., De Nys, R., Williamson, J. E., Heasman, M., and Steinberg, P. D. 2005. Settlement of larval blacklip abalone, *Haliotis rubra*, in response to green and red macroalgae. *Marine Biology*, 147: 1155-1163.
- Huggett, M. J., McMahon, K., and Bernasconi, R. 2018. Future warming and acidification result in multiple ecological impacts to a temperate coralline alga. *Environmental Microbiology*, 20: 2769-2782.
- Hunt, H., and Scheibling, R. 1997. Role of early post-settlement mortality in recruitment of benthic marine invertebrates. *Marine Ecology Progress Series*, 155: 269-301.
- Hurd, C. L. 2015. Slow-flow habitats as refugia for coastal calcifiers from ocean acidification. *Journal of Phycology*, 51: 599-605.
- IPCC. 2014. Climate Change 2014: Synthesis Report. Contribution of Working Groups I, II and III to the Fifth Assessment Report of the Intergovernmental Panel on Climate Change

[Core Writing Team, R.K. Pachauri and L.A. Meyer (eds.)]. IPCC, Geneva, Switzerland. 151 pp.

Johnson, C. R., Banks, S. C., Barrett, N. S., Cazassus, F., Dunstan, P. K., Edgar, G. J., Frusher, S. D., et al. 2011. Climate change cascades: shifts in oceanography, species' ranges and subtidal marine community dynamics in eastern Tasmania. *Journal of Experimental Marine Biology and Ecology*, 400: 17-32.

Johnson, M. D., and Carpenter, R. C. 2012. Ocean acidification and warming decrease calcification in the crustose coralline alga *Hydrolithon onkodes* and increase susceptibility to grazing. *Journal of Experimental Marine Biology and Ecology* 434–435: 94–101.

Kain, J. M. 1982. Morphology and growth of the giant kelp *Macrocystis pyrifera* in New Zealand and California. *Marine Biology*, 67: 143-157.

Kamenos, N. A., Burdett, H. L., Aloisio, E., Findlay, H. S., Martin, S., Longbone, C., Dunn, J., et al. 2013. Coralline algal structure is more sensitive to rate, rather than the magnitude, of ocean acidification. *Global Change Biology*, 19: 3621-3628.

Kram, S., Price, N., Donham, E., Johnson, M. D., Kelly, E., Hamilton, S., and Smith, J. 2015. Variable responses of temperate calcified and fleshy macroalgae to elevated pCO₂ and warming. *ICES Journal of Marine Science: Journal du Conseil*, 73: fsv168.

Kroeker, K. J., Kordas, R. L., Crim, R., Hendriks, I. E., Ramajo, L., Singh, G. S., Duarte, C. M., et al. 2013. Impacts of ocean acidification on marine organisms: quantifying sensitivities and interaction with warming. *Global Change Biology*, 19: 1884-1896.

Legrand, E., Riera, P., Bohner, O., Coudret, J., Schlicklin, F., Derrien, M., and Martin, S. 2018. Impact of ocean acidification and warming on the productivity of a rock pool community. *Marine Environmental Research*, 136: 78-88.

Legrand, E., Riera, P., Lutier, M., Coudret, J., Grall, J., and Martin, S. 2019. Grazers increase the sensitivity of coralline algae to ocean acidification and warming. *Journal of Sea Research*, 148-149: 1-7.

Lueker, T. J., Dickson, A. G., and Keeling, C. D. 2000. Ocean pCO₂ calculated from dissolved inorganic carbon, alkalinity, and equations for K₁ and K₂: validation based on laboratory measurements of CO₂ in gas and seawater at equilibrium. *Marine Chemistry*, 70: 105-119.

Marchini, A., Ragazzola, F., Vasapollo, C., Castelli, A., Cerrati, G., Gazzola, F., Jiang, C., et al. 2019. Intertidal mediterranean coralline algae habitat is expecting a shift toward a reduced growth and a simplified associated fauna under climate change. *Frontiers in Marine Science*, 6: 106.

Martin, S., Cohu, S., Vignot, C., Zimmerman, G., and Gattuso, J. P. 2013. One-year experiment on the physiological response of the Mediterranean crustose coralline alga, *Lithophyllum cabiochae*, to elevated pCO₂ and temperature. *Ecology and Evolution*, 3: 676-693.

Martin, S., and Gattuso, J. P. 2009. Response of Mediterranean coralline algae to ocean acidification and elevated temperature. *Global Change Biology*, 15: 2089-2100.

- Martínez, B., Radford, B., Thomsen, M. S., Connell, S. D., Carreño, F., Bradshaw, C. J. A., Fordham, D. A., et al. 2018. Distribution models predict large contractions of habitat-forming seaweeds in response to ocean warming. *Diversity and Distributions*, 24: 1350-1366.
- Martone, P. T., Alyono, M., and Stites, S. 2010. Bleaching of an intertidal coralline alga: untangling the effects of light, temperature, and desiccation. *Marine Ecology Progress Series*, 416: 57-67.
- McCoy, S. J. 2013. Morphology of the crustose coralline alga *Pseudolithophyllum muricatum* (Corallinales, Rhodophyta) responds to 30 years of ocean acidification in the Northeast Pacific. *Journal of Phycology*, 49: 830-837.
- McCoy, S. J., and Kamenos, N. A. 2015. Coralline algae (Rhodophyta) in a changing world: integrating ecological, physiological, and geochemical responses to global change. *Journal of Phycology*, 51: 6-24.
- McGraw, C. M., Cornwall, C. E., Reid, M. R., Currie, K. I., Hepburn, C. D., Boyd, P., Hurd, C. L., et al. 2010. An automated pH-controlled culture system for laboratory-based ocean acidification experiments. *Limnology and Oceanography: Methods*, 8: 686-694.
- Mehrbach, C., Culberson, C. H., Hawley, J. E., and Pytkowicz, R. M. 1973. Measurement of the apparent dissociation constants of carbonic acid in seawater at atmospheric pressure. *Limnology and Oceanography*, 18: 897-907.
- Mills, K. E., Pershing, A. J., Brown, C. J., Chen, Y., Chiang, F.-S., Holland, D. S., Lehuta, S., et al. 2013. Fisheries management in a changing climate: lessons from the 2012 ocean heat wave in the northwest Atlantic. *Oceanography*, 26: 191-195.
- Mundy C.M., and Jones, H.J. 2016. Tasmanian abalone fishery assessment 2015. Institute for Marine and Antarctic Studies (IMAS), University of Tasmania.
- Nelson, W. A. 2009. Calcified macroalgae critical to coastal ecosystems and vulnerable to change: a review. *Marine and Freshwater Research*, 60: 787-801.
- Noisette, F., Duong, G., Six, C., Davoult, D., and Martin, S. 2013. Effects of elevated pCO₂ on the metabolism of a temperate rhodolith *Lithothamnion corallioides* grown under different temperatures. *Journal of Phycology*, 49: 746-757.
- O'Leary, J. K., Barry, J. P., Gabrielson, P. W., Rogers-Bennett, L., Potts, D. C., Palumbi, S. R., and Micheli, F. 2017. Calcifying algae maintain settlement cues to larval abalone following algal exposure to extreme ocean acidification. *Scientific Reports*, 7: 5774.
- Ordoñez, A., Kennedy, E. V., and Diaz-Pulido, G. 2017. Reduced spore germination explains sensitivity of reef-building algae to climate change stressors. *PLoS ONE*, 12.
- Pearce, C. M., and Scheibling, R. E. 1991. Effect of macroalgae, microbial films, and conspecifics on the induction of metamorphosis of the green sea urchin *Strongylocentrotus droebachiensis* (Mueller). *Journal of Experimental Marine Biology and Ecology*, 147: 147-162.
- Pinsky, M. L., and Fogarty, M. 2012. Lagged social-ecological responses to climate and range shifts in fisheries. *Climatic Change*, 115: 883-891.

Qui-Minet, Z. N., Coudret, J., Davoult, D., Grall, J., Mendez-Sandin, M., Cariou, T., and Martin, S. 2019. Combined effects of global climate change and nutrient enrichment on the physiology of three temperate maerl species. *Ecology and Evolution*, 9: 13787-13807.

R Core Team 2019. R: A language and environment for statistical computing. R Foundation for Statistical Computing, Vienna, Austria. URL: <https://www.R-project.org/>.

Reyes-Nivia, C., Diaz-Pulido, G., and Dove, S. 2014. Relative roles of endolithic algae and carbonate chemistry variability in the skeletal dissolution of crustose coralline algae. *Biogeosciences*, 11: 4615-4626.

Rich, W. A., Schubert, N., Schläpfer, N., Carvalho, V. F., Horta, A. C. L., and Horta, P. A. 2018. Physiological and biochemical responses of a coralline alga and a sea urchin to climate change: implications for herbivory. *Marine Environmental Research*: 100-107.

Ries, J. B. 2011. Skeletal mineralogy in a high-CO₂ world. *Journal of Experimental Marine Biology and Ecology*, 403: 54-64.

Robbins, L. L., Hansen, M. E., Kleypas, J. A., and Meylan, S. C. 2010. CO₂calc—A user-friendly seawater carbon calculator for Windows, Max OS X, and iOS (iPhone). U.S. Geological Survey Open-File Report 2010, 1280: 17.

Roberts, R. 2001. A review of settlement cues for larval abalone (*Haliotis spp.*). *Journal of Shellfish Research*, 20: 571-586.

Roberts, R. D., Barker, M. F., and Mladenov, P. 2010. Is settlement of *Haliotis iris* Larvae on coralline algae triggered by the alga or its surface biofilm? *Journal of Shellfish Research*, 29: 671-678.

Roleda, M. Y., Cornwall, C. E., Feng, Y., McGraw, C. M., Smith, A. M., and Hurd, C. L. 2015. Effect of ocean acidification and pH fluctuations on the growth and development of coralline algal recruits, and an associated benthic algal assemblage. *PLoS ONE*, 10: e0140394s.

Schindelin, J., Arganda-Carreras, I., Frise, E., Kaynig, V., Longair, M., Pietzsch, T., Preibisch, S., et al. 2012. Fiji: an open-source platform for biological-image analysis. *Nature Methods*, 9: 676-682.

Schoenrock, K. M., Schram, J. B., Amsler, C. D., McClintock, J. B., Angus, R. A., and Vohra, Y. K. 2016. Climate change confers a potential advantage to fleshy Antarctic crustose macroalgae over calcified species. *Journal of Experimental Marine Biology and Ecology*, 474: 58-66.

Smith, J. N., Mongin, M., Thompson, A., Jonker, M. J., De'ath, G., and Fabricius, K. E. 2020. Shifts in coralline algae, macroalgae, and coral juveniles in the Great Barrier Reef associated with present-day ocean acidification. *Global Change Biology*, 26: 2149-2160.

Smith, S. V., and Key, G. S. 1975. Carbon dioxide and metabolism in marine environments. *Limnology and Oceanography*, 20: 493-495.

Sordo, L., Santos, R., Barrote, I., and Silva, J. 2019. Temperature amplifies the effect of high CO₂ on the photosynthesis, respiration, and calcification of the coralline algae *Phymatolithon lusitanicum*. *Ecology and Evolution*, 9: 11000-11009.

Tahil, A. S., and Dy, D. T. 2015. Effects of reduced pH on larval settlement and survival of the Donkey's ear abalone, *Haliotis asinina* (Linnaeus 1758). *Philippine Journal of Science*, 144: 21-29.

Uthicke, S., Pecorino, D., Albright, R., Negri, A. P., Cantin, N., Liddy, M., Dworjanyn, S., et al. 2013. Impacts of ocean acidification on early life-history stages and settlement of the coral-eating sea star *Acanthaster planci*. *PLoS ONE*, 8: e82938.

van Oppen, M. J. H., Oliver, J. K., Putnam, H. M., and Gates, R. D. 2015. Building coral reef resilience through assisted evolution. *Proceedings of the National Academy of Sciences*, 112: 2307.

Vásquez-Elizondo, R. M., and Enríquez, S. 2016. Coralline algal physiology is more adversely affected by elevated temperature than reduced pH. *Scientific Reports*, 6: sre19030.

Vogel, N., Cantin, N. E., Strahl, J., Kaniewska, P., Bay, L., Wild, C., and Uthicke, S. 2016. Interactive effects of ocean acidification and warming on coral reef associated epilithic algal communities under past, present-day and future ocean conditions. *Coral Reefs*, 35: 715-728.

Webster, N. S., Soo, R., Cobb, R., and Negri, A. P. 2011. Elevated seawater temperature causes a microbial shift on crustose coralline algae with implications for the recruitment of coral larvae. *The ISME Journal*, 5: 759-770.

Webster, N. S., Uthicke, S., Botté, E. S., Flores, F., and Negri, A. P. 2013. Ocean acidification reduces induction of coral settlement by crustose coralline algae. *Global Change Biology*, 19: 303-315.

Whalan, S., and Webster, N. S. 2014. Sponge larval settlement cues: the role of microbial biofilms in a warming ocean. *Scientific Reports*, 4: 4072.

Wolf-Gladrow, D. A., Zeebe, R. E., Klaas, C., Körtzinger, A., and Dickson, A. G. 2007. Total alkalinity: The explicit conservative expression and its application to biogeochemical processes. *Marine Chemistry*, 106: 287-300.

Appendices

Appendix 5.1: Latitude and longitude of all three sites where crustose coralline algal (CCA) cover was estimated *in situ* by divers taking photo quadrats.

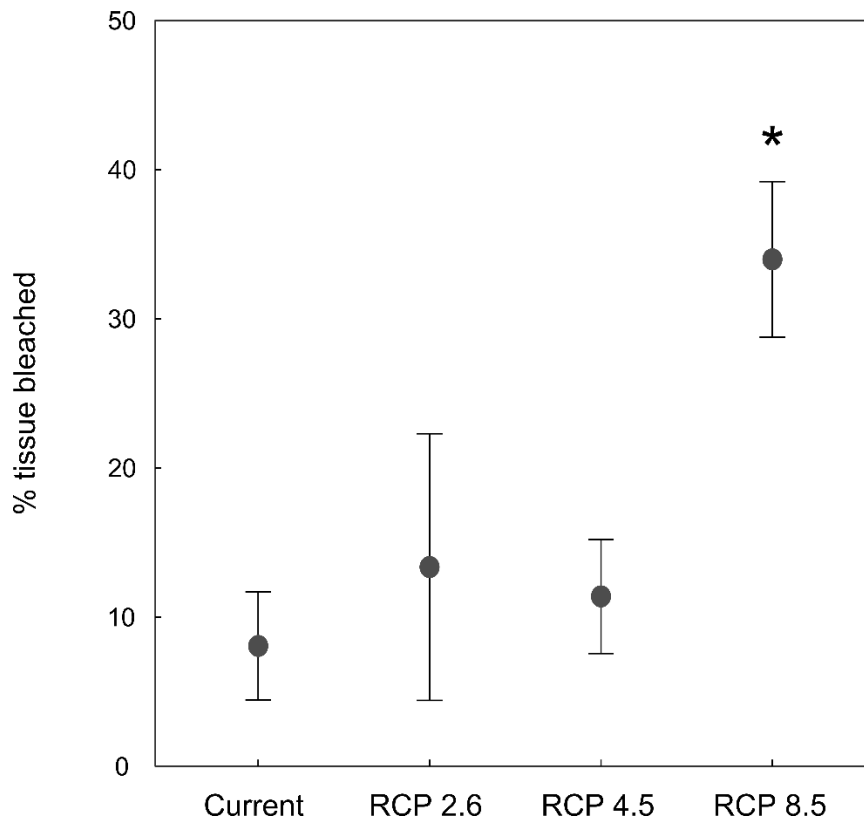
Coordinates (latitude, longitude)	
Site 1 (Bicheno)	41.870240° S, 148.303234° E
Site 2 (Coal Point)	43.335287° S, 147.324707° E
Site 3 (Mouldy Hole)	43.595252° S, 146.922055° E

Appendix 5.2: Target pH_T at every 4-hour water refresh for each treatment. Lights were turned on at 6 am and turned off at 6 pm.

	Current	RCP 2.6	RCP 4.5	RCP 8.5
	Target pH _T	Target pH _T	Target pH _T	Target pH _T
2am	7.95	7.85	7.75	7.60
6am	7.85	7.75	7.65	7.50
10am	7.95	7.85	7.75	7.60
2pm	8.05	7.95	7.85	7.70
6pm	8.15	8.05	7.95	7.80
10pm	8.05	7.95	7.85	7.70

Appendix 5.3: Analysis of Variance (ANOVA) table of a one-way ANOVAs comparing % bleaching of CCA tissue between treatments with the outlier in RCP 2.6 included. Df = degrees of freedom, SS = sums of squares, MS = mean square. Significant effects ($\alpha = 0.05$) have p-values displayed in bold.

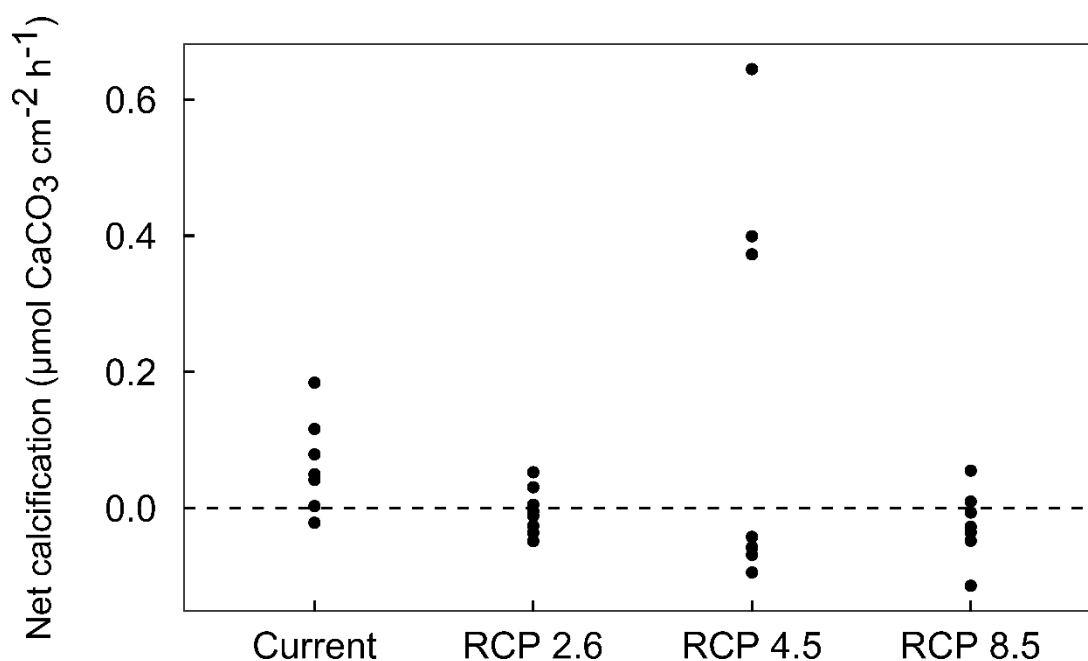
	Df	SS	MS	F-value	<i>p</i> - value
Treatment	3	3301	1100	4.08	0.016
Residuals	28	7551	270		



Appendix 5.4: % tissue bleached of crustose coralline algae (CCA) cultured for 29 days under current ocean pH and temperature and pH and temperature projected by 2100 under the RCP emission scenarios (low = RCP 2.6, medium = RCP 4.5 and high RCP 8.5, IPCC 2014). Data includes the outlier removed in the RCP 2.6 scenario in the main text. Treatments with an asterisk were significantly different from the Current scenario at $\alpha = 0.05$ in the a-priori planned comparisons. Data are presented as means \pm standard error, $n = 8$ for all treatments.

Appendix 5.5: Analysis of Variance (ANOVA) table of a one-way ANOVAs comparing net calcification rates of CCA assemblages between treatments. The three outliers removed from the RCP 4.5 scenario in the main text are included. Df = degrees of freedom, SS = sums of squares, MS = mean square.

	Df	SS	MS	F-value	<i>p</i> - value
Treatment	3	0.123316	0.041105	1.70	0.198
Residuals	26	0.640003	0.024615		



Appendix 5.6: Net calcification rates ($\mu\text{mol CaCO}_3 \text{ cm}^{-2} \text{ h}^{-1}$) of crustose coralline algae (CCA) cultured for 29 days under current ocean pH and temperature and pH and temperature projected by 2100 under the RCP emission scenarios (low = RCP 2.6, medium = RCP 4.5 and high RCP 8.5, IPCC 2014). The three outliers removed from the RCP 4.5 scenario in the main text are included. Data are presented as points for each replicate, $n = 8$ in RCP 2.6 and RCP 4.5, $n = 7$ in Current and RCP 8.5.

Appendix 5.7: Mean $\text{pH}_T \pm$ standard deviation (SD) measured in tanks every two hours for each scenario. Note that SD values are asymmetric as they were calculated as the concentration of H_3O^+ ions and subsequently converted back to pH_T on the log scale.

	Current		RCP 2.6		RCP 4.5		RCP 8.5	
	pH_T	SD	pH_T	SD	pH_T	SD	pH_T	SD
2am	7.91	-0.06, +0.07	7.81	-0.06, +0.07	7.72	-0.07, +0.09	7.63	-0.07, +0.08
4am	7.87	-0.05, +0.06	7.78	-0.06, +0.07	7.70	-0.06, +0.08	7.60	-0.08, +0.09
6am	7.82	-0.08, +0.10	7.73	-0.07, +0.08	7.65	-0.08, +0.09	7.56	-0.07, +0.09
8am	7.79	-0.06, +0.07	7.69	-0.06, +0.07	7.62	-0.08, +0.09	7.52	-0.07, +0.09
10am	7.84	-0.08, +0.09	7.74	-0.08, +0.09	7.67	-0.06, +0.07	7.57	-0.07, +0.09
12pm	7.91	-0.04, +0.05	7.79	-0.06, +0.07	7.69	-0.06, +0.07	7.56	-0.06, +0.06
2pm	7.97	-0.07, +0.09	7.86	-0.08, +0.11	7.79	-0.07, +0.09	7.65	-0.06, +0.07
4pm	8.07	-0.06, +0.06	7.94	-0.07, +0.08	7.83	-0.07, +0.08	7.67	-0.07, +0.09
6pm	8.06	-0.06, +0.06	7.94	-0.06, +0.07	7.87	-0.07, +0.08	7.73	-0.08, +0.09
8pm	8.04	-0.07, +0.09	7.93	-0.07, +0.08	7.85	-0.08, +0.10	7.72	-0.09, +0.11
10pm	8.00	-0.05, +0.06	7.90	-0.06, +0.07	7.81	-0.07, +0.08	7.70	-0.07, +0.09
12am	7.97	-0.04, +0.05	7.86	-0.06, +0.07	7.78	-0.06, +0.07	7.68	-0.07, +0.08

Chapter 6. General Discussion

This thesis examined the effects of global ocean change on seaweeds in key habitat of the commercially important blacklip abalone (*Haliotis rubra*) in eastern Tasmania. The impacts on these seaweeds are likely to have flow on effects to *H. rubra* and the magnitude and nature of these effects are likely to differ across life stages. The field survey (Chapter 2) indicated that the nutritional quality at the southern (cooler) sites was higher than at the northern (warmer) site. This was driven primarily by a higher abundance of nutritious red seaweeds at the southern sites. The low abundance of reds at the northern site may reflect an ongoing compositional change of understory seaweeds in response to climate driven changes in oceanic conditions. Chapter 3 highlighted the importance of using fluctuating pH, mimicking diel oscillations in the field, in experimental treatments. Differential responses to fluctuating pH were observed for two abundant understory red seaweeds. Significant interactions between fluctuating pH and ocean acidification were detected for *C. lambertii* but were not detected for *P. dilatatum*. These contrasting responses suggest misleading results are likely to be attained if static pH is used in experimental treatments. *Phyllospora comosa*, the primary habitat-forming brown seaweed for *H. rubra*, was tolerant to combined warming and acidification in conjunction with marine heatwaves (Chapter 4). This tolerance was likely driven by an increase in the saturation state of fatty acids, which maintained optimum membrane fluidity at higher temperatures. A higher saturation state of fatty acids in conjunction with the detected decrease in nitrogen content may reduce the nutritional quality of *P. comosa* under global ocean change. This, along with reductions in % tissue nitrogen detected under acidification in *C. lambertii*, could reduce *H. rubra* productivity in a future ocean. Crustose coralline algae (CCA) were highly sensitive to global ocean change and are likely to be negatively affected as early as 2030 (Chapter 5). These impacts may have flow on effects to *H. rubra* populations by reducing settlement rates of larvae that require the CCA to induce settlement and metamorphosis.

Current communities: have they already changed?

The field survey conducted in Chapter 2 provided a baseline of the composition and nutritional quality of abundant understory seaweeds in three sites in eastern Tasmania. In general, the two southern sites (site 2 and 3) were more similar than the northern site (site 1). This is unsurprising given that site 2 and 3 were much closer geographically and have similar temperature regimes (Appendix 2.4 - 2.6). The habitat-forming brown seaweed *P. comosa* was the primary component of the overstory across the three sites, with *E. radiata* also abundant at sites 1 and 2. The understory differed considerably between the northern and southern sites, with the main difference being a significantly lower abundance of fleshy red seaweeds at site 1 relative to the southern sites. Crustose coralline algal (CCA) cover (measured in Chapter 3) was similar across all three sites, although was slightly lower at site 3.

The low abundance of reds at the northern sites poses the question of whether reds were once abundant at this site but have declined due to ongoing global ocean change. A poleward extension of the East Australian Current (EAC) has occurred in Tasmania since the 1940s that has caused the warm, nutrient poor EAC to become the dominant water mass influencing the mid to north-eastern region (Ridgway, 2007; Johnson et al., 2011). Significant impacts on the seaweeds have occurred as a result of this extension. There has been a 95 % decline in the abundance of the giant kelp (*Macrocystis pyrifera*) since 1980 (Johnson et al., 2011) and a substantial loss of kelp cover due to overgrazing by the range extended sea urchin *Centrostephanus rodgersii* (Ling et al., 2009; Johnson et al., 2011). While it is yet to be investigated, it is likely that other seaweed species such as the reds have declined in this region, either due to negative effects of global ocean change on seaweed growth and reproduction or due to overgrazing by urchins. Given the high nutritional quality and palatability of the reds observed here and in other studies (Fleming, 1995a; Fleming, 1995b; Schmid et al., 2018), it is likely that the reds are preferentially grazed by urchins. However, whether this would translate to overgrazing in the field is unclear; at the depth our survey was

conducted (7 m) high water motion would likely reduce the abundance of urchins (Velimirov and Griffiths, 1979), potentially limiting their ability to reduce understory biomass.

The decline in *M. pyrifera* itself is also likely to have influenced the composition of understory seaweeds. Changes in biomass or density of the overstory assemblage influences sub-canopy light levels, water motion, sedimentation and rates of scour by kelp fronds (Kennelly, 1989; Wernberg et al., 2005; Layton et al., 2019), all of which influence understory biomass and species composition (Breda and Foster, 1985; Kennelly, 1989; Wernberg et al., 2005). There are substantial differences in morphology between *M. pyrifera* and *P. comosa* (i.e. *M. pyrifera* forms dense surface canopies, whereas *P. comosa* canopies are smaller and typically sub-surface), it is likely that since the decline of *M. pyrifera* at least some or all of the factors described above have been altered in rocky reef ecosystems in eastern Tasmania. Given that loss of *M. pyrifera* cover has been shown to alter understory assemblages in other regions (Dayton et al., 1984; Reed and Foster 1984; Clark, Edwards and Foster., 2004), it is likely that there has been flow on effects to understory biomass and species composition in Tasmania. Identifying whether there has been broad-scale changes in the understory and what the drivers of any changes are should be a priority of future research. Doing so will allow us to make more informed predictions of how communities of seaweeds in eastern Tasmania may change in a future ocean and allow the implementation of any mitigation strategies.

Indirect effects of global ocean change are likely to have differential effects on the life-stages of *H. rubra*

The responses of the seaweeds to global ocean change in the laboratory experiments indicated that there may be significant indirect impacts on *H. rubra*. These impacts are likely to differentially affect each life stage. The larval and post-larval stages are considered some

of the most challenging in terms of survival (Hunt and Scheibling, 1997) and these stages were identified as most likely to be indirectly affected by impacts on seaweed. Growth, photosynthesis, and calcification of CCA exposed to combined warming and acidification were negatively affected, even in near future conditions. If these negative effects were to occur in the field, it would likely cause reductions in *H. rubra* larval settlement, due to reductions in CCA cover or the capacity of the CCA and the associated microbial community to induce settlement. This has been observed in abalone (Tahil and Dy, 2015) and other invertebrates (Doropoulos et al., 2012; Uthicke et al., 2013; Huggett et al., 2018), however, effects are not always negative (Whalan and Webster, 2014; O'Leary et al., 2017; Espinel-Velasco et al., 2018). Although, *H. rubra* settlement can be induced by non-calcareous algae such as *Ulva spp.*, rates are typically highest on CCA (Huggett et al., 2005), indicating future reductions in settlement rates could be substantial. Changes in the microbial community associated with the CCA may also affect the post-larval phase which feed on the microbial community (Daume et al., 1997). Although this thesis did not test whether there was a shift in the microbial community structure under global ocean change, this effect has been observed on both corallines (Webster et al., 2011; Huggett et al., 2018) and kelp (Qiu et al., 2019) exposed to combined warming and acidification. However, whether changes in the microbial community would confer a negative effect to *H. rubra* is unclear and requires investigation.

The indirect effects of global ocean change on juveniles and adults of *H. rubra* are likely to be complicated. The primary habitat-forming seaweed *P. comosa* was tolerant to both marine heatwaves and global ocean change due to an adjustment in fatty acid composition. However, whether the acclimation mechanism is capable of withstanding longer heatwaves projected in the future is unclear (Frölicher et al., 2018; Oliver et al., 2018a; Oliver et al., 2018b). Furthermore, the response of *P. comosa* to global ocean change in the field is likely to be mediated by competitive interactions with other species (Falkenberg et al., 2013a; Kroeker et al., 2013; Falkenberg et al., 2015). The kelp *E. radiata* was abundant in the overstory at sites

1 and 2, likely competing with *P. comosa*. *E. radiata* is predicted to be negatively impacted by both acidification and warming (Britton et al., 2016; Martínez et al., 2018; Qiu et al., 2019), which may lead to declines in its abundance. This could confer a competitive advantage to *P. comosa* in the field, potentially increasing the proportion favourable overstory habitat for *H. rubra*.

A key mechanism through which *H. rubra* juveniles and adults are likely to be indirectly affected by global ocean change is through declines in the nutritional quality of the seaweeds it feeds on (Rossoll et al., 2012; Duarte et al., 2016). A decrease in the proportion of polyunsaturated fatty acids (PUFA) to saturated fatty acids (SFA) was observed in juvenile *P. comosa* under combined warming and acidification (Chapter 4). PUFA, particularly long-chain ($\geq C_{20}$) PUFA (LC-PUFA) are particularly important for animal nutrition (Galloway et al., 2012; Wells et al., 2017) and are positively correlated with elevated growth rates in abalone (Mai et al., 1996; Nelson et al., 2002). As such, any reduction in PUFA is likely to reduce the nutritional quality of this species to *H. rubra* in a future ocean. Whether these changes are likely to be widespread across species is unknown as this thesis did not investigate other species. However, there is evidence to suggest that this response is common: a reduction in PUFA in response to elevated temperature has been observed in the laboratory for red (Becker et al., 2010), green (Gosch et al., 2015) and brown species (Schmid et al. in review), and decreases in PUFA are correlated with increasing temperatures in field studies (Kim et al., 1996; Schmid et al., 2017). However, with the exception of *P. angustum* there were no clear seasonal patterns in PUFA or SFA content in the field survey (Chapter 2) that indicated temperature was the primary driver. Furthermore, the only study that has assessed how ocean acidification influences fatty acid composition in seaweeds found no effects (van der Loos et al., 2019). These findings suggest that the effects of global ocean change on availability of PUFA and LC-PUFA to *H. rubra* is likely to be complicated. There is evidence to suggest there may be a general decrease in the PUFA content of seaweed

communities, but this will likely be influenced by species-specific variation in responses and interactions of global ocean change with other environmental factors known to influence fatty acid composition such as light, salinity and nutrient concentrations (Floreto et al., 1993; Gordillo et al., 2001; Hotimchenko, 2002; Khotimchenko and Yakovleva, 2005; Kumar et al., 2010).

Nitrogen content of seaweeds is also a key determinant of growth rates in *H. rubra* (Fleming, 1995a) and any change in nitrogen content is likely to indirectly affect *H. rubra*. In Chapter 3 there was a reduction in the nitrogen content of the red seaweed *C. lambertii* in response to ocean acidification (importantly, this decrease was only detectable under realistic pH fluctuations), and in Chapter 4 a decrease in the nitrogen content of *P. comosa* was detected under combined warming and acidification (Appendix 4.6). Both of these species were abundant in our field survey and widespread reductions in nitrogen content of these species could have significant impacts on *H. rubra* productivity. These impacts could be further exacerbated if reductions in nitrogen content are widespread across species, but whether this is the case is unclear. There was no reduction in nitrogen content in *P. dilatatum* (Chapter 3) or other red and brown seaweeds from Tasmania exposed to acidification (Britton et al., 2016; van der Loos et al., 2019). In contrast, studies from other regions have shown C:N ratios in seaweeds increase under acidification (Falkenberg et al., 2013b; Gutow et al., 2014). In the field survey, nitrogen content was generally higher in winter relative to summer in both reds and browns, but whether temperature was the driver of this is unknown. Although temperature is elevated in summer, inorganic nitrogen concentrations of the seawater are typically lower (Fairhead and Cheshire, 2004; Flukes et al., 2015), which can decrease internal nitrogen levels in seaweeds (Brown et al., 1997). This means it was not possible to separate the effects of temperature and inorganic nitrogen concentrations. However, given that the increased influence of the EAC is also likely to reduce nutrient concentrations in the

future in eastern Tasmania (Ridgway, 2007; Johnson et al., 2011), it would appear that an overall reduction in the nitrogen content of the seaweeds in Tasmania is likely.

Limitations/key questions remaining

This thesis has contributed new knowledge on how seaweeds that are key to the life cycle of *H. rubra* may respond to climate change. However, there are still gaps in our understanding, limitations of what can be inferred from the data and further questions arising from results presented in these chapters. The nutritional quality survey highlighted that there was a significant difference in the nutritional quality and composition of seaweeds at each site, however, the drivers of this are unclear. A range of factors can influence the species composition or nutritional quality of understory seaweeds including light, temperature, nutrient concentrations and wave exposure (Breda and Foster, 1985; Kennelly, 1989; Gordillo et al., 2001; Hotimchenko, 2002; Goldberg, 2005; Wernberg and Goldberg, 2008; Schmid et al., 2017). While it was not possible to determine the drivers of changes in species composition or nutritional quality in the field in this thesis, conducting research into possible drivers would provide essential information for predicting how *H. rubra* may be impacted in the future. Undertaking an intensive field survey with a hierarchical sampling design at numerous sites along a latitudinal gradient and high-resolution monitoring of environmental drivers would assist in identifying the main drivers and predicting how communities may respond to future changes in ocean conditions.

This thesis assessed the nutritional quality of seaweed assemblages in the field and investigated how broad indicators (PUFA and % N) would be altered under global ocean change in the laboratory. Although broad indicators are useful in that they can identify patterns and are cost effective, changes in specific compounds are likely to drive impacts on growth and reproduction in *H. rubra*. For example, PUFA from the n-3 and n-6 families have

been identified as being important for abalone nutrition in feeding studies (Mai et al., 1996; Nelson et al., 2002) and field surveys (Guest et al., 2008). While % nitrogen serves as a proxy for protein content (Angell et al., 2016), the specific amino acid combinations in the proteins likely being important for nutrition. As such, identifying specific compounds required for nutrition, by concurrent analysis of seaweed and abalone tissue in the field (e.g. Guest et al., 2008) or by targeted feeding experiments (e.g. Mai et al., 1996; Nelson et al., 2002) should be a priority of future research. These experiments could be supplemented by further physiological experiments examining changes in the biochemical composition of key species to global ocean change. Doing so will provide a clearer understanding of how nutritional quality of seaweeds in eastern Tasmania are likely to change in the future and assist in determining whether the prior catch rates of *H. rubra* will be sustainable in a future ocean.

Another question arising from this research was whether the impacts on the CCA would result in a reduction in larval settlement or negatively impact post-larvae. Although the results provided a clear indication that CCA cover is likely to be reduced under global ocean change, this thesis was unable to determine whether these changes would alter larval settlement rates or influence the microbial community on the CCA surface. A key area of future research is to identify whether the impacts on CCA reduce the proportion of larvae settling, whether they can settle on different substratum and what impacts changes in the microbial community may have on post-larvae. Larvae of *H. rubra* are able to settle in response to species of seaweeds other than CCA (Huggett et al., 2005), but this is generally at a reduced rate and it is unclear if the settlement rates would be sufficient to compensate for losses in CCA cover. The surface biofilm has a key role in inducing abalone settlement (Daume et al., 1999; Roberts et al., 2010) and understanding whether changes in composition are likely to occur, what effect this has on settlement rates and its quality as a food source for post-larvae are key questions to address. Targeted laboratory experiments that culture both CCA and *H. rubra* larvae under current and future ocean conditions and examine how this

influences microbial communities and settlement rates in a reciprocal transplant experiment would be a useful approach to advance our knowledge of how global ocean change may impact recruitment and post-larval feeding in *H. rubra*.

A final consideration is that the responses of seaweeds to global ocean change in this thesis were all measured in the laboratory. Although the laboratory experiments in this thesis all mimicked the field as close as possible, by including factors such as realistic fluctuations in pH, it is still an artificial setting and lacks the dynamic conditions that occur naturally such as variable light and nutrient regimes, fluctuating wave energy and species interactions.

However, given that manipulating both pH and temperature in a way that represents how they will change in the future is very difficult and costly to do in the field, laboratory experiments such as these are still extremely valuable. By performing these experiments in a controlled environment, it is possible to identify how species respond to a stressor and understand the physiological mechanisms that underpin these responses. By understanding these mechanisms, it improves our ability to predict how other species may respond, particularly if subsequent studies find that the mechanisms are widespread amongst functional groups.

Inorganic carbon uptake strategy as a tool to predict responses of seaweeds to global ocean change

Inorganic carbon uptake strategy (i.e. CCM vs non-CCM species) has been suggested as a physiological trait that can predict how seaweeds will respond to ocean acidification (Hepburn et al., 2011; Cornwall et al., 2017; van der Loos et al., 2019). Non-CCM species are predicted to benefit from elevated CO₂ if they are carbon limited under today's concentrations, while species that have a CCM are predicted to benefit if they can down-regulate the CCM. However, these broad responses are likely to be mediated by other factors such as elevated temperature. To date, non-CCM seaweeds from Tasmania have not benefited from elevated CO₂ concentrations in experimental studies (Cornwall and Hurd, 2019; van der

Loos et al., 2019; Chapter 3), although some species increase net photosynthetic rates (Cornwall and Hurd, 2019; Chapter 3). Reasons for this are unclear but may be related to species-specific sensitivity to increased $[H^+]$ (Roleda et al., 2012; van der Loos et al., 2019). In contrast, CCM seaweeds from Tasmania generally down regulate the CCM in response to elevated CO_2 , which is typically beneficial (van der Loos et al., 2019; Chapter 4), but not for *E. radiata* (Britton et al., 2016).

Based on these responses, CCM seaweeds in eastern Tasmania may gain a competitive advantage over non-CCM seaweeds in a future ocean. Most non-CCM seaweeds identified in eastern Tasmania are red understory algae (Cornwall et al., 2015), and any reductions in competitive ability may lead to a decline in their future abundance. Given that the abundance of nutritious reds may be an important driver of abalone productivity, this could reduce abalone productivity in a future ocean, with seaweed communities becoming similar to those observed at site 1 (Chapter 2): an understory biomass comprised predominately of brown seaweeds. Future research that examines the importance of inorganic carbon uptake strategy relative to other factors such as increased temperature or species-specific sensitivity to $[H^+]$, in determining the response of seaweeds to global ocean change is required. This will assist our ability to make broad predictions of how seaweed assemblages may change in a future ocean and how these changes may affect invertebrate grazers that rely on them.

Projecting forward/conclusions

The primary aim of this thesis was to determine how seaweeds that are key to the life cycle of *H. rubra* will respond to global ocean change and infer how these changes may affect *H. rubra*. Figure 6.1 is a conceptual diagram highlighting the ways in which *H. rubra* relies on seaweeds, how these seaweeds may be impacted under global ocean change and the likely indirect effects on *H. rubra*. The indirect effects are likely to differentially affect each life-

history stage with larvae and post-larvae the most susceptible, through impacts on CCA. The effects on juveniles and adults are likely to be subtle with little evidence that a decline in the primary habitat-forming seaweed *P. comosa* will occur in eastern Tasmania. However, there may be declines in the nutritional quality of the seaweeds utilised by *H. rubra* as a food source, which could have flow on effects to *H. rubra* populations. Determining the drivers of changes in nutritional quality in the field and how it interacts with global ocean change is a key area of future research, which will assist in determining sustainable catch rates of *H. rubra* in eastern Tasmania.




Way in which <i>H. rubra</i> relies on seaweed	Impact of global ocean change on seaweeds	Likely indirect effect on <i>H. rubra</i>	Potential ecological consequences
Habitat	Primary habita- forming seaweed, <i>Phyllospora comosa</i> tolerant	 Minimal impacts	N/A
Food source	Reductions in PUFA and nitrogen content	 Reduction in food quality	Reduced growth, reproductive output
Settlement substrate	Reductions in growth, calcification and increased bleaching of crustose coralline algae	 Reduction in the proportion of settlement substrate	Reduced recruitment success

Figure 6.1: Conceptual diagram showing the ways in which the blacklip abalone (*Haliotis rubra*) relies on seaweed (left), the impacts of global ocean change on these seaweed detected in laboratory experiments (middle left), the likely indirect effects on *H. rubra* arising from the impacts on the seaweeds (middle right) and the potential ecological consequences of the indirect impacts (right). Red arrows refer to negative impacts and the grey dash refers to no impact.

References

- Angell, A. R., Mata, L., de Nys, R., and Paul, N. A. 2016. The protein content of seaweeds: a universal nitrogen-to-protein conversion factor of five. *Journal of Applied Phycology*, 28: 511-524.
- Becker, S., Graeve, M., and Bischof, K. 2010. Photosynthesis and lipid composition of the Antarctic endemic rhodophyte *Palmaria decipiens*: effects of changing light and temperature levels. *Polar Biology*, 33: 945-955.
- Breda, V. A., and Foster, M. S. 1985. Composition, abundance, and phenology of foliose red algae associated with two central California kelp forests. *Journal of Experimental Marine Biology and Ecology*, 94: 115-130.
- Britton, D., Cornwall, C. E., Revill, A. T., Hurd, C. L., and Johnson, C. R. 2016. Ocean acidification reverses the positive effects of seawater pH fluctuations on growth and photosynthesis of the habitat-forming kelp, *Ecklonia radiata*. *Scientific Reports*, 6.
- Brown, M. T., Nyman, M. A., Keogh, J. A., and Chin, N. K. M. 1997. Seasonal growth of the giant kelp *Macrocystis pyrifera* in New Zealand. *Marine Biology*, 129: 417-424.
- Clark, R. M., Edwards, M.S., and Foster, M.S. 2004. Effects of shade from multiple kelp canopies on an understory algal assemblage. *Marine Ecology Progress Series* 267:107-119.
- Cornwall, C. E., and Hurd, C. L. 2019. Variability in the benefits of ocean acidification to photosynthetic rates of macroalgae without CO₂-concentrating mechanisms. *Marine and Freshwater Research*, 71: 275-280.
- Cornwall, C. E., Revill, A. T., Hall-Spencer, J. M., Milazzo, M., Raven, J. A., and Hurd, C. L. 2017. Inorganic carbon physiology underpins macroalgal responses to elevated CO₂. *Scientific Reports*, 7: 46297.
- Cornwall, C. E., Revill, A. T., and Hurd, C. L. 2015. High prevalence of diffusive uptake of CO₂ by macroalgae in a temperate subtidal ecosystem. *Photosynthesis Research*, 124: 181-190.
- Daume, S., Brand-Gardner, S., and Woelkerling, W. J. 1999. Preferential settlement of abalone larvae: diatom films vs. non-geniculate coralline red algae. *Aquaculture*, 174: 243-254.
- Daume, S., Brand, S., and Woelkerling, J. 1997. Effects of post-larval abalone (*Haliotis rubra*) grazing on the epiphytic diatom assemblage of coralline red algae. *Molluscan Research*, 18: 119-130.
- Dayton, P. K., Currie, V., Gerrodette, T., Keller, B.D., Rosenthal, R., and Tresca, D.V. (1984). Patch Dynamics and Stability of Some California Kelp Communities. *Ecological Monographs* 54(3): 254-289.
- Doropoulos, C., Ward, S., Diaz-Pulido, G., Hoegh-Guldberg, O., and Mumby, P. J. 2012. Ocean acidification reduces coral recruitment by disrupting intimate larval-algal settlement interactions. *Ecology Letters*, 15: 338-346.

- Duarte, C., López, J., Benítez, S., Manríquez, P. H., Navarro, J. M., Bonta, C. C., Torres, R., et al. 2016. Ocean acidification induces changes in algal palatability and herbivore feeding behavior and performance. *Oecologia*, 180: 453-462.
- Espinel-Velasco, N., Hoffmann, L., Agüera, A., Byrne, M., Dupont, S., Uthicke, S., Webster, N. S., et al. 2018. Effects of ocean acidification on the settlement and metamorphosis of marine invertebrate and fish larvae: a review. *Marine Ecology Progress Series*, 606: 237-257.
- Fairhead, V. A., and Cheshire, A. C. 2004. Rates of primary productivity and growth in *Ecklonia radiata* measured at different depths, over an annual cycle, at West Island, South Australia. *Marine Biology*, 145: 41-50.
- Falkenberg, L. J., Connell, S. D., Coffee, O. I., Ghedini, G., and Russell, B. D. 2015. Species interactions can maintain resistance of subtidal algal habitats to an increasingly modified world. *Global Ecology and Conservation*, 4: 549-558.
- Falkenberg, L. J., Russell, B. D., and Connell, S. D. 2013a. Contrasting resource limitations of marine primary producers: implications for competitive interactions under enriched CO₂ and nutrient regimes. *Oecologia*, 172: 575-583.
- Falkenberg, L. J., Russell, B. D., and Connell, S. D. 2013b. Future herbivory: the indirect effects of enriched CO₂ may rival its direct effects. *Marine Ecology Progress Series*, 492: 85-95.
- Fleming, A. E. 1995a. Digestive efficiency of the Australian abalone *Haliotis rubra* in relation to growth and feed preference. *Aquaculture*, 134: 279-293.
- Fleming, A. E. 1995b. Growth, intake, feed conversion efficiency and chemosensory preference of the Australian abalone, *Haliotis rubra*. *Aquaculture*, 132: 297-311.
- Floreto, E. A. T., Hirata, H., Ando, S., and Yamasaki, S. 1993. Effects of temperature, light intensity, salinity and source of nitrogen on the growth, total lipid and fatty acid composition of *Ulva pertusa* kjellman (Chlorophyta). *In Botanica Marina*, p. 149.
- Flukes, E., T. Wright, J., and Johnson, C. 2015. Phenotypic plasticity and biogeographic variation in physiology of habitat-forming seaweed: response to temperature and nitrate. *Journal of Phycology*, 51.
- Frölicher, T. L., Fischer, E. M., and Gruber, N. 2018. Marine heatwaves under global warming. *Nature*, 560: 360-364.
- Galloway, A. W. E., Britton-Simmons, K. H., Duggins, D. O., Gabrielson, P. W., and Brett, M. T. 2012. Fatty acid signatures differentiate marine macrophytes at ordinal and family ranks. *Journal of Phycology*, 48: 956-965.
- Goldberg, N. 2005. Temporal variation in subtidal macroalgal assemblages at Black Island, Recherche Archipelago. *Journal of the Royal Society of Western Australia*, 88: 65-71.
- Gordillo, F., Jiménez, C., Goutx, M., and Niell, X. 2001. Effects of CO₂ and nitrogen supply on the biochemical composition of *Ulva rigida* with especial emphasis on lipid class analysis. *Journal of Plant Physiology*, 158: 367-373.

- Gosch, B. J., Lawton, R. J., Paul, N. A., de Nys, R., and Magnusson, M. 2015. Environmental effects on growth and fatty acids in three isolates of *Derbesia tenuissima* (Bryopsidales, Chlorophyta). *Algal Research*, 9: 82-93.
- Guest, M. A., Nichols, P. D., Frusher, S. D., and Hirst, A. J. 2008. Evidence of abalone (*Haliotis rubra*) diet from combined fatty acid and stable isotope analyses. *Marine Biology*, 153: 579-588.
- Gutow, L., Rahman, M. M., Bartl, K., Saborowski, R., Bartsch, I., and Wiencke, C. 2014. Ocean acidification affects growth but not nutritional quality of the seaweed *Fucus vesiculosus* (Phaeophyceae, Fucales). *Journal of Experimental Marine Biology and Ecology*, 453: 84-90.
- Hepburn, C. D., Pritchard, D. W., Cornwall, C. E., McLeod, R. J., Beardall, J., Raven, J. A., and Hurd, C. L. 2011. Diversity of carbon use strategies in a kelp forest community: implications for a high CO₂ ocean. *Global Change Biology*, 17: 2488-2497.
- Hotimchenko, S. V. 2002. Fatty acid composition of algae from habitats with varying amounts of illumination. *Russian Journal of Marine Biology*, 28: 218-220.
- Huggett, M. J., De Nys, R., Williamson, J. E., Heasman, M., and Steinberg, P. D. 2005. Settlement of larval blacklip abalone, *Haliotis rubra*, in response to green and red macroalgae. *Marine Biology*, 147: 1155-1163.
- Huggett, M. J., McMahon, K., and Bernasconi, R. 2018. Future warming and acidification result in multiple ecological impacts to a temperate coralline alga. *Environmental Microbiology*, 20: 2769-2782.
- Hunt, H., and Scheibling, R. 1997. Role of early post-settlement mortality in recruitment of benthic marine invertebrates. *Marine Ecology Progress Series*, 155: 269-301.
- Johnson, C. R., Banks, S. C., Barrett, N. S., Cazassus, F., Dunstan, P. K., Edgar, G. J., Frusher, S. D., et al. 2011. Climate change cascades: shifts in oceanography, species' ranges and subtidal marine community dynamics in eastern Tasmania. *Journal of Experimental Marine Biology and Ecology*, 400: 17-32.
- Kennelly, S. J. 1989. Effects of kelp canopies on understory species due to shade and scour. *Marine ecology progress series*. Oldendorf, 50: 215-224.
- Khotimchenko, S. V., and Yakovleva, I. M. 2005. Lipid composition of the red alga *Tichocarpus crinitus* exposed to different levels of photon irradiance. *Phytochemistry*, 66: 73-79.
- Kim, M.-K., Dubacq, J.-P., Thomas, J.-C., and Giraud, G. 1996. Seasonal variations of triacylglycerols and fatty acids in *Fucus serratus*. *Phytochemistry*, 43: 49-55.
- Kroeker, K. J., Micheli, F., and Gambi, M. C. 2013. Ocean acidification causes ecosystem shifts via altered competitive interactions. *Nature Climate Change*, 3: 156-159.
- Kumar, M., Kumari, P., Gupta, V., Reddy, C. R. K., and Jha, B. 2010. Biochemical responses of red alga *Gracilaria corticata* (Gracilariales, Rhodophyta) to salinity induced oxidative stress. *Journal of Experimental Marine Biology and Ecology*, 391: 27-34.

- Layton, C., Shelamoff, V., Cameron, M. J., Tatsumi, M., Wright, J. T., and Johnson, C. R. 2019. Resilience and stability of kelp forests: the importance of patch dynamics and environment-engineer feedbacks. *PLoS ONE*, 14: e0210220.
- Ling, S. D., Johnson, C. R., Frusher, S. D., and Ridgway, K. R. 2009. Overfishing reduces resilience of kelp beds to climate-driven catastrophic phase shift. *Proceedings of the National Academy of Sciences of the United States of America*, 106: 22341-22345.
- Mai, K., Mercer, J. P., and Donlon, J. 1996. Comparative studies on the nutrition of two species of abalone, *Haliotis tuberculata* L. and *Haliotis discus hannai* Ino. V. The role of polyunsaturated fatty acids of macroalgae in abalone nutrition. *Aquaculture*, 139: 77-89.
- Martínez, B., Radford, B., Thomsen, M. S., Connell, S. D., Carreño, F., Bradshaw, C. J. A., Fordham, D. A., et al. 2018. Distribution models predict large contractions of habitat-forming seaweeds in response to ocean warming. *Diversity and Distributions*, 24: 1350-1366.
- Nelson, M. M., Leighton, D. L., Phleger, C. F., and Nichols, P. D. 2002. Comparison of growth and lipid composition in the green abalone, *Haliotis fulgens*, provided specific macroalgal diets. *Comp Biochem Physiol B Biochem Mol Biol*, 131: 695-712.
- O'Leary, J. K., Barry, J. P., Gabrielson, P. W., Rogers-Bennett, L., Potts, D. C., Palumbi, S. R., and Micheli, F. 2017. Calcifying algae maintain settlement cues to larval abalone following algal exposure to extreme ocean acidification. *Scientific Reports*, 7.
- Oliver, E. C. J., Benthuyssen, J. A., Bindoff, N. L., Hobday, A. J., Holbrook, N. J., Mundy, C. N., and Perkins-Kirkpatrick, S. E. 2017. The unprecedented 2015/16 Tasman Sea marine heatwave. *Nature Communications*, 8: 16101.
- Oliver, E. C. J., Donat, M. G., Burrows, M. T., Moore, P. J., Smale, D. A., Alexander, L. V., Benthuyssen, J. A., et al. 2018a. Longer and more frequent marine heatwaves over the past century. *Nature Communications*, 9.
- Oliver, E. C. J., Lago, V., Hobday, A. J., Holbrook, N. J., Ling, S. D., and Mundy, C. N. 2018b. Marine heatwaves off eastern Tasmania: trends, interannual variability, and predictability. *Progress in Oceanography*, 161: 116-130.
- Qiu, Z., Coleman, M. A., Provost, E., Campbell, A. H., Kelaher, B. P., Dalton, S. J., Thomas, T., et al. 2019. Future climate change is predicted to affect the microbiome and condition of habitat-forming kelp. *Proceedings of the Royal Society B: Biological Sciences*, 286.
- Reed, D.C., and Foster, M.S. 1984. The effects of canopy shadings on algal recruitment and growth in a giant kelp forest. *Ecology*, 65(3), 937-948. doi:10.2307/1938066
- Ridgway, K. R. 2007. Long-term trend and decadal variability of the southward penetration of the East Australian Current. *Geophysical Research Letters*, 34: n/a-n/a.
- Roberts, R. D., Barker, M. F., and Mladenov, P. 2010. Is settlement of *Haliotis iris* larvae on coralline algae triggered by the alga or its surface biofilm? *Journal of Shellfish Research*, 29: 671-678.
- Roleda, M. Y., Morris, J. N., McGraw, C. M., and Hurd, C. L. 2012. Ocean acidification and seaweed reproduction: Increased CO₂ ameliorates the negative effect of lowered pH on

meiospore germination in the giant kelp *Macrocystis pyrifera* (Laminariales, Phaeophyceae). *Global Change Biology*, 18: 854-864.

Rossoll, D., Bermúdez, R., Hauss, H., Schulz, K. G., Riebesell, U., Sommer, U., and Winder, M. 2012. Ocean acidification-induced food quality deterioration constrains trophic transfer. *PLoS ONE*, 7.

Schmid, M., Guihéneuf, F., and Stengel, D. B. 2017. Ecological and commercial implications of temporal and spatial variability in the composition of pigments and fatty acids in five Irish macroalgae. *Marine Biology*, 164: 158.

Schmid, M., Kraft, L. G. K., van der Loos, L. M., Kraft, G. T., Virtue, P., Nichols, P. D., and Hurd, C. L. 2018. Southern Australian seaweeds: a promising resource for omega-3 fatty acids. *Food Chem*, 265: 70-77.

Tahil, A. S., and Dy, D. T. 2015. Effects of reduced pH on larval settlement and survival of the Donkey's ear abalone, *Haliotis asinina* (Linnaeus 1758). *Philippine Journal of Science*, 144: 21-29.

Uthicke, S., Pecorino, D., Albright, R., Negri, A. P., Cantin, N., Liddy, M., Dworjanyn, S., et al. 2013. Impacts of ocean acidification on early life-history stages and settlement of the coral-eating sea star *Acanthaster planci*. *PLoS ONE*, 8: e82938.

van der Loos, L. M., Schmid, M., Leal, P. P., McGraw, C. M., Britton, D., Revill, A. T., Virtue, P., et al. 2019. Responses of macroalgae to CO₂ enrichment cannot be inferred solely from their inorganic carbon uptake strategy. *Ecology and Evolution*, 9: 125-140.

Velimirov, B., and Griffiths, C. L. 1979. Wave-induced kelp movement and its importance for community structure. *In Botanica Marina*, p. 169.

Webster, N. S., Soo, R., Cobb, R., and Negri, A. P. 2011. Elevated seawater temperature causes a microbial shift on crustose coralline algae with implications for the recruitment of coral larvae. *The ISME Journal*, 5: 759-770.

Wells, M. L., Potin, P., Craigie, J. S., Raven, J. A., Merchant, S. S., Helliwell, K. E., Smith, A. G., et al. 2017. Algae as nutritional and functional food sources: revisiting our understanding. *Journal of Applied Phycology*, 29: 949-982.

Wernberg, T., and Goldberg, N. 2008. Short-term temporal dynamics of algal species in a subtidal kelp bed in relation to changes in environmental conditions and canopy biomass. *Estuarine, Coastal and Shelf Science*, 76: 265-272.

Wernberg, T., Kendrick, G. A., and Toohey, B. D. 2005. Modification of the physical environment by an *Ecklonia radiata* (Laminariales) canopy and implications for associated foliose algae. *Aquatic Ecology*, 39: 419-430.

Whalan, S., and Webster, N. S. 2014. Sponge larval settlement cues: the role of microbial biofilms in a warming ocean. *Scientific Reports*, 4: 4072.